Development of a new class of antivirals active against pox and measles viruses

Submitted for the degree of Doctor of Philosophy

Laura Farleigh

2014

Cardiff University

DECLARATION

This work has not been submitted in substance for any other degree or award at this or any other university or place of learning, nor is being submitted concurrently in candidature for any degree or other award.

Signed …… (candidate) Date ……

STATEMENT 1

This thesis is being submitted in partial fulfillment of the requirements for the degree of ……(insert MCh, MD, MPhil, PhD etc, as appropriate)

Signed …… (candidate) Date ……

STATEMENT 2

This thesis is the result of my own independent work/investigation, except where otherwise stated.

Other sources are acknowledged by explicit references. The views expressed are my own.

Signed …… (candidate) Date ……

STATEMENT 3

I hereby give consent for my thesis, if accepted, to be available for photocopying and for inter-library loan, and for the title and summary to be made available to outside organisations.

Signed …… (candidate) Date ……

STATEMENT 4: PREVIOUSLY APPROVED BAR ON ACCESS

I hereby give consent for my thesis, if accepted, to be available for photocopying and for inter-library loans **after expiry of a bar on access previously approved by the Academic Standards & Quality Committee.**

Signed …… (candidate) Date ……

Acknowledgements

Firstly I would like to thank my primary supervisor Dr J. Bugert for his help and guidance throughout the project, I also thank my secondary supervisors Professor C. McGuigan and Dr A. Jones for all their additional advice.

I would like to thank the friends I have worked with in the Bugert group including Subuhi Sherwani, Asif Nizam, Niamh Blythe and Lucy Robinson.

I would also like to thank people in PHRMY for their contributions including Ranjith Pathirana and Karen Hinsinger for producing the ddBCNAs and Edd Sayers for assistance with the confocal.

Thank you to all those who contributed to data and provided reagents as mentioned throughout the thesis.

A special thank you to my friends and family particularly my parents who have provided unlimited support throughout my life.

Finally I give huge thanks to my boyfriend Chris who has helped and guided me through the whole of the writing process and been a source of constant support.

Summary

In this PhD project we show for the first time that novel dideoxy bicyclic pyrimidine nucleoside analogues (ddBCNAs) with L-chirality represent promising antiviral candidates for use against pox and measles viruses. We suggest a mechanism of action based on a cellular target. Our lead compound (Cf2642, with side chain C_9H_{18}–O–C_5H_{11}) is active against vaccinia virus (a surrogate poxvirus for smallpox) and measles virus, with IC_{50} concentrations of 0.19 and 7.5 µM, respectively. This is a 60-fold enhancement over cidofovir (viral DNA polymerase inhibitor; IC_{50} of 11.5 µM against VACV). A structure activity relationship was established, which was similar for both viruses, indicating a common and specific mechanism of action. Cf2642 does not inhibit HSV-1/2, influenza, adeno or yellow fever viruses. The mechanism of action for the ddBCNAs has been investigated and, though not defined, has been narrowed down. Based on our observations of drug activity in cell lines derived from various sources, we have suggested a cellular target for the ddBCNAs, most likely cellular membrane compartments or the proteins located therein. Though inhibition of vaccinia is observed within two hours of infection, we have shown that the ddBCNAs are unlikely to be entry inhibitors. Acidification of the extracellular medium was observed but, whilst it may be linked to the mechanism of action, this is not the cause of the antiviral effects. With a possible cellular target, toxicity was carefully evaluated. We have not observed significant cytotoxicity in any of our cell models. Antivirals active against cellular targets are less subject to viral resistance, which may develop rapidly with virus-targeting drugs. This could be critical since, there are currently no effective measles antiviral drugs available on the market, and resistance to measles RNA polymerase inhibitors and the potential antipoxviral drug cidofovir has already been described.

Abbreviations

- 6-wp (12,24,48 or 96) wp – 6 (12,24,48 or 96) well plate
- AraC – Cytosine arabinoside
- ATCC – American Tissue Culture Collection
- ATP – Adenosine Triphosphate
- bp – base pairs
- CC_{50} – 50% Cytotoxicity concentration
- CCLR – Cell culture lysis reagent
- CEV – Cell-associated enveloped virus
- CPE – Cytopathic effect
- ddBCNA – Di-deoxy bicyclic nucleoside analogues
- D- / L- IddU – D- / L-5-iodo-2,3-deoxyuridine
- DMEM – Dulbecco's modified Eagle's medium
- DMSO – Dimethyl sulphoxide
- EBV – Epstein Barr Virus
- EEV – Extracellular enveloped virus
- FBS – Foetal Bovine Serum
- GAGs – Glycosaminoglycans
- hCMV – Human Cytomegalovirus
- HIV-1/2 – Human Immunodeficiency virus type 1/2
- HSV-1/2 – Herpes Simplex Virus type 1/2
- IC_{50} – 50% Inhibitory concentration
- IEV – Intracellular enveloped virus
- IMV – Intracellular mature virus
- IV – Immature virion

- LB – Luria (liquid) broth for bacterial cultures
- MAPs – Microtubule associated proteins
- m IC323 – Measles virus wild type strain containing GFP gene
- MCV – Molluscum Contagiosum Virus
- mEdATCC – Measles virus Edmonston (vaccine) strain
- MoA – Mechanism of action
- moi – multiplicity of infection
- MVA – Modified Vaccinia Ankara
- mWT Fb – Measles virus wild type strain
- PBS – Phosphate Buffered Saline
- PFA – Paraformaldehyde
- pfu – plaque forming units
- pi – post infection
- RLU – Relative Light Units
- rpm – rotations per minute
- SAR – Structure activity relationship
- SSPE – Subacute sclerosing panencephalitis
- T25 (75 or 150) – 25 (75 or 150) cm^2 cell culture flask
- $TCID_{50}$ – 50% tissue culture infective dose
- To – Time of infection
- ToA – Time of addition
- UC – Universal container (25 mL)
- v3 – Vaccinia virus containing luciferase gene
- v300 – Vaccinia virus containing GFP gene
- VACV – Vaccinia virus

- VITF-2 – Virus intermediate transcription factor-2
- VPEF – Vaccina virus penetration factor
- vWR – Vaccinia virus Western Reserve stain
- VZV – Varicella zoster virus
- YFV – Yellow fever virus (vaccine strain)

Contents

Chapter one - Introduction	**1**
1.1 Di-deoxybicyclic nucleoside analogues	**1**
1.1.1 Background of nucleoside analogues as antiviral compounds	**2**
1.1.2 D- versus L-chirality	**4**
1.2 Poxvirus family	**5**
1.2.1 Vaccinia virus and its use as a vaccine	**6**
1.2.1.1 VACV Structure	**7**
1.2.1.2 VACV entry	**9**
1.2.1.3 VACV life cycle	**13**
1.2.1.4 VACV spread	**18**
1.2.2 Smallpox	**20**
1.2.3 MCV	**21**
1.2.4 Other poxviruses	**22**
1.2.5 Current antivirals against poxviruses	**23**
1.3 Paramyxovirus family	**26**
1.3.1 Measles virus	**28**
1.3.1.1 Measles genome and structure	**29**
1.3.1.2 Measles entry	**30**
1.3.1.3 Measles lifecycle	**31**
1.3.1.4 Measles syncytia formation (virus spread)	**32**

1.3.1.5 Measles vaccine **32**

1.3.1.6 Measles antivirals **34**

1.4 Antiviral drugs with cellular targets **35**

1.5 Aims of the PhD project **36**

Chapter two – Materials and Methods **37**

2.1 Materials **37**

2.1.1 Cell lines **37**

2.1.2 Antiviral compounds **38**

2.1.2.1 ddBCNAs **38**

2.1.2.2 Control compounds **40**

2.1.3 Viruses **40**

2.1.4 Equipment **41**

2.1.4.1 Plastics and glassware **41**

2.1.4.2 Other equipment **42**

2.1.4.3 Software **42**

2.2 Methods **43**

2.2.1 Cell culture methods **43**

2.2.1.1 Cell maintenance **43**

2.2.1.2 Thawing cells **43**

2.2.1.3 Freezing cells **43**

2.2.1.4 Mycoplasma testing **43**

2.2.1.5 Sub-culturing of cells **44**

2.2.1.6 Cell counting **44**

2.2.2 Virus stock production methods **45**

2.2.2.1 Optimisation of VACV stock production **45**

2.2.2.2 Standard VACV stock production **48**

2.2.2.3 Measles stock production **48**

2.2.2.4 Yellow fever virus stock production **49**

2.2.3 Quantification of virus stocks **49**

2.2.3.1 Optimisation of VACV plaque assays – shell vial method **49**

2.2.3.2 VACV plaque assay titrations **52**

2.2.3.2.1 Crystal violet solution **52**

2.2.3.3 $TCID_{50}$ virus quantification **52**

2.2.4 Recombinant VACV (v3 and v300) construction details **53**

2.2.4.1 PCR – gene of interest **54**

2.2.4.2 Digestion **55**

2.2.4.3 Gel electrophoresis and purification **55**

2.2.4.3.1 Stop buffer **56**

2.2.4.4 Ligation **56**

2.2.4.5 Transformation **56**

2.2.4.6 Preparation of agar plates and liquid bacterial growth medium **57**

2.2.4.7 Amplification and purification of plasmid DNA **57**

2.2.4.8 Transfection/Infection **58**

2.2.4.9 Plaque purification **58**

2.2.5 VACV (v3) firefly luciferase assay **58**

2.2.5.1 Optimisation of the v3 luciferase assay **58**

2.2.6 Microscopy methods **60**

2.2.6.1 Fixing cells for staining **60**

2.2.6.2 Cell staining and mounting onto slides **60**

2.2.6.2.1 Blocking buffer **61**

Chapter three – ddBCNA SARs against vaccinia virus **62**

3.1 Introduction **62**

3.2 Materials and methods **64**

3.2.1 Luciferase assay **64**

3.2.2 Cell range assay **65**

3.2.3 Time of addition assay **65**

3.2.4 Statistics **66**

3.2.5 Plaque size reduction assay **66**

3.2.6 IC_{50} claculations **66**

3.2.7 Wide field fluorescence microscopy **67**

3.2.8 Pilot *in vivo* assay **67**

3.3 Results **68**

3.3.1 Activity of ddBCNAs against VACV: luciferase assay **68**

3.3.1.1 Activity of D- versus L-ddBCNAs **68**

3.3.1.2 Activity of L-ddBCNAs with alkyl and ether side chains **72**

3.3.1.3 Activity of further modified L-ddBCNAs **76**

3.3.2 Activity of Cf2642 against VACV in alternative cell lines **79**

3.3.3 Cf2642 time of addition luciferase assay **81**

3.3.4 Activity of ddBCNAs in plaque size reduction assays **83**

3.3.5 Fluorescence microscopy of plaque development **87**

3.3.6 Pilot *in vivo* assay **89**

3.4 Discussion **91**

Chapter four – Activity against measles and virus panel **96**

4.1 Introduction **96**

4.2 Materials and methods **98**

4.2.1 MCV luciferase transcription reporter assay **98**

4.2.2 Yellow fever virus assay **101**

4.2.3 Measles assay **101**

4.2.4 Confocal microscopy **101**

4.2.5 Phase contrast microscopy **102**

4.2.6 Measles IC_{50} assay **102**

4.2.7 HSV-1, HSV-2, Adenovirus and Influenza IC_{50} Assays **103**

4.2.8 HIV-1 assay **103**

4.3 Results **104**

4.3.1 Activity of Cf2642 in HSV-1, HSV-2, Adenovirus and Influenza A 104

4.3.2 Cf2642 activity against YFV 106

4.3.3 Cf2642 activity against MCV using a transcription reporter assay 108

4.3.4 Cf2642 activity against HIV-1 110

4.3.5 Measles ddBCNA assay 112

4.3.6 Fluorescence confocal microscopy with mIC323 and v300 114

4.3.7 Microscopy of Cf2642 activity against measles in B95a cells 116

4.3.8 Microscopy of Cf2642 activity against mEdATCC in Vero cells 117

4.3.9 IC_{50} concentrations of ddBCNAs against mWT Fb 120

4.4 Discussion 123

Chapter five – Toxicity of ddBCNAs 127

5.1 Introduction 127

5.2 Materials and methods 128

5.2.1 Cell titer-glo kit 128

5.2.1.1 Cf2642 effect on viability using Cell titer-glo kit 129

5.2.1.2 CC_{50} calculations of the ether series of L-ddBCNAs 129

5.2.2 Caspase-glo 3/7 assay 130

5.2.3 Cell medium replacement assay 131

5.3 Results 132

5.3.1 Cell titer-glo assays and Cf2642 132

5.3.2 CC_{50} concentrations of the ether series of L-ddBCNAs 136

5.3.3 Caspase-glo 3/7 assay **138**

5.3.4 Caspase-glo 3/7 assay in EBV positive and negative cell lines **140**

5.3.5 Cell medium replacement assay **143**

5.4 Discussion **146**

Chapter six – Mechanism of action **152**

6.1 Introduction **152**

6.2 Materials and methods **154**

6.2.1 Flourescent vYFP-A3L confocal microscopy **154**

6.2.2 Acid wash **155**

6.2.3 3D reconstruction confocal microscopy **155**

6.2.4 Virus particle and cell counting **155**

6.2.5 Fluorescence microscopy of actin cytoskeleton plus other markers **156**

6.2.6 Time course – pH change of cell medium **157**

6.2.7 Cd63 staining **157**

6.2.8 IL-6 ELISA **158**

6.2.9 *In vitro* cell-free poxvirus transcription assay **158**

6.3 Results **158**

6.3.1 Cf2642 effect on vYFP-A3L entry into host cells **158**

6.3.2 Cf2642 effect on actin tail formation **164**

6.3.3 Change in pH of cell medium **166**

6.3.4 Cd63 confocal assay **170**

6.3.5 Other staining experiments **174**

6.3.6 Human IL-6 ELISA **176**

6.3.7 Cf2642 effect on transcription **178**

6.4 Discussion **180**

Chapter seven – General discussion **183**

7.1 Combining the findings of the project **183**

7.2 Future work with the ddBCNAs **195**

7.3 Addressing the aims of the project **197**

7.4 Merit of the project results **197**

References **199**

Supplementary material **218**

List of Publications and presentations **223**

List of Figures

Figure 1.1 – Structure of ddBCNAs 1

Figure 1.2 – Structure of deoxynucleoside analogues active against VZV 2

Figure 1.3 – Structure of VACV (IMV and EEV) 8

Figure 1.4 – Summary of VACV entry methods 10

Figure 1.5 – Summary of VACV lifecycle 16

Figure 1.6 – Mechanism of VACV spread 19

Figure 1.7 – Structure of measles virus 27

Figure 2.1 – Hemocytometer counting grid 45

Figure 2.2 – VACV stock collection optimisation 47

Figure 2.3 – Plaque assay optimisation (shell vial) 51

Figure 2.4 – Plasmid p300 53

Figure 2.5 - Plasmid p240 54

Figure 2.6 – Luciferase assay optimisation (moi) 60

Figure 3.1 – General structure of ddBCNAs 70

Figure 3.2 – Luciferase assay: activity against VACV of D-ddBCNAs 71

Figure 3.3 – Structure of the L-ddBCNAs with alkyl and ether side chains 74

Figure 3.4 – Luciferase assay: SAR against VACV of the alkyl and ether ddBCNAs 75

Figure 3.5 – General structure the further modified L-ddBCNAs 77

Figure 3.6 – Luciferase assay: activity against VACV for the further modified ddBCNAs 78

Figure 3.7 – Luciferase assay: activity of Cf2642 in a range of cell lines 80

Figure 3.8 – Cf2642 time of addition assay 82

Figure 3.9 – ddBCNA effect on VACV plaque size 85

Figure 3.10 – IC_{50} concetrations of selected ddBCNAs 86

Figure 3.11 – Fluorescence microscopy: effect of Cf2642 on VACV plaque development 88

Figure 3.12 – Luciferase readings from the pilot *in vivo* assay 90

Figure 3.13 – Luciferase assay data plus IC_{50} concentrations for the ether ddBCNAs 95

Figure 4.1 – Plasmid p240 100

Figure 4.2 - Plasmid p238 100

Figure 4.3 – Cf2642 activity against yellow fever virus 107

Figure 4.4 – Cf2642 activity against MCV 109

Figure 4.5 – Cf2642 dose response against HIV-1 111

Figure 4.6 – Activity of ddBCNAs against measles virus 113

Figure 4.7 – Confocal images of effect of ddBCNAs against GFP expressing measles and VACV 115

Figure 4.8 - Microscopy of Cf2642 against mWT Fb and mEdATCC in B95a cells 118

Figure 4.9 - Microscopy of Cf2642 against mEdATCC in Vero cells 119

Figure 4.10 – IC_{50} concentrations of ddBCNAs against measles virus 122

Figure 4.11 – IC_{50} against measles and luciferase plus IC_{50} against VACV combined SAR 126

Figure 5.1 – Cell titer-glo kit reaction 128

Figure 5.2 – Caspase-glo 3/7 kit reaction 130

Figure 5.3 – Cf2642 effect on B95a cell viability 134

Figure 5.4 - Cf2642 effect on Vero cell viability 134

Figure 5.5 - Cf2642 effect on RK13 cell viability 135

Figure 5.6 - Cf2642 effect on BSC-1 cell viability 135

Figure 5.7 – Effect of Cf2642 on caspase 3/7 in range of cells 139

Figure 5.8 - Effect of Cf2642 on caspase 3/7 in range of EBV+/- cells 142

Figure 5.9 – Cell medium replacement effect on viability 145

Figure 5.10 – Comparison of CC_{50} and IC_{50} concentrations for ether ddBCNAs 147

Figure 6.1 - Confocal images of effect of Cf2642 on distribution of VACV 160

Figure 6.2 – Confocal 3D reconstruction of acid washed cells 161

Figure 6.3 – Comparison of virus particle/cell counts in Cf2642 treated/untreated cells 163

Figure 6.4 – Fluorescence microscopy of Cf2642 effect on cellular actin 165

Figure 6.5 – Cell medium pH time course – low cell count 167

Figure 6.6 - Cell medium pH time course – high cell count 169

Figure 6.7 – Confocal microscopy: Cf2642 effect of cd63 distribution 171

Figure 6.8 – Fluorescence intensity values across Cf2642 treated/untreated cells 172

Figure 6.9 – Cell selected for the fluorescence intensity readings 173

Figure 6.10 – Confocal microscopy of Cf2642 effect on VACV factories 175

Figure 6.11 – ELISA: ddBCNA effect on human IL-6 levels 177

Figure 6.12 – Cf2642 effect on *in vitro* transcription of MCV and VACV 179

List of tables

Table 2.1 – Primers used for v300 construction 55

Table 3.1 – Conditions used for *in vivo* assay 68

Table 3.2 – Side chains of the ddBCNAs 70

Table 3.3 – Side chains of the ether and alkyl series of L-ddBCNAs 74

Table 3.4 – Side chains and other structural details of the further modified ddBCNAs 77

Table 3.5 – IC_{50} concentrations selected ddBCNAs 86

Table 4.1 – Summary of ddBCNA activity against a range of viruses 105

Table 4.2 – IC_{50} concentrations of ddBCNAs against measles virus 121

Table 5.1 – CC_{50} concentrations of ether ddBCNAs 137

Chapter one - Introduction

1.1 Di-deoxybicyclic nucleoside analogues

Di-deoxybicyclic nucleoside analogues (ddBCNAs) are novel nucleoside analogues that have a bicyclic pyrimidine base with a hydrocarbon side chain at the C5 position and lack hydroxyl groups on both the 2' and 3' sites of the sugar moiety (2',3'-dideoxy sugar) (McGuigan et al. 2004; McGuigan et al. 2013). The general structure of these compounds is shown in figure 1.1. These were produced with the aim of developing new antiviral compounds.

All ddBCNAs described herein were produced by the McGuigan group of Cardiff University, School of Pharmacy and Pharmaceutical Sciences. Initial activity of the ddBCNAs was discovered against human cytomegalovirus (hCMV) with the compound Cf1821, a D-enantiomer with an alkyl side chain of ten carbons in length. This compound was further optimised in order to determine the structure with the best activity. In the process of optimisation, it was found that switching from the D- to the L-enantiomer configuration produced compounds with increased activity against vaccinia virus (VACV). In addition, the L-configuration was later found to be active against measles virus.

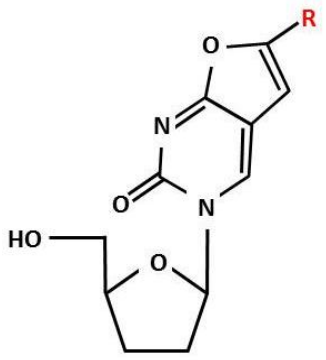

Figure 1.1 General structure of the ddBCNAs. The R group represents the hydrocarbon side chain which is varied to produce different ddBCNAs.

1.1.1 Background of BCNA nucleoside analogues as antiviral compounds

In 1999 McGuigan et al. published data describing a new series of compounds that displayed highly selective antiviral activity against Varicella Zoster Virus (VZV). These compounds (bicyclic furano pyrimidine 2'-deoxynucleosides) were deoxynucleoside analogues with a bicyclic base region, (structures shown in figure 1.2) and displayed fluorescent properties. They are unique in that other reported nucleoside analogues displaying activity against VZV also show activity against Herpes simplex virus (HSV), whereas these compounds do not. Human cytomegalovirus (hCMV) and VACV were also tested but were not affected.

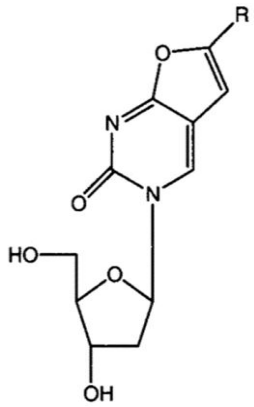

Figure 1.2 The structure of the deoxybicyclic nucleoside analogues active against VZV. The series produced, included alkyl side chains (R) ranging from C5 to C12.

They were discovered as by products of the Pd-catalysed coupling of terminal alkynes with 5-iodo-nucleosides, the reaction used for the production of 5-alkynyl-2'-deoxyuridines. A structure activity relationship (SAR) profile, based on the length of the alkyl side chain of these novel deoxynucleoside analogue compounds was produced, with the optimum activity being observed when the side chain was 8-10 carbons long. These compounds were found to have 300 fold greater activity against VZV than the control drug acyclovir and displayed no signs of cytotoxicity *in vitro* (McGuigan et al. 1999). These compounds were not active against thymidine kinase-deficient strains of VZV, suggesting that they are activated by VZV kinases to their 5'-phosphate forms.

In attempts at optimisation of these structures, the addition of halogen atoms (F, Cl, Br, I) at the end of the alkyl chain was tested though no significant differences in

antiviral activity was observed. No cytotoxity was observed for these compounds either. Furthermore, (prior to the cyclisation step) intermediate compounds in the synthesis of the deoxy bicyclic nucleoside analogues were also tested for activity. These compounds do not have the bicyclic structure and have an alkynyl group at the start of the side chain. These intermediate compounds displayed reduced antiviral activity and showed signs of cytotoxicity against the cells tested (Brancale et al. 2000).

Further analysis of the structure found that their activity could be significantly improved by the introduction of a phenyl ring group into the side chain of the compounds (McGuigan et al. 2001). The addition of an ether group in the alkyl side chain of these compounds significantly reduced the lipophilicity, however the antiviral activity was also reduced by around 1000 fold. These studies highlighted the requirement of the hydrophobic side chain in these compounds for optimum activity. Due to the high activity and low toxicity of the compounds with alkyl side chains, the selectivity index (toxic concentration divided by the active concentration) is very high at >5000. This rises to one million for the compounds containing a phenyl ring in the side chain. As such they represent anti-VZV drug candidates of great potential (McGuigan et al. 2001). Modifications elsewhere in the molecule were also attempted. It was found that sulphur, but not nitrogen, may be substituted into the furano ring in place of oxygen to maintain antiviral effect. However elsewhere in the molecule little variation in structure was permitted without loss of activity. Aryl substitutions at the C5 position of the furano ring abolished the activity and sugar variation (arabino- and ribo- analogues) also significantly reduced the antiviral activity.

Following on from these studies, further investigations revealed that 2',3'-dideoxy sugar analogues of these compounds became selective and potent inhibitors of hCMV but lost their activity against VZV. This confirmed that the 3' hydroxyl group is required for activity against VZV. The intermediate length side chains on the dideoxy compounds displayed a similar range of activity to the current anti-hCMV drug gancyclovir. The compounds were also tested against human

immunodeficiency virus type 1 and type 2 (HIV-1 and HIV-2), HSV-1 and HSV-2 but were found to be inactive against these viruses (McGuigan et al. 2004).

Interestingly these new compounds did not act as nucleoside analogues in their inhibition of hCMV. Time of addition (ToA) assays suggested that they may inhibit a stage of the hCMV replication cycle before DNA synthesis. The SAR profiles of the compounds also indicated little difference in activity between side chains of 8 and side chains of 12 carbons in length. In contrast, the SAR of the deoxy- compounds against VZV indicated that a change in side chain length of just 2 carbons altered the activity by 100 fold. This suggests that the new compounds are not required to interact with the precise kinases or DNA polymerases of hCMV (McGuigan et al. 2004). It was the further study of these dideoxy nucleoside analogues against hCMV that led to the production of the ddBCNAs described in this project.

1.1.2 D- versus L-chirality

Chirality is the term used to describe molecules that have the same chemical formula but are arranged in such a way that they form mirror images of each other. The chirality of molecules may be described in different ways; here the D- and L-configuration is used. The D- or L- configuration is based on the molecule glyceraldehyde. Therefore, stating that the molecule of interest has D- or L- chirality is effectively stating that it is similar to the D- or L- form of glyceraldehyde respectively (Voet and Voet, 2004).To determine whether a particular molecule such as and amino acid should be described as D- or L- configuration the 'CORN' rule is applied. This rule states that, with the hydrogen (H) atom pointing away from the viewer, if the groups **CO**OH, **R** and **N**H_2 are arranged clockwise then the compound is the D- configuration and if they are arranged anti-clockwise then it is the L-configuration (Berg et al. 2006; Voet and Voet, 2004). Naturally, amino acids usually exist in the L- configuration while the ribose of DNA and RNA is usually in the D-configuration (Breslow and Cheng, 2009).

Initial antiviral activity against hCMV was described using ddBCNAs with D-chirality. The initial hit for these D-compounds against hCMV with a 50% inhibitory concentration (IC_{50}) of 2.6 μM was named Cf1821 which has an alkyl side chain

length of 10 carbons. During structure optimisation, an ether group was introduced into the side chain. This led to the production of Cf2095, a D-enantiomer ddBCNA with the side chain C9-O-C5, which displayed improved activity against hCMV (IC_{50} 0.5 μM) as compared to the initial lead Cf1821. This compound was also found to have some activity against VACV. An L-enantiomer equivalent of Cf2095 was produced and named Cf2642. This no longer showed activity against hCMV but showed much improved activity against VACV.

Following on from this discovery, this project was initiated which included testing further modifications of both D- and L-ddBCNAs in order to optimise their structures for activity against VACV and to look into determining the mechanism of action (MoA) of these novel compounds. Further activity against measles virus led to a patent application (McGiugan et al. 2013).

1.2 Poxvirus family

There are two subfamilies of poxviruses within the poxvirus family: the Entomopoxvirinae, which contains three genera and infect only insects, and the Chordopoxvirinae, which contains ten genera and infects a wide range of mammals and birds (Haller et al. 2014). There are two poxviruses that will infect only humans; Smallpox (variola virus) and Molluscum Contagiosum virus (MCV). However, many animal poxviruses may also cause disease in humans (Melquiot and Bugert, 2004; Moss, 1991).

Poxviruses are large viruses, with a brick shaped/ovoid morphology. Their structure is known as complex since they are neither helical nor icosahedral, but have a unique dumbbell shaped core. The genome of poxviruses consists of linear double stranded (ds) DNA ranging between 130-360 kbp (Hughes et al. 2010). Replication occurs completely in the cytoplasm of the host cell and, as such, they were thought to be less dependent on host functions and able to replicate in cells that do not contain a nucleus (Schramm and Krijnse Locker, 2005). However other studies have found that host nuclear proteins recruited by the virus play important roles in poxvirus replication (Sivan et al. 2013). This indicates that although the nucleus is

not the site of replication of poxviruses it is required by the virus for efficient replication.

1.2.1 Vaccinia virus and its use as a vaccine

Vaccinia virus (VACV) from the genus Orthopoxvirus is of particular interest as it was the first animal virus to be visualised microscopically, to be accurately titered and to be purified and analysed. The virus was successfully used as the smallpox vaccine, which lead to variola virus being the first virus to be eradicated through the organisation of a global vaccination campaign (Behbehani, 1983). There is evidence to suggest that the vaccine can induce long term protection against smallpox infection (Hammarlund et al. 2003).

Despite the success of this vaccine, it can be associated with severe complications (Lane and Miller, 1971), especially in individuals with skin problems such as eczema (Engler et al. 2002) and for individuals with defective innate immunity. Complications were due to the high levels of VACV replication and spread from the initial site of inoculation (Bray, 2003). In such instances, antiviral therapies would be beneficial.

First attempts at immunisation against smallpox involved the process of variolation where a healthy individual was inoculated using variola virus obtained from the lesions of an infected individual (Arita, 1979). This method was replaced by the safer method of using cowpox virus after it was demonstrated by Edward Jenner to also provide protection from smallpox. Cowpox was later replaced with VACV. The first VACV vaccines used included Dryvax, Lister and Copenhagen strains produced in the skin of live animals. Dryvax (Wyeth laboratories, Marietta, PA) for example was produced in calf skin infected with the NYCBH strain of VACV (Rosenthal et al. 2001).

Since the eradication of smallpox, other versions of VACV vaccine have been produced in an attempt to reduce complications associated with this virus. A new version produced in Vero cells (tissue culture adapted) from a plaque purified clone of Dryvax has been produced called ACAM2000 (Artenstein et al. 2005). Although it

appears that the rates of unintentional transfer are similar between the two types of vaccine (Tack et al. 2013).

Other vaccine strains include Paris strain (France), Copenhagen strain (Denmark), Bern strain (Switzerland), Ankara strain (Turkey), Temple of Haven and Vaccinia Tian Tian strains (China) and the Dairen strain (Japan). Each of these stains varying in the levels of adverse effects. Further attempts to produce vaccines with reduced adverse effects have involved attenuating the virus by passaging in alternative hosts (e.g. Modified Vaccinia Ankara; MVA, which was passaged in chick embryo fibroblast cells over 570 times) and through genetic engineering (e.g. NYVAC, which has deletion of 18 open reading frames) (Jacobs et al. 2009).

1.2.1.1 Vaccinia structure

The VACV genome is about 190 000 base pairs (bp) in length, and consists of ds linear DNA with covalently closed ends, which is packaged into the core. VACV has four different forms of infectious virion. These include the intracellular mature virus (IMV), the intracellular enveloped virus (IEV), the cell-associated enveloped virus (CEV) and the extracellular enveloped virus (EEV). The most common of these is the IMV which remains inside the host cell until cell lysis, at which point it is then able to infect other cells. The IEV is the intermediate virus between the IMV and the CEV/EEV and is produced when the IMV is wrapped with intracellular membranes. The IEV is then transported to the cell membrane on microtubules. The CEV can induce actin tails at the surface of the cell that propel it away from the infected cell and allow it to spread to nearby cells. The EEV allows the virus to spread to cells even further away from the host cell (while the initial replication process is ongoing in the original cell). CEV and EEV are physically the same and differ only in their location in relation to the host cell. The CEV and EEV contain one less membrane than the IEV since one is fused with the plasma membrane when the virus particle is released (Smith et al. 2002). The general structures of the IMV and the EEV are shown in figure 1.3.

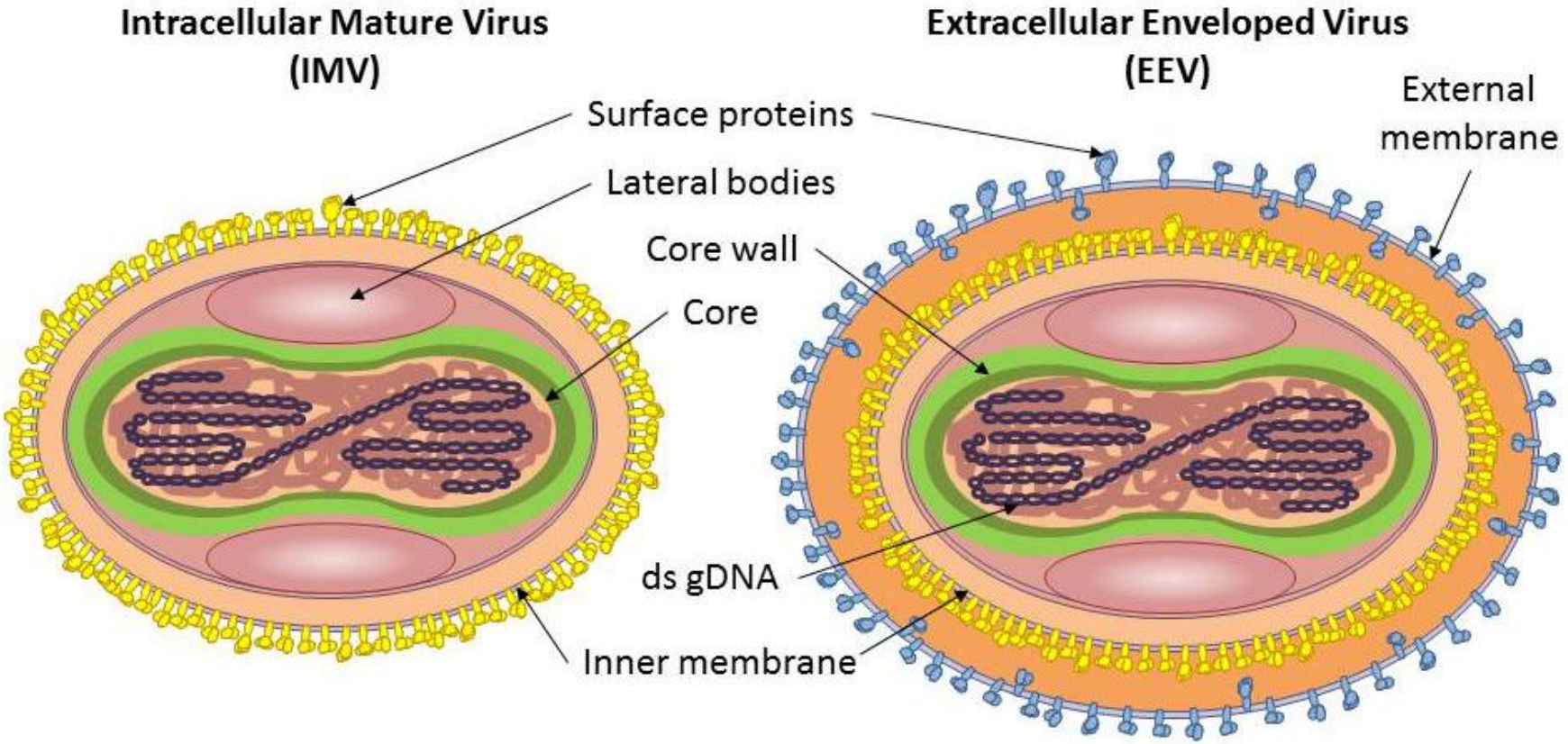

Figure 1.3 Structures of VACV IMV and EEV. The EEV form of the virus possesses an extra external membrane envelope. The core of the virus packages the ds genomic DNA (ds gDNA). The complete virus structure contains lateral bodies, the function of which is not entirely clear (Schmidt et al. 2013). (Adapted from viralzone.expasy.org)

The proteins and properties that make up the different forms of VACV vary, meaning that using a virus vaccine of only IMV particles does not lead to full protection against orthopoxvirus infection. Both EEV and IMV forms of the virus need to be present to initiate an adequate immune response (Roberts and Smith, 2008). In addition inactivated forms of vaccinia vaccine do not induce sufficient immune response. Individuals initially treated with the inactivated virus vaccine, that are later treated with the live vaccine, showed similar response levels to those given just the live vaccine (Kaplan et al. 1965).

The IMV is more robust than the other forms of VACV and is more effective at spreading the virus between hosts. However, it is less suitable for spreading the virus within the host when compared with the CEV and EEV forms (Townsley et al. 2005). This is due to the fact that it remains inside the cell until cell lysis, delaying its opportunity to infect other cells. The other obstacle for the IMV is that it is more readily recognised by antibodies as it contains most of the viral membrane proteins. The CEV and EEV forms, on the other hand, have membranes that have been derived from the host and as such also contain some of the host's membrane proteins. This protects the virus, to some extent, from antibody binding and provides the virus with increased opportunities for receptor binding with host cells (Smith et al. 2002).

1.2.1.2 VACV entry

Attempts to determine the exact mechanism of VACV entry into cells have been complicated by the fact that VACV exists in different infectious forms with different numbers of membranes (Moss, 2006). Each of the different forms contains the same DNA and protein core. The different forms of VACV enter the cells by different mechanisms (Vanderplasschen et al. 1998). In many cases of viral entry, just one or two fusion proteins are enough to control entry. For example measles virus requires only two proteins for viral attachment and fusion (measles F and H proteins, discussed later in the introduction, section 1.3.3). In the case of VACV this is more complicated as there are four proteins that have been found responsible for attachment to the cell and a further 12 in a complex that are involved with cell

entry and are conserved between poxvirus species (Moss, 2012). There are two different routes of entry that the IMV form may use depending on the extracellular pH or the pH of cellular endosomes. These include direct fusion with the cell membrane or uptake through endocytosis (figure 1.4).

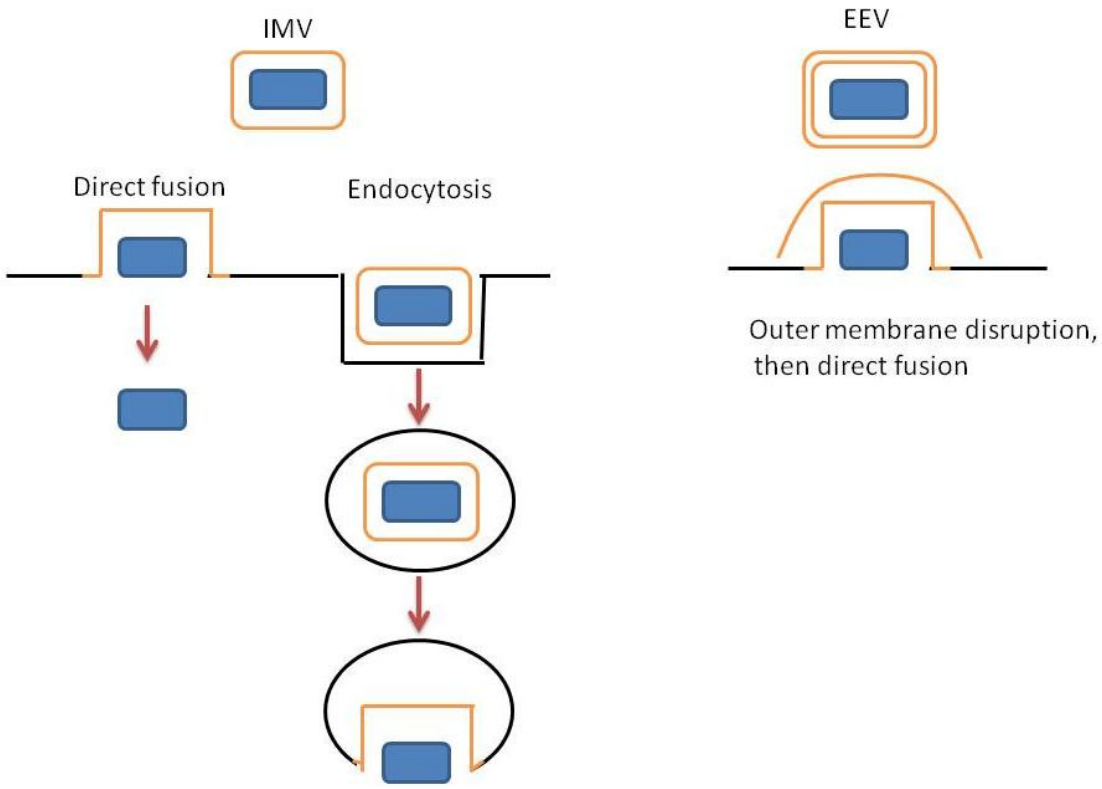

Figure 1.4 A summary of the methods of entry of the IMV and EEV forms of VACV. The IMV may enter the cell either through direct fusion with the membrane or by a form of endocytosis, the endocytosed virus particle must then fuse with the membrane of the vesicle to release the core into the cytoplasm. The EEV particles must shed their outer membrane before fusion with the plasma membrane may occur. Adapted from Roberts and Smith (2008).

The fact that VACV have so many proteins linked to entry, combined with the fact that the sequences that encode them do not resemble those observed in other viruses, suggests that VACV enter cells by a unique method. In some instances, the use of inhibitors of cellular processes was found to have an effect on the ability of the virus to enter the host. These were mainly processes involved with actin remodelling/polymerisation (e.g. blebbistatin) or the tyrosine kinases that mediate

actin cytoskeletal changes (e.g. genistein). The overall result in these cases was that the virus could still attach to the cell membrane but the core could not enter the cell, i.e. fusion was inhibited (Laliberte et al. 2011).

The most common form of VACV is the IMV. This form has just a single phospholipid bilayer that contains non-glycosylated viral proteins. For the majority of enveloped viruses, fusion occurs when the envelope of the virus fuses with the host cell plasma membrane. There is evidence to suggest that the IMV form of VACV also enter cells in this way (Roberts and Smith, 2008). However, evidence suggests that the IMV may also enter the cell by an internalisation (endocytic) method such as macropinocytosis (Mercer and Helenius, 2009) after the induction of blebbing at the cell surface through the presence of phosphatidyserine exposed on the viral membrane (Mercer and Helenius, 2008). The virus induces activation of p21 activated kinase 1 (PAK1). The requirement for exposed phosphatidylserine on the virus membrane suggests that the virus uses apoptotic mimicry to enter the host cell. Cells treated with Blebbistatin (an inhibitor of myosin II preventing blebbing) and exposed to VACV showed significantly reduced rates of infection. This suggests that the blebbing caused by VACV, on contact with the host, is important for efficient virus entry (Mercer and Helenius 2008). This method of entry was observed with the Western Reserve (vWR) strain of VACV IMV, however other methods of macropinocytosis have been observed with different strains of VACV. The International Health Department-J strain of VACV (IHD-J) was found to induce and lengthen filopodia. The differences observed were found to be partly due to differences in the levels of cellular Rho GTPases (induced by the virus) between the different strains (Mercer et al. 2010).

The method of entry utilised by VACV likely depends on a series of factors including the pH, the strain of the virus, and the type of host cell it is entering. It has been found that the IMV contains a set of viral fusion proteins that are conserved across poxvirus species, including A21, A28, H2, and L5 (Townsley et al. 2005). They are associated with each other, and other proteins on the membrane of the IMV. It has been demonstrated that knocking out any one of these proteins results in an IMV

that is unable to enter the cell (and is no longer infectious). This work highlighted the importance of these proteins in the entry process (Senkevich et al. 2005).

VACV entry to the cell is pH dependant. VACV may enter cells through a low pH mediated endosomal pathway. This method of entry is inhibited by drugs that prevent acidification of endosomes for example balfilomycin (Townsley et al. 2006). Two VACV proteins A25 and A26 have been described as fusion suppressors as they prevent the direct fusion of the IMV with the membrane at a neutral pH. Entry through low pH dependent endocytosis is not inhibited by these proteins. It is likely that these proteins act as fusion modulators to prevent random fusion of the IMV with cell membranes until required for a new infection (Chang at al. 2010) and to allow the release of newly produced virions from the surface of the host cell.

The EEV form of the virus requires an additional stage for viral entry. Here, disruption of the fragile outer membrane of the virus occurs before the internal IMV is able to fuse with the host membrane (figure 1.4). This disruption of the outer membrane occurs after interaction with glycosaminoglycans (GAGs) on the membrane of the host cell. Viral proteins B5 and A34 are required for this process (Roberts et al. 2009). Were the EEV to fuse directly with the membrane without this stage, the internalised IMV would have to undergo shedding of its intact membrane in order to be able to release its viral core in the cytoplasm. Other evidence highlighting the importance of this extra stage is that viral proteins involved with fusion and entry, are in the membrane of the IMV (Moss, 2012). These need to be exposed, by disruption of the outer membrane of the EEV before entry can take place.

No specific cellular receptors have been determined for the entry of VACV. However, evidence suggests that depletion of cholesterol inhibits VACV entry, suggesting that glycosphingolipid-cholesterol enriched microdomains (lipid rafts) are required for VACV entry (Moss, 2006). When the raft disrupting drug methyl-β-cyclodextrin was used to treat BSC40 cells that were subsequently infected with VACV, it was found that the infectivity of the virus decreased with increasing concentrations of the drug. This indicates that the cholesterol enriched lipid rafts

are needed for entry of the virus into the cell. However they are not necessary for binding of the virus to the host cell membrane. Virus proteins interact with lipid rafts during penetration (Chung et al. 2005). Several cellular lipid raft associated proteins are required for the entry of IMV particles. These include vaccinia virus penetration factor (VPEF) which is detected on lipid rafts and on vesicular structures in the cytoplasm (Huang et al. 2008), CD98 which is required for entry but not attachment (Schroeder et al. 2012) and Intergin β1 which activates PI3K/Akt signalling and mediates endocytosis (Izmailyan et al. 2012).

1.2.1.3 VACV life cycle

After the viral core has entered the cell by one of the methods explained above, the core is transported further into the cell cytoplasm along microtubules. It enters what is known as a virus factory within the cytoplasm. The virus factories are made using specific host cell components (Wileman, 2006) recruited by the virus, plus proteins synthesised by the virus forming a structured specific viral organelle (Condit, 2007). The core of the virus consists of structural proteins and tightly packaged DNA. It also contains transcription enzymes that are required to initiate DNA replication. Within minutes of cell entry, early transcription occurs and viral mRNA is released through pores in the surface of the core (Broyles, 2003). The genes that are expressed during early transcription are those involved with DNA replication, evasion of the host immune response and modification of host components that the virus takes advantage of. After the completion of early transcription, there is a stage of intermediate transcription involving genes that encode regulatory proteins and initiators of late transcription. The structural proteins that make up the core of the newly formed virus, and the enzymes that are required for initiating transcription in the next cell, are transcribed late in the replication process (Moss, 1991).

Early VACV transcription can be induced *in vitro* in the absence of cells using a specific buffer (Bugert et al. 1998; Shand et al. 1976). This indicates that VACV particles contain all their necessary components for early mRNA production (Broyles, 2003) including DNA-dependent RNA polymerase and may initiate early

transcription immediately after entry into the host cell. In the cell however it has been shown that the early mRNAs accumulate in granular structures some distance from the viral cores. These mRNA granules recruit host cell translation components, indicating that these granular mRNA sites are where protein synthesis occurs (Mallardo et al. 2001). Further to this, it has been demonstrated that the site of DNA replication is in a separate location within the cell, specifically at the cytosolic side of endoplasmic reticulum (ER) membranes. As the infection progresses further, ER cisternae are recruited to the site, enclosing it with membranes (Mallardo et al. 2002).

It has been suggested that although the virus particles contain the necessary components for early transcription and may undergo induced transcription *in vitro* under specific conditions, they require cellular factors for their intermediate transcription. The virus intermediate transcription factor 2 (VITF-2) protein, involved with the intermediate transcription observed *in vitro* may be isolated from uninfected HeLa cells, but not from cells that are nonpermissive to VACV. It has been shown that RK13 cells which are conditionally permissive do not contain the VITF-2 protein, however wild type strains are able to replicate in these cells. Mutant strains that lack the K1L gene cannot replicate in RK13 cells but may replicate in cell lines that contain VITF-2. This line of work suggests that VITF-2 is a cellular protein required by the virus for intermediate transcription and that the K1L gene is possibly linked to the upregulation of VITF-2 (Rosales et al. 1994).

VACV has several host range genes that are involved with its ability to grow in certain cells lines. For example, the E3L, K1L, C7L and B5R genes are essential for growth in HeLa, RK13, MRC-5 and vero cells respectively. Often host range genes are involved with the evasion of the host immune responses to the virus (Chung et al. 1997).

The first structures observed during the VACV replication process are oval shaped and package DNA within. These structures are known as immature virions (IV). The IV is transformed into the classic brick shaped IMV by proteolytic cleavage of core proteins. It is currently unclear exactly how the IMV obtains its single lipid bilayer.

Though evidence suggests that during the assembly of viral particles, the IMV obtains its membrane through an open membrane intermediate that derives its structure through scaffold proteins on the convex side (Suárez et al. 2013). The assembly of the IMV particles is a complex process involving folding of cisternal and tubular domains (Griffiths et al. 2001).

At the IMV stage, replication ends for the majority of VACV particles and they are released from the cell upon cell lysis. For some of the particles, the next stage in replication is transportation from the virus factory along microtubules to the golgi/early ensosomes of the cell. Here they are wrapped in host cell derived membranes (Tooze et al. 1993) to form intracellular enveloped virions (IEV). These IEV are further transported along microtubules to the cell membrane. The outer membrane fuses with the plasma membrane of the cell, releasing the EEV form of the virus. The virions that remain in contact with the cell upon release are known as CEV and can induce the cell to produce actin tails that propel the virus particle away from the surface of the cell (Blasco and Moss, 1992). A summary of the lifecycle of VACV is shown in figure 1.5.

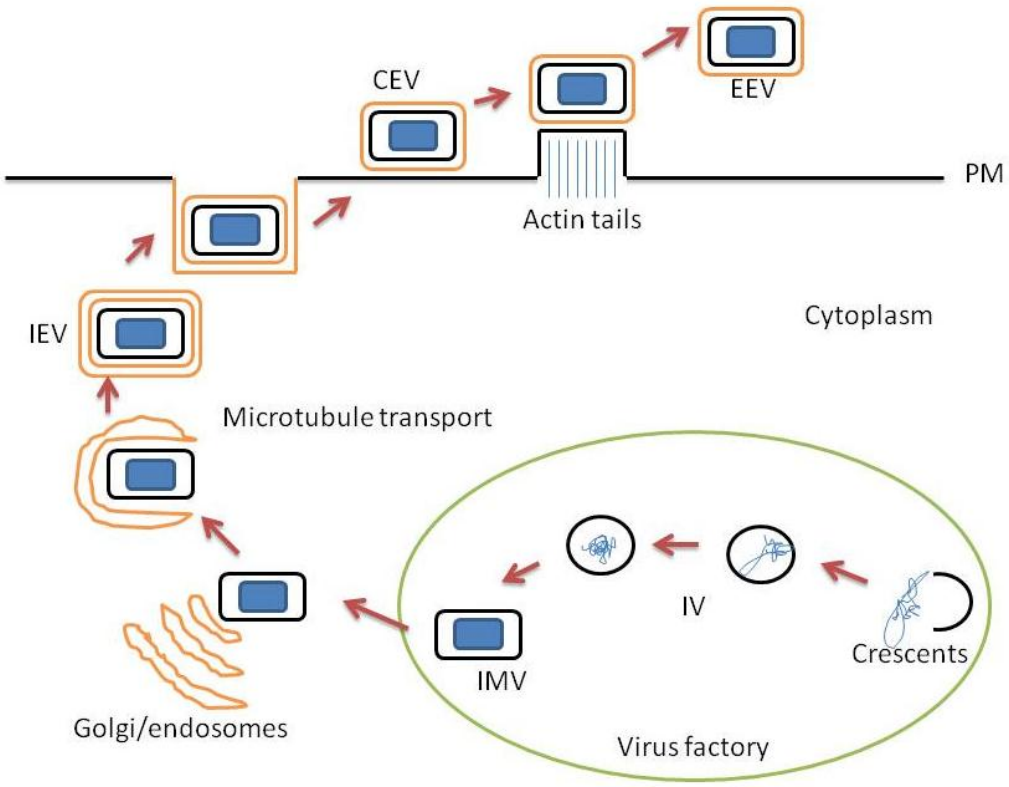

Figure 1.5 VACV lifecycle. After entry and early transcription, the construction of new VACV particles occurs within virus factories. Here the IMV form of VACV is produced. In most cases this is where the lifecycle ends and the IMV particles are released upon cell lysis. Some IMV particles however get transported along microtubules to the golgi/endosomes where they are wrapped in membranes to form the IEV. The IEV is transported to the plasma membrane and released by fusion of the outer membrane of the IEV with the plasma membrane. The released particles are the CEV/EEV forms of VACV. Figure adapted from Smith et al. (2002).

It was discovered that the IEV form of VACV use microtubule based transport, using a recombinant VACV with GFP fused to the membrane protein F13L. Live fluorescence microscopy of this virus detected movement of the particles at a rate consistent with microtubule based transport (~3 µm/s). In further support of this, the movement of the particles can be inhibited using the microtubule depolymerising drug nocodazole (Geada et al. 2001).

It was once thought that the viral gene A27L was responsible for the microtubule transport of IMV particles. However it has been demonstrated that mutant strains of VACV with this gene deleted are still capable of bidirectional transport along

microtubules, as the IMV are able to be transported by both kinesin and dynein motors (Ward, 2005). Instead the deletion of A27L leads to VACV that are unable to form enveloped forms of the virus. The interaction between the IMV and the motor proteins appears to be weaker than between the IEV and the motor proteins. The IEV contain the protein A36 which interacts with kinesin (Ward and Moss, 2004). It was noted that the intracellular microtubule based transport precedes actin based motility observed at the membrane of the cell only (Rietdorf et al. 2001).

It has been shown that during VACV infection the microtubule organising centre becomes reorganised in a manner similar to that observed with an upregulation of microtubule associated proteins (MAPs). Two VACV proteins were also found to have properties similar to MAPs and could mediate direct binding of viral cores to microtubules *in vitro* (Ploubidou et al. 2000).

The protein kinesin-1, but not kinesin-2, was found to have roles at several stages of VACV replication; including transport of the viral core to the site of DNA replication and assembly, then for transporting the newly formed virions to the golgi for wrapping and then transporting the IEV to the membrane for egress (Schepis et al. 2007). During the replication of VACV, newly formed IEV are transported from the cytoplasm of the cell to the plasma membrane on microtubules in a kinesin-1 dependant manner. When they reach the membrane, the fusion with the membrane is actin dependant (Arakawa et al. 2007).

Autophagy is a part of the host cell innate immune response against viral infections, however many viruses have developed mechanisms by which they can exploit this system to aid their replication/spread (Kudchodkar and Levine, 2009). VACV however appear not to take advantage of autophagy as part of the replication cycle as they have been shown to be able to replicate in cells that are deficient for autophagy (Zhang et al. 2006). In fact VACV have been found to inhibit cellular autophagy, through the conjugation of ATG12 (modifier protein of autophagy) to ATG3 (substrate of ATG12) which in turn leads to the lipidation of LC3 (microtubule associated light chain-3 protein) (Moloughney et al. 2011). Therefore the virus is able to evade this host defence mechanism.

1.2.1.4 VACV spread

In cell monolayers VACV demonstrate cytopatic effect (CPE) known as a plaque. Plaques are holes in the monolayer of cells where the cells have been infected by the virus and lysed. Each plaque is formed by one initial virus which replicates and spreads to form a visible plaque after 3 days (Dulbecco, 1952). The rapid rate at which a VACV plaque edge spreads suggests that it is not solely reliant on the rate of the virus' replication cycle alone, i.e. the spread suggests that the virus spreads from one cell to the next every 75 minutes while the life cycle VACV is known to be 8 hours. As such, the virus must have an alternative method of spreading from one cell to the next that occurs before the full replication cycle of the virus in one cell is complete. When cells become infected with VACV the virus expresses surface proteins A33 and A36, which mark the cell as infected. When another VACV comes into contact with a cell already expressing these proteins, actin tail formation is induced. VACV then binds to these tails and is propelled away from the infected cells and towards uninfected cells (figure 1.6). Proteins A33 and A36 are vital for the correct functioning of this mechanism (Doceul et. al 2010).

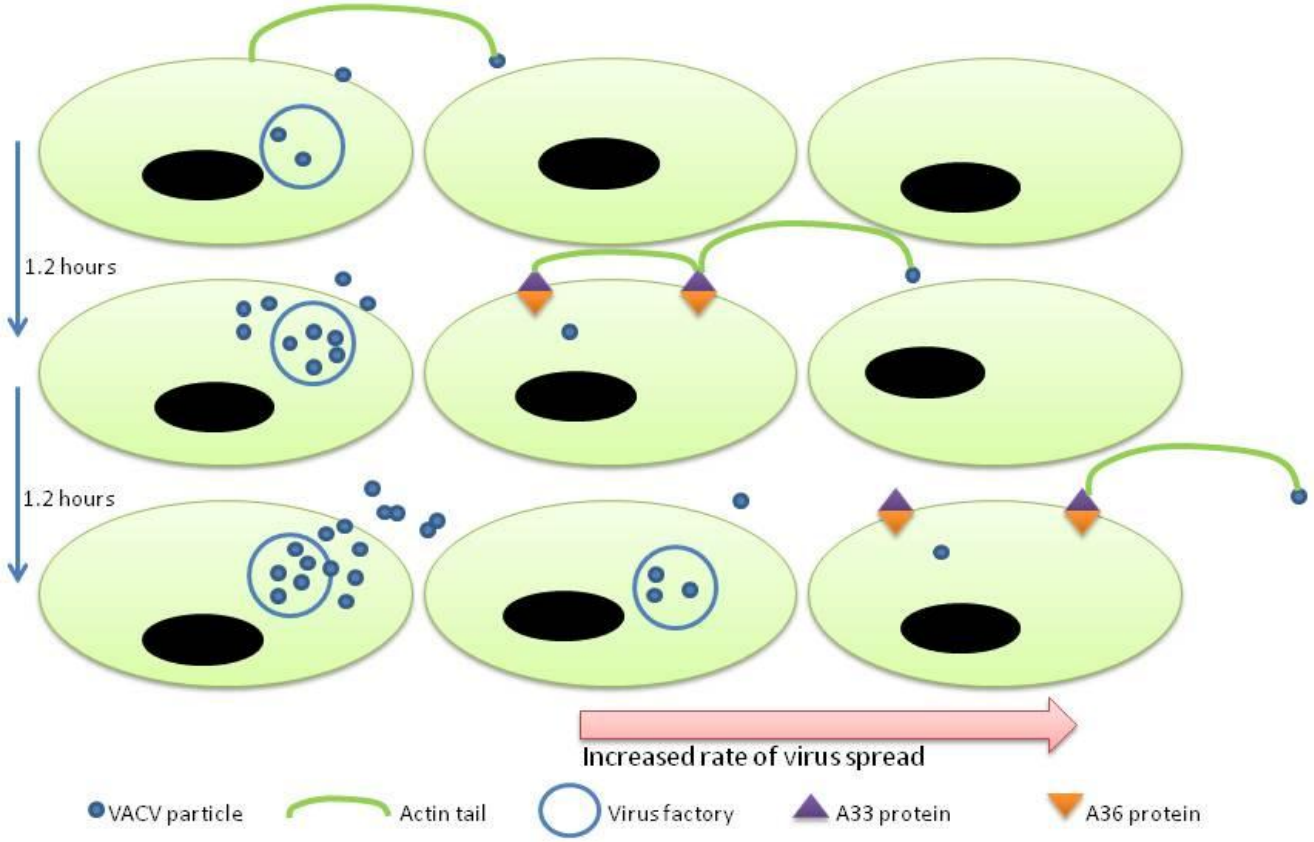

Figure 1.6 VACV spread by the activation of actin tails by A33 and A36 protein expression at the surface of infected cells. Incoming VACV particles are propelled away from infected cells by the actin tails towards other (uninfected) cells (figure adapted from Doceul et al. 2010).

It has been demonstrated that actin polymerisation is greatly enhanced when CEV VACV recruits clathrin and a transcription factor, activating protein 2 (AP-2). Clathrin induces the clustering of A36 with neural Wiskott-Aldrich syndrome protein (N-WASP; regulator of actin polymerisation), which initiates the polymerisation of actin through the Arp 2/3 complex. The clustering that occurs also has the benefit of stabilising the N-WASP which enhances continued actin tail production (Humphries et al. 2012). This recruitment of clathrin is only transient and as soon as the actin tails are initiated, the clathrin disappears (Schmidt and Mercer, 2012). The clathrin recruitment is involved with the release of VACV from the host cell (Humphries and Way, 2013).

F13L gene is involved in the wrapping of the IMV to form IEV. It has been found that deletion of this gene leads to a form of VACV that is no longer able to produce the EEV form of the virus and is unable to produce plaques in cell culture. This indicates that this gene is essential in the egress and spread of VACV (Blasco and Moss, 1991). Mutant strains of VACV with the deletion of F13L (vRB12) may be used to produce recombinant forms of VACV by inserting a functional F13L gene along with the gene of interest (Blasco and Moss, 1995), this provides a clear selection method for the recombinant virus as it will produce plaques in three days. A deletion of the K4L gene (a homologue of F13L) was found to have no effect on the production of plaques and EEV formation (Blasco and Moss, 1991).

1.2.2 Smallpox

Small pox is a serious and, in many cases, lethal infection caused by the variola virus. There are two forms of the variola virus; a minor form that leads to death in less than 1% of cases and a major form that causes life threatening illness with a mortality rate of 30% (Geddes, 2006). Many of the survivors of the disease can be left with scarring or blindness. The infection is spread through the respiratory system. It is a highly infectious virus that may remain active for long periods (24 hours) in an aerosolised form (Wehrle et al. 1970).

This disease was declared eradicated in 1980 after a widespread vaccination campaign (Geddes 2006). Vaccination against this virus was stopped in 1972.

However recent threats of bioterrorism, specifically the event of a smallpox outbreak, have re-ignited interests in finding suitable treatments (Bray, 2003). Smallpox was declared among the most likely candidates to be used as a bioweapon by a panel of Russian bioweapons experts (Henderson, 1999). In the meantime, the remaining stocks of the vaccine have been preserved and new versions are in production for fast administration should the need arise. This is critical since the majority of today's population would be susceptible to the virus (Geddes, 2006). However it would take time for the vaccine to be administered at levels sufficient for protection and support from antiviral compounds would be essential.

Today, there are only two laboratories in the world (one in the USA and one in Russia) that contain the remaining official stocks of this virus for research purposes. This however does not include any illegal stocks that may still exist elsewhere (McFadden, 2010). There is also technology available that would allow the virus to be regenerated in a laboratory setting as has been described using poliovirus (Cello et al. 2002).

Another drawback of the vaccine is that it may lead to side effects which may be severe, and in some cases lethal. This is often due to over replication of VACV. In such instances, antiviral drugs would be beneficial. Immunocompromised individuals and those with skin conditions such as dermatitis and eczema are particularly vulnerable to complications resulting from smallpox vaccination (Bray 2003).

1.2.3 MCV

Since the eradication of smallpox virus, MCV has become the most common pox virus of clinical significance. MCV is a member of the *Poxviridae* family and it has its own genus; *Molluscipoxvirus* (Esposito, 1991). MCV is a pathogen that produces multiple wart-like protrusions on the skin with a concave centre. These secrete debris that contains infectious particles. The disease is not considered serious and in healthy individuals it can clear up within a year without intervention. However it is very common in children and immune-suppressed individuals where it can persist

for several years with increased numbers of lesions, causing discomfort for the patient (Buckley and Smith, 1999). To date, there are no specific therapeutic treatments for this infection. In some cases the infection may be treated by physical removal of the growths (Van der Wouden et al. 2009).

MCV is a difficult pathogen to study due to the fact that it will not grow in cell culture. It will infect cells in culture and produce early gene transcripts but the infection is terminated at this stage. It is a strictly human disease, so there are no animal models that are able to support the infection. Other methods of studying this virus have been developed including a PCR quantification method and luciferase transcription reporter system (Sherwani et al. 2012).

The length of the genome of MCV is similar to that of VACV, but it has a much higher GC content. The genome of MCV encodes around 182 proteins, 105 of which correspond with proteins found in the orthopoxivirus strains. (Senkevich et al. 1997)

1.2.4 Other poxviruses

Human monkeypox virus is another pathogen that has recently emerged as a threat to human health. Monkeypox virus causes serious illness in humans, similar in nature to the infection caused by small pox. The disease can spread to humans through contact with infected animals or other humans. Incidences of it have increase greatly in the Democratic Republic of Congo since use of the small pox vaccine was stopped (Rimoin et al. 2010).

Cowpox is another poxvirus with the ability to infect humans. Though it is rare, rates of infection have increased since the end of small pox vaccination (Vorou et al. 2008). In most cases this infection is mild and self-limiting, however in the immunocompromised and those with skin conditions such as eczema (especially children) (Pelkonen et al. 2003) the disease can be more serious and in some cases fatal. The range of animal hosts capable of supporting this infection has also increased. Transmission of this virus is through animal contact (Nitsche and Pauli, 2007).

1.2.5 Current antivirals against poxviruses

Even though the most serious of poxviruses (small pox) was eradicated, the study of antiviral treatments against poxviruses is still very relevant today. As described, there is concern that this virus could re-emerge as a weapon in bioterrorist attacks. The vaccine would not be ideal in all cases (section 1.2.1) and would likely take time to be administered; therefore the support of the vaccine with antiviral drugs would be essential.

Furthermore, other poxviruses (such as monkeypox virus and MCV) still cause infections in humans and these would benefit from antiviral treatments. Some of the research into antiviral compounds has been discussed below.

Many antiviral drugs are based on nucleotide or nucleoside structures. These analogues may compete with standard nucleotides for incorporation into the growing nucleotide chain by polymerases (De Clercq and Neyts, 2009). This incorporation leads to termination of the growing nucleotide chain and prevents successful replication of the virus' genetic material. Whilst initially effective the virus may develop resistance, altering the polymerase in a way that prevents the nucleotide/nucleoside analogue from binding.

An example of this type of antiviral compound is cidofovir (approved for the treatment of hCMV in AIDS patients), which is the suggested experimental drug for the treatment of smallpox (in the event of an emergency outbreak). This compound is a nucleotide analogue; (S)-1-(3-hydroxy-2-phosphonylmethoxypropyl) cytosine. Cidofovir was initially discovered as a selective inhibitor of hCMV (Snoeck et al. 1988), but was later found to have antiviral activity against other DNA viruses including poxviruses (Andrei and Snoeck, 2010). It is an inhibitor of viral DNA polymerase and therefore it prevents viral DNA replication. This drug is not ideal for this purpose as it has to be administered intravenously and has the severe side effect of nephrotoxicty (Skiest et al. 1999). Vaccinia strains that are resistant to cidofovir have also been described, although their virulence and growth are reduced in comparison to wild type strains (Becker et al. 2008). Ether lipid analogues of cidofovir have been produced and were found to protect mice from

lethal mousepox infections. They may be administered orally with improved bioavailability (Buller et al. 2004).

An ether-lipid analogue of cidofovir, CMX001, has also been shown to be active against several DNA viruses, including poxviruses. It may be administered orally instead of intravenously and has been shown to cause little in the way of nephrotoxicity. It displays the same protective effect as cidofovir when used against a lethal dose of ectromilia (mousepox virus) in mice. This protective effect was still observed when the mice were treated up to 5 days pi (Parker et al. 2008).

A study by Bray and Roy (2004) indicated that, in the event of an outbreak, cidofovir may be used as a prophylaxis against small pox to complement vaccination. With the addition of an alkoxyalkanol ether side-chain, which allows absorption in the gut, the treatment could be administered orally or aerosolized, alleviating the nephrotoxicity caused by the drug when given intravenously (Bray and Roy. 2004). Furthermore, the idea that antiviral compounds could be used as a prevention method for small pox was tested before its eradication using methiazone. Unfortunately, the drug methisazone was found to have minimal effects (Heiner et. al. 1971). Methisazone was the first antiviral drug used clinically against poxviruses. This compound inhibits a late stage in viral protein synthesis and reports suggested that it helped reduce the severity of the complications associated with vaccination. However, due to a lack of controlled trial data, its precise effects could not be verified (Jaroszyn, 1970). It is toxic if administered systemically and as such clinical use of this compound has since ceased.

Other efforts to produce new drugs active against poxviruses have yielded ST-246 (Yang et al. 2005), a molecule that targets the F13L protein of the virus (Duraffour et al. 2008). This compound has shown antiviral activity greater than that of cidofovir against VACV, cowpox and camelpox viruses in three dimensional cell culture rafts as well as monolayers, where the effect could be seen as reduction in the size of the plaques (Duraffour et al. 2007). It has also been found to be effective at protecting mice from lethal doses of VACV and ectromelia virus *in vivo* (Yang et al. 2005). Of note, ST 246 resistant strains of VACV have been characterised (Yang

et al. 2005). Furthermore, a study has indicated that treatment using ST-246 in combination with CMX001 has increased efficacy against VACV and cowpox virus when compared to either of these drugs alone (Quenelle et. al. 2007), indicating that combination therapies may be useful against poxvirus infections.

Small interfering RNAs (siRNAs) targeting specific VACV genes B1R and G7L have been shown to have antiviral activity against VACV and monkeypox viruses, when used alone or in combination with Cidofovir. These siRNAs also display antiviral activity against Cidofovir resistant strains of VACV (Vigne et al. 2009).

Another example of a drug recently described as being active against VACV and cowpox virus is terameprocol (a methylated derivative of nordihydroguaiaretic acid). This reduces the spread of the virus by inhibiting the formation of actin tails at the surface of infected cells (Pollara et al. 2010). Terameprocol had previously been associated with antiviral and anti-inflammatory effects and was recently shown to be safe in phase I clinical trials as a potential anti cancer therapy. It was generally well tolerated when administered intravenously to 25 patients with tumours (Smolewski, 2008) and when administered as an intravaginal ointment to assess its potential at interrupting transmission of HIV, HPV and HSV (Khanna et al. 2008). The amount of virus produced by individually infected cells is not reduced by terameprocol, however overall virus production is reduced as the virus is unable to spread via actin tails to uninfected cells. It is not clear what the exact target of this compound is that leads to the inhibition of the actin tails (Pollara et al. 2010).

Nigericin, a carboxylic ionophore, displays antiviral activity against VACV, with a 50% inhibitory concentraion (IC_{50}) of 7.9 nM. It inserts easily into biological membranes and facilitates the exchange of K^+ ions for H^+ ions, thereby altering the electrochemical gradient across the membranes. Its antiviral effect was not due to the prevention of viral entry into the host cell. Instead, it has been found to inhibit early and late gene transcription as well as DNA replication, though the precise MoA has not yet been defined. Nigericin has a selectivity index of 1038 although was found to be more toxic than cidofovir and ST 246 in *in vivo* experiments (Myskiw et al. 2010).

During those periods where vaccinations against small pox using VACV were necessary, it was found that therapies were required to counteract the complications caused by the vaccination. Several therapies were tested during this period although the exact effects of the therapies were not entirely clear as the immune response was not taken into account. Vaccinia immune globulin (VIG) was collected from recently vaccinated individuals to be administered to those patients showing complications. (Kempe, 1956) Though improvement could be seen in many cases, administration of the VIG treatment was required several times over several weeks before a full recovery was observed. However, it was unclear whether the improvement was due to the treatment or the patient's own immune response.

Research into the use of other nucleoside analogues as antiviral drugs is ongoing. Interferon and interferon inducers have been shown to have potential in the treatment of vaccinia complications (Bray 2003). Recently a new nucleoside inhibitor of orthopoxviruses was described named KAY-2-41. This compound is a 1'-methyl-substituted 4'-thiothymidine nucleoside and shows activity in the micromolar range with little toxicity. Selected KAY-2-41 resistant strains of VACV, cowpox and camelpox display mutations in the viral thymidine kinase indicating that the MoA of this compound relies on its interaction with this enzyme (Duraffour et al. 2014).

1.3. Paramyxovirus family

The paramyxovirus family include viruses with a negative sense single-stranded RNA genome and a lipid envelope that is derived from the host cell membrane. They are generally spherical in structure with a helical nucleocapsid. Viral glycoproteins are inserted into the lipid envelope and extend out of the surface of the virus. These proteins include the hemagglutinin (H) and fusion (F) proteins, which are required for viral attachment and membrane fusion with the host cell respectively (Yanagi et al. 2006). The structure is shown in figure 1.7.

The replication of the paramyxoviridae family is thought to occur completely in the cytoplasm of the host cell (Kingsbury, 1991).

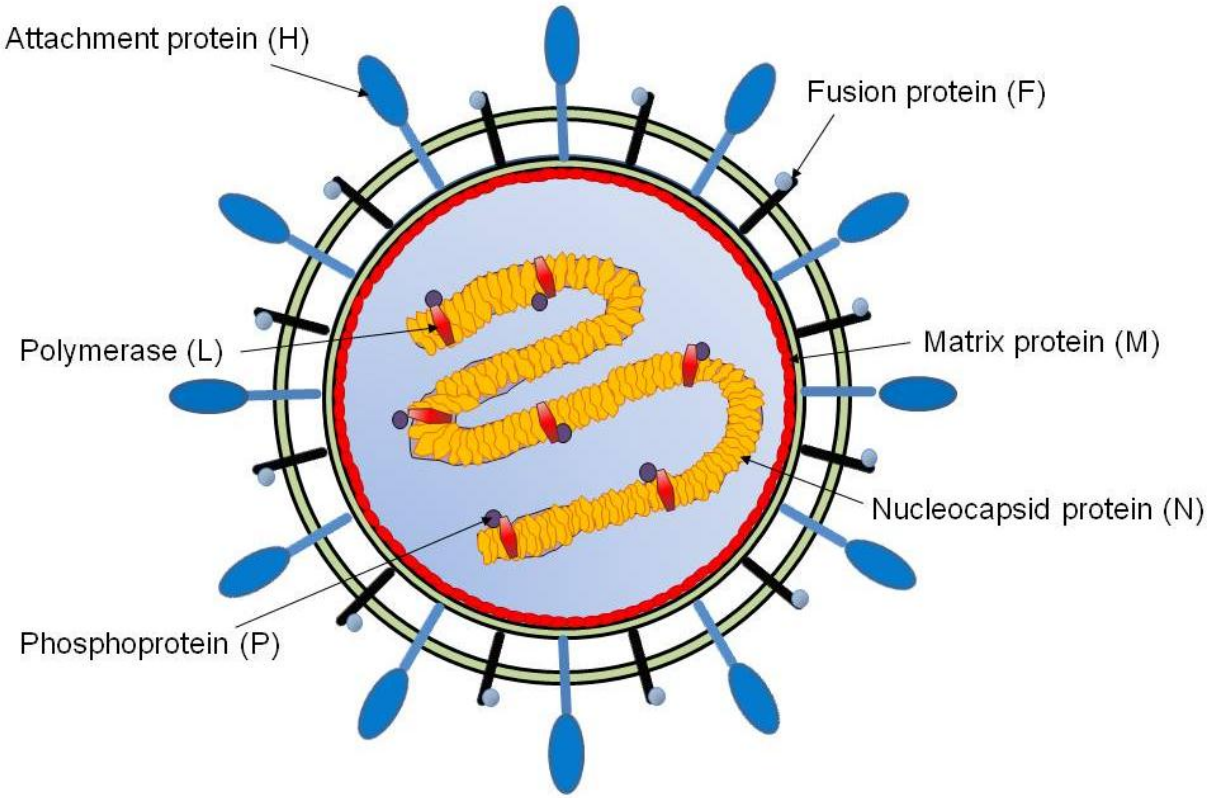

Figure 1.7 The structure of measles virus. The envelope membrane contains the glycoproteins attachment/hemagglutinin (H) and fusion (F). The matrix protein (M) is located in the inner leaf of the membrane. The genome is packaged into a helical structure with the nucleocapsid (N) protein. The polymerase/large (L) and phopho (P) proteins are also located on the genome. (Figure adapted from Griffin, 2007).

1.3.1 Measles virus

The Measles virus is a member of the Paramyxovirus family, morbillivirus genus and spreads via the respiratory system. Measles virus is one of the most infectious viruses - one case of infection can lead to 12-18 subsequent infections in a susceptible population. Exposure of susceptible individuals to an infected individual leads to transfer of the infection in 90% of cases (Sabella, 2010). Measles infection induces long lasting immunity to the virus. Therefore in order for the virus to continually propagate through a population, it must consist of over 250 000 people. Measles virus is a strictly human pathogen and therefore could not have emerged until the population reached this size. Measles virus is closely related to the Rinderpest virus (RPV) which infects cattle. It is thought that measles virus could have evolved from this virus at a time when humans and cattle were often in close proximity (Furuse et al. 2010).

Measles is initially acquired through the respiratory system by inhalation of infectious particles. At first the virus replicates in dendritic cells, lymphocytes and lymphatic tissues before spreading to other organs. The symptoms of measles infection begin around 10-12 days after initial exposure to the virus and include fever, coughing, coryza and conjunctivitis (Rima and Duprex, 2006). A maculopapular rash occurs 2-4 days after the initial symptoms present. The rash appears on the face and the neck area before spreading to the extremities over the course of around 3-7 days. Koplick's spots may also be seen in the mouth of infected individuals a day before the start of the rash (Perry and Halsey, 2004).

Whilst measles is usually a mild infection, it can lead to complications that, in some instances, can be lethal. Measles is one of the leading causes of child deaths worldwide (Hussey and Clements, 1996).

Often measles infection can lead to pneumonia, which is the most common cause of measles associated deaths. The measles itself may be the direct cause of the pneumonia (e.g. in the case of giant cell pneumonia) or pneumonia can be caused by a secondary opportunistic infection that occurs as a result of a suppressed immune system caused by the initial measles infection. Indeed, many deaths are

the result of secondary infection by another virus, bacteria or parasite that occurs at a stage when the host is in an immunosuppressed state (Moss et al. 2004).

Complications caused by measles virus occur at an increased rate in individuals with immunodeficiency (Kaplan et al. 1992) and they can affect any organ system within the body and range in severity from mild to fatal (Perry and Halsey, 2004). Subacute sclerosing panencephalitis (*SS*PE) is a rare complication that may be fatal and occurs when the virus spreads to the central nervous system and may develop years after the initial infection (Bellini et al. 2005). It is not treatable with any currently available drugs. Measles during pregnancy may also lead to severe complications (Atmar et al. 1992) such as premature birth, spontaneous abortion and maternal death (Ogbuanu et al. 2014).

1.3.1.1 Measles genome and structure

Measles virus has a negative sense single stranded RNA genome of 15 894 nucleotides in length. The genome contains six genes plus small leader and trailer regions. The genes encoded by the measles genome are N, P/V/C, M, F, H and L (figure 1.7). The N gene encodes the nucleocapsid protein which forms the capsid structure of the virus and packages the RNA genome of the virus. Phosphorylation of specific sites on the nucleocapsid protein is responsible for controlling viral gene expression and consequently the growth rate of the virus (Sugai et al. 2013). P, V and C are encoded by overlapping regions of the genome. P encodes the phospho protein and this forms an essential part of the polymerase structure (Devaux and Cattaneo, 2004). V encodes the V-protein that inhibits the host interferon signalling response (Ohno et al. 2004). C encodes the C-protein which is involved with the inhibition of interferon signalling and in regulating polymerase activity (Bankamp et al. 2005). M encodes the matrix protein, which is situated on the inner layer of the membrane and is hydrophobic. It is involved with regulating RNA synthesis (Iwasaki et al. 2009). F encodes the fusion protein that mediates fusion of the viral envelope with the plasma membrane of the host, in-turn allowing entry of the viral core into the host cell. H encodes the hemagglutinin glycoprotein that is involved with attaching the virus to the host cell prior to fusion (Zhang et al. 2005). Finally L

encodes the large protein that provides the enzymatic activity required for the RNA polymerase complex (Duprex et al. 2002).

1.3.1.2 Measles entry

The wild type strain of measles uses the cellular receptor signalling lymphocyte activation molecule (SLAM), also known as CD150, to enter cells (Tatsuo et al. 2000). The SLAM receptor is present on lymphocytes, dendritic cells and macrophages, and so when carrying out experiments with the wild type measles virus in the laboratory, the marmoset B cell line B95a is used. These cells are adherent and have been transformed with Epstein-Barr virus (EBV). The infection of these immune system cells leads to immune suppression in infected individuals (Yanagi et al. 2002). The vaccine strain of measles, the Edmonston strain, may use the SLAM receptor but also uses the CD46 receptor to enter cells (Dorig et al. 1993). The CD46 receptor is present on all nucleated cells and so there is a wider range of cells that may be used for experiments involving this strain. It has been found that there is another method of virus entry that does not use either the SLAM receptor or the CD46 receptor. SLAM negative cells showed autofluorescence when infected with a wild type measles virus strain expressing GFP (IC323-EGFP), indicating that the virus was still able to enter the cells, though less efficiently. The virus was not able to form syncytia in SLAM-negative cells therefore inhibiting its ability to spread (Hashimoto et al. 2002). The receptor PVRL4 (Nectin-4; a human tumour cell marker) is able to act as a receptor for binding and entry of wild type measles into epithelial cells of lung, colon and breast adenocarcinoma cell lines (Noyce et al. 2011). There also exists a SLAM negative cell line that has been shown to allow syncytia formation by a SLAM independent mechanism in the presence of Wild type measles virus. This cell type is small airway epithelial cells (SAEC) (Takeuchi et al. 2003).

The measles virus glycoprotein complex interacts with the lipid raft domains on the host cell membrane. This interaction alters the recruitment and segregation of signalling components. This in-turn interferes with cell signalling pathways and leads to immunosuppression in the host because the SLAM positive immune cells

are no longer able to proliferate (Avota et al. 2004). In recent years, studies of the way that measles gets in and out of host cells have altered the assumption that the virus is a respiratory infection. Instead current thought suggests that it is an infection of the immune system through SLAM positive cells, analogous to HIV-1 (Rima and Duprex, 2011).

Binding, fusion and entry of measles virus are mediated by glycoprotein spikes in the envelope that are made up of attachment (H) and the fusion (F) proteins. The RNA genome, N, P, and L proteins form the nucleocapsid which is tethered to the envelope by the matrix protein. Binding of measles virus to the host cell membrane causes the activation of pH-independent fusion of the measles envelope with the cell membrane and subsequent entry of the nucleocapsid into the host cell.

1.3.1.3 Measles lifecycle

There are many stages of the virus' life cycle that are unique to the virus and that don't involve the use of host cell mechanisms. These represent potential targets for therapeutics. However the virus also uses host cell components during its replication cycle. Sphingosine kinase (SK) is a host cell enzyme that catalyses the production of sphingosine 1-phosphate and regulates several cellular processes. This enzyme has been found to be a regulator of measles infection. Inhibition of SK further inhibits NF-κb activation by measles virus. This is essential for efficient measles replication. This indirect mechanism highlights SK as an essential cellular factor for measles replication (Vijayan et al. 2014). Measles proteins have been found to interact with a wide range of host cell proteins and in doing so, the virus takes advantage of the host cell machinery for its own benefit. For example, measles (and other viruses) phosphorylate the initiation factor eIF2α that functions as part of the cell's translation machinery. This inhibits the translation of cellular mRNA, and allows the virus to use it for its own benefit (Rima and Duprex, 2011).

The actin and microtubule cytoskeleton is required for replication and maturation of measles virus. However inhibition of either of these structures does not inhibit syncytia formation (Berghall et al. 2004). It has been found that using compounds that either disrupt or stabilise actin filaments, affects measles replication in

different ways. Stabilisation of actin filaments inhibited the release of newly produced particles, indicating that actin dynamics are required for the budding of measles from the cell membrane. Disruption of actin filaments results in inhibition of the transport of the newly formed nucleocapsids to the plasma membrane (Dietzel et al. 2013).

1.3.1.4 Measles syncytia formation (virus spread)

The fusion of measles virus with the host cell is initiated by the hemagglutinin glycoprotein and entry into the cell is initiated by the interaction of the fusion protein with the cell membrane. As the infection progresses, newly formed glycoproteins accumulate at the cell membrane, leading to the fusion of the cell with other cells in-turn resulting in the formation of syncytia (Wild et al. 1991).

It has been shown that members of the paramyxoviridae family induce autophagy in the cell in order to aid virus spread to the next cell (Delpeut et al. 2012). It was also observed that membrane fusion is mediated by viral glycoproteins that lead to the induction of autophagy in the cell. The wild type and Edmonston strains of measles activate autophagy through different mechanisms. The Edmonston strain can activate early autophagy immediately upon infection through the CD46 receptor and the scaffold protein GOPC. Replication of the virus induces successive waves of autophagy. Wild type (SLAM dependant) measles are unable to take advantage of the early autophagy, but can instead induce and exploit the late and sustained phase of autophagy (Richetta et al. 2013).

1.3.1.5 Measles Vaccine

Enders and Peebles were the first to grow measles virus in tissue culture (Enders et al. 1954), using primary human kidney cells, and inoculate them with the blood from a child with measles (David Edmonston). The primary cell lines were replaced with continuous monkey kidney cells lines (Vero and CV-1) for the growth of this virus which ultimately became the vaccine (Edmonston) strain of measles.

The measles vaccine has been very successful and involves the use of a live-attenuated virus. Given that this successful anti measles vaccine exists, and that

there is no animal reservoir for the virus to otherwise thrive in, it should theoretically be possible to eradicate measles (Bellini and Rota, 2011). However this has not occurred to date and is partly due to individuals opting against vaccination for themselves and/or their children. The highly infective nature of the virus means that it rapidly reappears when levels of vaccination decrease in the population. Highlighting this, only 5 to 6% of the population need be susceptible to the virus for it to cause outbreaks. Therefore the level of herd immunity (percentage of the population required to be immune to the virus to prevent outbreaks) would need to be over 95% (Plemper and Hammond, 2014).

Another factor detracting from the vaccines success is that its effectiveness is reduced when administered to infants less than 12 months of age. This is due to the interference of maternal antibodies in their not-yet-developed immune systems. Maternal measles antibodies are often lost at 4 to 9 months and infants are susceptible to the virus until such a time as they are vaccinated (usually at 12-13 months of age in the UK). Occasionally in cases where maternal antibodies persist in infants beyond the age of 12 months, the effectiveness of the vaccine is reduced (Albrecht et al. 1977). Today a second dose is recommended at the age of 40 months to 5 years to ensure that full protection is established (Le Menach et al. 2014).

Prior to the development of the vaccine, 95-98% of children would catch measles before the age of 18 years. Indeed, individuals would make efforts to increase the chances of their children catching measles early in life. This was considered preferable to the risk of exposing their children to a disease of increased severity in adulthood. The introduction of the vaccine has lead to the prevention of around 5 million child deaths per year, with the assumption that the fatality rate is 2-3% (Perry and Halsey, 2004). Despite the successful vaccine, outbreaks of measles virus are still common, and as such antiviral compounds would be of great clinical benefit.

1.3.1.6 Measles Antivirals

At present there are no measles antiviral drugs available on the market. With the eradication of the virus proving difficult, the development of safe antivirals against measles virus would be a useful tool in the control of the virus – especially in cases where vaccination is not an option. Several treatments, including Ribavirin, interferon-alpha (IFNα) treatments, high-dose vitamin A and measles specific immune globin (Ig), have been shown to reduce some of the effects of the virus in some instances. However there are issues associated with each of these treatments that make them unsuitable for use in controlling measles on a larger scale (Barnard, 2004).

The ideal antiviral therapy for measles virus would be a small molecule inhibitor that is safe, effective, inexpensive to produce and stable. Attempts to produce such a drug have as yet failed to cover all of these criteria and, as such, there remains space in the market for an effective measles antiviral treatment (Plemper and Snyder 2009).

Ribavirin is a guanoside ribonucleic analogue that has demonstrated antiviral activity against several viruses *in vitro*. There have been five mechanisms of action described for this compound including inhibition of ionosine monophosphate dehydrogenase, immunomodulatory effects, interference with viral RNA capping, inhibition of viral polymerase and mutagenesis due to incorporation of the drug into the viral genome (Graci and Cameron, 2006). It has been successful in treating some cases of measles pneumonitis (Forni et al. 1994). This compound however has not been accepted for clinical use against measles due to issues with side effects, specifically haemolytic anaemia (Lin et al. 2004). Due to the potential beneficial effects of this compound attempts at producing safer analogues of Ribavirin have been described.

The compound 5-Ethynyl-1-β-D-Ribofuranosylimidazole-4-Carboxamide (EICAR) and other related compounds that are structurally similar to ribavirin have been shown to have broad antiviral activity, similar to but more effective than that of ribavirin.

The compound EICAR is thought to act on the enzyme inosine-5'-monophosphate (IMP) dehydrogenase, which converts IMP to xanthosine 5'-phosphate (XMP). XMP then catalyses the production of GTP. As expected based on this mechanism, the addition of GTP to the antiviral assay involving EICAR diminished its antiviral activity (De Clercq et al. 1991).

A series of small molecule inhibitors of measles were designed to inhibit its entry into the host cell by targeting the hydrophobic pocket near the C terminal heptad repeat of the measles F protein. Mutation of the residue Val94 and surrounding residues within this hydrophobic pocket have a significant effect on the fusion of the virus with the host. The molecules designed, including the initial lead OX-1 (active at 50 µM) and the optimised AS-48 (active between 600-3000 nM depending on virus strain), displayed inhibition of measles virus entry. During the research into these compounds it was also demonstrated that resistance of the virus to these compounds was achievable through mutations at specific locations on the F protein (Prussia et al. 2008).

Peptides derived from the structure of the C terminal heptad repeat section of measles F protein have also demonstrated antiviral potential. They have been shown to protect SLAM transgenic mice from lethal measles infections (Welsch et al. 2013).

A recent small molecule inhibitor of the morbillivirus polymerase has been described named ERDRP-0519. This molecule is orally available and has been shown to protect ferrets from lethal morbillivirus (canine distemper virus; CDV) infections (Krumm et al. 2014).

1.4. Antiviral drugs with cellular targets

Drugs that are produced to target a specific part of the virus have the disadvantage that the virus may mutate and become resistant to the drug. Therefore recently there has been a change in focus towards compounds that have a host target that is required by the virus as part of its lifecycle (Schwegmann and Brombacher, 2008). As well as reducing the chance of the virus developing resistance to the drug, they

have the added benefit of antiviral activity against other viruses that take advantage of the same host mechanism (Krumm et al 2011). The disadvantage of targeting host cell components is the increased potential for unwanted side effects (Yan et al. 2013).

1.5 Aims of the PhD project:

1. To test the activity of novel D- and L-ddBCNAs against VACV and quantify their activity with the aim of determining structure activity relationships.

2. To test the lead compounds against a panel of other viruses (including measles) and quantify their activity in order to determine how this compares with their activity against VACV.

3. To test the toxicity of the lead compounds against cell lines used in the antiviral assays in order to confirm that the antiviral effect is not due to loss of cell viability

4. To investigate the mechanism of action of the lead ddBCNAs.

Chapter two - Materials and Methods

2.1 Materials

2.1.1 Cell lines

- **293:** (ATCC, CRL-1573) - human embryonic kidney cells (HEK-293), easily transfectable, transformed with adenovirus 5 DNA.
- **3T3**: (ATCC, CRL-1658) - Fibroblasts derived from Swiss Albino mouse embryo cells.
- **A431**: (ATCC, CRL-1555) - Human skin (squamous carcinoma) epithelial cells derived from 85 year old female.
- **A549:** (ATCC, CCL-185) - Human lung epithelial cells from a lung carcinoma derived from a 58 year old male.
- **B95a**: (IZSBS – Istituto Zooprofilattico Sperimentale, Brescia, Italy) – Marmoset B lymphocyte cell line derived from B95 8 cells and adapted to be attached. Immortalised using Epstein Barr virus (EBV).
- **BJ-1**: (Clontech) - Human foreskin fibroblasts derived from a newborn male. Stably transfected with human telomerase (Bodnar et al. 1998).
- **BJAB**: (MRC – gift of Fabien Blanchet) - B cell line derived from human origin. Require RPMI 1640 instead of DMEM.
- **BSC-1:** (ATCC, CCL-26) – Grivet monkey kidney epithelial cells.
- **CV-1:** (ATCC, CCL-70) – Fibroblast cells derived from African green monkey kidneys.
- **HaCaT:** (German cancer research centre, DKFZ) - Spontaneously immortalised human skin keratinocyte cells.
- **HeLa**: (ATCC, CCL-2) – Human epithelial cells: established from the cervical adenocarcinoma of a black 31 year old female. This cell line contains Human Papilloma Virus 18 oncogenes (E6 and E7) (DeFilippis et al. 2003).
- **HFF**: (ATCC, SCRC-1041) – Human foreskin fibroblasts, derived from newborn male.

- **HFFFtc:** (gift of G. Wilkinson) – Human foetal foreskin fibroblasts (HFFF tert car). Immortalised by human telomerase expressing the cocxsackie adenovirus receptor (CAR).
- **HUH7**: (gift of Bartenschlager group, University of Heidelberg) - Derived from human liver carcinoma of 57 year old Japanese male. Epithelial hepatoma cells.
- **Ramos**: (MRC - gift of Fabien Blanchet) - B cell line derived from human origin. Require RPMI 1640 instead of DMEM.
- **RK13:** (ATCC, CCL-37) – Derived from 5 week old rabbit kidney epithelial cells. Susceptibility to several poxviruses has been reported. The cells are positive for keratin by immunoperoxidase staining. The cells are positive for bovine viral diarrhea virus (BVDV).
- **TK- 143**: (ATCC, CRL-8303) - Human osteocarcoma cell line lacking the thymidine kinase enzyme.
- **Vero:** (ATCC, CCL-81) - African green monkey kidney epithelial cells. They have high susceptibility to a wide range of viruses.

2.1.2 Antiviral compounds

2.1.2.1 ddBCNAs

All of the ddBCNA compounds used in this project were produced/synthesized by the McGuigan group in the Cardiff School of Pharmacy and Pharmaceutical Sciences by Ranjith Pathirana and Karen Hinsinger using the methods described in a recently published manuscript. This describes the chemistry involved in producing these L-enantiomer compounds and this is briefly summarised below (McGuigan et al. 2013). The method used to produce L-ddBCNAs is more complicated than that used for the D-ddBCNAs. The production of the D-ddBCNAs can begin with D-5-iodo-2,3-dideoxyuridine (D-IddU) made from D-2-deoxyuridine which is commercially available. L-2- deoxyuridine is not commercially available and, therefore more steps are required to reach the L-5-iodo-2,3-dideoxyuridine (L-IddU) starting point for the

various L-ddBCNAs. The starting compound used in this process is L-arabinose. Six further steps are required from this point to produce L-IddU.

When the compound reaches the stage of L-IddU, the required L-ddBCNA structures are produced by coupling the L-IddU with a series of acetylenes using the Sonogashira reaction with a Palladium catalyst. Extra steps are also required for the production of the ether side chains as opposed to the commercially available alkyl- and arylacetylenes. Two alternative methods were used in the synthesis of the ether side chains depending on the target ethers required. The first method involved the mesylation of alkyl-1-ols, which were then coupled with different alcohols to give the final ethers. In the second method, alcohol starting materials were transformed into mesylated compounds and then reacted with selected alkynols to obtain the ethers. The final ddBCNAs were analysed spectroscopically and chromatographically to determine structure and purity before testing in antiviral assays (McGuigan et. al. 2013).

All the ddBCNAs were assigned inventory numbers to refer to without giving away structural information. The use of inventory numbers ensured that IP was maintained and enabled double blind biological assays to prevent investigator bias. The inventory numbers all started with 'Cf' (the compounds were developed in Cardiff) followed by a four digit number based on the order in which the compounds were produced. Throughout this thesis the compounds will be referred to by their inventory numbers. The structure of each of the compounds is described in chaper 3 section 3.3.1.

The ddBCNAs were received from the McGuigan laboratory in a lyophilised form. In the Bugert laboratory each compound was dissolved in dimethyl sulphoxide (DMSO) to make a stock solution of 10 mM, which was stored at -20^{o}C. The required concentrations of the compounds were made prior to each experiment by diluting relevant volumes of the stock solution in DMEM.

2.1.2.2 Control compounds

- **Wortmannin:** (W3144; Sigma-Aldrich) – Specific covalent inhibitor of phosphoinositide 3-kinases (PI3Ks) (Wymann et al. 1996).
- **Cidofovir:** (C5874; Sigma-Aldrich) – Viral DNA polymerase inhibitor. Used as antiviral treatment against CMV in AIDS patients. Also shown to be active against VACV (Magee et al. 2005).
- **Ribavirin:** (R9644; Sigma-Aldrich) - An anti-viral drug displaying antiviral activity against a range of viruses *in vitro* and *in vivo* (Graci and Cameron, 2006).
- **Cytosine arabinoside (AraC):** (C6645; Sigma-Aldrich) – Chemotherapy agent that interferes with DNA synthesis (Grant, 1998).
- **Staurosporine:** (S6942; Sigma-Aldrich) – Cytosine-β-d-arabinofuranoside hydrochloride, apoptosis inducer (Bertrand et al. 1994).
- **Chloroquine:** (C6628; Sigma-Aldrich) – Anti-malarial drug that accumulates in lysosomes and raises lysosomal pH (Homewood et al. 1972).

2.1.3 Viruses

- **vWR:** (Gift from Bernhard Moss, NIH-NIAID, to Joachim Bugert) - Vaccinia Western reserve strain - Wild type vaccinia virus.
- **v3:** (constructed by Joachim Bugert) - Firefly luciferase expressing VACV - Modified VACV to express firefly luciferase under the control of the synthetic early/late poxviral promoter (Blasco and Moss, 1995) using pRB21-based donor plasmid p240. Details of the production of this virus are described in section 2.2.4.
- **v300:** (constructed by Laura Farleigh) - VACV expressing GFP - VACV modified to express enhanced green fluorescent protein under the control of the synthetic early/late promoter using the pRB21 based donor plasmid p300. Full details for the production of this virus are described in section 2.2.4.

- **vRB12:** (gift from Bernhard Moss to Joachim Bugert) - Plaque-less mutant VACV containing faulty F13L gene (ΔF13L) responsible for producing large plaques. This virus will not produce visible plaques within three days pi.
- **vYFP-A3L:** (Gift from Michael Way; unpublished construct) - VACV modified to express YFP attached to a structural (core) protein of VACV (A3L).
- **mWT Fb:** (gift from Jurgen Schneider-Schaulies, Universitat Wurzburg, Germany) - Wild type measles virus (Erlenhofer et al. 2002).
- **mIC323:** (gift from Yusuke Yanagi, NIID, Tokyo, Japan) - Wild type measles modified to express GFP (Hashimoto et al. 2002).
- **mEdATCC:** (ATCC-VR24) - Edmonston vaccine strain of measles virus.
- **YFV:** (STAMARIL, Sanofi Pasteur MSD; gift of Thomas Junghanss,Tropenambulanz Heidelberg) - Yellow fever virus vaccine strain.
- **Adenovirus 5:** (ATCC VR-5).
- **HSV-1:** (NCPV 17+) - Herpes simplex virus type 1.
- **HSV-2:** (NCPV 132349) - Herpes simplex virus type 2.
- **Influenza A:** (gift of Dietmar Katinger, Polymun Scientific) - Strain H1N1, NS1 116 GFP fusion.
- **MCV:** (Obtained from collection of lesions from molluscum patients, Heidelberg, Germany, between 1999-2003) - Samples were dounce homogenised prior to use.
- **HIV-X4:** (Fabien Blanchet laboratory) - HIV-1 strain that uses the CXCR4 receptor for entry.

2.1.4 Equipment

2.1.4.1 Plastics and glassware

2.5 mL, 10 mL and 25 mL Stripettes (Costar). T25, T75 and T150 flasks with filter caps (CellStar, Greiner bio-one). 96-wp, 48-wp, 24-wp, 12-wp, 6-wp, (CellStar, Greiner bio-one), clear bottom black 96-wp (Corning). 25 mL universal containers (UC; Sterillin UK) and 7 mL Bijous (Greiner bio-one). Sterile 1.5 mL screw cap eppendorf tubes (Greiner, bio-one). 1 mL cryotubes plus coloured caps (Nunc).

Pipette tips 10 µL, 200 µL, 1 mL, 5 mL (VWR). Falcon tubes 15 mL and 50 mL (Greiner). Glass 16 mm coverslips (Marienfeld, Laboratory Glassware). Glass slides (Superfrost, Thermo Scientific). Sterile 25 cm cell scrapers (Fisherbrand). 8.25 cm plastic disposable plates (Sterillin UK).

2.1.4.2 Other equipment

Eliptical shaker ('The Belly Dancer', STOVALL, life sciences incorporated). Centrifuge (CR412, Jouan). Microcentrifuge (IEC, MicroMax). Biosafety Class II cabinet (MicroFlow). Incubators (MCO-17A, Sanyo electric). Confocal miscroscope (Leica SP5 confocal laser scanning microscope) equipped with Ar (488 nm) and HeNe (543 nm, 633 nm) lasers and a 63X oil immersion objective. Widefield microscope (Leica, SP5, DMIRB) with camera (QI Imaging Retiga Exi FAST Cooled Mono 12- bit Camera). Phase contrast microscope (Olympus, CK40), equipped with digital microscope camera (Polaroid). 96-wp plate reader (FLUOstar OPTIMA (BMG labtech). NanoDrop spectrophotometer (ND 1000, Thermo Scientific). Thermal cycler for PCR (PTC-100, Peltier Thermal Cycler). Vacuum pump (Fisherbrand). Automatic pipette (Pipetus, Hirschmann, Laborgerate). Incubators (MC0-17A, Sanyo Electric). Shaking incubator (Gallenkamp). UV transilluminator (BIORAD). Electrophoresis gel chambers (Hoeffer-Pharmacia). Water bath (GRANT; SUB14). Magnetic stirrer (BIBBY; HB501). Heat block (GRANT; QBT2). Pipettes; 10 µL, 50 µL, 200 µL, 1000 µL (BIOHIT).

2.1.4.3 Software

Graphs depicting results were produced in Microsoft Excel. Paired T tests performed using SPSS (IBM). IC_{50} and CC_{50} concentrations were calculated using GraphPad Prism 6. Plaque measurements and virus particle/nuclei counting performed using Image J (version 1.47). Leica software used to obtain images on the confocal microscope. FLUOstar OPTIMA plate reader software for luminescence readings. Nanodrop (ND 1000, V3.3) software for measuring DNA concentrations.

2.2 Methods

2.2.1 Cell culture methods

2.2.1.1 Cell maintenance

Cells were grown in 1x Dulbecco's Modified Eagles Medium (DMEM) containing 4.5g/L glucose and L-glutamine without sodium pyruvate (Gibco, Life Technologies, Paisley, UK) supplemented with 10% (*v/v*) foetal bovine serum (FBS; Gibco, life technologies, LOT: 41G6401K) unless stated otherwise. Cells cultured in the absence of antibiotics until required for assay when penicillin/streptomycin (Gibco, life technologies) was added. All cells stored in incubators at 37^{o}C with 5% CO_2.

2.2.1.2 Thawing cells

Cells were removed from the freezer and allowed to thaw quickly at 37^{o}C. Immediately after thawing they were transferred into a sterile T75 flask containing 10 mL cell medium (DMEM containing 10% FBS). These were incubated for four hours for the cells to settle then the cell medium was removed and replaced with fresh medium to remove all traces of DMSO.

2.2.1.3 Freezing cells

Cells were routinely frozen for storage over longer periods and to maintain stocks. Cells at 70-80% confluence were suitable for freezing. After trypsinising, 10 mL of PBS was added to the cells and they were transferred to a 25 mL UC. These were then centrifuged at 1000 rpm for 5 minutes. PBS was decanted from the pellet of cells. These were then resuspended in 2 mL of freeze medium (47.5% DMEM, 47.5% FBS and 5% DMSO [Sigma-Aldrich, UK]), and the cells were transferred into 2x 1mL cryotubes which were placed into the -70^{o}C freezer. For long term storage after initial freezing at -70^{o}C, cells were ideally transferred into liquid nitrogen (-196^{o}C).

2.2.1.4 Mycoplasma testing

Mycoplasma contaminations were ruled out by routine testing by mycoplasma PCR (Geneflow). Over the course of the work there was one case of mycoplasma

contamination in B95a cells. These cells were discarded and cells at various passage numbers were thawed from previous stocks and retested until the results were negative. All other cells tested were clear of contamination over the course of the work.

2.2.1.5 Sub-culturing of cells

Cells were routinely sub-cultured for experiments/maintenance. Before reaching confluence (~70-80%) cells were detached from the flask using TrypLE (Gibco, life technologies). Cell medium was removed, cells were washed once with TrypLE (1 mL for T25, 2 mL for T75 or 4 mL for T150 flask). This was discarded and replaced with fresh TrypLE (0.5 mL for T25, 1 mL for T75 and 2 mL for T150 flask). The cells were placed in the (37^{o}C) incubator for ~5 minutes to allow the cells to detach (microscopical examination confirmed the detachment of the cells). These could then be removed from the flask, counted and placed into mulitiwell plates for experiments, or discarded for maintenance. The number of cells used were $5x10^4$/well in 96wp, $1x10^5$ in 48wp, $2.5x10^5$ in 24wp, $5x10^5$ in 12wp and $1x10^6$ in 6-wp. The remaining cells in the flask were resuspended in fresh cell medium (5 mL for T25, 10 mL for T75, 20 mL for T150).

2.2.1.6 Cell counting

After trypsinisation 10 µL of evenly suspended cells (cells pipetted three times to ensure they were evenly dispersed) were added to 90 µL of diluted (1:5 dilution in sterile PBS) 0.4% trypan blue solution (Sigma). These were mixed well and 10 µL of the cell/trypan blue suspension was then pipetted into a hemocytometer (washed prior to use with 70% ethanol) and left for a few minutes to allow the trypan blue to stain dead cells. The hemocytometer counting grid consists of 9 large squares, the cells in the four corners of the grid (see figure 2.1) of the hemocytometer were counted and the average of the four counts was calculated. The volume in one corner square (consisting of 16 smaller squares) is equal to 0.1 mm^3 (as it has an area of 1 mm^2 and a depth of 0.1 mm) so the concentration of cells per mL is the average number of cells counted in one corner x 10^4/mL. This was originally diluted

1:10 in the trypan blue solution so the number of cells in the original stock is 10 times greater than this (i.e the average cell count x 10^5/mL).

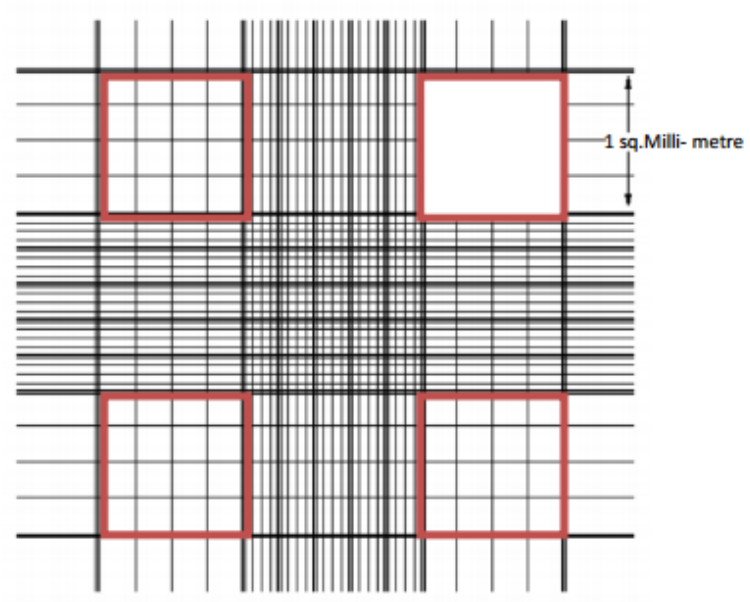

Figure 2.1 Hemocytometer counting grid, the cells are counted in each of the four corner squares (outlined in red) and the average is calculated. The number of cells in the stock is the average number of cells in one corner x10^5/mL allowing for the dilution in trypan blue/PBS (figure from www.humanimmunologyportal.com).

2.2.2 Virus stock production methods

2.2.2.1 Optimisation of VACV stock production

In order to produce stocks of VACV with high titres a time course experiment was carried out that determined the optimum collection time for the virus stocks. Four T75 flasks of each of 4 cell lines (HeLa, RK13, CV-1 and 3t3) were infected with v3 virus at an moi of 0.1. One of each of the four flasks was then frozen after one, two, three or four days and the subsequent titres were calculated (by plaque assays described section 2.2.3.2). Separate titres were calculated for the supernatant (sn; containing the virus particles released from the cells into the cell medium) and the pellet supernatant (psn; containing the virus particles remaining within the cells) collected (collection protocol described in section 2.2.2.2).

The data generated (figure 2.2) suggests that the best time to collect VACV stocks is after two days for all the cells tested, with the exception of 3t3 cells where the optimum stock collection was four days post infection. It is noteworthy that even after four days the stock generated in 3t3 cells does not reach levels as high as those in the other cell lines tested. This is likely to be due to the fact that VACV does not infect and replicate as well in 3t3 cells as in the others. As such, it takes longer for new virus particles to be produced in this cell line. In almost all cases shown in figure 2.2, the supernatant shows a higher titer than the equivalent pellet supernatant. The supernatant v3 virus grown in HeLa cells was selected for use in the majority of antiviral experiments. The v3 virus grown in this way gave better luminescence signals in the luciferase assays compared with the virus grown in other cell lines (data not shown) and gave good titres of virus in both the supernatant and pellet supernatant although the highest titer overall was seen in the supernatant of RK13 cells at over $1x10^7$ pfu /mL.

Between the time of infection and the second day the number of viral particles increases as they infect the cells and fulfil their replication cycle. It appears that after the 2 day optimum collection time (in most cases) the titer of the virus decreases from this point. This observation is probably due to the fact that it takes two days for all of the cells in the flask to become infected. After this time there are no cells left to infect and the virus particles start to disintegrate, ultimately leading to a reduction in the number of infectious particles in the stock. This observation emphasises the need to collect the virus at the optimum time in order to achieve the highest titers for the virus stocks.

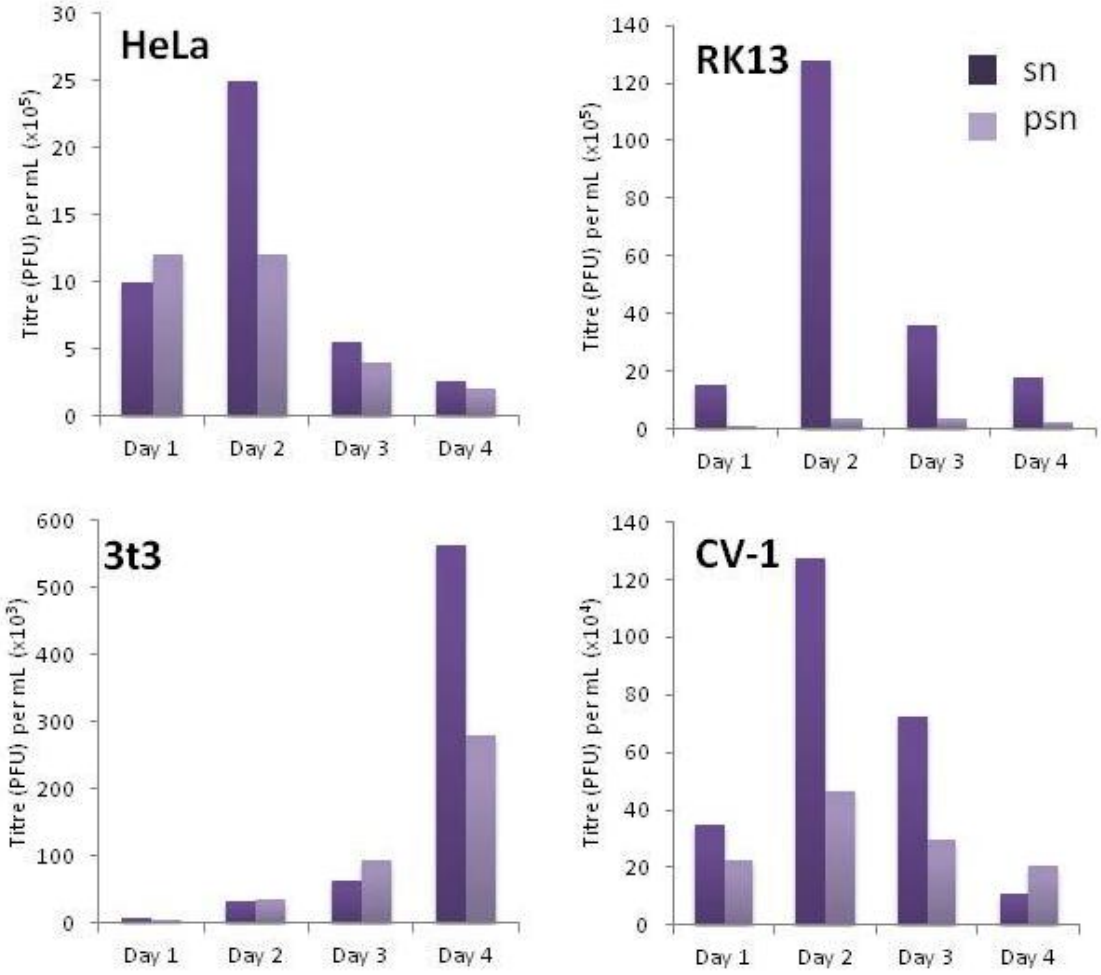

Figure 2.2 VACV stock production kinetic experiment in different cell lines, showing that the optimum time after infection for collection of the virus stocks is two days in the case of all cells apart from 3t3 cells where a four day incubation leads to higher titers. Separate titers were calculated form the supernatent (sn) and the pellet supernatent (psn).

2.2.2.2 Standard VACV stock production

Large titers of stocks were grown in T150 flasks of HeLa cells as these produced high titers in both the sn and psn. The effects of the ddBCNAs appeared more apparent in the luciferase assays in RK13 cells when using virus produced in HeLa cells compared with the other stocks (data not shown). Confluent cells (~80%) were infected with the VACV at an moi of 0.1 and incubated for 2 days. The virus was collected by transferring the supernatant into a 25 mL UC and scraping the cells from the surface of the flask into 10 mL of PBS, this was then transferred into another UC. The UCs were then centrifuged at 1000 rpm for 5 minutes in order to pellet the cells. Cell supernatant was removed from the pellet and frozen in a 50 mL falcon tube to use as virus sn which contains a mixture of intracellular mature virus (IMV) from lysed cells and extracellular enveloped virus (EEV). The PBS from the cell pellet was discarded and both of the pellets of cells were resuspended into the same 1 mL of PBS. This cell suspension was transferred to a sterile 1 mL eppendorf tube and frozen and thawed 3 times in order to disrupt the cell membranes and release the intracellular virus. This was then centrifuged at 10 000 rpm for 5 minutes and the supernatant was collected into another sterile eppendorf and frozen. This solution containing mostly IMV was designated the pellet supernatant (psn).

Further purification of the virus (OPTIMEM/sucrose gradient centrifugation as described in Townsley et al. 2006) was only essential for the study of virion components and was thus not required for the antiviral experiments in this project. It was found that purification of VACV had no effect of the results of the antiviral assays and resulted in a reduced virus titer (Bugert laboratory, unpublished results).

When making stocks of other strains of VACV the results from the same method was used. Stock titers were determined by plaque assay.

2.2.2.3 Measles stock production

In order to obtain high stocks of measles virus, stocks were grown up in a series of passages. Initially one T75 flask of ~80% confluent B95a cells was infected with measles (mWT Fb) in 2 mL volume. The flask was tilted from side to side over a

period of 15 minutes to allow adsorption of the virus onto the cells. The flask was topped up with 8 mL DMEM and the cells were left to incubate at 37^{o}C for 48 hours. The cells were scraped from the flask and transferred, along with the medium into a 14 mL falcon tube. This was frozen at -70^{o}C and thawed at 37^{o}C.The sample was centrifuged at 2000 rpm for 15 minutes at room temperature. The supernatant (kept on ice between steps) was collected and used for the next round of infection. The 10 mL collected medium was used to infect a T150 containing B95a cells at ~80% confluency. The flask was tilted from side to side over a period of 15 minutes at room temperature to allow the virus to adsorb to the cells. The flask was topped up with a further 10 mL DMEM and left to incubate at 37^{o}C for 48 hours. This was collected as before and the supernatant obtained was used to infect a further four T150 flasks of B95a cells at ~80% confluency (5 mL collected supernatant per flask) which were left for a further 48 hours at 37^{o}C. This final stock was collected as before and, after the centrifugation step, FBS (20% of the supernatant volume) was added to the collected supernatents. These were then aliquoted into separate 1 mL cryotubes and frozen at -70^{o}C for storage. The same method was also used for growing up stocks of mEdATCC in Vero cells. Stock titers were determined by $TCID_{50}$ assays (section 2.2.3.3) of syncytia formation in B95a/Vero cells.

2.2.2.4 Yellow fever virus stock production

Vero cells grown in a T75 flask at ~80% confluency were infected with 100 µL of the newly received vaccine stain of Yellow fever virus. This was left to incubate for 3 days (when CPE is observed) before collection. The supernatant was used to infect a T150 of ~80% confluent Vero cells in order to increase the stocks. The virus stock was collected using the same method as was used for collection of measles virus stocks (section 2.2.2.3). Stock titers were determined by $TCID_{50}$ assays (section 2.2.3.3) of CPE in Vero cells.

2.2.3 Quantification of virus stocks

2.2.3.1 Optimisation of VACV plaque assays – Shell vial method

It has been demonstrated that when carrying out *in vitro* virus assays the level of infection may be improved by including a centrifugation step (Osborn and Walker,

1968) termed shell vial. The effect of using a shell vial was tested for three vaccinia stocks produced in different cell lines (RK13, BSC-1 and HeLa).

Titration of three stocks of vWR, produced in these three cell lines, was carried out in duplicate for each of the virus stocks. The process carried out on the first plate of the pair, involved applying the virus to the cells in a series of dilutions and then applying the overlay to the infected cells after a 45 minute incubation period. The second plate was treated in the same way except that during the incubation period, before the addition of the overlay, the plates were centrifuged at 5000 rpm for 15 minutes (i.e. shell vial).

This optimisation assay indicated that the stock titres generated were higher if treated with shell vial than they were if not. The amount by which the shell vial increased the titre varied depending on which cell line the VACV was produced in. For VACV produced in RK13 cells, the increase was over six fold, in BSC-1 cells it was over two and a half times increased and in HeLa cells was almost 10 fold higher (figure 2.3)

This effect is likely due to centrifugation forcing the virus particles into close proximity to the 'target' cells so there is an increased chance of them binding and inducing an infection before the addition of the overlay. This means that the centrifugation step leads to more accurate calculations of the titers. Without it there may be more infectious particles/ plaque forming units (PFU) in the stock than cause plaques in the assay (i.e. the virus particles are not binding before the addition of the overlay to the cells). Based on these observations, the shell vial method was adopted for all further plaque assay titrations of VACV stocks, in an effort to reduce underestimation of the number of virus particles in the stocks.

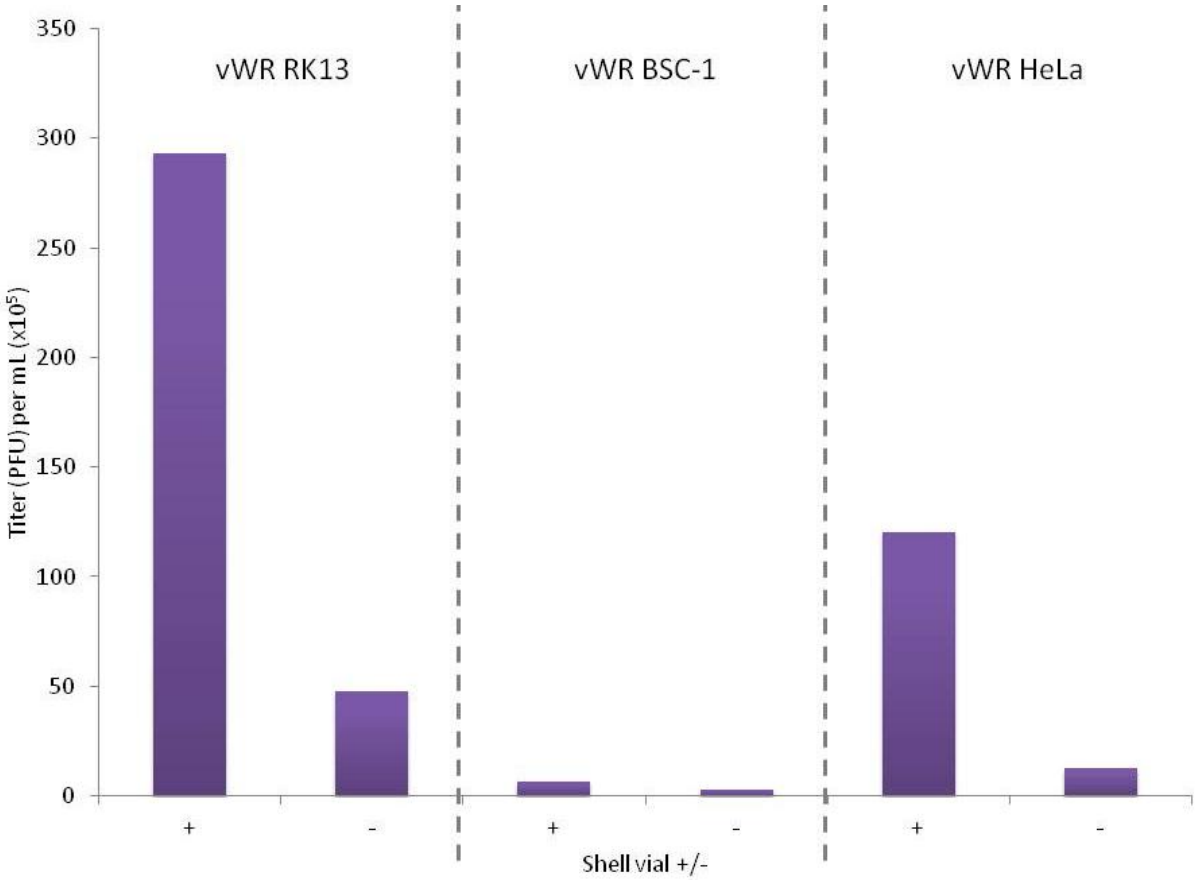

Figure 2.3 The effect of shell vial culture on the calculated titer (as PFU/mL) for VACV produced in three different cell lines. The centrifugation step in the shell vial method increases the titer calculated in the three cell lines. The titer of the BSC-1 cells was increased by around two and a half times, the titer of the RK13 cells was increased by around 6 times and in the case of the HeLa cells the titer was increased by almost 10 fold by the shell vial. + denotes results generated using shell vial. - denotes results generating without shell vial.

2.2.3.2 VACV plaque assay titrations

BSC-1 cells were seeded into a 24-wp and left to settle overnight to full confluency. Stock virus was prepared in a series of dilutions ($1x10^{-2}$ - $1x10^{-7}$). These were applied to the plate in quadruplet, 500 µL per well. The plate was then centrifuged at 5000 rpm for 15 minutes and left to incubate and allow the virus to settle for a further 30 minutes. The wells were topped up to 1 mL with 500 µL of overlay (consisting of 50% Avicel and 50% DMEM containing penicillin/streptomycin; Gibco). The plates were then left for three days before collection. After this time the sn was removed from the cells and the cells were gently washed twice with 1 mL PBS. The cells were then stained with 400 µL per well of Crystal violet solution (section 2.2.3.2.1) and left for 4-6 hours. The crystal violet was removed by plunging the plates into cold water. Excess water was shaken off and the plates were left to dry before the plaques in each well were counted. Titers were calculated as the average number of plaques in the wells (where they were countable) multiplied by ten to the power of the dilution factor of those wells, whilst also taking into account the original volume that was used to inoculate the cells (i.e. 500 µL/well).

2.2.3.2.1 Crystal violet solution:

5 g Crystal violet was dissolved in 100 mL 37% formalin, 200 mL 100% ethanol and 700 mL distilled water. 35 mL 2M Tris-base and 10 g $CaCl_2$ was added and stirred until dissolved the solution was then topped up to 2 L with distilled water.

2.2.3.3 $TCID_{50}$ virus quantification

To calculate the titers of viruses that did not form plaques (i.e. mWT Fb, mEdATCC and YFV) the 50% tissue culture infective dose ($TCID_{50}$) method was used. Cells (B95a for mWT Fb and Vero for mEdATCC or YFV) were grown to ~80% confluency in 96-wp. A series of 10 dilutions of virus plus two mocks (8 times repeated) were added to the cells. Cells were incubated for three days before being assessed for CPE. $TCID_{50}$ concentrations were calculated based on the method previously described by Reed and Muench (1938). An estimation of the number of virus

particles in the stock may be made based on the average lowest dilution at which CPE is observed.

2.2.4. Recombinant VACV (v300 and v3) construction details

The construction of these viruses was based on the methods published by Blasco and Moss (1995). This involves the use of a virus with a faulty gene (ΔF13L) which renders it unable to produce large plaques. The plasmid used for the recombination (pRB21- ampR) includes a complete copy of the F13L gene, so any virus that takes up the plasmid will be able to produce large plaques. The gene of interest is inserted under the control of the synthetic early/late poxvirus promoter (Blasco and Moss, 1995). When the gene is inserted into the plasmid and recombinant virus is made, upon infection with the recombinant virus the gene of interest will be transcribed along with the F13L gene. In the case of v300 virus the eGFP gene was inserted into the pRB21 plasmid to produce the plasmid p300 (figure 2.4). For v3 virus the firefly luciferase gene was inserted in order to produce the plasmid p240 (figure 2.5). This plasmid was also used for the transcription reporter assay (chapter 4, section 4.3.3).

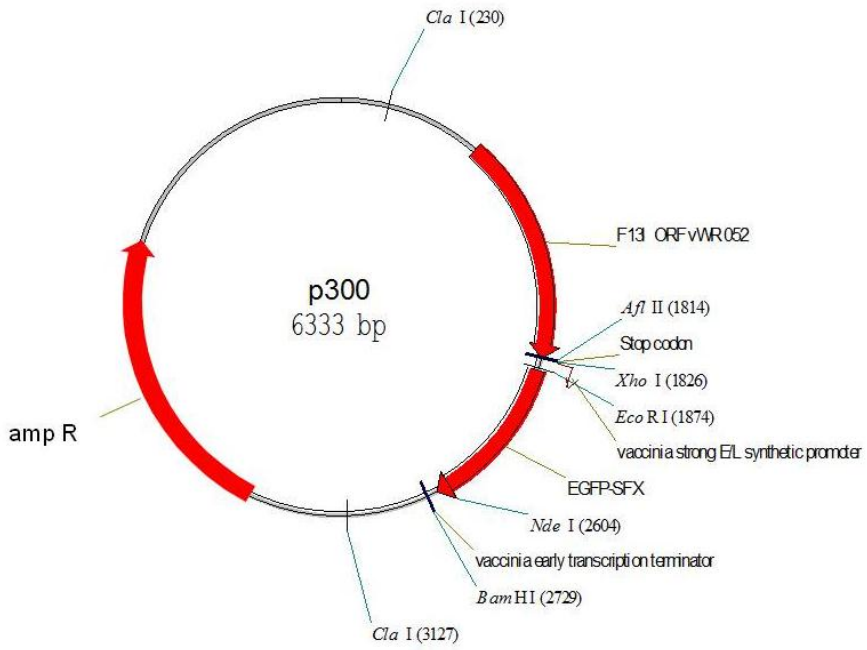

Figure 2.4 Plasmid p300 produced from pRB21 with the eGFP gene inserted used to produce v300 strain of VACV. The plasmid also contains an ampicillin resistance gene for selection.

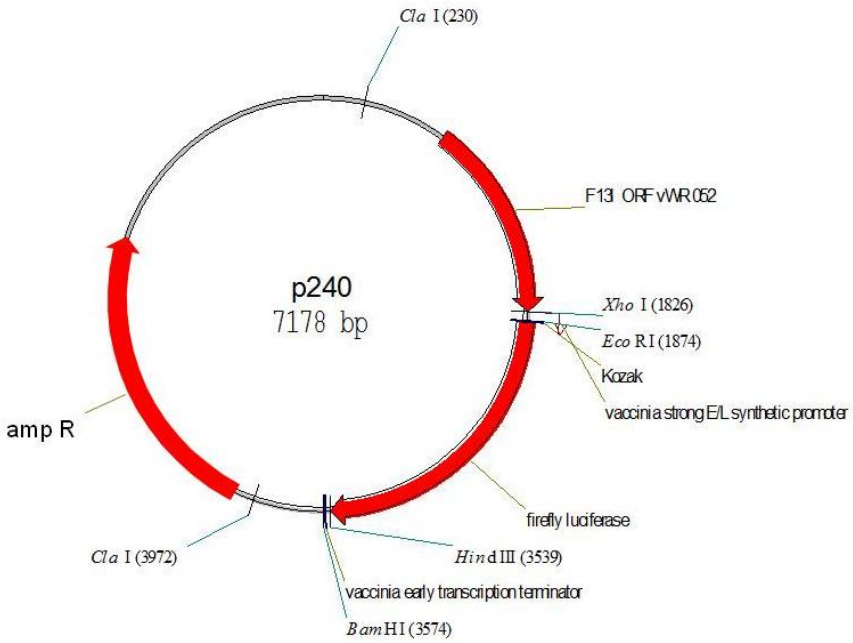

Figure 2.5 Plasmid p240 produced from pRB21 with the firefly luciferase gene inserted to produce v3 virus. The plasmid also contains an ampicillin resistance gene for selection.

2.2.4.1 PCR – gene of interest

For the v300 virus, the eGFP gene was amplified by PCR from the plasmid pIRESneo eGFP, using primers designed to contain the restriction sites EcoRI and NdeI (Table 2.1). The PCR reaction consisted of 40 µL H_2O (sterile injection water; BRAUN), 5 µL 10X Buffer I (Accuprime), 2 µL nucleotides (TaKaRa), 1 µL template (pIRESneo eGFP; 0.01ug/ul), 0.5 µL of each primer (5' primer Eco-K-eGFP and 3' primer Nhe-pst-V5S-ndeI-egfp; shown in table 2.1) and 0.5 µL Taq polymerase (Accuprime-INVITROGEN). The cycling conditions used were two minutes at 96^{o}C followed by 25 cycles of one minute 96^{o}C, two minutes at 55^{o}C and three minutes at 72^{o}C. Loading dye (15 µL) was added to the PCR product and analysed and purified using a gel prep kit (see section 2.2.4.2.2).

Primer	Sequence
5’ primer Eco-k-egfp	5‘-CTTCGTgaattcGCCACCATGGTGAGCAAGGGCGAGGAG
3’ primer Nde-pst-V5S-ndeI-egfp	5'-CTTCGTGCTAGCCTGCAGTTACGTAGAATCGAGACCGAGGAGAGGGTTAGGGATAGGCTTACCTTTTTCGAACTGCGGGTGGCTCCAcatatgCTTGTACAGCTCGTCCATGCCGAG- egfp

Table 2.1 The sequences of the primers to amplify the GFP gene for the construction the v300 virus. The restriction sites are underlined and in lower case.

2.2.4.2. Digestion

The PCR product (5 µL) and plasmid vector pRB21 (5 µL) were each analysed and purified from an agarose gel using a Qiagen gel extraction kit (section 2.2.4.3). Both the PCR product and plasmid vector were digested with the restriction enzymes EcoRI and NdeI (2 µL each; 10 U/µL) in 10X SURECUT buffer A (5 µL; ROCHE) in a total volume of 50 µL (using 36 µL injection water) , incubated at 37^{o}C for two hours. This was mixed with 15 µL loading buffer and analysed on a gel. The bands were again gel purified (QIAquick- Qiagen protocol, section 2.2.4.3), to remove small DNA fragments, and ligated following the protocol in section 2.2.4.4.

2.2.4.3 Gel electrophoresis and purification

In order to asses that the correct DNA was present at each stage of the cloning process, the samples were seperated by gel electrophoresis. The DNA samples were inserted into the wells of a 2% agarose gel housed in a vertical gel electrophoresis instrument (Hoeffer-Pharmacia) with 1X electrophoresis buffer used as the running buffer. Molecular weight ladders (1kb and 100bp) (Fermentas) were also loaded into the gel as markers. The running of the gel took ~60-90 minutes at 100V. Ethidium bromide solution (20 µL of 200 µg/mL solution in a tray of distilled water) was used to stain the DNA for a couple of minutes and the gel was viewed using a BIORAD UV transilluminator.

After PCR amplification and digestion of the DNA, a gel extraction kit was used to purify the required DNA. The samples were run on a 6 well vertical gel. In order to ensure that the purified DNA was not damaged, the following steps were taken to ensure that the required product was not exposed to UV and Ethidium bromide. The two centre wells were used for the DNA ladders (1kb and 100bp) while the adjacent wells were loaded with 10% of the DNA sample. Meanwhile the two outer wells were loaded with the remaining 90% of the sample. Before staining with ethidium bromide the two outer lanes were cut off the gel. The rest of the gel was stained and the bands resulting from the 10% of PCR product were used to assess the location of the required DNA. Based on this location, the remaining 90% of the DNA samples was then excised and purified using Qiagen gel extraction kit. After cutting the required sections out of the strips, they may then also be stained and viewed to ensure that the required DNA has been removed successfully.

2.2.4.3.1 Stop buffer: 50% Sucrose (Sigma), 7 M Urea (Sigma), 0.1 M EDTA (Fisher-scientific), 0.01% Bromphenol blue (Sigma).

2.2.4.4 Ligation

The digested PCR product and the vector were ligated together. This involved mixing 5 µL of the digested PCR product, plus 1 µL of the digested plasmid vector, and 2 µL glycogen with 100 µL -20^{o}C ethanol. This mixture was centrifuged for 15 minutes at 13 000 rpm, to pellet the DNA and bring the vector and insert into close proximity. The ethanol sn was discarded and the pellet was incubated at 50^{o}C for 5 minutes to dry. The pellet was resuspended in 10 µL ligation mix consisting of 1 µL T4 DNA ligase (Invitrogen), 2 µL 5X T4 DNA ligase buffer (Invitrogen) and 7 µL sterile injection water. The ligation reaction was stored overnight at 4^{o}C.

2.2.4.5 Transformation

The product of the ligation was used to transform chemically competent Top10 bacteria (One Shot TOP10 chemically competent E.Coli; Life Technologies) by heat shock transformation. This method involved thawing the bacteria slowly on ice, then adding 5 µL of ligated DNA to the cells on ice. The tube was placed on a heat

block at 37^{o}C for 5 minutes and returned to the ice for 5 minutes. SOC buffer (250 µL) was added to the cells and they were left to recover on the heat block at 37^{o}C for one hour. The transformed bacteria (100 µL) were spread onto an Ampicillin (Sigma; 1 µL/mL of 100mg/mL stock) LB (Sigma) agar (Merck) plate and 50 µL was put into a bijou containing 1 mL LB broth containing Ampicillin. This acted as a control in case no colonies grew on the plates. The plates and the bijou were incubated overnight at 37^{o}C and subsequent plate colonies were picked and grown up in 10 mL LB containing Ampicillin at 37^{o}C overnight. One mL of the transformed bacteria from the grown up cultures were frozen for storage on beads (Cryobank) at -20^{o}C. Plasmid from the remaining 9 mL of bacteria was purified using the MiniPrep kit (Qiagen).

2.2.4.6 Preparation of agar plates and liquid bacterial growth medium:

Agar plates were prepared by dissolving agar base (7.8g) in 200 mL of distilled water. The solution was sterilised in an autoclave at 121^{o}C for 20 minutes. The agar was cooled in a water bath for 20 minute at 45^{o}C, before adding ampicillin (1 µL/mL of 100 mg/mL stock). 20 mL was poured into each 8.25 cm plastic disposable plate. The plates were left overnight to cool and set before storing at 4^{o}C.

Liquid bacterial growth broth- Luria Bertani (LB; Sigma) was prepared by diluting the recommended volume in distilled water. This was sterilised by autoclaving at 121^{o}C for 20 minutes and was stored at room temperature. Ampicillin was added to the required amount of LB broth prior to use.

2.2.4.7 Amplification and Purification of Plasmid DNA

Purification of the plasmid DNA from the grown up bacteria was carried out using a MiniPrep kit (Qiagen). Further stocks of the plasmid could be produced by growing up one bead in 10 mL/100 mL LB containing Ampicillin at 37^{o}C overnight in a shaking incubator and purified using the QIAprep spin miniprep kit or Qiagen plasmid midi kit (100) (Qiagen).

2.2.4.8 Transfection/Infection

This plasmid was used to transfect BSC-1 cells in 6-wp. For the transfection (200 µL) Opti-MEM reduced serum medium (Gibco Invitrogen) was used to dilute (2 µg) plasmid DNA (p300/p240). Turbofect *in vitro* transfection reagent (Fermentas) (4 µL) was then added to the diluted DNA. The transfection mix was incubated at room temperature in the dark for 15 minutes before spotting onto the cells. The cells were simultaneously infected with vRB12 virus and left to settle for 1 hour. The wells were then topped up with 2 mL per well of low melting point (LMP) agarose (Bio-Rad). The plates were left at room temperature for at least 30 minutes to allow the agarose to set, before being returned to the incubator. The cells were observed over a period of three days.

2.2.4.9 Plaque purification

Plaques that formed over three days contained the recombinant virus and were selected for purification. Using a 2.5 mL pipette, a plug of the LMP agarose at the location of a plaque may be removed from the plate. This was transferred into a sterile eppendorf tube containing 500 µL DMEM which was then frozen at -70^{o}C and thawed three times in order to release the virus particles from the agarose plug. The DMEM containing the virus was used to infect another 6-wp containing BSC-1 cells, and the process was repeated. This was done a total of three times to ensure that the final virus obtained was all recombinant from one clone. The final plug in 500 µL DMEM was used to grow up larger stocks of the recombinant virus using the method described in section 2.2.2.2.

2.2.5 VACV (v3) firefly luciferase assay

2.2.5.1 Optimisation of the v3 luciferase assay

Optimisation experiments were carried out to determine the most suitable conditions to obtain significant luminescence signals in the luciferase assays. The first of these was to find out what amount of virus should be added to obtain sufficient measurable signals. The background signals for cells that have no v3 virus is an average af around 500 relative light units (RLU). Bearing this in mind, the ideal

signals in the presence of the virus is at least a few thousand/ tens of thousands RLU. If the signals are reaching the levels of hundreds of thousands then there is a risk of exceeding the maximum readable signal. The settings used for reading the luminescence signals lead to a maximum possible reading of just under 2 million. It was found that using an moi of 0.2 of the v3 (grown in HeLa cells) infecting RK13 cells was sufficient to produce a signal in the range of around 25 thousand RLU (figure 2.6), which is around 50 times greater than the background signal (~500 RLU). Using a small moi in the luciferase assays has the added benefit of conserving the virus stocks. For this reason it was possible to use the same batch of the v3 grown in HeLa cells for all of the luciferase antiviral assays. This reduced the chance of error between experiments due to subtle variation between virus stocks.

The optimum collection time for the luciferase assay has previously been determined by this group (data not shown). It was found that two hours was sufficient to produce a suitable signal from the v3 virus. This collection time has other advantages as it focuses solely on the early stage of the VACV lifecycle, i.e. cell entry and early viral transcription. Another benefit is that the assay has a short turn-around time, producing results within a single day. Also, the 96-wp format of the assay ensures that it is possible to test the effect of several compounds against VACV simultaneously. This assay became the standard first step for testing new ddBCNA compounds. Those that did not display improved activity against VACV at this stage were not selected for further study.

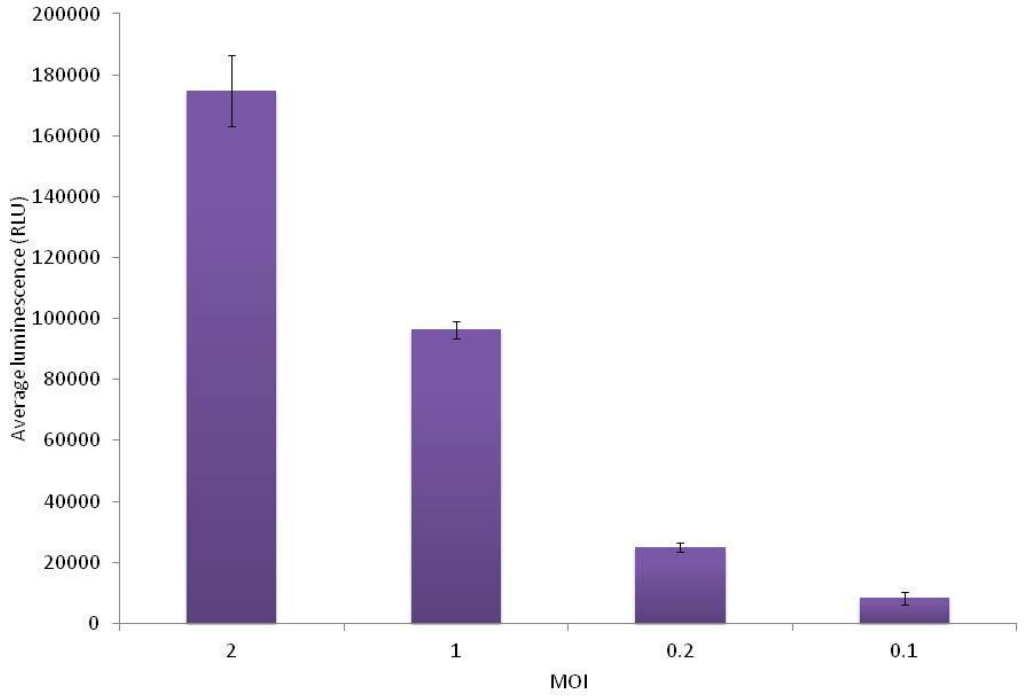

Figure 2.6 The luminescence signals from v3 (HeLa) at different moi after two hours in RK13 cells. Error bars ± 1 standard deviation.

2.2.6 Microscopy methods

2.2.6.1 Fixing cells for staining

After the required experiment had been performed, cells were fixed onto coverslips by removing the medium and applying 500 µL/well 3% paraformaldehyde (PFA; Sigma) for 15 minutes. This was then removed and the cells were washed two times with PBS and stored at 4°C until staining.

2.2.6.2 Cell staining and mounting onto slides

Coverslips were initially placed face down onto 100 µL blocking buffer (section 2.2.6.2.1) on a sheet of parafilm (Sigma) in a box and left to block for 30 minutes at 37^{o}C. They were then transferred to a box containing a new sheet of parafilm with 100 µL/coverslip of the primary antibody at the recommended dilution in blocking buffer and left to attach at 37^{o}C for 1 hour. The coverslips were dipped into a beaker of PBS to wash off the excess primary antibody while the excess PBS was

carefully removed from the coverslip using a tissue. The coverslips were then placed into another box with fresh parafilm with 100 µL/ coverslip of the required secondary antibody at the recommended dilution in blocking buffer. These were then left at 37^{o}C to incubate for one hour. The coverslips were rinsed again by dipping them into PBS, the excess PBS was removed from the coverslips by dabbing the edges with a tissue. Slides were prepared by placing 3 µL of Vectashield containing DAPI (Vector laboratories) onto them. The coverslips were then placed cells down onto the Vectashield on the slide. The coverslips on the slides were left for 5-10 minutes to dry before the edges were sealed using clear nail varnish. These were allowed to dry before storage at 4°C. The coverslips were analysed by fluorescence microscopy.

2.2.6.2.1 Blocking buffer

Solution A: 100 ml PBS was used to dissolve 1.5 g Tris (Fisher-Scientific), the pH was adjusted with 2N HCl (Sigma) to pH 7. Then 1.45 g NaCl (Sigma) was added followed by 0.46 g EDTA (Fisher-Scientific). 125 µl Tween 20 (Fisher-Scientific) was added using a 200 µl pipette with the end of the tip cut off (because Tween 20 is a viscous liquid which does not pipette easily with a narrow tip). The solution was stirred using a magnetic stirrer until it had completely dissolved. Solution B: 125 ml of 1X PBS was heated separately in a 45^{o}C water bath. Then 5 g bovine serum albumine (fraction V; Sigma) was added followed by 0.625 g gelatine (Sigma). The solution was stirred until dissolved.

Solutions A and B were combined and topped up to 250 mL with 1X PBS. This was run through a NALGENE sterile filter (250 ml set) and stored in a sterile T75 cell culture flask.

Chapter Three – ddBCNA structure activity relationships against Vaccinia virus

3.1 Introduction

The novel compounds (ddBCNAs) used in this PhD project were synthesized from D-IddU (for the D-ddBCNAs) using the Sonogashira reaction method, or from L-arabinose (for the L-ddBCNAs) through 6 reaction steps to produce L-IddU. The required L-ddBCNAs were then produced from the L-IddU using the same method as for the D-ddBCNAs (McGuigan et al. 2013). The ddBCNAs were produced by the McGuigan group at the the School of Pharmacy and Pharmaceutical Sciences of Cardiff University. Previous nucleoside analogues had been shown to have antiviral activity (McGuigan et al. 2004). The ddBCNAs tested here are based on these original analogues but have been modified in an attempt to improve activity. The first ddBCNA compound found to show activity against hCMV was Cf1821, a D-ddBCNA with the side chain C10 (McGuigan et al. 2004). The structure of Cf1821 was further optimised to produce the compound Cf2095, also a D-enantiomer but with the side chain C9-O-C5. This modification improved the activity against hCMV. Cf2095 was then produced with the same general structure but in the L-enantiomer form. This was named Cf2642 and no longer displayed antiviral activity against hCMV. Critically however, it did show considerable activity against VACV (McGuigan et al. 2013).

The first aim of this project was to confirm and quantify the activity of Cf2642 against VACV. Furthermore, alternative L-enantiomer ddBCNAs (produced by the McGuigan group) were tested in order to determine if the structure of the ddBCNAs could be optimised to increase the antiviral effect against VACV. As such, another aim of this chapter was to test novel ddBCNA structures and compare the activity of the novel L- and D-enantiomers with the activity of a selection of D-enantiomers that had previously been produced by the McGuigan group.

Initially steps were taken to determine the optimum conditions for antiviral experiments and for the preparation of viral stocks for use in them. These optimisation experiments are described in chapter 2 (sections 2.2.2.1, 2.2.3.1 and 2.2.5.1). The initial testing method for any newly produced ddBCNAs was the luciferase assay using v3 (VACV modified to express firefly luciferase; details in chapter 2, section 2.2.4) that produces firefly luciferase under the control of a synthetic early/late poxvirus promoter (Blasco and Moss, 1995). Using the luciferase assay, structure activity relationships (SAR) were established for the L-ddBCNAs based on the length of their alkyl/ether side chains. The SAR was used to gain information about how the structure of the ddBCNAs relate to its antiviral activity. This was used to determine which specific parts of a molecule were responsible for the activity and to inform further optimisations.

The luciferase assay was also used to compare the activity of the lead compound (Cf2642) against VACV in a variety of different cells lines. The aim of said experiment was to determine if the compound could inhibit the virus in a selection of different cellular hosts (of both human and animal origin), and if so, to what extent.

A ToA assay was carried out using a luciferase reporter assay. This was done to determine the amount of time that the addition of the drug may be delayed before the antiviral effect can no longer be observed, i.e. to determine if the compound remains active against VACV if added at a later stage during viral infection.

Plaque assays (carried out over 4 days) were used to determine if the ddBCNAs inhibited plaque formation by VACV. The effect of the active ddBCNAs could be seen as a reduced plaque size phenotype. Plaque sizes were measured and used to calculate IC_{50} concentrations against VACV for the compounds. The IC_{50} of a given compound is the concentration at which the compound inhibits the viral activity by 50%, i.e. in this case the concentration at which the size of the plaque size reduced by 50% of the no drug control. An SAR was established for the selected L-ddBCNA

compounds based on their IC_{50} concentrations (section 3.3.5). This SAR was compared to the luciferase SAR for the same compounds.

Wide field fluorescence microscopy was carried out on BSC-1 cells that had been infected with vYFP-A3L and either treated with Cf2642 or left untreated. The cells were then imaged in order to accurately visualise the effect of the ddBCNAs on the virus during plaque development.

3.2 Materials and methods

3.2.1 Luciferase assay

RK13 cells were seeded into 96-wp and left overnight to settle and reach confluency. Cells were treated 30 minutes prior to viral infection, with each of the ddBCNAs at 10 µM and a no drug (DMEM only) control in triplicate, v3 was then added to the wells at a multiplicity of infection (moi) of 0.2. Cells were collected 2 hours post infection (pi). The cell supernatant was removed and 100 µL of 1 × cell culture lysis reagent (CCLR) (Promega, Madison, WI) per well was added before the plate was agitated on an orbital shaker for 15 minutes. The plate was then frozen and stored at −20 °C. After thawing, 20 µL of each of the samples was transferred to a black 96-wp (NUNC, Roskilde, Denmark) and processed with 10 µL of the luciferase assay substrate and buffer II (Promega, Madison, WI). The luminescence, as relative light units (RLU) was measured in a 96-well luminescence plate reader (FLUOstar OPTIMA FL, BMG Labtech). The percentages of the treated versus the no drug control readings were calculated.

This method was based on the technique known as poxvirus infection luciferase assay (PILA), described previously by Levy et al. (2010), however instead of using the transfection reporter system and transfecting the cells with the plasmids containing the luciferase gene, the VACV itself was modified to contain the firefly luciferase gene (v3), giving a direct firefly luciferase signal on viral entry into the cell. This eliminated the need for a Renilla control plasmid that is typically used to indicate the level of transfection.

3.2.2 Cell range assay

A range of different cells were seeded in a 96-wp at $5x10^4$ cells per well (6 wells of each cell type were plated). The cells selected included a range of human epithelial and fibroblast cells as well as cell lines derived from animals, in order to provide further information about the activity of Cf2642. The cells used were human epithelial- (HUH7, A431, A549, HeLa and HaCaT), human fibroblast (HFF, HFFFtc and BJ-1), marmoset B lymphocyte (B95a), monkey epithelial (BSC-1, Vero and CV-1) and rabbit epithelial cells (RK13) (full details of all cell lines are given in chapter 2, section 2.1.1).

The panel of cells were treated 30 minutes prior to infection with 10 µM Cf2642 or left untreated in triplicate. The cells were then infected with v3 at an moi of 0.2. The cells were collected 2 hours pi (medium was removed and replaced with 100 µL per well of 1 x CCLR, shaken for 15 minutes on an orbital shaker and then frozen at -20^{o}C). The effect of the drug in each of the cell types was calculated as a percentage of the readings in the absence of drug.

3.2.3 Time of Addition assay

RK13 cells were seeded into a 96-wp and left overnight to settle and reach confluency. These were then treated in triplicate with 10 µM of Cf2642 at a range of times in relation to the time of infection (T_0). These times were 30 minutes before infection and 2 hours, 4 hours, 6 hours, and 8 hours pi. A second 96-wp plate of RK13 cells was treated in the same way but with DMEM in place of Cf2642 – this plate acted as a control. This was carried out to compensate for the effect of the change in the volume at each of the time points. All cells were then collected 12 hours pi. The medium was removed and replaced with 100 µL per well of cell (1 x CCLR), shaken for 15 minutes on an orbital shaker and then frozen at -20^{o}C. Luminescence readings were measured using the 96-wp luminescence plate reader. The activity of the ddBCNAs was calculated as a percentage of the values measured for the DMEM control plate at each of the corresponding time points.

3.2.4 Statistics

In order to determine which compounds reduced the luciferase signal by a statistically significant amount as compared with the no drug control, P values were calculated. This was done by performing paired t tests using SPSS software that compared the luminescence readings (RLU) from each of the drug conditions with the equivalent no drug control readings.

3.2.5 Plaque size reduction assay

BSC-1 cells were seeded in 24-wp and left overnight to settle and reach confluency. These were pre-treated with a series of dilutions of drug (50, 5, 0.5, 0.1, and 0.05 µM) as well as a no drug control, in quadruplet. These were then infected with ~20 plaque forming units (pfu) of v3 per well. The plate was centrifuged at 5000 rpm for 15 minutes, and the virus was allowed to adsorb onto the cells for 45 minutes. The drug and the virus were removed and replaced with 0.5 mL DMEM containing the drug at double the required concentration. This was diluted to the required concentration by the addition of 0.5 mL Avicel overlay (50% Avicel, 50% DMEM containing 1% P/S). The plates were incubated for 4 days and were then rinsed 2 x with 1 mL/well PBS and stained with 400 µL/well crystal violet stain for 4−6 h. The plates were submerged in water to remove the crystal violet stain and left overnight to dry. After drying the plates were scanned at 600 dpi and the area of each plaque was measured individually using Image J software. Cidofovir (a viral DNA polymerase inhibitor) and AraC (a DNA synthesis inhibitor) were included in the assays as positive controls.

3.2.6 IC_{50} calculations

An IC_{50} concentration of a compound is the concentration of that compound that inhibits the viral activity by 50%. In this case IC_{50} values were defined as the concentration of ddBCNA that reduced plaque size (area, measured in pixels) by 50% in comparison to cells infected in the absence of antiviral. The final IC_{50} values for all virus/antiviral combinations are each calculated as the mean of three repeats. IC_{50} values were calculated for each drug using the GraphPad Prism

software (GraphPad Software, Inc.). In this software the log of the concentrations was entered plus the average plaque size for each concentration. Since the log of 0 cannot be defined, a theoretical concentration was used for the untreated cells i.e. in this instance the concentration was entered as -4, the log of 0.0001 (µM).

3.2.7 Wide field fluorescence microscopy

BSC-1 cells were seeded onto 12-wp containing coverslips and left overnight to settle and reach confluency. These were infected with ~20 pfu/well of vYFP-A3L and half were treated with Cf2642 at 50 µM, while the other half were treated with a DMEM (no drug) control. One of each of the treated and untreated coverslips was fixed after one day, two days and three days. The cells were stained with phalloidin-594 to visualise the actin cytoskeleton (in red) and mounted onto slides using Vectashield containing DAPI to visualise the nuclei (in blue). The edges of the coverslips were sealed using clear nail varnish. The cells were imaged using the wide field fluorescence microscope and images were taken of each of the conditions. The exposure time required to visualise the virus was 1000 ms in the presence of the drug and 400 ms in its absence.

3.2.8 Pilot *in vivo* assay

The *in vivo* assay was carried out by Dr J Bugert and Dr A Ager, under the home office project licence of Dr A Ager (PPL no. 30/2635). The experiment was designed with the aim of determining if the lead compound Cf2642 could reduce the level of VACV infection in mice. The experiment involved the use of 24 black-6 female mice, three mice were used for each infection/treatment condition. The 8 conditions are summarised in table 3.1. The drug or control, as well as $2x10^6$ pfu of v3 (grown in TK- cells), were injected into the peritoneal cavity of the mice. Cf2642 was dissolved in DMSO and mixed with the virus prior to the injection. After 3 days the mice were euthanized and the ovaries were collected for testing. During VACV infection of mice the virus accumulates in the ovaries. Therefore the reason for collecting these was to see if the level of virus accumulation was reduced by Cf2642. One ovary from each mouse was dounce homogenised. Samples of each were then used to

infect a 96-wp of RK13 cells. These were collected after two hours as described for other luciferase assays (section 3.2.1) and luminescence readings were taken.

Condition number	Virus added	Drug added (mg/kg)
1	$2x10^6$ v3 (TK-)	No drug
2	No virus	No drug
3	$2x10^6$ v3 (TK-)	Cf2642 (10)
4	$2x10^6$ v3 (TK-)	Cf2642 (50)
5	$2x10^6$ v3 (TK-)	Cf2642 (100)
6	No virus	Cf2642 (10)
7	No virus	Cf2642 (100)
8	No virus	Cidofovir (50)

Table 3.1 The 8 conditions used in the pilot *in vivo* assay. The other columns indicate which mice received virus and which received drug (concentrations bracketed).

3.3 Results

3.3.1 Activity of ddBCNAs against VACV as determined by luciferase assay:

3.3.1.1 Activity of D- versus L-ddBCNAs

Early attempts at modifying the structure of the ddBCNAs to improve activity involved producing alternative compounds with D-chirality. However, recently L-enantiomers have been studied and found to have increased activity against VACV (McGuigan et al. 2013).

All ddBCNA compounds produced were tested using a two hour luciferase reporter assay with v3 in RK13 cells. This method provided an indication of how active these compounds were against VACV. Critically for experiment planning, the output of this assay was rapid (less than one day) (as described in section 3.2.1).

The readouts determined which of the compounds would be further investigated for activity. The results also allowed for optimisation of the structure since the most

active compounds provided a base to work from in any attempts to improve the structure further.

Initially, two L-ddBCNAs (Cf2642 and Cf2644), the original D-enantiomer lead Cf2095, and a series of 12 newly synthesised D-compounds were tested. The structures of these compounds are described in figure 3.1 and table 3.2. The compounds were applied to the cells at a concentration of 50 µM which was sufficient to ensure that the maximum effect of each could be established.

The resulting data (figure 3.2) indicated that the two L-compounds (Cf2642 and Cf2644) displayed the greatest reduction in the luciferase activity of v3 in RK13 cells over the course of two hours. Cf2642 caused a reduction in signal from v3 to just 20% of the luminescence signals generated in the no drug control. The reduction caused by Cf2644 was similar (~25%).

Despite being inferior to the reduction observed with the L-compounds, some D-compounds (with alternative modifications) did show improved activity against VACV ($P < 0.05$) as compared to the original D-compound Cf2095. For example, Cf2762 reduced the luciferase signal to ~40% of that of the no drug control ($P < 0.01$) whilst Cf2095 reduced the signal to only ~75% ($P < 0.05$).

The clear difference in activity between the best of these D-compounds compared to the L-compounds led to the decision that further synthesis of compounds would focus on the L-enantiomer form of drug, with the structures of the lead L-ddBCNAs Cf2642 and Cf2644 acting as the baseline for further optimisation i.e. the new compounds produced were similar to Cf2642/Cf2644 but had subtle alterations (for example, increasing/decreasing the number of carbon atoms in the hydrocarbon side chain). The subsequent compounds were tested in parallel to establish SAR.

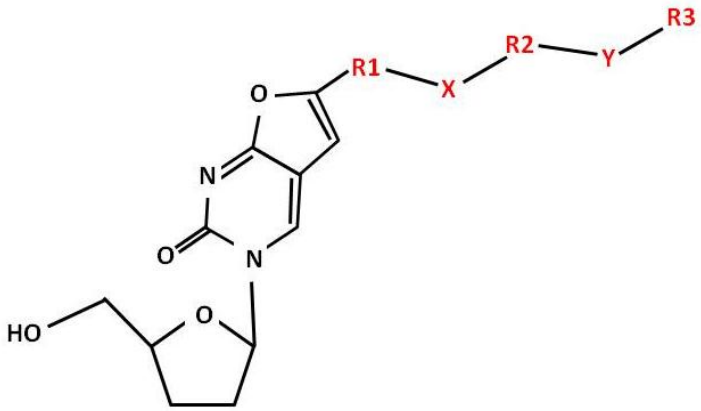

Figure 3.1 The main chemical structure of the ddBCNAs. Variable sections are indicated in red and the modifications at each of these sections are described in table 3.2.

CF	Chirality	R1	X	R2	Y	R3
2642	L	C9	O	C5	-	-
2644	L	C10	-	-	-	-
1821	D	C10	-	-	-	-
2095	D	C9	O	C5	-	-
2641	D	C5	O	C4	O	C4
2643	D	C9	S	C5	-	-
2645	D	C2	O	C12	-	-
2653	D	C4	O	C10	-	-
2749	D	C9	O	C5	-	Ph
2750	D	C9	O	C4	-	Ph
2754	D	C9	O	C4	-	CHex
2755	D	C9	O	C2	-	2-Nap
2756	D	C9	O	C2	-	PClPh
2760	D	C9	O	C3	O	Bn
2762	D	C9	O	C2	-	mClPh
2779	D	C9	O	C2	-	pBrPh

Table 3.2 The structure of the side chains of the ddBCNAs.

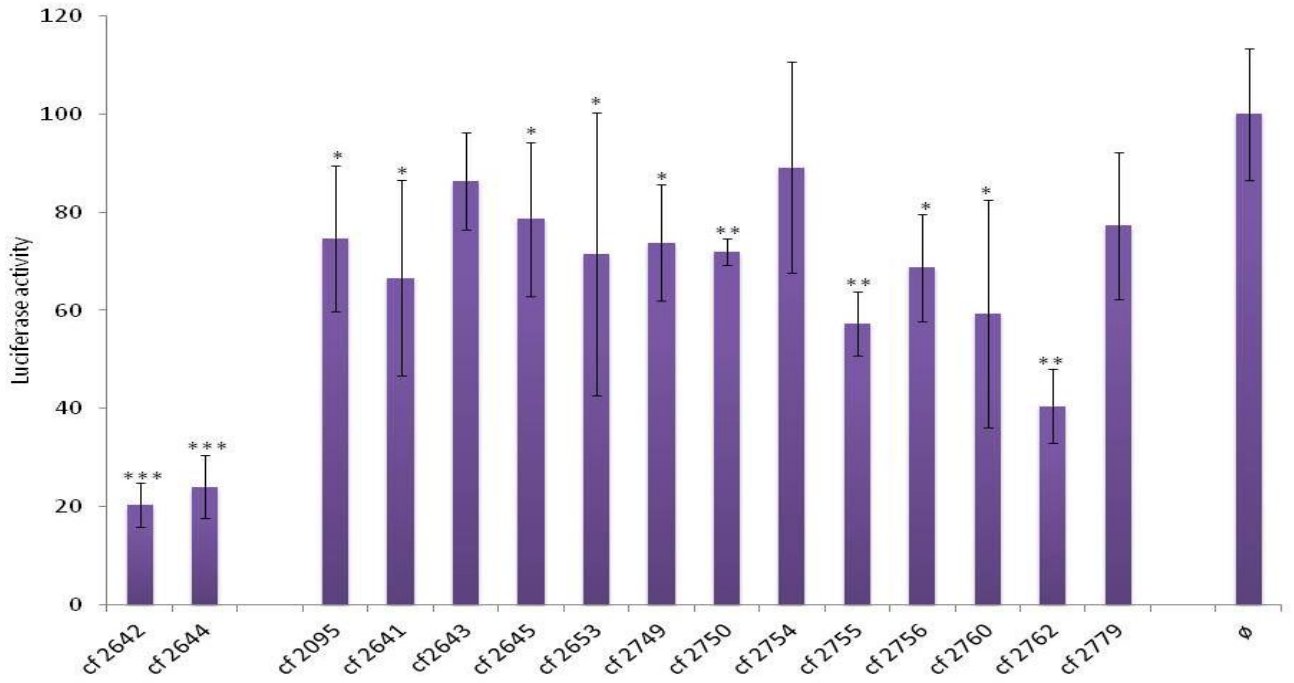

Figure 3.2 Luciferase signals for two L-ddBCNAs and 13 D-ddBCNAs as compared to a no drug control (Ø) Average of 3 independent luciferase assays as a percentage of the signal generated with the no drug control. Infection with v3 at moi 0.2 in RK13 cells pre-treated for 30 minutes with each of the compounds indicated in the graph at 50 µM. Collection at 2 hour pi. Error bars ± 1 standard deviation. * P <0.05, ** P <0.01, *** P <0.001. Although visually the data suggests that the D-ddBCNAs are not having as much of an effect against the VACV than the L-ddBCNAs, only three of them fail to show a significant decrease in luciferase activity (Cf2643, Cf2754 and Cf2779). The remaining compounds correlate with varying levels of reduced signal (as indicated by decreasing P values). The compounds that reduce the virus to the greatest extent include both of the L-ddBCNAs described (Cf2642 and Cf2644). None of the D-ddBCNAs show as big an effect. However three of them (Cf2750, Cf2755 and Cf2762) do show improvement over the original D-ddBCNA (Cf2095).

3.3.1.2 Activity of L-ddBCNAs with alkyl and ether side chains

The first set of modifications made to the L-ddBCNAs used the structures of Cf2642 and Cf2644 (as described in section 3.3.1.1) as a base to work from. Cf2644 contains an alkyl side chain of 10 carbon atoms in length. Cf2642 contains an ether side chain with the structure C9-O-C5. The modifications made to these compounds were subtle and involved simply altering the length of the alkyl/ether side chain. In doing this an SAR could be established and the optimum side chain length could be determined. The basic structure of these compounds is shown in figure 3.3 and each of the modifications is listed in table 3.3.

Figure 3.4 indicates that L-ddBCNAs with alkyl and ether side chains have a clear SAR. There is a correlation between increasing length of the side chain and resulting activity levels of the compound. However, this correlation plateau's beyond an alkyl side chain length of 9 carbons. This is probably due to the fact that the lipophilicity of the compounds increases as the chain length increases and they become progressively harder to dissolve for experiments. The addition of an ether group to the side chain decreases the lipophilicity, thereby allowing for additional carbons to be added to the side chain.

The ether series of compounds all had 9 carbon atoms before the ether group. The number of carbons after the ether group was then altered to determine the SAR for the ether series. The series portrayed an SAR with the optimum length being 4/5 carbons after the ether group. The data also shows that the optimum ethers performed better than the optimum alkyls. Therefore it was decided that ethers would be used for further optimisation and testing against the viruses with particular focus on Cf2642/Cf3208.

To avoid bias, investigators were blinded to the structures of all compounds during the process of optimisation. Two of the older preparations of active L-ddBCNAs (Cf2642 and Cf2644) were included in the assay as positive controls. When the structures of the new compounds were revealed, it was found that the 'newly produced' Cf3208 had the same structure as the original lead Cf2642. As expected,

the activity levels of newly synthesised Cf3208 were similar to the levels observed for Cf2642 (an older stock). This was also the case with the alkyl series; Cf3155 had the same structure as the original compound Cf2644, and they both showed very similar activity. To avoid confusion from this point forward only the original names of these two compounds will be used, i.e. Cf2642 and Cf2644.

Using paired t tests in SPSS, P values were calculated for each of the compounds to determine which reduced the signal by a significant amount in comparison to the no drug controls. The compounds Cf3176 and Cf3156 were the only two that appeared to be inactive ($P > 0.05$). The remaining compounds showed significantly improved activity levels as compared to the untreated control - two compounds, Cf3177 and Cf3174, with P values less than 0.05 and all others with P values less than 0.01.

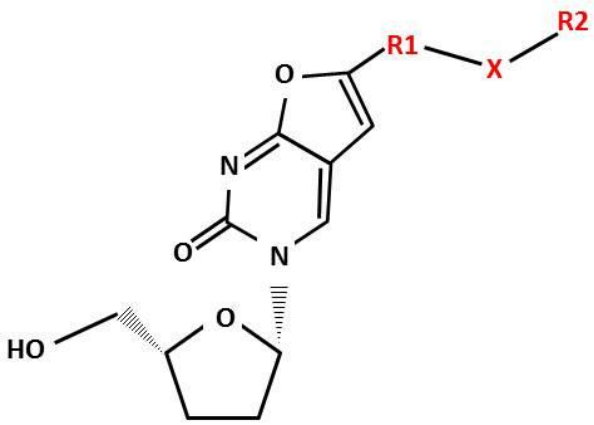

Figure 3.3 The main chemical structure of the L-ddBCNAs with alkyl and ether side chains. Variable sections are indicated in red and the modifications at each of these sections are described in table 3.3

CF	R1	X	R2
3176	Ph	-	C4
3177	Ph	-	C5
3153	C6	-	-
3174	C7	-	-
3154	C8	-	-
3175	C9	-	-
3155 (2644)	C10	-	-
3156	C12	-	-
3210	C9	O	C2
3204	C9	O	C3
3207	C9	O	C4
3208 (2642)	C9	O	C5
3209	C9	O	C6

Table 3.3 The structures of each of the side chains for the alkyl and ether series of L-ddBCNAs.

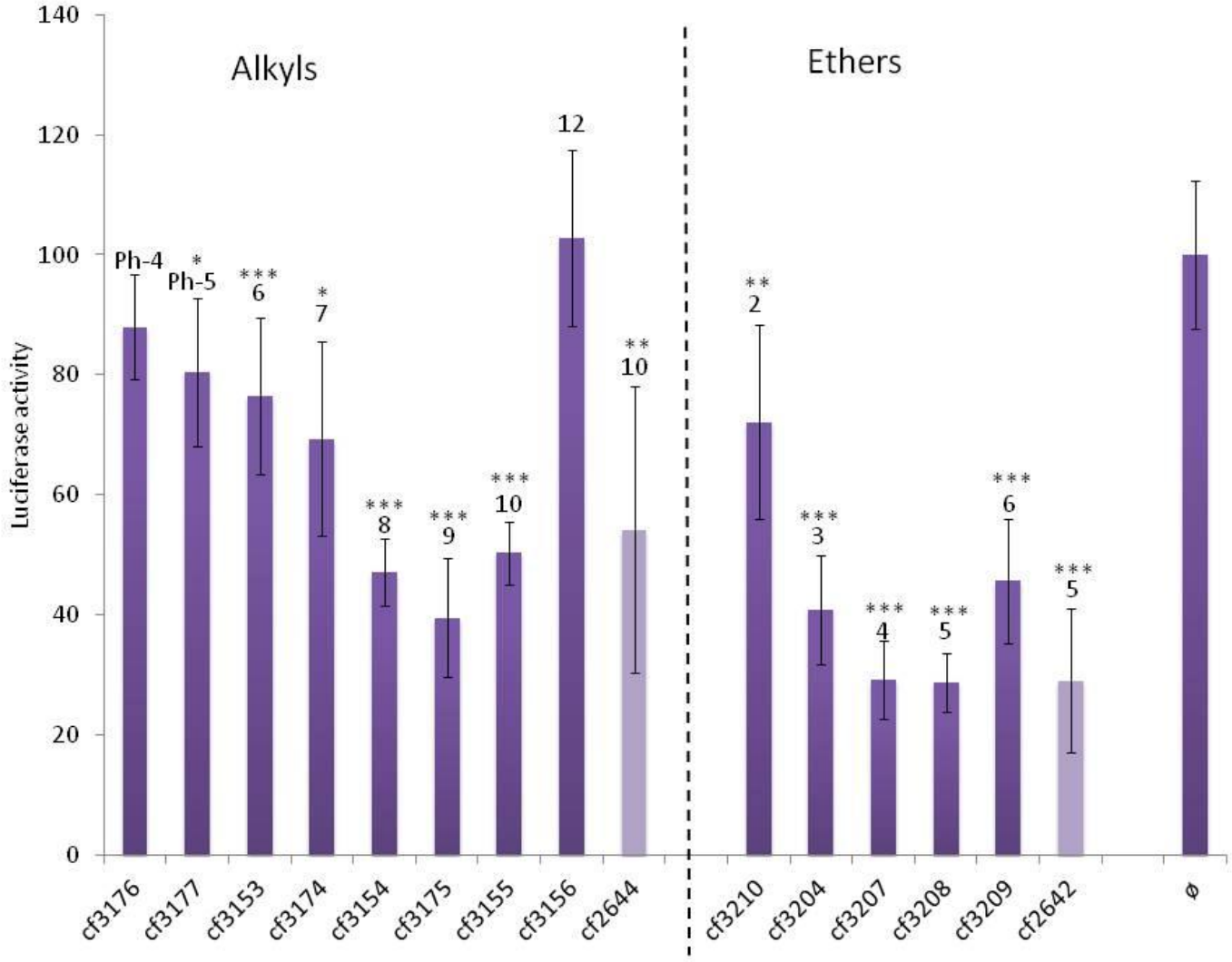

Figure 3.4 L-ddBCNAs with alkyl (left section) and ether (right section) side chains of increasing length. The length of carbon side chain is indicated above each bar. For the ether series the number above the bar represents the number of carbons after the ether group. Full structural information is provided in figure 3.3 and table 3.3. Lightly shaded bars represent the original L-ddBCNAs included as positive controls. These had matched structures in the newly produced series; Cf2644 and Cf2642 were identical to Cf3155 and Cf3208 respectively. As expected, these duplicates showed similar activity levels.

Luciferase assay in RK13 cells pre-treated with 10 µM of stated compounds and infected with v3 at moi of 0.2. Ø = no drug. Collection two hours pi. Error bars ± 1 standard deviation.

* P <0.05, ** P <0.01,
*** P <0.001

3.3.1.3 Activity of further modified L-ddBCNAs

The best performer at this stage was still Cf2642, a compound with an ether side chain C9-O-C5. As such this side chain structure was chosen as the basis for further modifications to the L-ddBCNAs. Of the resulting modified compounds, two maintained the same side chain structure but were altered elsewhere in the molecule, four maintained the same side chain length but had the ether group moved to an alternative position and four had branched groups added after the ether group. The structures of the modified compounds are summarised in figure 3.5 and table 3.4.

These compounds were all tested using a two hour luciferase assay in RK13 cells. It was found that, barring one compound (Cf3242) which reduced the luminescence signal to less than 20% of the no drug control, none of them displayed better activity against VACV than Cf2642 (figure 3.6). As discussed later in this chapter (section 3.3.5), Cf3242 was ruled out as a potential drug candidate due to its increased toxicity against the cells. Beyond the original leads Cf2642 and Cf2644, four of the new compounds (Cf3242, Cf3230, Cf3231 and Cf3232) reduced the luciferase signals to less than 50% as compared with the no drug control ($P < 0.001$). Of the remaining compounds, all showed a significant reduction in signal compared to the control (Cf3253, Cf3254, Cf3392 and Cf3332 $P < 0.01$; Cf3393 and Cf3458 $P < 0.05$).

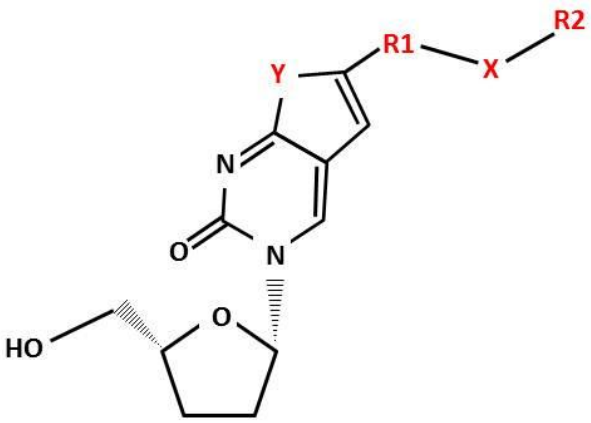

Figure 3.5 The main chemical structure of the L-ddBCNAs with further modifications. Variable sections are indicated in red and the modifications at each of these sections are described in table 3.4

CF	R1	X	R2	Y
3230	C8	O	C6	O
3231	C4	O	C10	O
3232	C1	O	C13	O
3242	C9	O	C5	NMe
3253	C9	O	C5	NH
3254	C13	OH	-	O
3392	C9	O	isobutyl	O
3393	C9	O	*sec*-butyl	O
3332	C9	O	isopropyl	O
3458	C9	O	*tert*-butyl	O

Table 3.4 The further modified L-ddBCNAs and their structures.

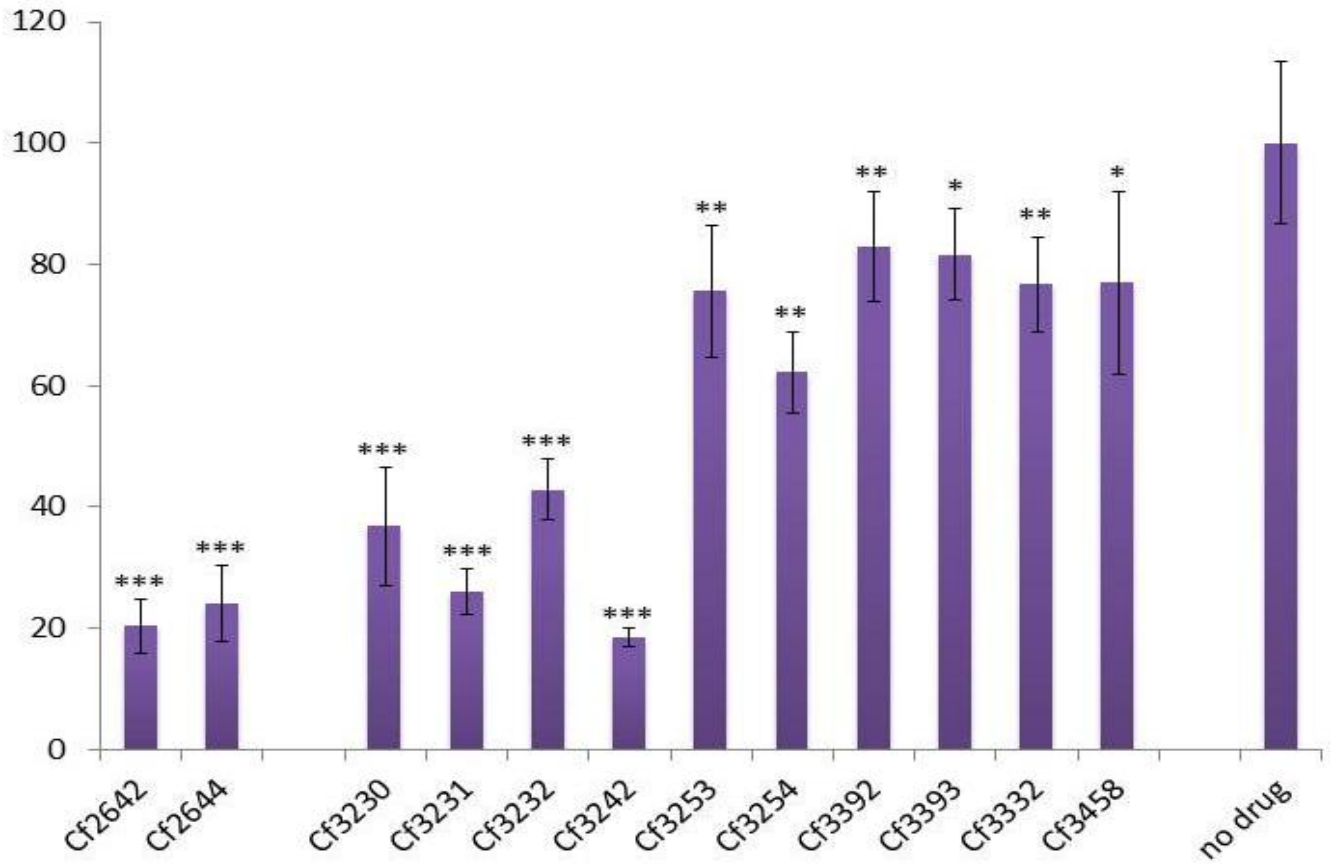

Figure 3.6 Luciferase assay in RK13 cells showing the luciferase activity of v3 in the presence of all further modified L-ddBCNAs (at 10 μM). Results are shown as a percentage of the no drug control readings. Cf3242 is the only other compound that showed greater antiviral activity than Cf2642. Error bars ±1 standard deviation. * P <0.05, ** P <0.01, *** P <0.001.

3.3.2 Activity of Cf2642 against VACV in alternative cell lines

The activity of Cf2642 was tested against v3 using a two hour luciferase assay in a variety of cell lines in order to ascertain how well it worked in an alternative host. A selection of human epithelial and fibroblast cells were tested as well as animal-derived cell lines (the nature of these cell lines are described in chapter 2 section 2.1.1). Cells were selected to cover a range of different human and animal origins in order to confirm an effect of the drug in relevant cell lines. The strength of the luminescence signals displayed in these cell lines are presented in figure 3.7A. The data indicate that there is considerable variability in the signals generated between the cell lines. Human epithelial HUH7 cells produced the largest luminescence signals whilst human fibroblast cell lines and monkey lymphocytic B95a cells gave the lowest luminescence signals.

In order to account for the variability in luminescence signals generated by the various cell lines, the readings for the cells containing Cf2642 were calculated as a percentage of control cells (of the same origin) that received no drug. This provided an indication as to how well the drug worked against the virus in each of the cell lines tested (figure 3.7B). It can be seen that there is some level of antiviral activity of the compound in each cell line and that this varies from cell to cell. Of note, however, is the fact that the differences between the readings in the presence and absence of Cf2642 were significant in all the cell lines tested (CV-1, BJ-1, HaCaT and B95a, $P < 0.05$; A431, A549, HUH7, HFF, HFFFtc, BSC-1 and Vero, $P < 0.01$; HeLa and RK13, $P < 0.001$). It is clear that the activity is highest in the RK13 cells. As such these cells were used for all downstream luciferase assays involved in compound optimisation.

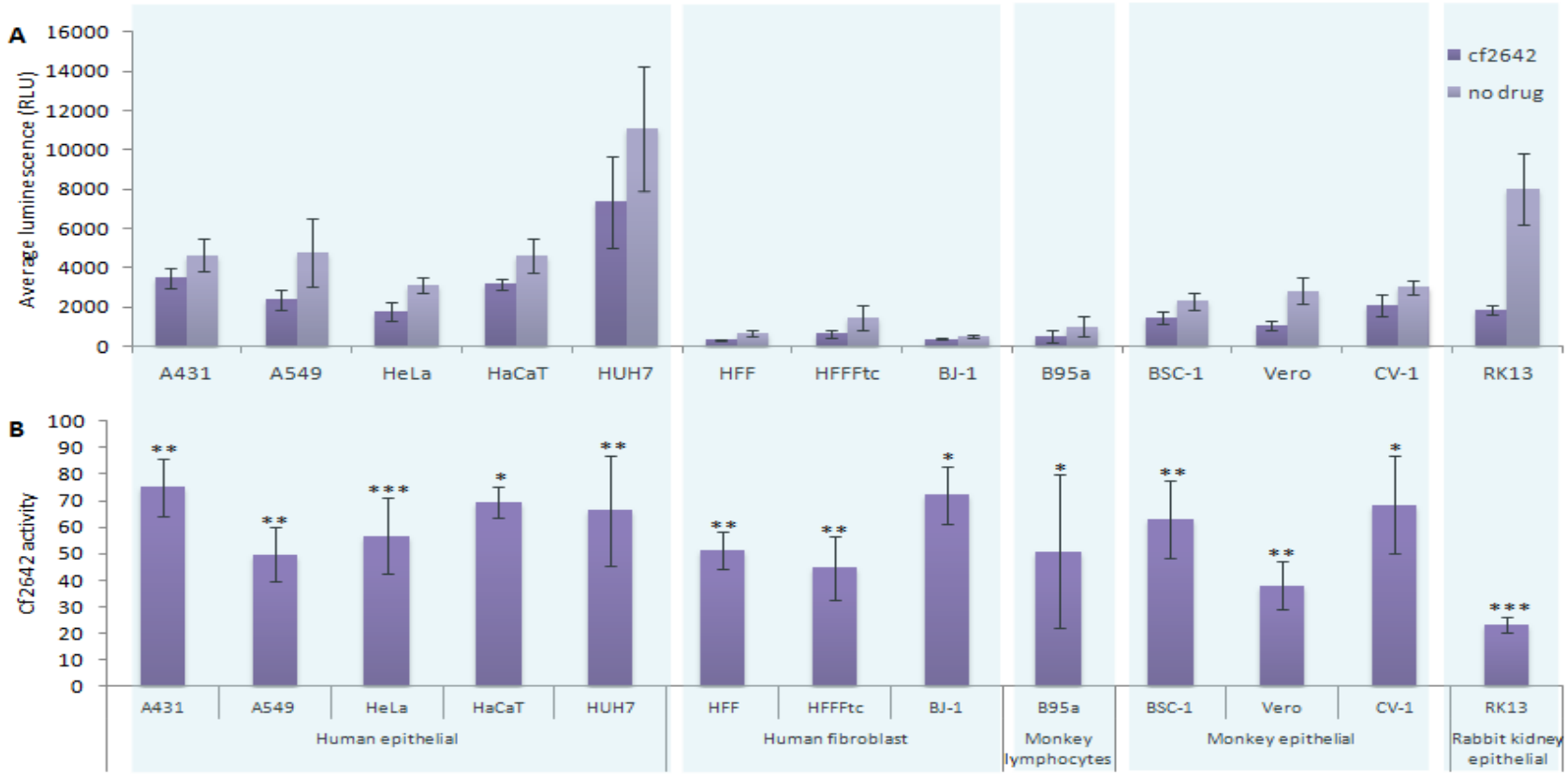

Figure 3.7 Luciferase assays displaying the effect of Cf2642 on v3 activity in different cells, including (human epithelial) A431, A549, HeLa, HaCaT, HUH7, (human fibroblast) HFF, HFFFtc, BJ-1, (monkey lymphocytes) B95a, (monkey epithelial) BSC-1, Vero, CV-1 and (rabbit epithelial) RK13. A: shows the average luminescence readings with and without drug. B: shows Cf2642 activity as a percentage of the no drug control. Error bars ± 1 standard deviation. * P<0.05, ** P<0.01, *** P<0.001.

3.3.3 Cf2642 time of addition luciferase assay

Another luciferase assay in RK13 cells was carried out in order to determine if the drug still had an effect on the virus when added at different stages of v3 infection. Cf2642 was added at a series of time points; prior to (30 minutes), at the same time as (To), and after viral infection (ranging from two to eight hours). Cells were collected for luciferase readings at 12 hours pi. The greatest effect on viral activity was observed when the drug was added before or at the same time as the virus (figure 3.8). However, the drug appears to still have an effect on the virus even when added 8 hours after the initial infection, as indicated by a ~50% reduction in the luminescence signal. Whilst the latter observation is non-significant ($P > 0.05$), the data is still suggestive of an effect. The results for the addition of Cf2642 at each of the other time points were statistically significant ($P < 0.01$). Of note, there is no statistical difference in activity between cells that were pre-treated, and those which had the drug added at the same time as the virus ($P = 0.937$).

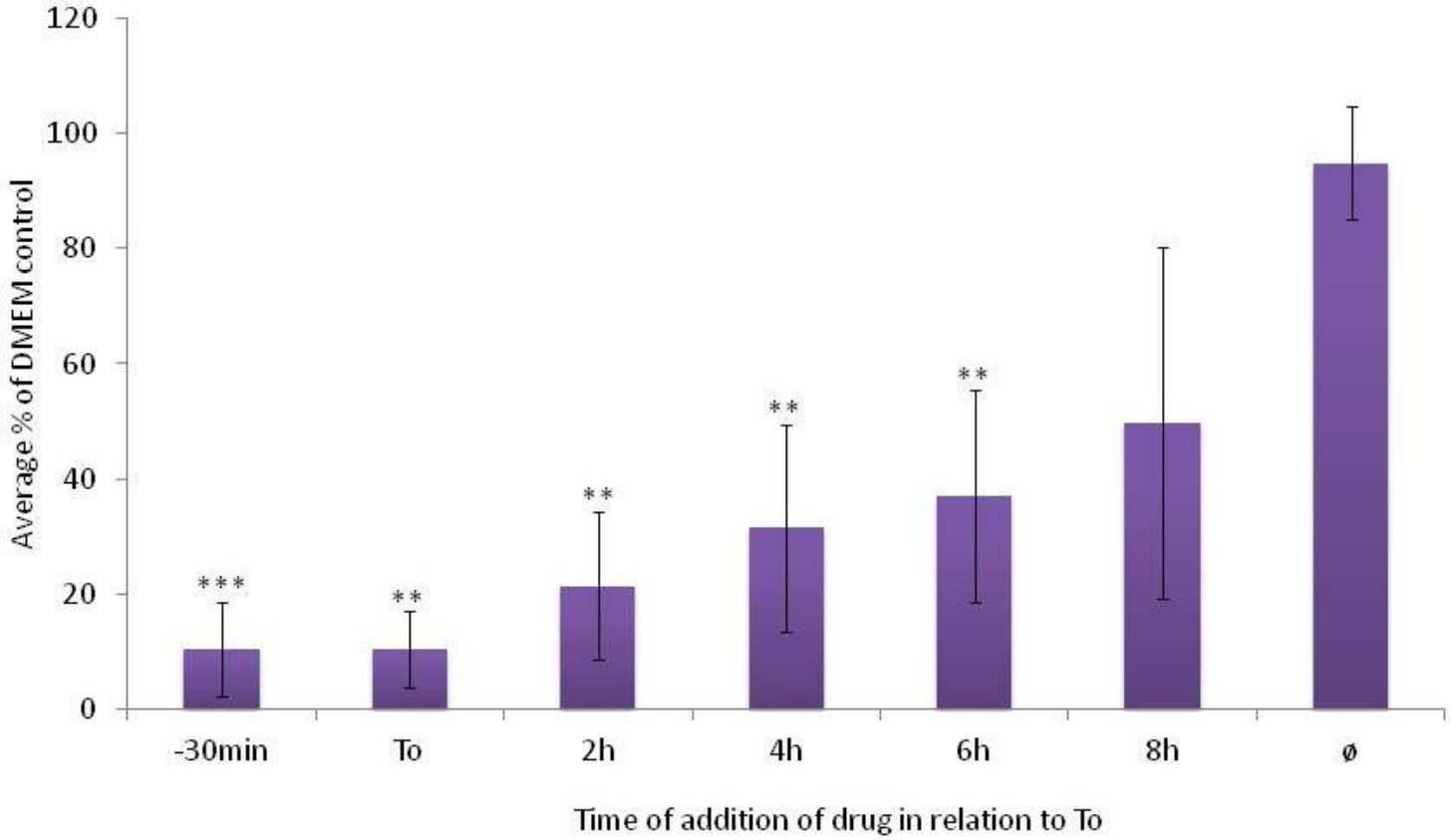

Figure 3.8 The effect of Cf2642 (10 µM) on the luminescence signal from v3 infection in RK13 cells when added at 30 minutes prior to infection, To and 2, 4, 6, and 8 hours pi. Collection at 12 hours pi. The results are shown as a percentage of the DMEM time of addition control. Ø = no drug. Error bars ±1 standard deviation. ** P <0.01, *** P <0.001

3.3.4 Activity of ddBCNAs in plaque size reduction assays

Plaque assays are a well established method of studying antiviral effects in cell culture (Porterfield, 1959). This method was chosen as a further means of measuring ddBCNA activity against VACV. The effect of the ddBCNAs was observed as a reduction in the size of the plaques but they had no effect on the total number of plaques formed.

The ether series of L-ddBCNAs were tested in four day plaque assays in triplicate. To demonstrate the output of the plaque assays, example data representing the greatest (Cf2642), smallest (Cf3210) and most toxic (Cf3242) responses to the compounds, are displayed in figure 3.9 along with Cidofovir as a positive anti-poxviral control.

Cf2642 was the most active of the compounds in the majority of the assays, displaying small plaques at drug concentrations of 50, 5 and 0.5 µM. Of note, this decrease in plaque size only occurred at Cf2642 concentrations above 0.1 µM. Merely by visualising the data (figure 3.9), it is evident that the concentration required to reduce the plaque size by 50% is between 0.1 and 0.5 µM. However, to confirm this, Image J software was used to accurately measure the area (in pixels) of each individual plaque. By inputting these measurements into curve fitting software (GraphPad), an accurate IC_{50} concentration was generated (IC_{50} concentrations shown in table 3.5 and figure 3.10). This value was determined to be 0.19 µM for Cf2642.

Cf3210 appears the least active of the L-ddBCNAs tested, with a calculated IC_{50} value of 12.9 µM. In support of this, it is clear from the plaque images that the size of the plaque doesn't decrease until drug concentrations of 50 µM are used. The remaining L-ddBCNAs tested induced plaque size changes somewhere between those displayed by Cf2642 and Cf3210.

Cf3242 appeared to have activity greater than Cf2642 in the luciferase assay (figure 3.6) and was therefore included in the plaque assays along with three other compounds (Cf3230, Cf3231 and Cf3232) that were among the most active in the

luciferase assay (figure 3.6). Conversely, the plaque assays suggest that Cf3242 is not as active against VACV as Cf2642 – with plaque reduction not occurring unless drug concentrations of at least 5 μM are used. It had a calculated IC_{50} of 2.4 μM. In addition, it is clear that the compound displays toxicity against the host cells (figure 3.9) as indicated by a lack of crystal violet staining (which in turn indicates a lack of viable cells) four days after drug addition (at a concentration of 50 μM).

The control drug Cidofovir appears to eliminate the plaques completely at the highest concentration, and shows some reduction in plaque size at the 5 μM. The calculated IC_{50} for this drug was 11.45 μM. AraC which also included as a control, also displays reduced plaque size phenotype in the plaque assays and displays an IC_{50} concentration of 0.93 μM.

Another observation of note when carrying out the plaque assays was that in the wells containing higher concentrations of ddBCNAs, the cell medium became yellow over the course of the experiment. This effect appeared to correlate with the activity of the ddBCNAs, i.e. the most active ddBCNAs changed the medium yellow at a lower concentration than the less active ones. This significance of this observation is discussed further in chapter 6 and 7.

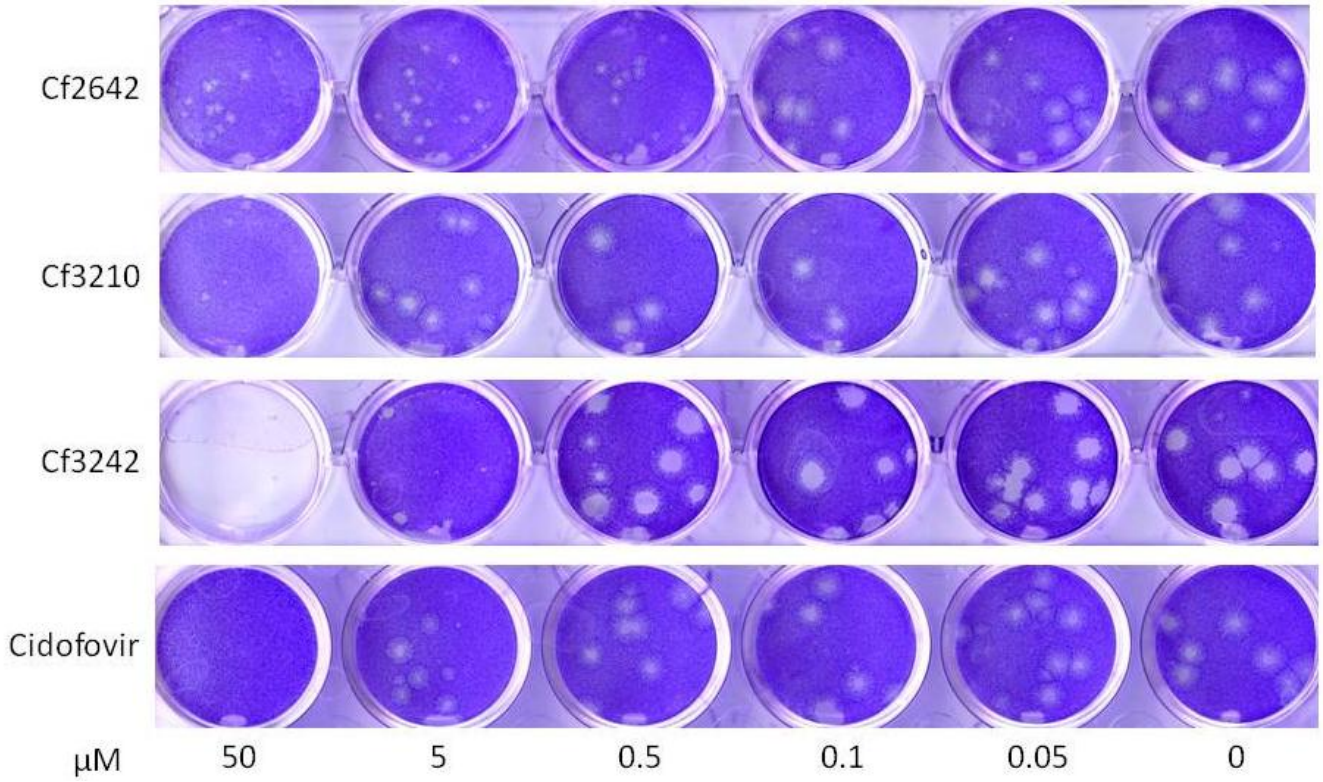

Figure 3.9 Cf2642, Cf3210, Cf3242 and Cidofovir at different concentrations in BSC-1 cells infected with ~20 pfu/well v3 over four days. After infection, cells were stained with crystal violet and scanned in order to analyse plaque sizes. A small plaque size phenotype is observed at lower concentrations in the most active compounds, (e.g. at 0.5 µM in the case of Cf2642) than it is in the less active compounds (e.g. small plaques can only be seen at 50 µM of Cf3210). Cf3242 displays toxic effects at 50 µM, observed as a complete lack of crystal violet staining (in-turn indicating a lack of cells in the well).

Compound	IC_{50} (μM)
Cf3210	12.9
Cf3204	1.9
Cf3207	1.8
Cf2642	0.19
Cf3209	0.19
Cf3230	1.7
Cf3231	2.2
Cf3232	3.4
Cf3242	2.4
Cidofovir	11.5
Ara C	0.93

Table 3.5 IC_{50} concentrations calculated using plaque size measurements for the ether series plus four ddBCNAs with other modifications. Cidofovir and AraC have also been included as positive controls.

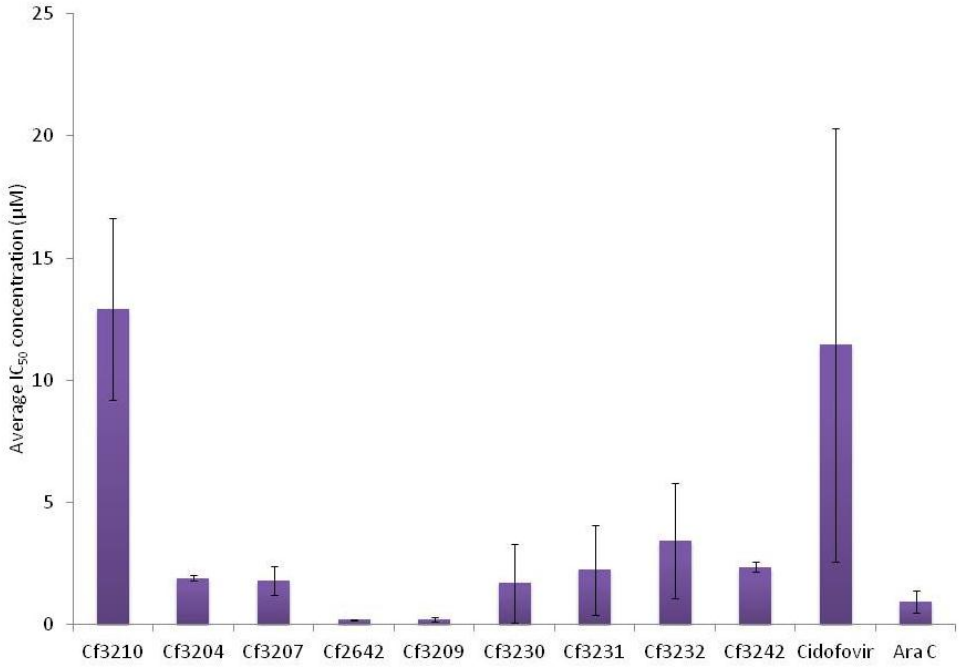

Figure 3.10 The calculated IC_{50} concentrations of the ether series of ddBCNAs (Cf3210, Cf3204, Cf3207, Cf2642 and Cf3209) plus four other (best performer) ddBCNAs (Cf3230, Cf3231, Cf3232 and Cf3242). Cidofovir and AraC were also included as controls. Error bars ± 1 SD based on three independent experiments.

3.3.5 Fluorescence microscopy of plaque development

BSC-1 cells were infected with ~10 pfu per well of vYFP-A3L and then were either treated with 50 μM Cf2642, or left untreated. Cells were fixed after one, two and three days pi. Cells were stained with phalloidin-594 (to visualise the actin cytoskeleton in red) and mounted with Vectashield containing DAPI (to visualise the nuclei in blue). Fluorescence microscopy images are presented in figure 3.11.

After one day the untreated cells showed signs of the formation of small plaques surrounded by cells containing many virus particles. The cells that had been treated with Cf2642 also showed signs of plaque formation, though they appeared smaller than the untreated equivalents. There were some virus containing cells around the edge of these small plaques, however these were fewer in number than in those untreated.

Another point to note is that in order to photograph the signs of the vYFP-A3L in the treated cells, the exposure time needed to be much longer than for the untreated cells, 1000 ms compared with just 400 ms. The greater exposure time required, indicates a reduced number of fluorescent virus particles within the Cf2642 treated cells i.e. suggesting that the drug is having an effect.

Both trends noted above (i.e. smaller plaques and reduced exposure time for the treated cells) continued into two and three days pi, suggestive of a real and prolonged effect for Cf2642 against the virus.

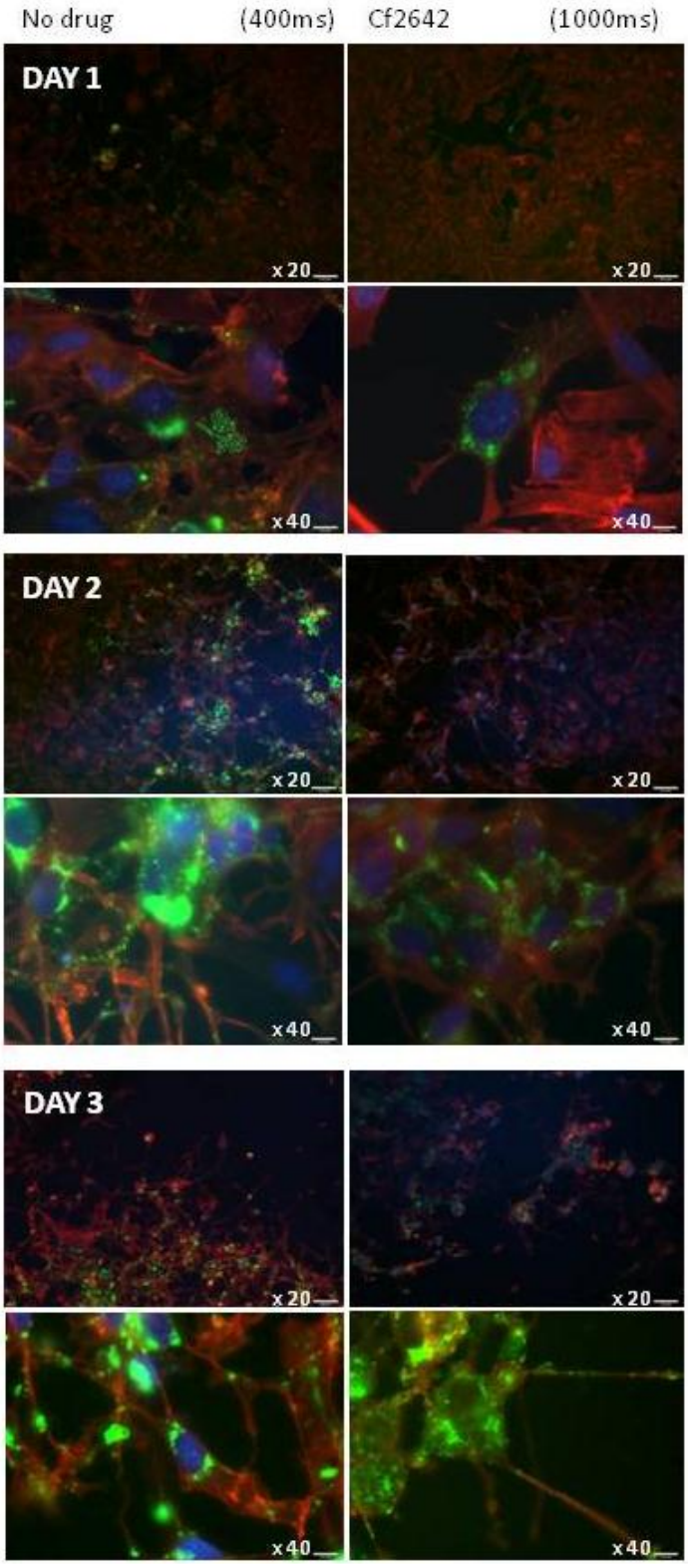

Figure 3.11 BSC-1 cells seeded in a 12-wp + coverslips, infected with ~10 pfu/well vYFP-A3 and either untreated or treated with 50 µM Cf2642. Cells were fixed after 1, 2 and 3 days. Cells were photographed using a fluorescence wild field microscope. Exposure time was 400 ms for untreated cells and 1000 ms for Cf2642 treated cells. The intensity of the viral fluorescence is greater in the absence of the drug suggesting there are more viral particles present than in the Cf2642 treated cells.

3.3.6 Pilot *in vivo* assay

The results of the animal experiment proved inconclusive (figure 3.12). Luminescence levels were used to provide an indication of the quantity of v3 accumulation in the ovaries of the mice. Unexpectedly, the level of luminescence in untreated mice infected with v3 (~200 000 RLU) was lower than in some of those that were treated (up to ~250 000 RLU). Considering the drug dilution results alone for infected mice, it seems that the drug does have a slight dose dependant inhibitory effect on the virus (~250 000 RLU at 10 mg/kg, ~170 000 RLU at 50 mg/kg and ~150 000 RLU at 100 mg/kg). As expected the luminescence from the ovaries of the mice that were not infected with virus was equivalent to the background luminescence (<1000 RLU).

In terms of toxicity, the drugs seemed to be well tolerated by the mice – with no indications of harm or discomfort occurring throughout the course of the experiment.

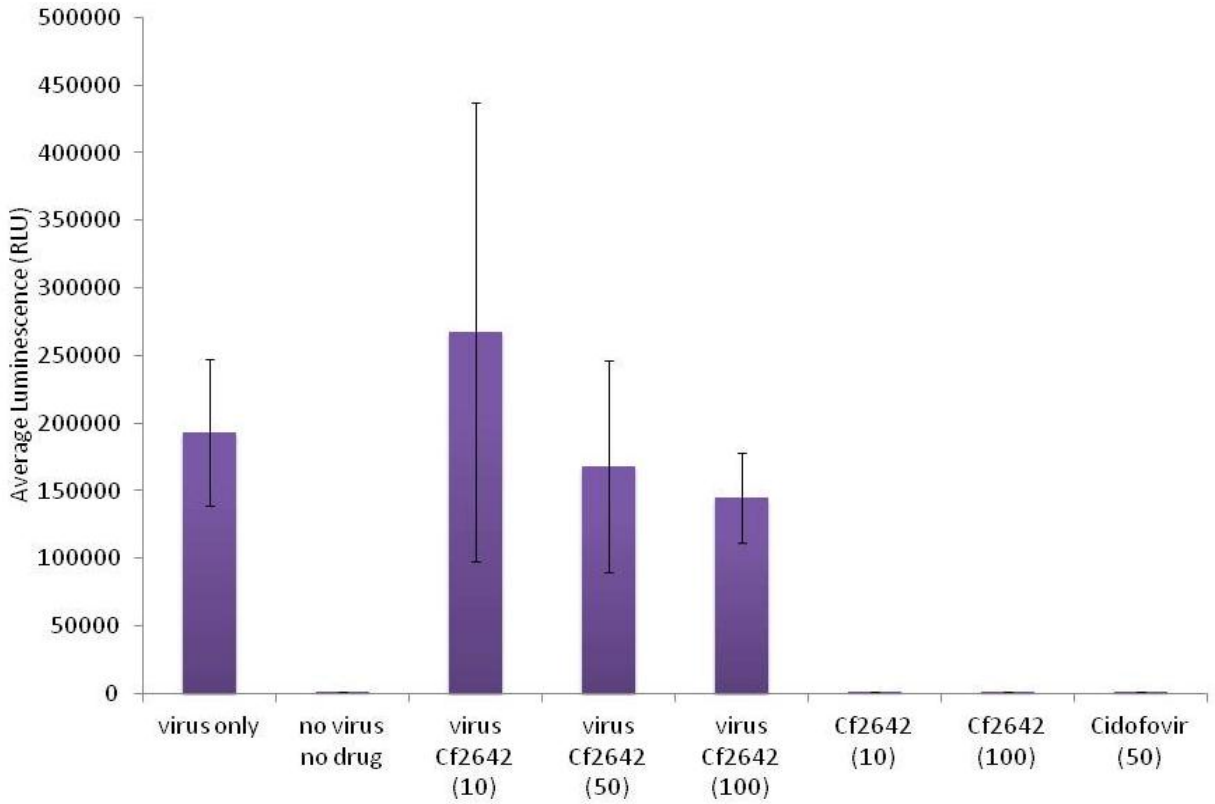

Figure 3.12 *In vivo* Cf2642 assay - the accumulation of v3 in the ovaries of mice. Average luminescence in relative light units from three mice ovary collections. Error bars ± 1 standard deviation. The uninfected mice in the presence or absence of drug display background levels of luminescence (<1000 RLU). The results from the Cf2642 dilution series suggest an inhibitory effect as the luminescence decreases with increasing concentrations. However the signals from the untreated, infected mice turned out to be lower than when treated with 10 mg/kg Cf2642 so the inhibitory effect of Cf2642 could not be confirmed from this assay alone.

3.4 Discussion

Before commencing work on the antiviral assays in this project, certain aspects of the assays and virus stock production methods were optimised. The results of the method optimisations are described in chapter 2. All modified and optimised conditions were subsequently used to generate the data described here on in.

The antiviral assays described in this chapter repeatedly demonstrate that, of the ddBCNAs tested, the compound Cf2642 appears the most effective at inhibiting VACV infection. The only exception to this was luciferase assay data generated for Cf3242 which showed a greater reduction in the luminescence signal (to <20% of the no drug control). However Cf3242 was later found to have a higher IC_{50} concentration than Cf2642 and also displayed clear signs of toxicity in the plaque assay. Based on the overwhelming data pointing to Cf2642 having the strongest antiviral effect, all subsequent assays of activity against VACV focussed on this drug.

The apparent antiviral effect of Cf2642 was tested in a variety of different cell types that had been infected with v3. This data indicated that Cf2642 inhibited the virus in all of the cell types tested, though the extent of this inhibition varied between them.

In order to compare the effect of the ddBCNAs between the different cells, the results for the antiviral effect of the ddBCNAs in this assay were calculated as a percentage of no drug control for each cell type. This was particularly important in this assay because variation in the luminescence signal between the cell types in the absence of the drug could be observed. This is possibly due to the fact that some cells may be more easily infected with VACV than others. In cells where the virus can enter easily, there would likely be a greater luminescence signal produced than in those where the virus cannot enter so easily. Another reason for the variety in luminescence signals may be because the method of cell counting is not entirely precise, especially in cell lines that have a tendency to aggregate after trypsinisation. As such, although every attempt was made to ensure that equal

numbers of cells were placed into each well, there may have been some disparity between the starting numbers of cells.

Cell size may also have been an issue. Cells that are larger will approach confluence at an increased rate as compared to the same number of smaller cells within wells of the same capacity. For example, HUH7 cells are larger than B95a cells – we observed that $5x10^4$ cells per well of the former approached confluence while the latter did not fill the well.

The ability of Cf2642 to function in different cell lines is an important observation. Previous experience has shown that the effects of novel antivirals cannot always be replicated in different cell lines. For example N-methanocarbathymidine ((N)-MCT) a carbocyclic thymidine analogue showing antviral activity against orthpoxvirus infection, was found to have significant variation in activity between different cell lines (Smee et al. 2006). The ability of Cf2642 to function in different cell types (albeit at different levels) supports its use as a potential novel antiviral. Furthermore, the data presented here can potentially provide an insight into its MoA. The possible MoA will be discussed further in chapters 6 and 7.

A ToA assay was carried out to determine if the drug maintained antiviral effects when administered at later stages of infection. Here Cf2642 was added at a series of time points relative to infection, ranging from 30 minutes prior to - 8 hours pi. The data ultimately suggests that adding the drug at different times made little difference to the antiviral effect. Whilst the signal at the 8 hour time point was not significantly lower than the control reaction, this is likely due to large variation resulting from anomalous readings. These anomalous readings are as a result of some of the luminescence signals generated from the later collection times exceeding the maximum readable signal by the luminometer

The above findings are useful for a number of reasons. Firstly, the fact that the drug can be administered at various stages before and after viral infection is informative for future laboratory based testing. Indeed the observation that there is no benefit to adding the drug 30 minutes prior to infection suggests that this routine practice

isn't necessary (though, for the sake of consistency, the 30 minute drug pre-treatment step was maintained for future assays). Also, it is possible that the data could be clinically relevant – though it is of course difficult to extrapolate from *in vitro* data to *in vivo* systems.

Relating to this though is the information the ToA data infers about the MoA of the drug. ToA assays have been used to gain insights as to the MoA of antiviral compounds (Daelemans et al. 2011). This provided information about the MoA of the ddBCNAs based on the time that the addition of the drug may be delayed before a loss of antiviral effect is observed. For example if the compound was inhibiting the entry stage of infection alone, this would imply that if the drug was added after the viral entry had already occurred there would be no antiviral effect observed.

Plaque assays were carried out to determine the effect of the ddBCNAs on the formation of plaques by VACV. Following the observation that the ddBCNAs reduced the size of the VACV plaques, the area of each of the plaques was measured to quantify the effectiveness of each of the ddBCNAs by producing IC_{50} concentrations. Again the data pointed to Cf2642 as being the compound with the greatest antiviral activity.

When comparing the IC_{50} concentrations of the ether series of ddBCNAs to their luciferase activity data, there appears to be a correlation between the two. Indeed, the SAR profiles of each of the assays follows a similar pattern (figure 3.13). This pattern indicates that the activity of these compounds is specific as altering the structure of them by even a small amount can have a large effect on their activity. This effect has previously been observed with a series of deoxynucleoside analogues active against VZV where it was found that an alkyl side chain length of 8-10 carbon atoms was required for optimum activity (McGuigan et al. 1999).

Wide field fluorescence microscopy of plaques in the presence and absence of Cf2642 indicated a clear reduction in the number of fluorescent virus particles when the drug was added. This was made clear as the level of exposure needed to

capture the viral fluorescence in the treated cells was much higher than for the untreated cells with normal infection levels (1000 ms compared with 400 ms). This effect could be seen after one day and the trend continued over the course of the three days. The series of images taken during this experiment provided further evidence for the ddBCNAs ability to reduce infection by VACV.

Based on the encouraging findings made in *in vitro* systems, a preliminary experiment in an animal system (specifically mice) has been carried out and is included here as a further discussion point. The mice appear to be unaffected by the presence of the drug in their system, in turn suggesting that the drug is well tolerated and toxicity isn't a factor. The issue of toxicity will be discussed further in chapter 5.

Though there is perhaps a trend toward decreasing virus burden as drug levels are increased, the data does not confirm an antiviral effect for Cf2642 in mice. Further tests are needed to validate this negative finding since it is possible that various confounding factors might have influenced the result. For example, the results could have been affected by the fact that some of the drug appeared to precipitate out of solution after injection into the mice, reducing the full antiviral effect of the compound. As such, further repeats involving animals would require that the drug be administered in a way that ensured that it remained completely in solution.

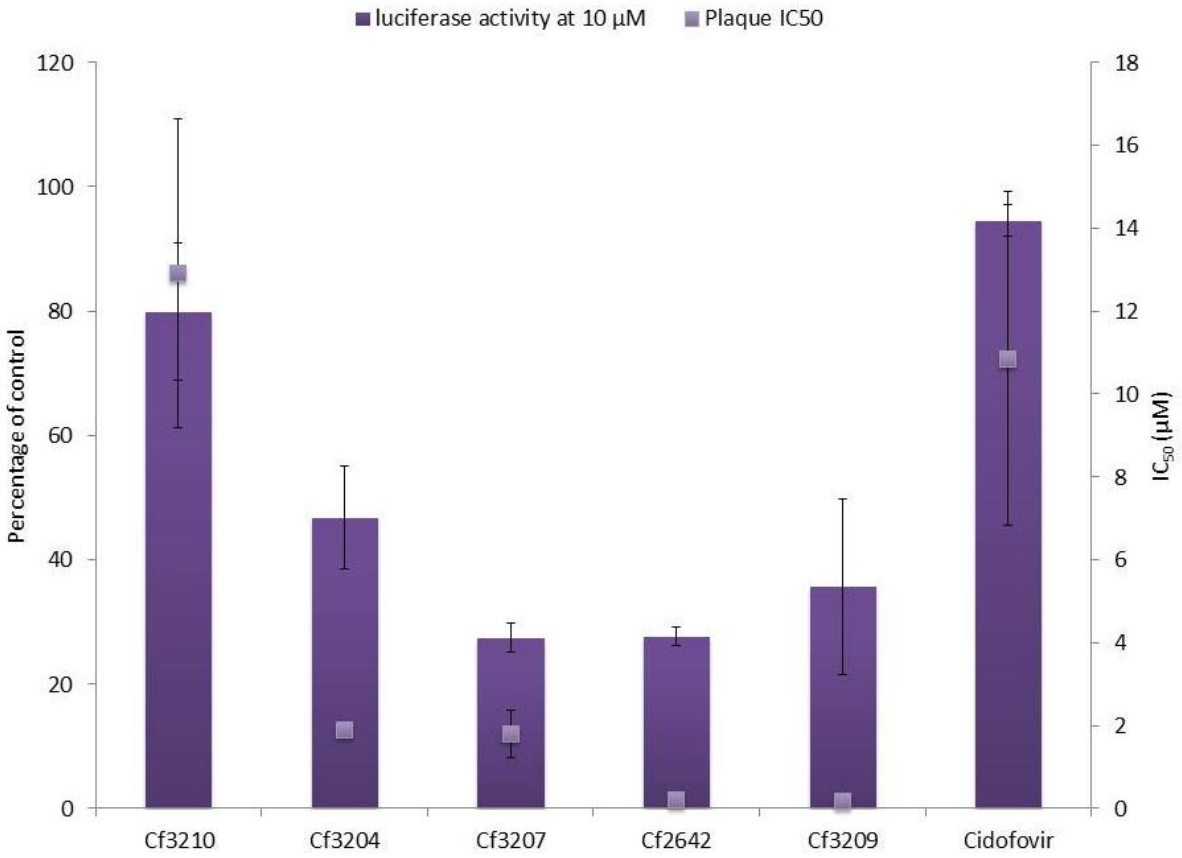

Figure 3.13 The calculated IC_{50} concentrations from the plaque assays in BSC-1 cells over four days for the ether series of L-ddBCNAs overlaid onto previously shown data from the two hour luciferase SAR in RK13 cells for the ether series. The graph shows a similar trend in the SAR using the data from both assays.

Chapter four – Activity of ddBCNAs against measles and virus panel

4.1 Introduction

The D-ddBCNAs described in this thesis were initially developed for antiviral activity against hCMV. In contrast, the L-ddBCNA equivalents of these were found to not be active against hCMV. However they do display antiviral activity against VACV. In chapter 3, it was confirmed that these compounds are clearly having an inhibitory effect against VACV, and this effect was quantified using a series of independent assays. Whilst this observation is an interesting one, it is not of huge clinical importance. This is because the smallpox virus (the most serious of the poxviruses) has been declared eradicated. Despite this there is still interest in potential anti-viral compounds against the smallpox virus due to increasing concerns about the possibility of bioterrorism and the release of smallpox. Indeed, whilst there are only two official stocks of smallpox virus remaining worldwide, there is a distinct possibility that unknown illegal stores exist elsewhere. For this reason the vaccinia vaccine, that acts against the smallpox virus, has been produced in large quantities for use in the event of such an outbreak.

Beyond this, the only drug capable of protecting against an outbreak of smallpox, is cidofovir. However, this drug can have severe nephrotoxic side effects (Skiest et al. 1999). Indeed, the overall aim of studying the ddBCNA's activity against VACV was to act as the groundwork for determining their suitability against other poxviruses of greater clinical relevance, for example MCV. This is the only remaining strictly human poxvirus. It affects many children and immune deficient individuals (Buckley and Smith, 1999). It produces uncomfortable wart like protrusions on the skin that secrete infectious particles. In the immunosuppressed state these may persist for years if left untreated.

Furthermore, if it were demonstrated that the ddBCNAs displayed activity MCV, as well as VACV, this would provide proof of concept of the possibility of utilising their antiviral effects against other poxviruses such as monkeypox (of which there are

increasing infections in parts of Africa) and smallpox (in case of an outbreak). Here it was demonstrated that Cf2642 has an antiviral effect on MCV.

In addition to poxviruses, the ddBCNAs were tested against a panel of other viruses. This was firstly to determine if they displayed activity against other viruses of clinical importance. It also aimed to establish if there were viruses against which the compound did not work. It was important to make sure that the effect of the compounds was specific and not just a general effect that works against any virus. Whilst being of obvious clinical relevance, the data yielded from this combination of affected and unaffected viruses might provide insights as to the MoA (e.g. is there a shared feature amongst the viruses that are affected by the ddBCNAs). This is discussed further in chapter 7.

This chapter describes efforts to define the anti-viral activity of several ddBCNAs (though primarily Cf2642) against a series of viruses beyond VACV (e.g. MCV, HIV-1, measles (Wild type and Edmonston strains) and the vaccine strain of yellow fever virus (YFV)).

The choice of viruses tested was ultimately dependent upon which ones the Bugert group could get access to and whether suitable assays were available or could be developed for testing them. The viruses tested also had to correspond with the permissions given for the work being carried out (details of permissions: license holder 'Bugert lab' - HSE notification GM130/07.5: testing of candidate antiviral compounds for activity against viruses: laboratory strains, vaccine strains, wild types, and recombinant viruses expressing fluorescently tagged proteins using classical virus titrations and reporter assays).

Tests of Cf2642 against Influenza, Adenovirus, HSV-1 and HSV-2 had previously been carried out (by the Bugert group) though it was found to have no activity against these viruses. This chapter summarises and describes experiments carried out to determine activity of ddBCNAs in a series of viruses.

Briefly, the results of this chapter describe;

-Test of Cf2642 against YFV where it was found to have no activity.

-A transcription luciferase reporter assay with Cf2642 against MCV suggested anti-viral activity. This finding provided initial evidence that the effect of the ddBCNA is transferable between different poxviruses. As such, it may be possible to use the ddBCNAs to inhibit further poxviruses.

-Preliminary results of Cf2642 activity against HIV-1. This experiment indicated that Cf2642 had a possible effect against the HIV-1 virus. Although work on this virus is in the very early stages of development, if the antiviral effect of the ddBCNAs against HIV-1 could be confirmed, this too would be of clinical importance.

-Tests of selection of ddBCNAs against measles, where activity of the L-ddBCNAs against this virus was discovered serendipitously, indicated by a lack of syncytia formation. Further testing with the ether series of L-ddBCNAs in order to establish SAR against this virus and compare with the SAR against VACV.

4.2 Materials and Methods

4.2.1 MCV luciferase transcription reporter assay

This work was carried out by Ms Niamh Blythe with my technical support of cell culture and reporter assays (SARTRE technician post 2010). MCV cannot be grown in cell culture - it is able to complete the cell entry stage of the life cycle and produce early gene transcripts, but cannot complete the lifecycle beyond this stage. For this reason, to measure the effect of Cf2642 against this virus, the transfection-poxviral luciferase reporter system developed in 2010 by the Bugert laboratory (Sherwani et al. 2012) was used. This method quantitates transcription levels from a consensus poxviral early/late promoter (Chakrabarti et al. 1997).

Cells were seeded into a 96-wp and left overnight to settle and reach confluency. The cells selected for testing were 293, 3t3, BHK21 and RK13 cells, a selection of cells from four different hosts (human, mouse, hamster and rabbit respectively). The 293 cells in particular were selected as they have been demonstrated to be

more easily transfected than others according to the ATCC. The cells were simultaneously transfected with two plasmids, one (p240 shown in figure 4.1) containing the firefly luciferase gene under the control of a synthetic early/late poxvirus promoter (to measure poxvirus entry and early transcription) (Chakrabarti et al. 1997), the second (p238 shown in figure 4.2) containing the renilla luciferase gene (to act as a transfection control). The cells were infected with MCV (collected from patient lesions from Heidelberg Germany, the lesions were dounce homogenised prior to use in assays; equivalent moi of 5, calculated using quantitative PCR (Sherwani et al. 2012)). They were incubated for 16 hours before collection to allow time for a signal to develop. This was essential since the transfection method using MCV is much less sensitive than the infection with v3. The medium was removed from the cells and replaced with 100 µL 1 X CCLR, the cells were agitated on an orbital shaker for 15 minutes and then frozen at -20°C. After thawing, 20 µL of each sample was transferred into an opaque 96-wp and mixed with 10 µL firefly luciferase substrate. This process was done for four samples at a time to reduce the delay between the addition of the substrate and the measurements being taken. The luciferase readings measured using a 96-wp FLUOstar OPTIMA plate reader (set to read luminescence signals). A second set of luminescence readings were taken using a second 20 µL aliquot of each sample mixed with 20 µL Renilla luciferase. The firefly luminescence signals were normalised to the Renilla readings to compensate for the differing levels of transfection in each cell type.

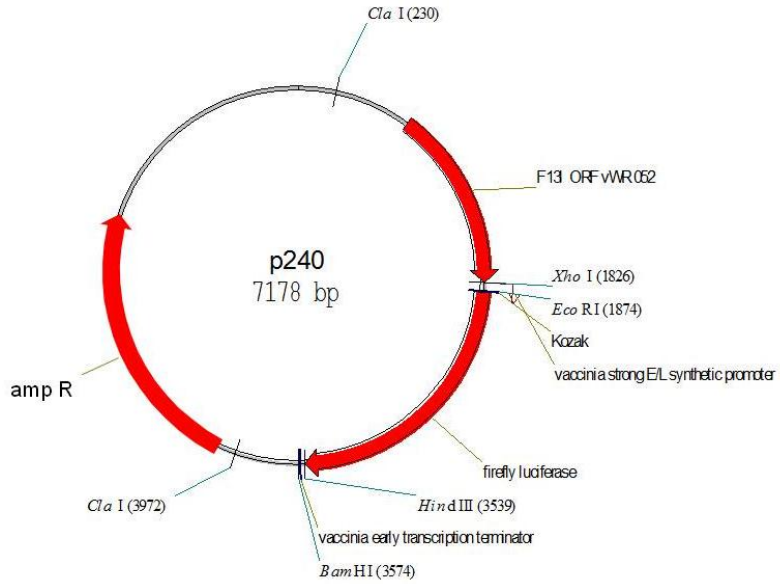

Figure 4.1 Plasmid p240 containing the firefly luciferase gene under the control of a synthetic early/late poxvirus promoter.

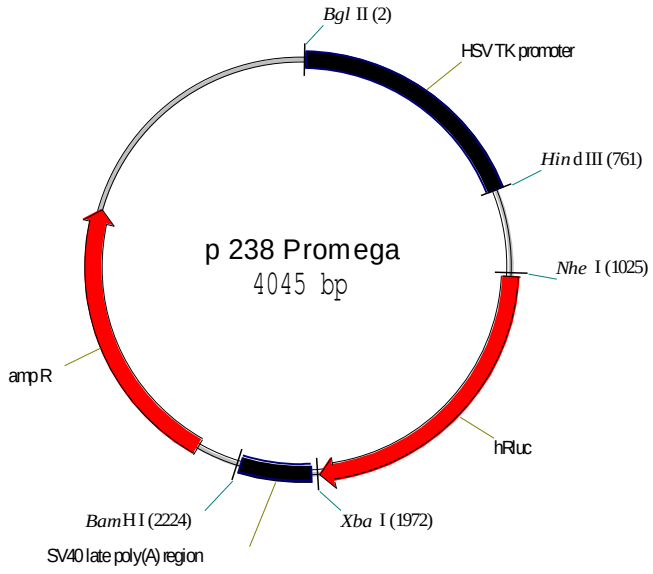

Figure 4.2 Plasmid p238 containing the Renilla luciferase gene to act as the transfection control.

4.2.2 Yellow fever virus assay

Vero cells were seeded into a 48-wp and left overnight to settle and reach confluency. One well of these was pretreated with Cf2642 at 10 µM. Another was treated with Cf3625 at 10 µM. This is an anti YFV compound (produced by the McGuigan group) which acted as a positive control i.e. cells treated with this had a phenotype consistent with a positive antiviral effect and reduced CPE. Despite the name, it must be noted that Cf3625 is **not** a ddBCNA.

Both drug treated wells were infected with YFV (moi 0.1). A further two wells were used and left untreated. One of these was infected with YFV while the other was used as a mock, to demonstrate the appearance of healthy uninfected cells. CPE of YFV was visible three days pi. Images of the cells were taken at this stage to assess the activity of the compounds.

4.2.3 Measles assay

A series of compounds were tested for activity against the Measles virus. The chosen compounds represented the best performers from the luciferase assays against VACV described in chapter 3 section 3.3.1. They were the L-ddBCNAs Cf2642 (old and new stocks to compare), Cf3232, Cf3175, Cf3242, and Cf2644, In addition, three D-ddBCNAs (Cf2643, Cf2095 and Cf1821) were included to determine if the D-enantiomers showed any activity against measles.

B95a cells were seeded into 24-wp and left overnight to settle and reach confluency. The cells were pretreated for 30 minutes with each of the selected compounds at 10, 5, 1, 0.5, 0.1 and 0 µM and infected with wild type measles virus (mWT Fb; moi 0.1). After 24 hours the cells were observed using an inverted phase contrast microscope and the activity of each of the compounds was determined by the absence of syncytia.

4.2.4 Confocal microscopy

B95a cells were seeded into an 8 well labtec slide and left overnight to settle and reach confluency. They were then pretreated with either a DMEM (no drug) control, Wortmannin (PI3 kinase inhibitor), Cf3242 or Cf2642 at 10 µM for 30 minutes. The cells were then infected with mIC323 and v300 and left for 24 hours

before fluorescence confocal images of the cells in each well were captured using a confocal miscroscope.

Cf3242 was included in this experiment since it was the ddBCNA compound that appeared to have the most improved activity against VACV in the luciferase assay (chapter 3 section 3.3.1.3) and it also displayed activity against measles at concentrations of 5 µM and above in the initial assay with mWT Fb. Cf2642 was included as the best performer against VACV in the luciferase assays and plaque assays. It also rated amongst the best performers in the initial measles assays.

4.2.5 Phase contrast microscopy

B95a cells were seeded into a 24-wp and left overnight to settle and reach confluency. These were used in two separate assays. The first tested Cf2642 at 10, 5, 1, 0.5, 0.1 and 0 µM against both mWT Fb and mEdATCC. Ribavirin was also included at concentrations of 5, 2, 1, 0.5, 0.1 and 0 mM as a control. The cells were pretreated with the drugs for 30 minutes before the addition of mWT Fb and mEdATCC. Images of each condition were captured using an inverted phase contrast microscope at 24 and 48 hours pi.

The second experiment was similar to the first though it tested Cf2642 against only mEdATCC in Vero cells. The reason mWT Fb was not used in this assay was because Vero cells do not have the SLAM receptor; therefore this strain cannot cause CPE in this cell line. Vero cells were seeded into a 24-wp and left overnight to settle and reach confluency. They were then pre-treated with Cf2642 and Ribavirin at the same concentrations as described above for 30 minutes before the addition of mEdATCC virus. Images of the cells were taken two days pi.

4.2.6 Measles IC_{50} assay

In order to quantify the activity of the ddBCNAs against measles virus, IC_{50} experiments were carried out using a similar method to the $TCID_{50}$ experiments for determining the titer of measles. B95a cells were seeded into a 96-wp and left overnight to settle and reach confluency. The cells were pre-treated for 30 minutes prior to infection using a variety of concentrations (100, 50, 10, 5, 1, 0 µM) of the alkyl series, ether series and best performers from the other modifications of L-

ddBCNAs. The alkyl and ether series were chosen in order to compare their activity against measles virus with the SAR profiles previously established against VACV. The wells were infected with 10 µL/well mWT Fb. The presence/absence of syncytia in each well was analysed using phase contrast microscopy after two days pi.
The IC_{50} concentration was then calculated using a similar statistical approach as the one described for the $TCID_{50}$ method for calculating virus titers (Reed and Muench, 1938). The IC_{50} in this case is the concentration of the compound that inhibits the CPE (syncytia formation) by 50% in comparison to cells infected in the absence of antivirals as an average of three experiments. Controls consisting of virus and cell only (no drug) and cell only (no virus and no drug) were included in each experiment.

4.2.7 HSV-1, HSV-2, Adenovirus and Influenza IC_{50} Assays

The following work was carried out by Dr J. Bugert. HSV-1/2, adenovirus 5, and Influenza A (H1N1, NS1 116 GFP fusion) were used to infect HFFF, BSC-1 cells, and MDCK cells respectively in 96-wp (10 drug dilutions, two mock, 8 times repeated) and evaluated 3 days pi for CPE in comparison to mock infected wells. Cells were grown in a 96-wp until 80% confluent. Cells were pre-treated with medium containing the appropriate amount of antivirals for 30 minutes prior to infection. Each well was infected with 100 pfu of HSV-1/2, adenovirus 5 or Influenza A and incubated in DMEM (without FBS or antibiotics) containing Cf2642 at concentrations ranging from 0 to 100 µM for 3 days. CPE was assessed by phase contrast microscopy. IC_{50} was defined as the concentration of antivirals that reduced the CPE by 50% (Reed and Muench, 1938) in comparison to cells infected in the absence of antivirals as an average of three experiments. Controls consisting of virus and cell only (no drug) and cell only (no virus/no virus and no drug) were included in each experiment.

4.2.8 HIV-1 assay

This work was carried out by Dr. Fabien Blanchet (Cardiff University). A pilot test of Cf2642 activity against the HIV-1 virus was performed in the MEDIC JBIOS CL3 laboratory as per Blanchet laboratory protocol (Blanchet, unpublished data). This

preliminary experiment was done by infecting immature primary dendritic cells (iDC) with HIV-1 in the presence and absence of Cf2642 at 50, 5, 0.5 and 0 µM. The cells were harvested at two, five and nine days pi and tested for percentage of Gag positive cells using FACS. The percentage of Gag positive cells provides an indication as to the level of HIV-1 infection as Gag is a HIV-1 viral protein that acts as the antigen present on the cells that are infected with the virus. Gag positive cells were detected with an antibody for the Gag protein. Gag positive cells were then counted using FACS flow cytometry. AZT is an anti-HIV-1 compound that, when included in the same type of assay (at 50 µg/mL,) maintains the level of Gag positive cells below 5% even up to 11 days pi.

4.3 Results

4.3.1 Activity of Cf2642 against HSV-1, HSV-2, Adenovirus and Influenza A

Prior to the start of this project the activity of Cf2642 against HSV-1, HSV-2, Adenovirus and Influenza A had been tested using a range of assays. It was found to be inactive against all of them. The compound had also been tested against MCV and was found to have some activity.

Tests of further viruses were carried out over the course of this project and yielded mixed results; Cf2642 showed no activity against Yellow Fever virus, showed possible activity against HIV-1, and showed definite activity against measles virus.

All anti-viral tests and the activity scores are outlines in table 4.1.

Virus	Cells tested	Activity
VACV	Variety	Active
Adenovirus 5	HFFF and BSC-1	Inactive
HSV-1	HFFF and BSC-1	Inactive
HSV-2	HFFF and BSC-1	Inactive
Influenza	MDCK	Inactive
YFV (vaccine)	Vero	Inactive
MCV	293, 3t3, BHK21 and RK13	Active
HIV-1	iDC	Possibly Active *
Measles Edmonston	B95a, BSC-1 and Vero	Active in B95a
Measles WT	B95a	Active

Table 4.1 A summary of activity of Cf2642 against different viruses (*preliminary data).

4.3.2 Cf2642 activity against YFV

Cf2642 activity against the vaccine strain of YFV was tested in Vero cells. In order to act as a positive control, a known anti-YFV compound Cf3625, was tested in parallel.

A CPE of untreated cells was visible after three days pi - specifically a reduction in size of and rounding of the cells. In the presence of Cf2642 the levels of CPE were very similar (figure 4.3) to the untreated cells. This observation suggests that Cf2642 is not active against YFV. In contrast to this, cells administered with Cf3625 had a normal/healthy appearance – similar to the appearance of the negative control (i.e. not infected) 'mock' cells.

Another point of note is that in parallel with signs of CPE the YFV caused the medium of the infected cells to become yellow. Meanwhile, the medium of cells administered with anti-YFV compound Cf3625 remained pink. This is in contrast to what was observed in assays of Cf2642 activity against VACV and measles, where the medium of the treated cells **did** become yellow.

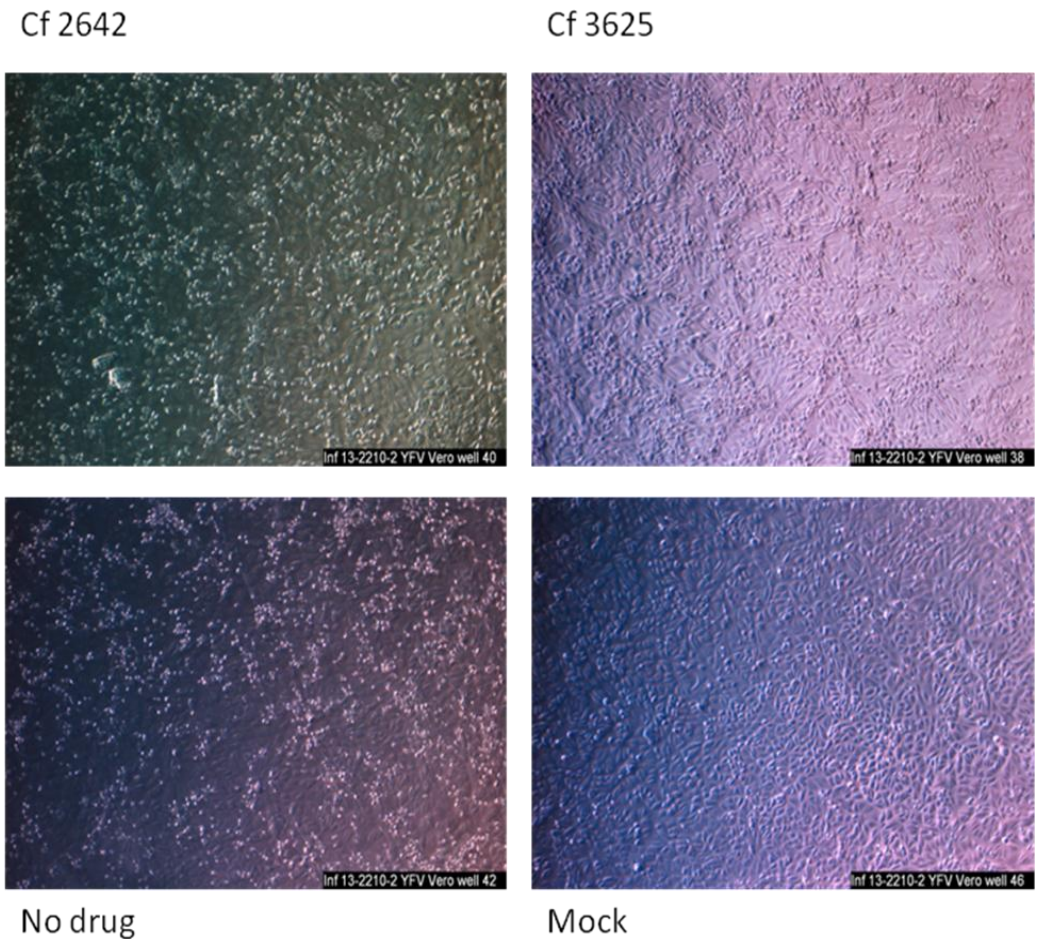

Figure 4.3 Yellow fever virus (vaccine strain) on Vero cells, three days pi. Cf2642 has no effect against the virus as the cells display the same level of CPE as the infected cells containing no drug. The positive control (Cf3625), included for comparison, shows no signs of CPE. The cells appear the same as the mock cells containing no virus. The colour of the medium in the infected wells in the absence of drug turned yellow with the appearance of CPE. The cells treated with Cf2642 had a similar appearance. The medium in the mock infected well remained pink, as did the medium in the well with the positive anti-YFV control Cf3625.

4.3.3 Cf2642 activity against MCV using a transcription reporter luciferase assay

A transcription reporter luciferase assay system was used (by the Bugert laboratory) to determine Cf2642 activity against MCV. Cells were simultaneously infected with MCV from patient samples and transfected with two plasmids. One of these plasmids contained the firefly luciferase gene under the control of a synthetic early/late poxviral promoter. The other plasmid contained the Renilla luciferase gene as a transfection control. Firefly luminescence signals were normalised to these Renilla signals in order to compensate for differences in the level of transfection between different experiments or cell lines.

The transfection method for the luciferase assay is not as sensitive as the method used for VACV, where the v3 virus produces its own firefly luciferase enzyme (described in chapter 2 section 2.2.4). For this reason the cells were allowed a longer incubation period in order to produce adequate luminescence signals. As such, the cells in this assay were collected 16 hours post infection/transfection.

Prior to the infection and transfection, half of the cells were pre-treated with Cf2642 while the others were used as untreated controls.

The luminescence readings indicated that the drug reduced the firefly luciferase signal suggesting that early MCV infection was inhibited by the Cf2642 (figure 4.4). This reduction in signal was evident in four cell lines and was found to be statistically significant in the 293 ($P<0.01$), 3t3 and RK13 cells ($P<0.05$).

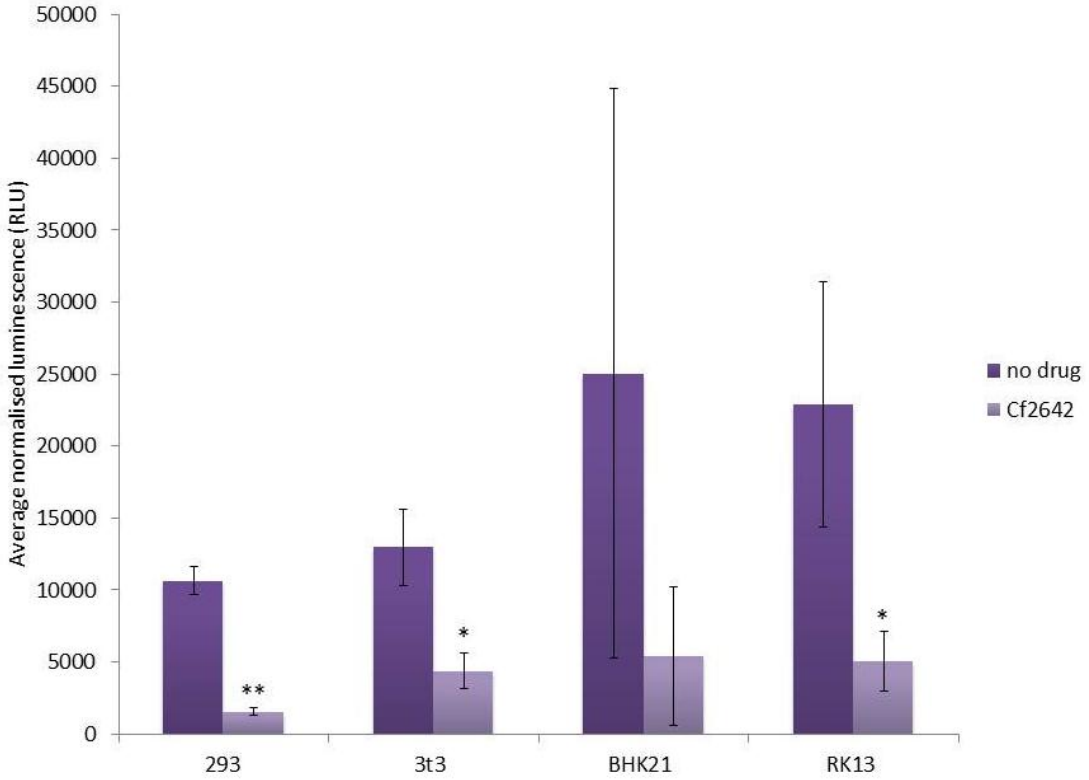

Figure 4.4 Luciferase transfection reporter assay in four different cell lines (293, 3t3, BHK21 and RK13) simultaneously infected with MCV and transfected with two plasmids, one containing the firefly luciferase gene under the control of a synthetic early/late poxviral promoter, and another containing the gene for Renilla luciferase. The firefly luciferase signals produced were normalised to the Renilla luciferase signals, in-turn giving an indication as to the level of transfection in each cell line. Cf2642 reduced the firefly signal in all tested cells and the reduction was found to be statistically significant in the 293, 3t3 and the RK13 cell lines. * $P < 0.05$, ** $P < 0.01$. Error bars ± 1 standard deviation. The reason for the large error bars in this figure is that BHK21 cells have a tendancy to aggregate, meaning that there is increased variation in the number of cells seeded into each well. The effect in the BHK21 cells could have been significant if not for the large standard deviations for the results in this cell line as there is a trend towards a reduction in signal in the presence of Cf2642. (Figure adapted from IBSc dissertation by Niamh Blythe).

4.3.4 Cf2642 activity against HIV-1

A pilot test of Cf2642 activity against the HIV-1 virus was attempted (by Dr Fabien Blanchet). Results are portrayed in figure 4.5. As expected, in untreated cells, the levels of viral infection increase as time goes on (4.08% at 2 days, 21.3% at 5 days and 44% at 9 days). This trend is apparent at all subsequent levels of drug concentration.

At the lowest concentration of Cf2642 tested (0.5 µM), there is a trend towards decreased levels of viral infection (1.75% at two days, 14.6% at five days and 29.5% at nine days – a decrease of 2.33%, 6.7% and 14.5% respectively as compared to the no drug control), immediately suggestive of a HIV-1 antiviral effect of the drug. Further to this, the virus levels decrease further at a drug concentration of 5 µM at five (8.84%) and nine (21.4%) days post infection – a decrease of 12.46% and 22.6% respectively as compared to the no drug control. Of note, this is not the case at two days pi (2.58%, only a 1.5% decrease vs no drug and a 0.25% increase compared with 0.5 µM Cf2642). At 50 µM Cf2642 (the highest concentration tested) the levels of HIV-1 increase at two days (6.75%, a 2.67% increase vs no drug). At five days pi, the trend towards decreasing viral levels continues (7.64%, a 1.2% decrease as compared to that observed at five days). However at nine days (26%), the trend reverses and a 4.6% increase as compared to the five day value is observed.

A typical level of infection observed in the presence of the HIV antiviral compound AZT (at 50 µg/mL) maintains the level of Gag positive cells below 5% up to 11 days pi. This shows that the Cf2642 is not as effective against the virus as this antiviral compound.

A coincident observation of this experiment was that, in the presence of Cf2642, the cell medium gradually became acidic. This was indicated by an increasingly yellow colour of the medium over the course of the experiment. This observation has been noted in other assays with the ddBCNAs for example the plaque assays chapter 3 (section 3.3.4) and the YFV assay (section 4.3.2). Further investigations into this effect are discussed later in chapters 5 and 6.

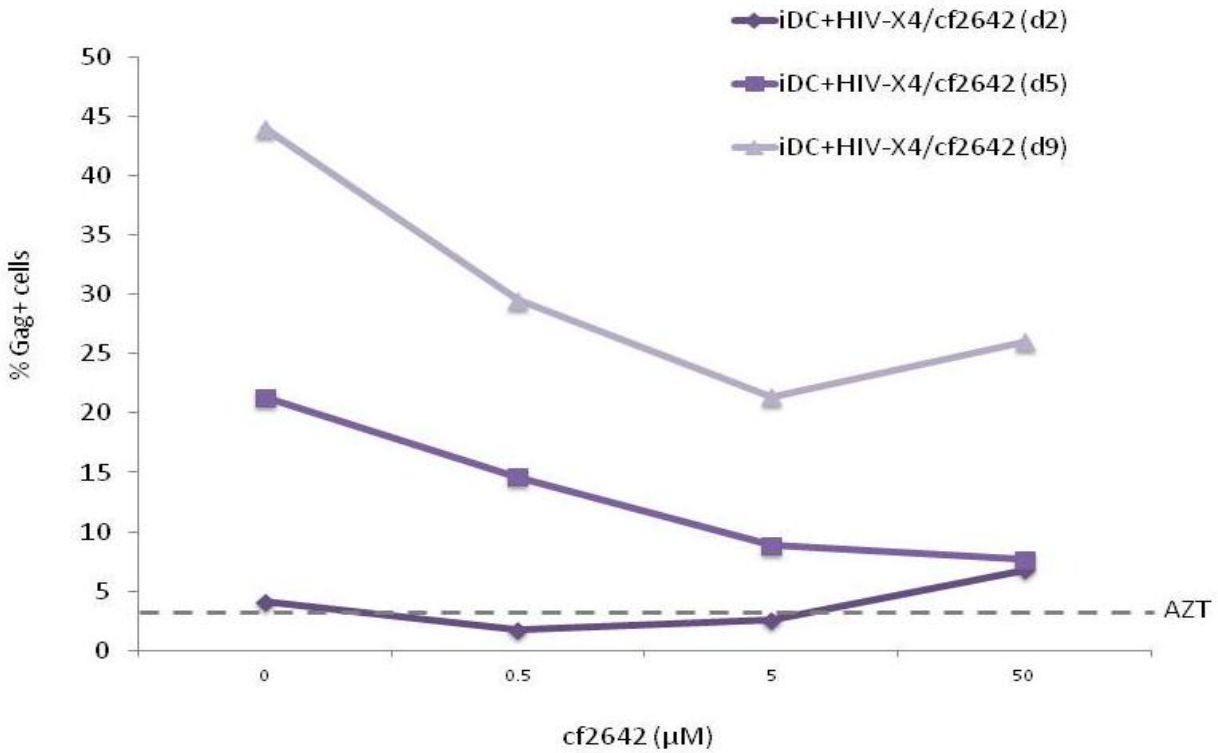

Figure 4.5 Dose response curves of Cf2642 (at 0, 0.5, 5 and 50 µM) activity against HIV. Cells collected after two (d2), five (d5) and nine (d9) days pi and percentage of Gag+ cells calculated by FACS. Although not included in this assay, the dotted line indicates a typical level observed of Gag+ cells in the presence of the HIV-1 antiviral AZT (at 50 µg/mL, which usually maintains the level of Gag positive cells below 5% up to nine days pi) for comparison. All conditions were carried out in iDC cells with HIV-X4, the darkest line (and diamond points) represents data collected two days pi, the medium coloured line (and square points) represents data collected five days pi and the lightest line (and triangle points) represents data collected nine days pi. (Graph generated from data produced by Fabien Blanchet).

4.3.5 Measles ddBCNA assay

An initial experiment to test the activity of the ddBCNAs against measles virus was carried out using a selection of both L- and D-ddBCNAs at a range of concentrations (from 0.1 to 10 µM). Their anti-viral activity was indicated by the absence of syncytia in B95a cells infected with wild type measles virus. Results are depicted in figure 4.6.

Here, Cf2642 (the best performing compound against VACV) showed activity against wild type measles virus at 1µM and above. Of note, both new and old stocks of Cf2642 were tested and displayed similar levels of activity from 1 µM and above. Activity was also observed at concentrations above 1 µM for Cf3232.

Three other L-ddBCNAs tested (Cf3175, Cf3242 and Cf2644) were selected from the best performers for activity against VACV in the luciferase assays. Cf3175, Cf3242 and Cf2644 indicated activity against the wild type measles at a concentration of 5 µM and above.

Finally, the D-ddBCNAs (Cf2095, Cf1821 and Cf2643) did not display any activity against the wild type measles virus at any of the concentrations used in this assay.

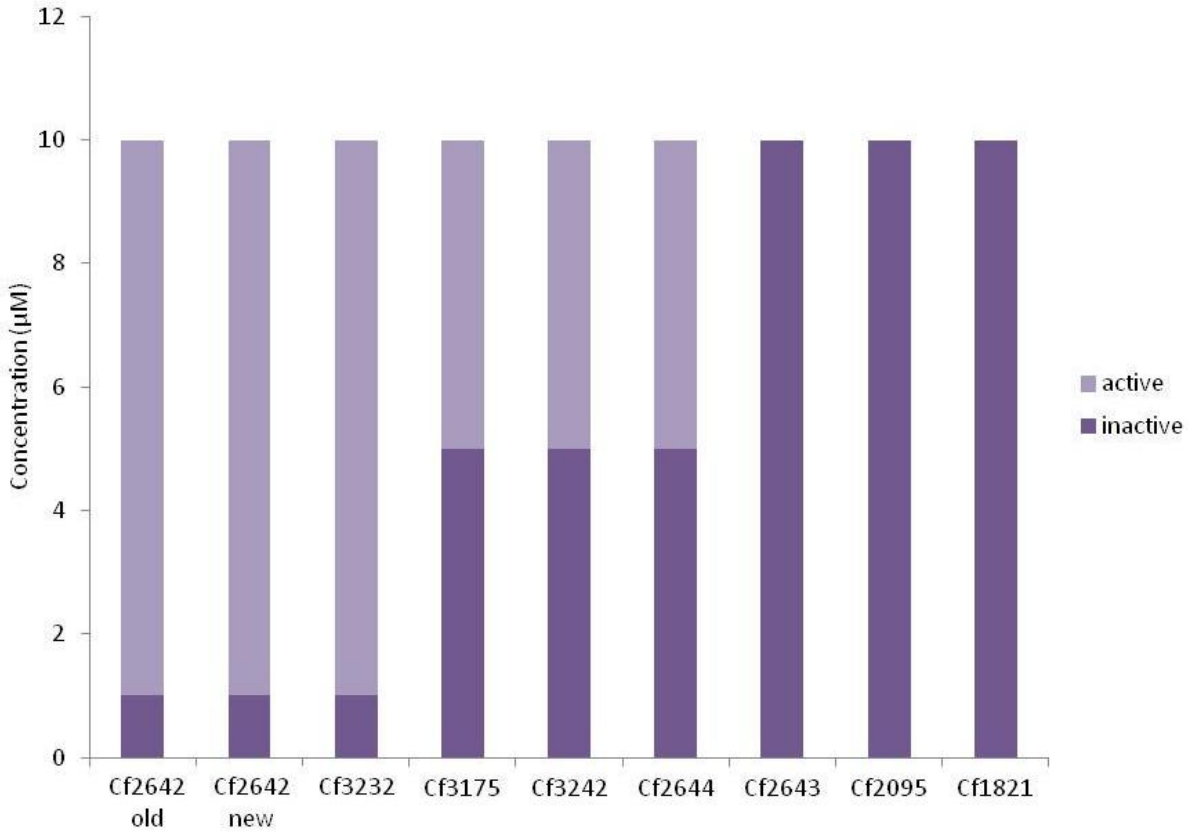

Figure 4.6 A selection of ddBCNAs tested against wild type measles in B95a cells over two days. Activity was determined by the absence of syncytia. New and old stocks of Cf2642 (the best performer against VACV) and Cf3232 are active against measles virus at concentrations of 1 µM and above. Other selected L-ddBCNAs (Cf3175, Cf3242, Cf2644) are active against the virus from 5 µM and above. The D-ddBCNAs (Cf2643, Cf2095 and Cf1821) are not active against the wild type measles virus at concentrations of up to 10µM.

4.3.6 Fluorescence confocal microscopy with mIC323 and v300

Described are the results of fluorescence microscopy of B59a cells, using mIC323 and v300 with the drugs Cf3242 and Cf2642. Wortmannin was also included as a control.

In the absence of any drug, the mIC323 produce large syncytia in the B95a cells, which are clearly visible with expression of GFP (figure 4.7 A). In the presence of the Wortmannin control there is a clear reduction in the levels of GFP expression (suggestive of a decrease in virus containing cells). Though the syncytia are not eradicated they are reduced in size.

The levels of GFP expression are further reduced in the Cf3242 and Cf2642 treated cells – with only 5-6 and 1-2 clearly visible small syncytia respectively.

In the wells infected with v300 there is a similar trend in GFP expression (figure 4.7 B), although VACV does not produce syncytia. In the absence of any drug there are many cells containing GFP. However the number of GFP-containing cells is reduced in the presence of Wortmannin and reduced further still in the presence of Cf3242 and Cf2642.

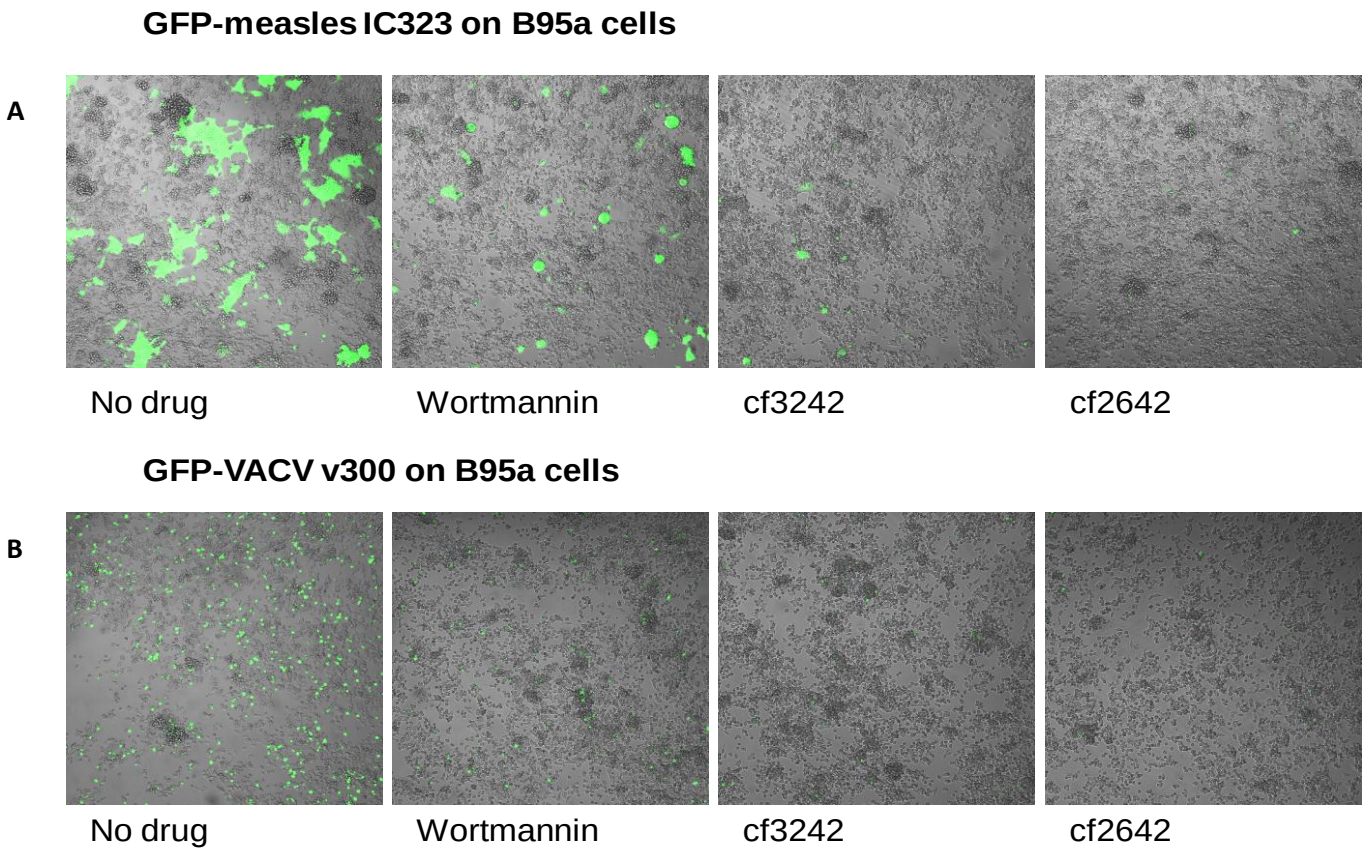

Figure 4.7 Confocal microscopy images of live B95a cells treated with no drug, Wortmannin, Cf3242 or Cf2642 (10 µM). A: Infected with mIC323 B: Infected with v300. Images taken 24 hour pi. Cf2642 and Cf3242 reduce the level of GFP expression caused by the viruses, to a greater extent than the control drug Wortmannin.

4.3.7 Phase contrast microscopy of Cf2642 activity against measles in B95a cells

Here the activity of Cf2642 against wild type (mWT Fb) and Edmonston (mEdATCC) strains of measles was tested in B95a cells, and compared with a Ribavirin control. Phase contrast images were taken at 24 and 48 hours pi (figure 4.8). It is clear that after 24 hours in the absence of drug, the measles have formed small syncytia in the cells. This effect can be seen for both wild type (1) and mEdATCC (2) strains of measles.

(1), In the cells infected with wild type virus the syncytia are still present at 0.5 µM and 1 µM Cf2642 (though they do appear smaller in the latter). Above this concentration it appears that syncytia formation is completely inhibited. This effect is increasingly evident at 48 hours pi. At lower concentrations of the compound (0 – 1 µM) the syncytia are larger in size and starting to detach from the surface of the plate. As the concentration increases beyond this, the cells maintain a normal and healthy appearance.

The Ribavirin control appears to inhibit syncytia formation by the wild type measles at a concentration of 0.5 mM and above after 24 hours and after 48 hours.

(2), In the case of the mEdATCC a similar effect is observed. Cf2642 inhibits the mEdATCC at the same concentrations as the wild type virus. In the case of the Ribavirin treated mEdATCC infections, there do not appear to be any syncytia at drug concentrations of 0.1 mM and above, even at 48 hours pi.

These observations indicate that the ddBCNAs are active against measles virus as they inhibit the formation of syncytia at low micromolar concentrations. The Ribavirin control is required at higher concentrations to have an effect on the measles virus syncytia formation. These findings suggest that the ddBCNAs are 100 times more active against measles than the control compound Ribavirin.

4.3.8 Phase contrast microscopy of Cf2642 activity against mEdATCC in Vero cells

Interestingly Cf2642 does not appear to have the same level of anti-viral activity against mEdATCC infected Vero cells as it showed against the virus in infected B95a cells (figure 4.9). There appears to be syncytia in all of the wells containing the drug, even at the highest concentration of 10 μM. In contrast, Ribavirin appears to inhibit the formation of syncytia at concentrations of 0.5 mM and above. This is the same level of inhibition as observed in the B95a cells. The mWT Fb strain of measles cannot be tested in Vero cells as this cell line does not contain the SLAM receptor that the wild type measles virus uses to gain entry into the host cell.

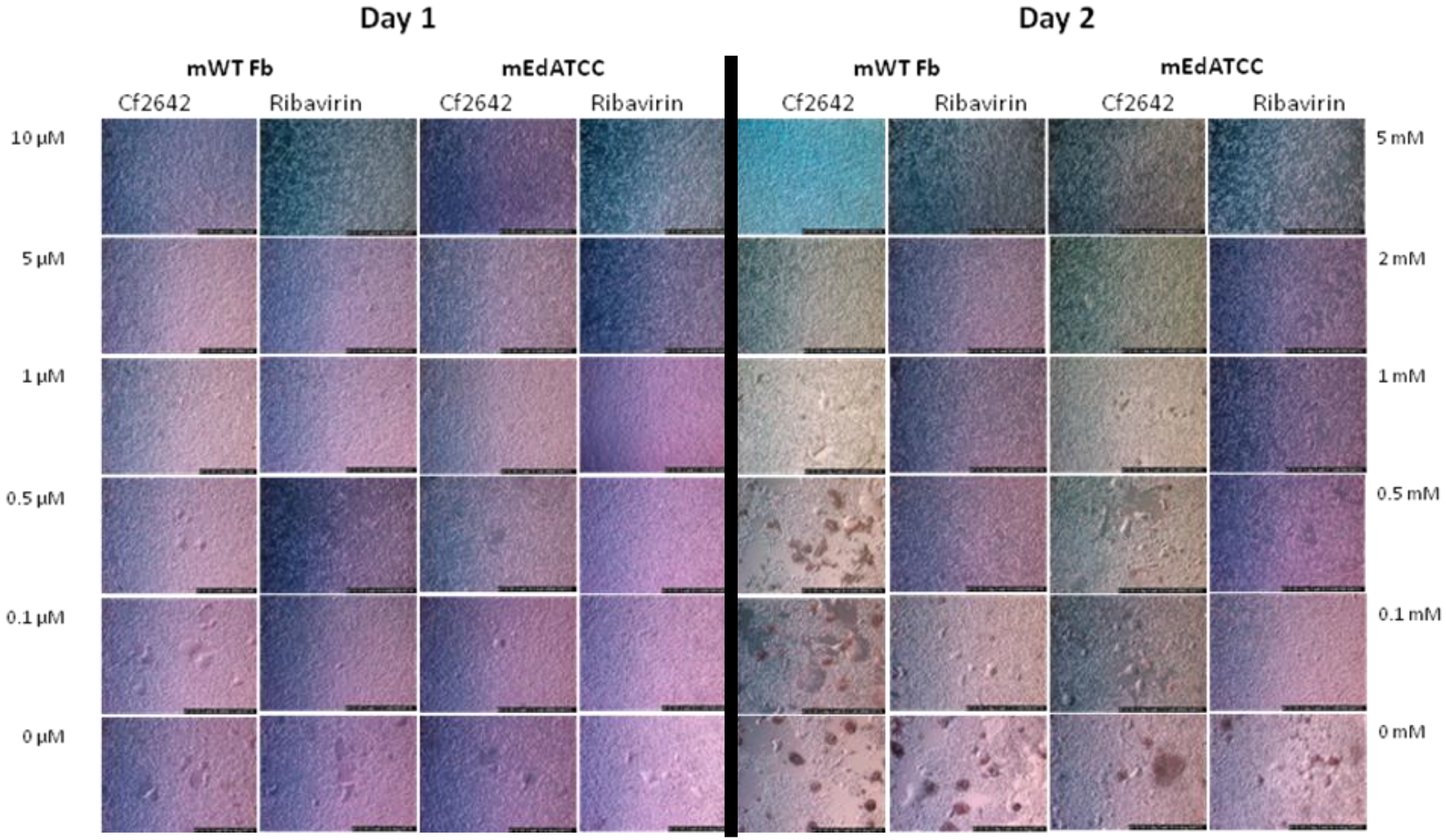

Figure 4.8 Activity of cf2642 and Ribavirin (concentrations displayed at the left and right of the figure respectively) against mWT Fb and mEdATCC strains in B95a cells. Syncytia formation is inhibited by Cf2642 at 5 µM and above. Ribavirin inhibits the formation of syncytia from 0.5 mM and above. Images were taken at 24 hours (left panels) and 48 hours (right panels) pi.

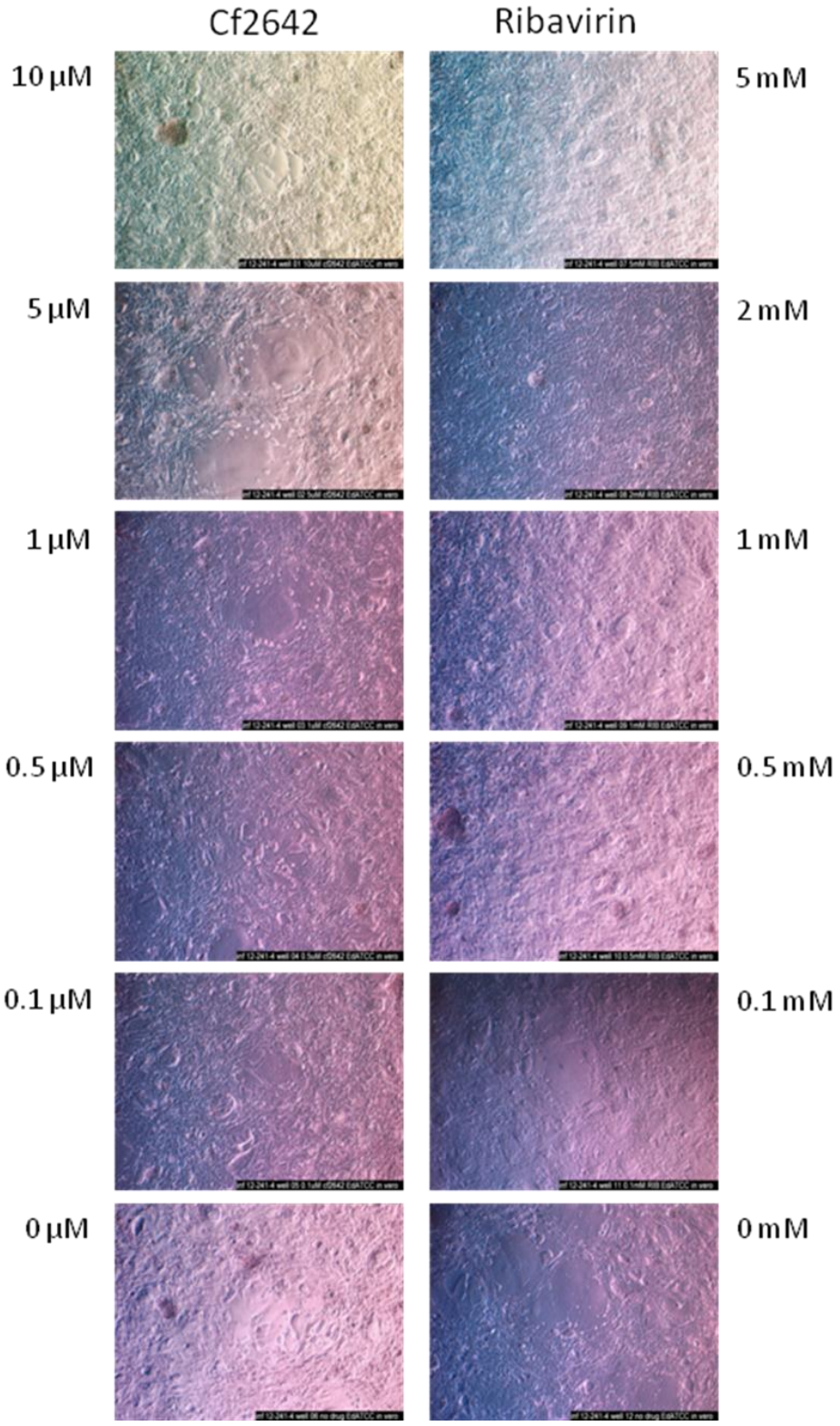

Figure 4.9 Vero cells infected with mEdATCC and treated with Cf2642 and Ribavirin (concentrations displayed at the left and right of the figure respectively). Images of the cells were taken 2 days pi. Syncytia can be seen at all concentrations of Cf2642, but are inhibited by ribavirin at concentrations of 0.5 mM and above. Syncytia are not as clearly visible in the Vero cells as in the B95a cells.

4.3.9 IC_{50} concentrations of ddBCNAs against mWT Fb

Measles IC_{50} values for the alkyl series, the ether series and the four best performers from the further modified L-ddBCNAs were generated (Table 4.2). This data demonstrates a clear SAR profile as the length of the side chain increases (figure 4.10). The SAR profiles for the alkyl and ether series of L-ddBCNAs against measles are very similar to those shown against VACV by the luciferase assay in chapter 3 section 3.3.2 The optimum alkyl L-ddBCNAs (Cf3175 and Cf3155) were found to have a IC_{50} concentration against measles of 7.5 µM, as did the lead compound Cf2642. Another of the compounds in the ether series (Cf3209) had an even lower IC_{50} concentration of 6.45 µM. Further to this, it appeared that one of the other modified L-ddBCNAs (Cf3230) had an even lower IC_{50} concentration of 3 µM. Two of the alkyl L-ddBCNAs were inactive with IC_{50} concentrations of >100 µM. The control compounds cidofovir (not active against measles) and ribavirin (active in the mM range of concentrations) also had IC_{50} concentrations of >100 µM.

It was again noticed that in this assay the colour of the cell medium became yellow in the presence of the active concentrations of the ddBCNAs.

Compound	IC_{50} concentration against measles (μM)
Cf3176	>100
Cf3177	>100
Cf3153	75
Cf3174	30
Cf3154	30
Cf3175	7.5
Cf3155	7.5
Cf3156	75
Cf3210	50
Cf3204	35
Cf3207	15
Cf2642	7.5
Cf3209	6.45
Cf3230	3
Cf3231	8.33
Cf3232	30
Cf3242	30
Ribavirin	>100
Wortmannin	70
Cidofovir	>100

Table 4.2 IC_{50} concentrations of ddBCNAs and controls against mWT Fb in B95a cells

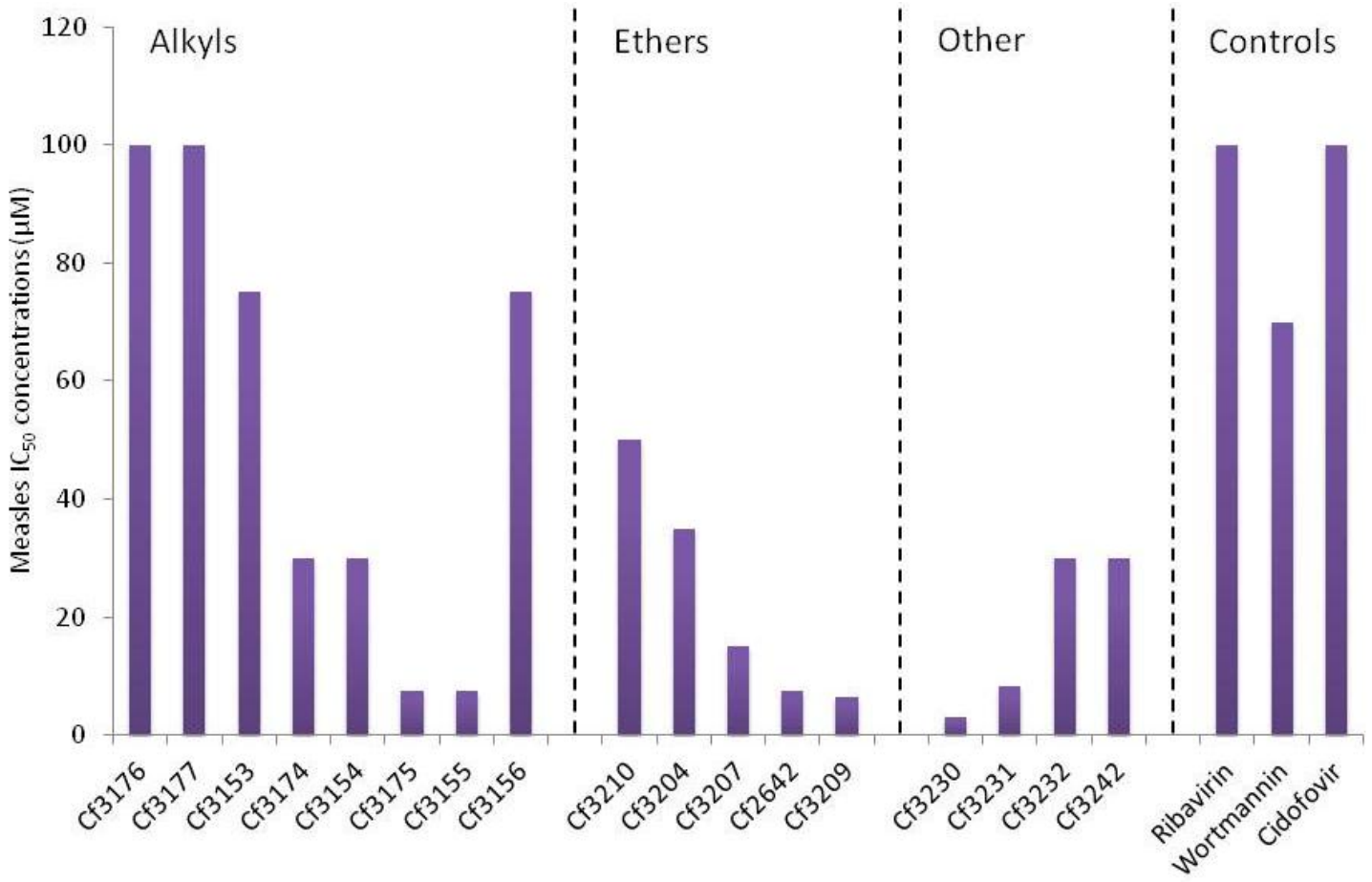

Figure 4.10 Measles IC_{50} concentrations using the ether and alkyl series of L-ddBCNAs plus the four most active from the alternatively modified L-ddBCNAs. The alkyl and ether series of L-ddBCNAs show SAR against measles, similar to those seen against VACV (Chapter 3 section 3.3.1.2).

4.4 Discussion

The first point to note from the data presented in this chapter is that the ddBCNAs are not active against all viruses. It was found that there was no apparent activity of Cf2642 against HSV-1, HSV-2, Adenovirus and Influenza A. It was also shown that there is no apparent activity of Cf2642 against YFV. These findings, although not of clinical significance, demonstrate that the ddBCNAs don't have a general effect that inhibits all viruses. Instead their activity is specific and only certain viruses are inhibited by whatever MoA these compounds operate through.

It was demonstrated that Cf2642 displayed antiviral activity against MCV. This finding has the further implication that the compound may be a potential antiviral drug candidate for clinical cases of MCV. As it also works against VACV the activity of the ddBCNAs may possibly be transferrable to other pox viruses of clinical significance such as Monkeypox or Smallpox in the case of a bioterrorist outbreak.

Considering the data generated in the experiment with HIV-1, it seems that there is a possible HIV-1 anti-viral effect of Cf2642 based on the trends loosely observed. However, it is clear that the correlation is not simple and thus, further testing is required. If the effect were confirmed this would be of great clinical importance due to the burden of HIV-1 infection. Worldwide 34 million people were living with HIV/AIDS at the end of 2011 (WHO website: www.who.int/gho/hiv/en/) with an estimated 96 000 of these in the UK (NHS website: http://www.nhs.uk/Livewell/STIs/Pages/HIV.aspx). AZT is a nucleoside analogue compound that inhibits the viral reverse transcriptase of HIV. This was the first approved compound to be used as a treatment against HIV. This drug slows down the replication of HIV in patients and can be used to prevent spread (e.g. from mother to baby during birth) but it does not inhibit viral replication entirely. As this compound has a specific viral target the virus has the potential to develop resistance to it. It is therefore critical that alternative compounds that act against the HIV-1 virus are developed (Jeeninga et al. 2001).

The observations in HIV-1 certainly warrants further investigation in order to confirm and quantify the effect of the ddBCNAs against the virus. The effect could

potentially be confirmed by using the rest of the ether series of L-ddBCNAs to determine if a similar SAR can be established as was observed against VACV and measles. If this was the case, then it would suggest the same MoA is involved against all three viruses.

The discovery of activity of the ddBCNAs against measles virus was very significant in terms of clinical relevance. This virus has a large impact worldwide. Even with the development of a successful vaccine, outbreaks still often occur due to the particularly high level of herd immunity (>95%) required to prevent the spread of this virus. Complications caused by measles infection remain one of the leading causes of infant mortality worldwide. There are currently no specific treatments for measles infection on the market. Based on this work the ddBCNAs were filed for a patent: US patent; Activity of ddBCNAs versus human cytomegalovirus, poxviruses and measles virus (2011-US patent # 13/193,343) (McGuigan et al. 2013).

In addition, regardless of its clinical relevance, the observed activity against measles virus proved very useful for further investigation of the ddBCNAs. This is because the wild type measles virus produces a clear CPE in the form of syncytia in B95a cells. This tendency toward syncytia formation makes a suitable model for measuring the activity of the compounds against measles.

It was found that the ether series of compounds demonstrated a clear SAR profile against the measles virus when plotting IC_{50} concentrations (figure 4.11). Critically, this SAR matched those previously observed against VACV using both luciferase and plaque assays (as described in chapter 3 section 3.4). As such, this relationship has now been observed in three independent cells lines infected with two different viruses. This offers strong evidence for the antiviral effects of these compounds. It also strongly suggests that they have a specific target as altering the length of the hydrocarbon side chain by a small amount has a significant effect on their activity. This also confirms that the ddBCNAs are not just having a general effect that could be achieved with any of their structural variations.

Of note, whilst the IC_{50} concentrations for the measles virus follow a similar trend to the VACV IC_{50} concentrations, they appear to be higher. This could imply that higher concentrations of the compounds are required to inhibit the measles virus to the same extent as VACV. However, the discrepancy could also be due to the timescales required for the two experiments; the measles IC_{50} experiments were collected at two days pi, whereas the VACV IC_{50} concentrations from the plaque assays were measured at four days pi.

When using the compound against the vaccine (mEdATCC) strain of measles virus, the variation in the effect in different cell lines represents an interesting observation. It is not clear exactly why the effect of Cf2642 is different against this virus strain in certain cell lines. However this finding could provide insights into the MoA of the drug based on the differences between the two virus strains and between the cell lines B95a and Vero. Potential insights into the observed effect will be discussed further in chapter 7.

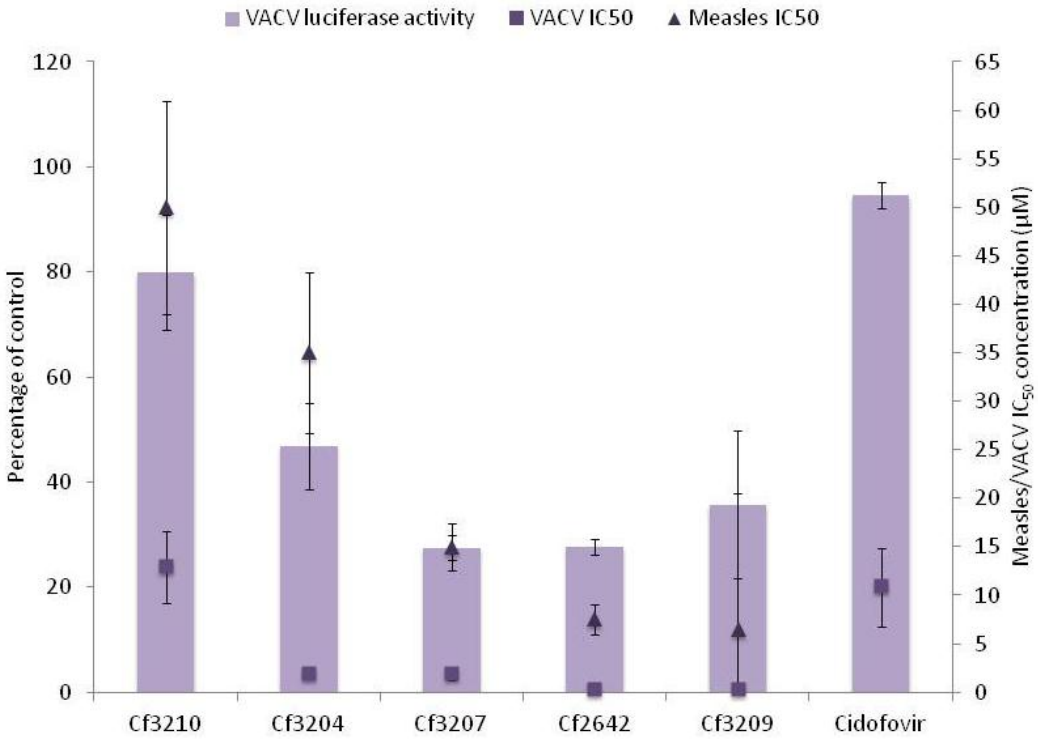

Figure 4.11 SAR profiles of the ether series of L-ddBCNAs against measles shown as IC_{50} concentrations (triangle points). The IC_{50} concentrations for these compounds show a similar SAR observed in VACV IC_{50} concentrations (square points) and luciferase assay data (bars). The left y-axis indicates the luciferase readings as percentage of control. The right y-axis indicates the concentrations for the measles IC_{50} and the VACV IC_{50} in µM. The results show that in all assays, Cf3210 is the worst performer. Taking all three assays into account the compound Cf2642 appears the best performer. Even though the measles IC_{50} concentration is slightly lower for Cf3209 the error bar on this point is larger and this compound did not perform so well in the luciferase assays.

Chapter five – Toxicity of ddBCNAs

5.1 Introduction

The activity of ddBCNAs against several viruses (including VACV, measles and possibly HIV-1) has been previously studied (as described in chapters 3 and 4). Regardless of the activity they show, an important consideration in the use of anti-viral compounds is their toxicity profile. This chapter describes efforts to test the toxicity levels of these compounds, at active concentrations, against a series of host cells. An understanding of their toxicity profiles is essential if they are to have any chance of being considered as viable clinical antiviral candidates. The toxicity testing of these compounds involved several assays that tested;

-ATP levels – Using the cell titer-glo kit (Promega), which measures the viability of cells based on the level of ATP (Crouch et al. 1993). The reaction uses ATP in the sample to convert Beetle luciferin into oxyluciferin. This leads to the production of light at levels directly proportional to the amount of ATP in the sample, thereby providing an indication as to the number of viable cells. This is a very sensitive method of viability detection (Petty et al. 1995).

-Caspase 3/7 levels – Using the caspase-glo 3/7 kit (Promega), which measures the levels of caspases 3 and 7 in the sample. The kit contains a substrate with a tetrapeptide (DEVD) sequence that is cleaved by the caspases. The cleaved DEVD sequence then acts as a substrate for a luciferase enzyme, leading to the production of light. The level of luminescence produced provides information as to the level of apoptosis in the sample as the caspases are effector enzymes of apoptosis (Thornberry and Lazebnik, 1998). This assay was performed to confirm that the ddBCNAs were not leading to apoptosis of the host cells.

-The effect of the pH of the medium - In previous assays involving the ddBCNAs it has been noted that high concentrations of the compounds correlated with a change in the colour of the cell medium form red to yellow. Since DMEM contains a pH indicator (phenol red) this change in colour could suggest that the

ddBCNAs are acting on the cells in a way that causes them to release acidic substances into the cell medium. The resulting decrease in the pH could potentially cause the cells to lose viability. In order to determine if any loss in viability is due to the presence of the compounds themselves or as an indirect result of decreasing pH of the cell medium, a simple assay of changing the cell medium (containing fresh Cf2642) on a daily bases was adopted. The resulting effect on cell viability was observed.

In combination, the results from these toxicity assays were used to gain insights as to the suitability of the ddBCNAs as drug candidates.

5.2 Materials and Methods

5.2.1 Cell titer-glo kit

The method selected for measuring the viability of cells in the presence/absence of drug was the cell titer-glo kit (Promega). This assay sensitively determines the viability of cells by measuring ATP – the amount of which is directly proportional to the number of viable cells present. The reaction employed in this method is shown in figure 5.1

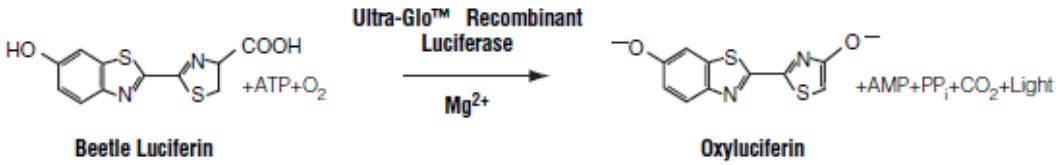

Figure 5.1 The reaction used by the cell titer glo kit to measure the ATP present in the sample. The level of ATP is directly proportional to the number of viable cells in the sample. (Figure from Promega cell titer-glo kit protocol)

This method has been described as the gold standard for viability assays as it determines the level of ATP present, rather than other methods such as MTT colourimetric assays (Petty et al. 1995). Measuring ATP provides a more accurate indication of the number of viable cells as the ATP is broken down very quickly after

cell death. In contrast, proteins may be more stable and take more time to break down.

5.2.1.1 Cf2642 effect on viability using Cell titer-glo kit

In order to determine how the ddBCNAs affect the viability of cells over a sustained period (here four days), a time course assay was carried out with the lead compound Cf2642. B95a, Vero, RK13 and BSC-1 cells (the same cell lines used in previous antiviral assays) were seeded into black (clear bottom) 96-wp and left overnight to settle and reach confluency. They were treated with different concentrations (50, 20, 10, 5, 1, 0 μM) of Cf2642. These concentrations were selected as they include the compound at active concentrations used in the antiviral assays (1, 5, 10 μM) and higher in order to determine the difference between active concentrations and toxic concentrations. Cell viability was measured at 6h, 12h, 24h, 48h, 72h and 96h time points using the cell titer-glo kit. This range of time points was selected to cover the full length of timescales used in previous antiviral assays. Each condition was carried out in triplicate. The aim of this experiment was to confirm that the apparent antiviral affects of the compounds was not simply due to the cells losing viability.

5.2.1.2 CC_{50} calculations of the ether series of L-ddBCNAs

Following on from the time course viability assay, the cell titer-glo kit assay was used again to calculate CC_{50} concentrations for the ether series of L-ddBCNAS including Cf2642. BSC-1 cells were seeded into a black (clear bottom) 96-wp and left overnight to settle and reach confluency. The cells were then treated with each of the ether series of ddBCNAs at different concentrations (0, 1, 10, 50 and 100 μM). The viability of the cells was measured using the cell titer-glo kit after four days and the values were used in GraphPad to calculate CC_{50} concentrations*. By using BSC-1 cells and measuring activity over four days, it was possible to directly compare these CC_{50} concentrations with the previously generated IC_{50} concentrations against VACV (as described in chapter 3 section 3.3.5).

*Of note, the ether L-ddBCNAs did not reduce the viability of the BSC-1 cells to 0% at concentrations of up to 100 µM. In order to force the program to produce a curve and calculate a CC_{50} as the half way point between 100% and 0% viability, a theoretical point was included. This value was included to assume the viability would be zero at a high concentration of the compound (e.g. 10 000 µM or 10mM). The reason for including this point was because without it the program calculates the halfway point between the values given. This leads to a much lower calculated CC_{50} value than the bar graphs for the viability would suggest.

5.2.2 Caspase-glo 3/7 assay

To assess whether the ddBCNAs lead to an increase in cellular apoptosis, the caspase-glo 3/7 kit was used. This kit contains a substrate with a DEVD sequence that is recognised and cleaved by caspases 3 and 7 (effector enzymes in apoptosis). This releases aminoluciferin. The free aminoluciferin acts as a substrate for the luciferase (also in the kit) which leads to a luciferase reaction and the production of light. The reaction is summarised in figure 5.2. The amount of light produced is proportional to the activity of caspases 3 and 7, and can be used as an indicator of the level of apoptosis in the cells.

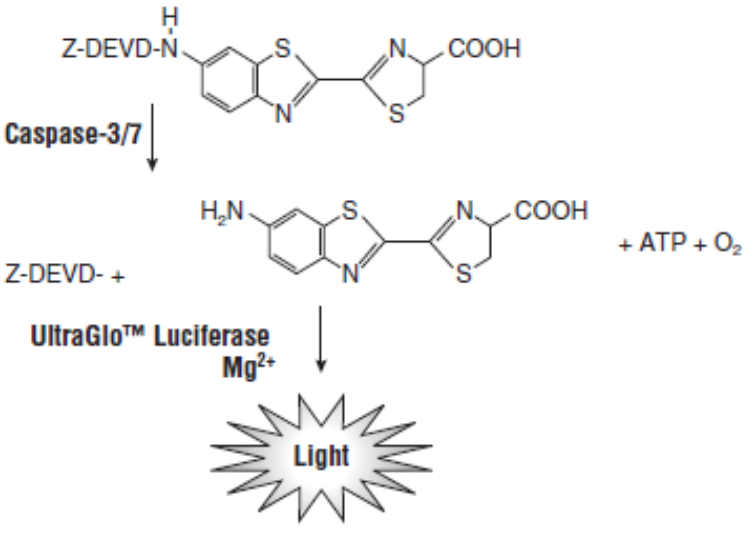

Figure 5.2 The reaction used by the Caspase-glo 3/7 kit to detect the levels of Caspases 3 and 7 in the sample. These provide an indication of the level of apoptosis in the sample (figure from Promega Caspase-glo 3/7 kit protocol).

As some of the results from the first Caspase-glo 3/7 assay suggested a possible effect of the presence of EBV in cells, a second experiment was performed that included a range of B cell lines with a known presence or absence of EBV. The presence or absence of EBV was confirmed (by Joachim Bugert) in each of the B cell lines using a PCR for EBV as described by Telenti et al. (1990). HeLa and RK13 cells were again included so as to allow for the comparison of the two data sets.

5.2.3 Cell medium replacement assay

It was noted in several previous experiments (described in chapter 3 section 3.3.5 and chapter 4 sections 4.3.2, 4.2.4 and 4.3.9) that the presence of the ddBCNAs correlated with a change in colour of the cell medium, possibly indicating a release of acidic substances from the treated cells. In order to determine if the effect of the ddBCNAs on the viability of the cells is a direct effect of the compounds or as an indirect result of decreasing pH of the medium, an assay was carried out that involved replacing the medium (± Cf2642) on a daily bases over the course of four days.

BSC-1 and B95a cells (24 wells of each) were seeded into a black (clear bottom) 96-wp and left overnight to settle and reach confluency. These were then pretreated for 30 minutes with Cf2642 (10 µM) or with a DMEM control. BSC-1 cells were infected with mEdATCC and B95a cells were infected with mWT Fb. Uninfected controls for each condition were also included and each condition was carried out in triplicate. Half of the wells had their medium (± Cf2642) changed every 24 hours, while the other half remained in the same medium. The viability of the cells was determined on the fourth day using the cell titer-glo assay kit.

5.3 Results

5.3.1 Cell titer-glo assays and Cf2642

To determine whether Cf2642 caused a loss in cell viability over the course of the antiviral assays described in previous chapters, an assay was carried out using the cell titer-glo kit. This involved applying Cf2642 at 50, 20, 10, 5, 1 and 0 µM of drug to B95a, Vero, RK13 and BSC-1 cells and measuring their viability after 6, 12, 24, 48, 72 and 96 hours. This was to ensure that the antiviral effect of the compound is not simply due to a loss in cell viability.

The cells that appeared to be most affected by the compound were the B95a cells (figure 5.3). For up to 24 hours, the cells appeared to maintain their viability at all of the included concentrations. At 48 hours however, loss in viability is evident at 5µM Cf2642, leading to readings that are only 40% of the no drug control. At 72 and 96 hours, cell viability levels decrease markedly when drug concentrations of 5 µM and above are used, with luminescence signals decreasing to ~5% and ~0% of the control respectively. Of note, inhibition of syncytia formation by mWT Fb in B95a cells has previously been observed at 24 hours pi, suggesting that the viability loss observed here at 48 hours pi is not the cause of this antiviral effect.

The Vero cells appear less affected than the B95a cells by Cf2642. As displayed in figure 5.4, they maintain full viability at all concentrations included in the assay for up to 48 hours. At 5 µM, cell viability starts to descend (to about 40%) between 48 and 72 hours. Above this concentration the viability is greatly reduced (to around 5-10% of the control) at 72 hours. At 96 hours the cells appear to have very little remaining viability (<5%) at concentrations of 5 µM and above. There also appears to be an anomalous peak in luminescence at the 5 µM concentration after 48 hours. The reason for this is not clear.

The effect on viability of RK13 cells appears to lie somewhere in between that observed for the B95a and the Vero cell lines – evidenced by a ~50% reduction in viability at the 48 hour time point (figure 5.5). Again this loss in viability is only observed at concentrations of 5 µM and above. The antiviral effect against VACV in

RK13 cells can be seen at only two hours pi. Therefore, as suggested in B95a cells, loss in cellular viability is unlikely to be responsible for the apparent antiviral effect of the compounds. At the 72 and 96 hour time points, cell viability is reduced to around 10% and 0% of the control respectively at concentrations of 5 µM and above.

Despite there being a ~20% decrease in viability levels compared with controls at concentrations of 5 µM and above at only 6 hours after addition, the BSC-1 cells appear to be less affected than the other cell lines tested (figure 5.6). They ultimately maintain viability at higher concentrations and longer time points i.e. the viability of the cells is still above 50% of the control even at the highest concentration (50 µM) after four days. This offers further evidence that the antiviral effect is not due to a loss in the viability of the cells.

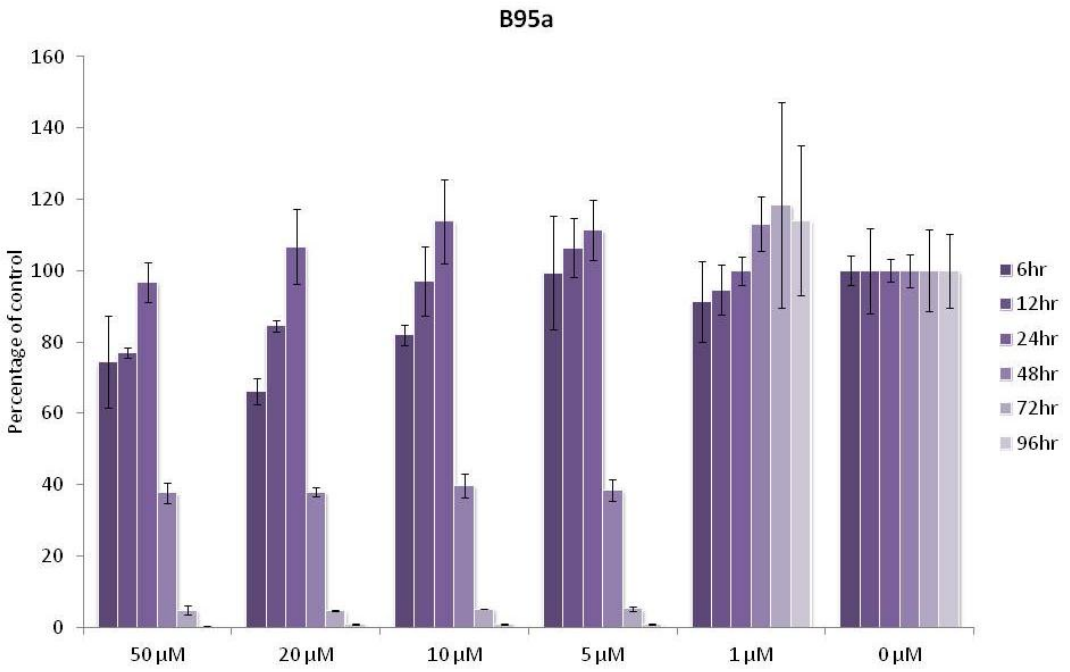

Figure 5.3 The effect of Cf2642 at 50, 20, 10, 5, 1 and 0 µM on the viability of B95a cells over 6, 12, 24, 48, 72 and 96 hours.

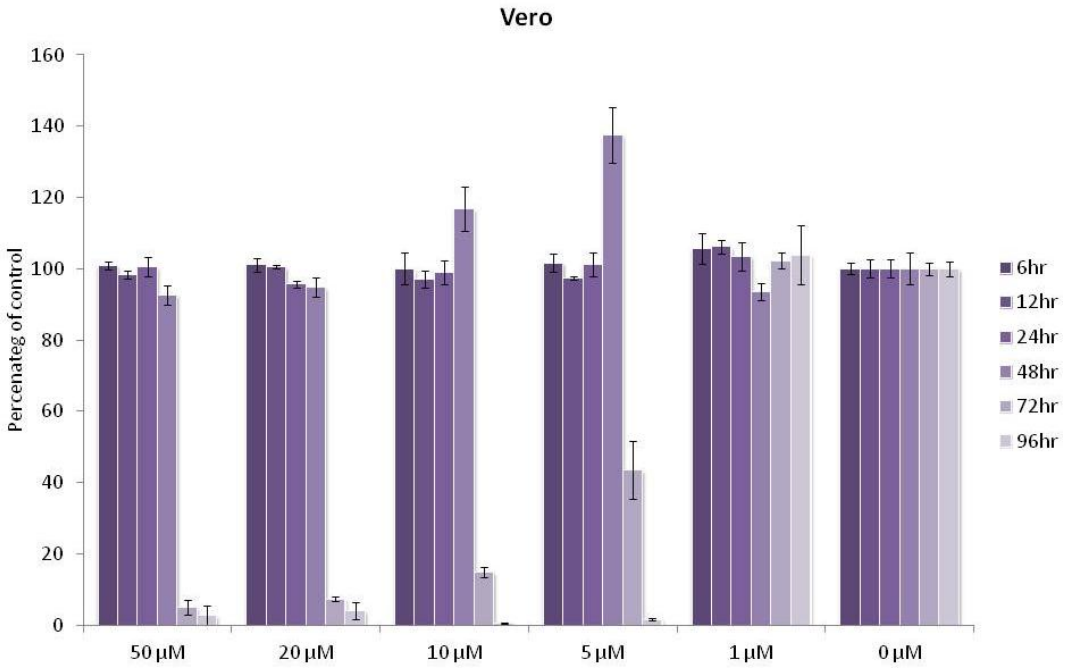

Figure 5.4 The effect of Cf2642 at 50, 20, 10, 5, 1 and 0 µM on the viability of Vero cells over 6, 12, 24, 48, 72 and 96 hours. The peak at 5 µM over 48 hours appears to be anomalous.

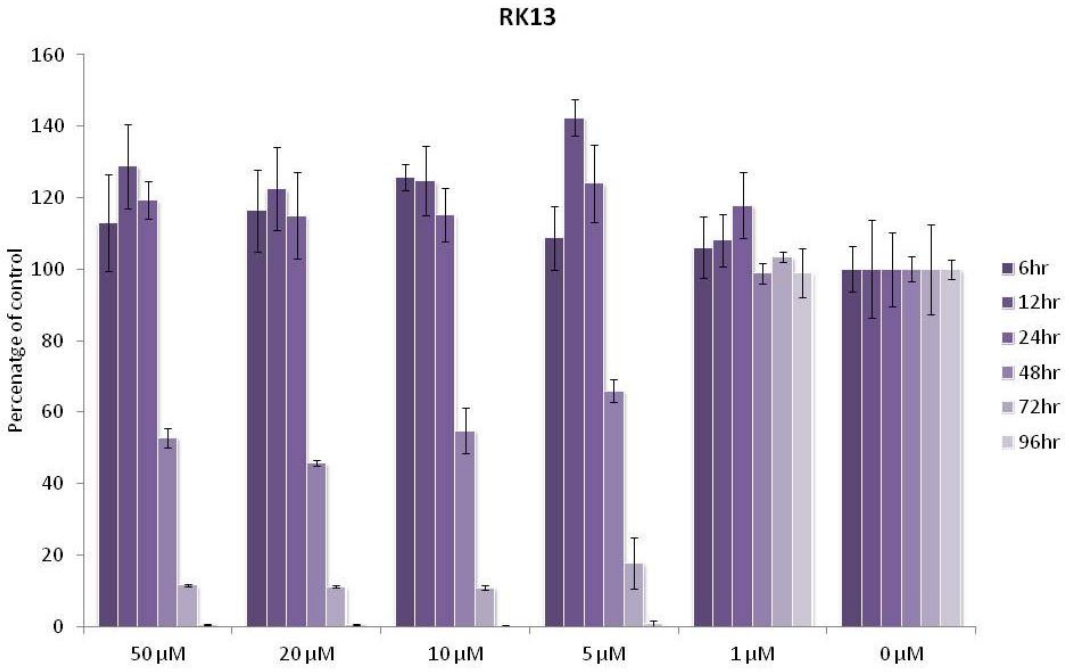

Figure 5.5 The effect of Cf2642 at 50, 20, 10, 5, 1 and 0 µM on the viability of RK13 cells over 6, 12, 24, 48, 72 and 96 hours.

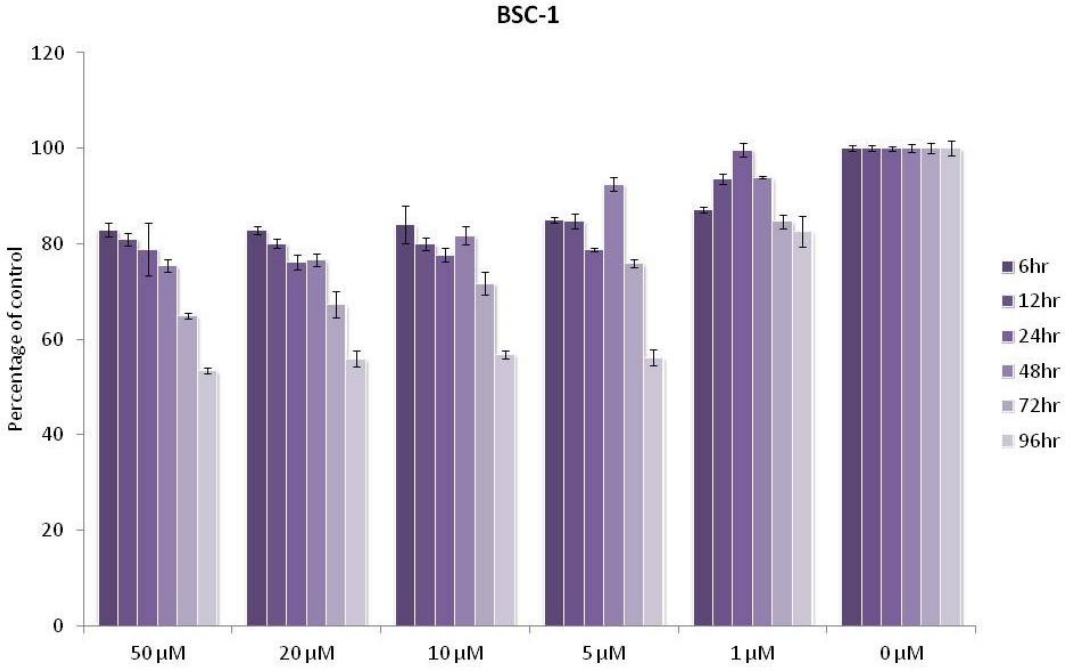

Figure 5.6 The effect of Cf2642 at 50, 20, 10, 5, 1 and 0 µM on the viability of BSC-1 cells over 6, 12, 24, 48, 72 and 96 hours.

5.3.2 CC_{50} concentrations of the ether series of L-ddBCNAs

Further assays using the cell titer-glo kit were carried out to test the ether series of L-ddBCNAs in BSC-1 cells at a range of concentrations over four days. CC_{50} concentrations were calculated and compared with the IC_{50} concentrations for the activity of the compounds against VACV in the same cell line over the same time period. This experiment was designed to calculate CC_{50} concentrations for the ether series of ddBCNAs to correspond with the IC_{50} concentrations against VACV calculated in chapter 3 section 3.3.5 This is why they were done in BSC-1 cells only over four days. The maximum concentration used in this assay was also increased as the results from the previous cell viability assays showed that in BSC-1 cells 50 µM Cf2642 did not decrease the viability to less than 50%.

The observed CC_{50} calculations are displayed in table 5.1. Interestingly the compounds expected to be the most active based on previous data (Cf2642, Cf3207, Cf3209) appear to have higher CC_{50} concentrations than those that previously showed less activity (e.g. Cf3210, Cf3204). The CC_{50} for the most active compound, Cf2642, was calculated to be 105 µM, whilst Cf3210 and Cf3204 had a calculated CC_{50} of 64.6 µM and 63.3 µM respectively.

The CC_{50} concentration for Cf2642 (105 µM) as compared to its IC_{50} concentration (0.19 µM), suggests that there is a good selectivity index (>500). Wortmannin was included in this assay as a control and was calculated to have a CC_{50} concentration of 22 µM. This is considerably lower than that of the ether series of L-ddBCNAs and suggests that they are less toxic.

Compound	CC_{50} (μM) in BSC-1 cells (4 days)
Cf3204	63.3
Cf3207	73.1
Cf2642	104.8
Cf3209	112.6
Cf3210	64.6
Wortmannin	22.3

Table 5.1 The CC_{50} concentrations calculated for the ether series of L-ddBCNAs using the cell titer-glo assays in BSC-1 cells over 4 days. These results are also presented in the discussion section 5.4 in the form of a bar graph that compares the CC_{50} concentrations with the IC_{50} concentrations.

5.3.3 Caspase-glo 3/7 assay

To assess whether the ddBCNAs lead to an increase in cellular apoptosis, the caspase-glo 3/7 kit was used to test the level of these caspases in a variety of cells treated with Cf2642 at 10, 1 and 0 µM for 24 hours. The reason for using these concentrations and testing over a 24 hour timescale was to cover the concentrations/timescales at which antiviral activity had previously been observed. The initial data indicated that Cf2642 causes an increase in apoptosis in B95a cells (figure 5.7); 1 µM of drug increased the luminescence signal (apoptosis) by 25%, while 10 µM increased the signal by >100% relative to the signal in the absence of drug. However, in other cell lines (namely BJAB, RK13, HFFF, A549 and BSC-1) there is no evidence for increased apoptosis. HeLa were also included and showed some increase in the luminescence signal in the presence of Cf2642.

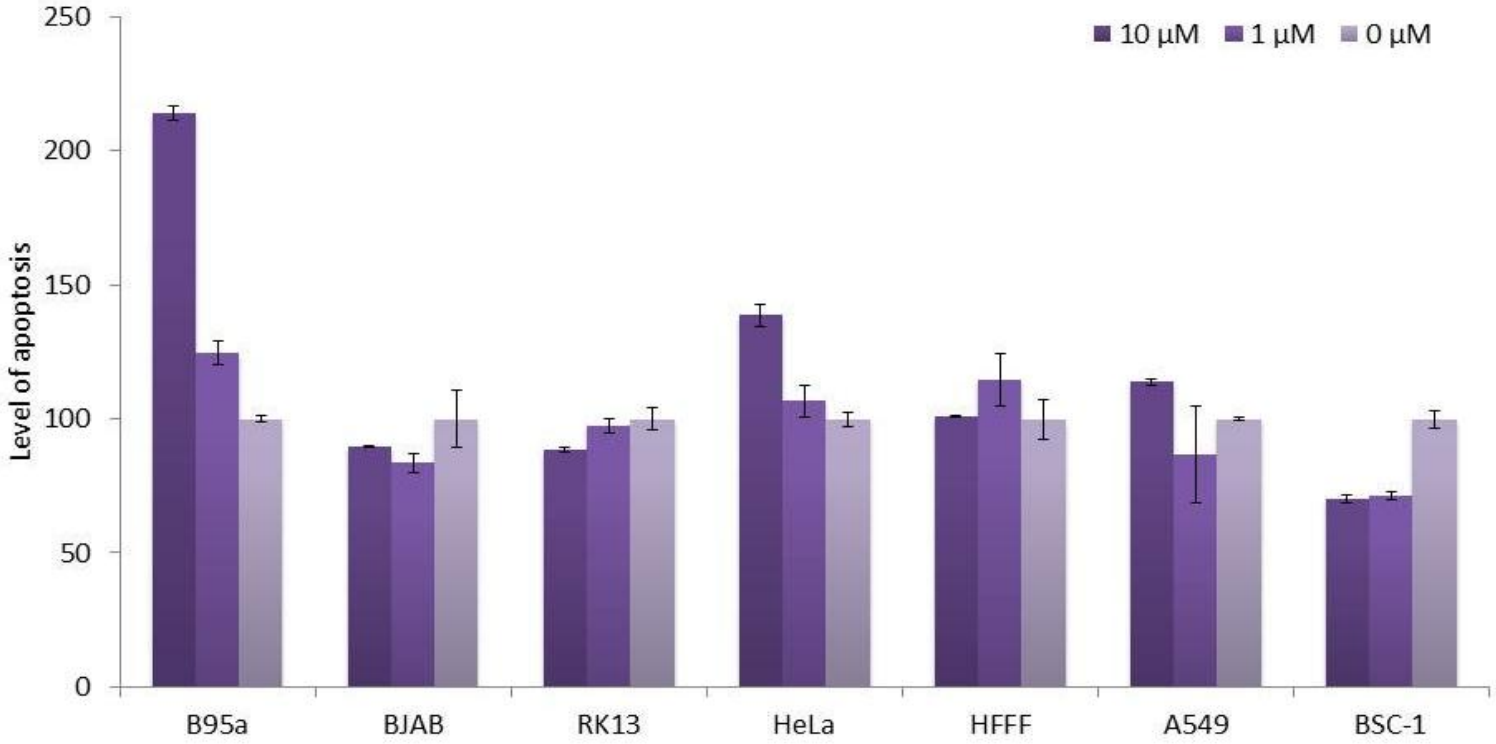

Figure 5.7 The effect of Cf2642 at 1 and 10 µM on the level of apoptosis (determined by the levels of caspases 3 and 7) in a range of cell lines. The values for the level of apoptosis were calculated as a percentage of the no drug readings. Cf2642 appears to double the level of apoptosis in B95a cells. The levels are increased by about 25% in HeLa cells, the caspase levels in the rest of the cells were relatively unaffected by Cf2642. Here the BJAB cells included are those from the Bugert laboratory.

5.3.4 Caspase-glo 3/7 assay in EBV positive and negative cell lines

B95a cells belong to a class of cell lines that have been transformed using EBV. Based on the positive results from the initial caspase assay (figure 5.7), it was suggested that the ddBCNAs may be leading to apoptosis in cell lines containing EBV. This was fuelled by the fact that BJAB cells included in the assay did not show any signs of increased apoptosis. BJAB cells are similar to B95a cells in that they are both derived from B cells, however BJAB are of human origin and were assumed to be EBV negative. To further investigate this effect, a second caspase assay was devised to test whether the ddBCNAs might induce apoptosis specifically in EBV containing cells, using a selection of B cells some of which were EBV positive and some EBV negative.

Prior to this second experiment the presence or absence of EBV was confirmed in each of the B cell lines using a PCR for EBV using the method of Telenti et al. (2010). The results of this PCR led to the surprising finding that the BJAB (from the Bugert laboratory) were actually EBV positive.

The cells used in the second round of testing were the B95a cells as before (EBV +), BJAB cells (human derived B cell line) from the Bugert laboratory (EBV +), BJAB cells from the MRC (EBV -), BJAB cells from MRC that have been incubated in medium from EBV + cells (i.e. EBV+ induced) and Ramos (another human derived B cell line that were EBV-). This was in an effort to confirm whether Cf2642 was leading to apoptosis specifically in EBV positive cell lines. This experiment involved direct comparison of EBV positive and EBV negative versions of the same cell line (i.e. BJAB). RK13 and Hela cells were also included in this assay to link the results with the previous apoptosis assay. Cf2642 was included at 10 µM as before but this time the second concentration was 20 µM instead of 1 µM in order to see if a clearer difference in effect could be established by using a higher concentration. Staurosporine (1 µM) was included in this assay as an apoptosis inducing positive control for comparison purposes. Results are displayed in figure 5.8.

All of the cells tested produced luminescence signals that were significantly increased by the presence of the positive control staurosporine. This result indicated that the caspase assay does reliably detect increases in the level of apoptosis.

In contrast to the initial caspase assay, the data this time indicate no clear difference in the levels of apoptosis in Cf2642 treated cells as compared to those that were untreated, regardless of drug concentration. This included the same B95a cells previously tested. The caspase levels appear to be 100% of that of the control (i.e. there is no increase in the level of apoptosis in the presence of Cf2642 over the cells containing no drug). In one case (the BJAB cells from the Bugert laboratory), it appears that the levels of caspase are actually reduced in the presence of Cf2642 (at 10 µM the caspase levels are ~50% of the no drug control).

From the results of this experiment Cf2642 was ruled out as an apoptosis inducer as it generally did not increase the levels of caspases 3 and 7. It was also assumed that it was unlikely that Cf2642 induces apoptosis in B95a cells as the initial result was not reproducible. It was concluded that apoptosis was not the cause of the antiviral effect observed with the ddBCNAs.

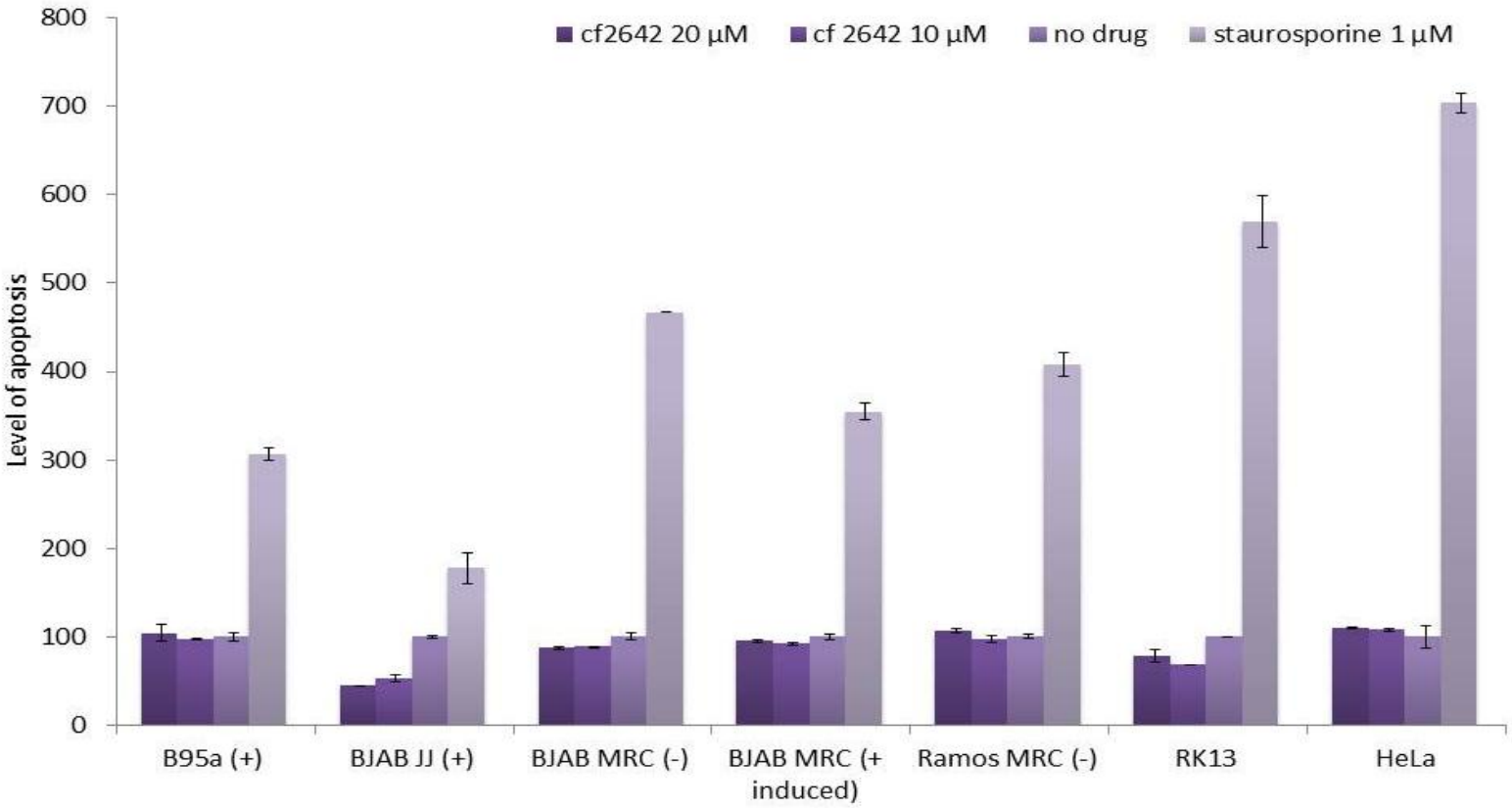

Figure 5.8 The effect of Cf2642 at 20 and 10 µM on the level of apoptosis (caspases 3 and 7 as percentage of no drug control) in a range of cell lines. Cells that are EBV positive are represented with (+) and the EBV negative with (-). HeLa and RK13 cells were also included. Staurosporine was added to each of the cells as an apoptosis inducing positive control. Cf2642 does not appear to increase the level of apoptosis in any of the cells tested. BJAB JJ are BJAB cells from the Bugert laboratory, BJAB MRC are BJAB cells obtained from MRC.

5.3.5 Cell medium replacement assay

Coincidental observations from previous tests of the ddBCNAs raised the question as to whether loss of cell viability could be an indirect consequence of the effect of the ddBCNAs. The medium of cells in the presence of active concentrations of the ddBCNAs changes in colour from red to yellow, which in turn indicates a reduction in the pH of the cell medium (that contains phenol red indicator). Here a method was devised where-by the cell medium (and drug) were replaced with fresh stocks, on a daily basis. This experiment was carried out in B95a and BSC-1 cells (the most and the least affected in the viability assays with the cell titer-glo assay described section 5.3.1), and the viability of the cells was measured after four days using the cell titer-glo kit.

The results of this experiment are presented in figure 5.9. Overall, it appears that in the absence of any virus the viability of both cell lines is improved when the medium/drug is replaced on a daily bases. For example, non-infected BSC-1 cells that were treated with Cf2642 and that had their medium changed daily, showed cellular viability levels approaching those observed in the no-drug control (123 000 RLU compared to 162 000 RLU respectively). However, cells treated in the same way but that were exposed to the same cell medium for four days showed a greatly reduced viability as compared with the no drug control (7000 RLU compared to 166 000 RLU). As expected, the control wells containing no drug showed little difference in viability whether the medium was changed or not. The latter result confirms that over the course of four days in DMEM, the cells are not losing viability as a result of their own metabolic waste products.

The same trends were also observed in the B95a cells - those that had their medium changed every day produced signals of 485 000 RLU (Cf2642 treated) compared with 434 000 RLU (untreated). The cells that were left in the same medium for four days produced values of 20 000 RLU (Cf2642 treated) and 367 000 (untreated).

Again, these data provide evidence that the drug itself is not leading to the loss in the viability of the cells. Instead, the side effect of the drug (i.e. change of pH of the medium) is actually the reason for the loss in viability.

In terms of the effect of medium change on the antiviral activity, Cf2642 treated BSC-1 cells infected with mEdATCC did not display improved viability above that of the no drug control with the readings taken being 80 000 RLU compared to 99 000 RLU respectively when the medium was changed daily. However the effect of the compound against mWT Fb in B95a cells suggests that treating the infected cells with fresh drug on a daily bases may increase the viability of the cells above that of the no drug control, in this case the luminescence values produced were 340 000 RLU (Cf2642 treated) compared with only 100 000 (untreated). This suggests that the Cf2642 is having an antiviral effect against the virus in this assay over four days without causing loss in viability of the cells itself as long as it is replaced with fresh medium and drug on a daily bases.

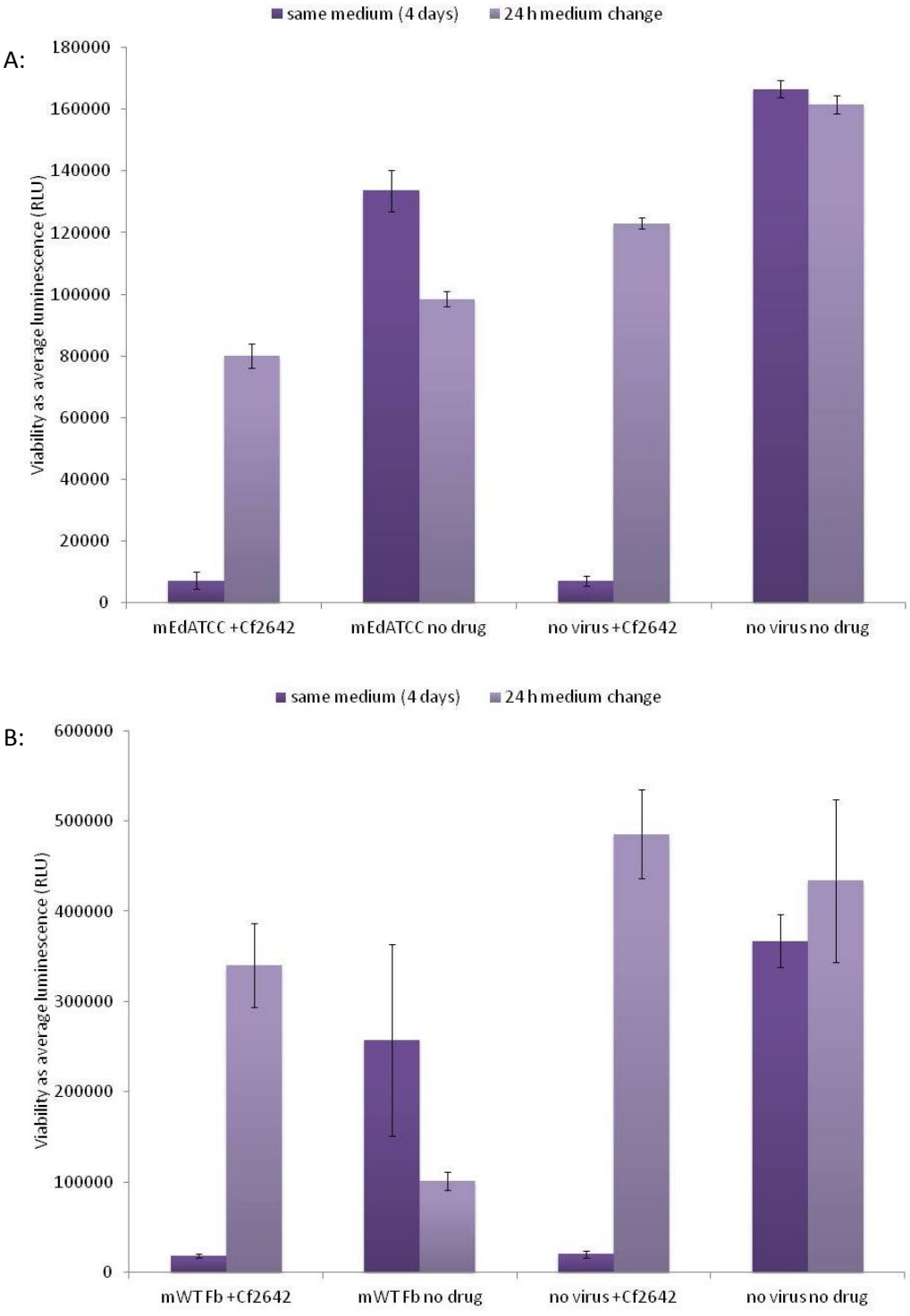

Figure 5.9 Cell viability readings taken after four days. Cells were either treated with Cf2642 (10 µM) or untreated. Half of the cells in each condition were either left for the four days with no change of medium, the other half had the medium (± Cf2642) changed on a daily bases. A: BSC-1 cells either infected with mEdATCC or uninfected, B: B95a cells either infected with mWT Fb or uninfected.

5.4 Discussion

The data presented here show that the ddBCNAs do not have a toxic effect on the host cell at active concentrations (i.e. the concentration previously shown to be necessary for the antiviral effect). For example, in BSC-1 cells exposed for four days, the CC_{50} concentrations of both Cf2642 and Cf3209 were calculated to be 105 µM and 112.6 µM respectively and the IC_{50} for both compounds was just 0.19 µM. Combined, these values produce a selectivity index for Cf2642 and Cf3209 in BSC-1 cells of 550 and 592 respectively (i.e. the concentration of drug that causes a 50% reduction in viability is over 500 times greater than the concentration that causes a 50% reduction in viral activity). However as the toxicity of the ether L-ddBCNAs appears to increase as the activity decreases, the selectivity index of the least active (Cf3210) is only 5. The intermediate compounds Cf3204 and Cf3207 display selectivity index values of 33 and 40 respectively. The selectivity index is an important consideration when developing compounds as potential drug candidates. The *in vitro* selectivity index for cidofovir against VACV has been shown to be 42 (Nettleton et al. 2000) although was higher against parapoxviruses (198-264). According to this data the *in vitro* selectivity index for Cf2642 against VACV is much higher than for the control drug cidofovir.

The CC_{50} concentrations generated here were plotted against the IC_{50} concentrations calculated in BSC-1 cells against VACV (chapter 3 section 3.3.5) in figure 5.10. The fact that the CC_{50} and IC_{50} concentrations do not follow the same trend across the ether series of L-ddBCNAs (i.e. the most toxic of the ddBCNAs appears to be the least active and vice versa) provides further evidence that the antiviral activity of the ddBCNAs is not simply due to their effect on host cell viability.

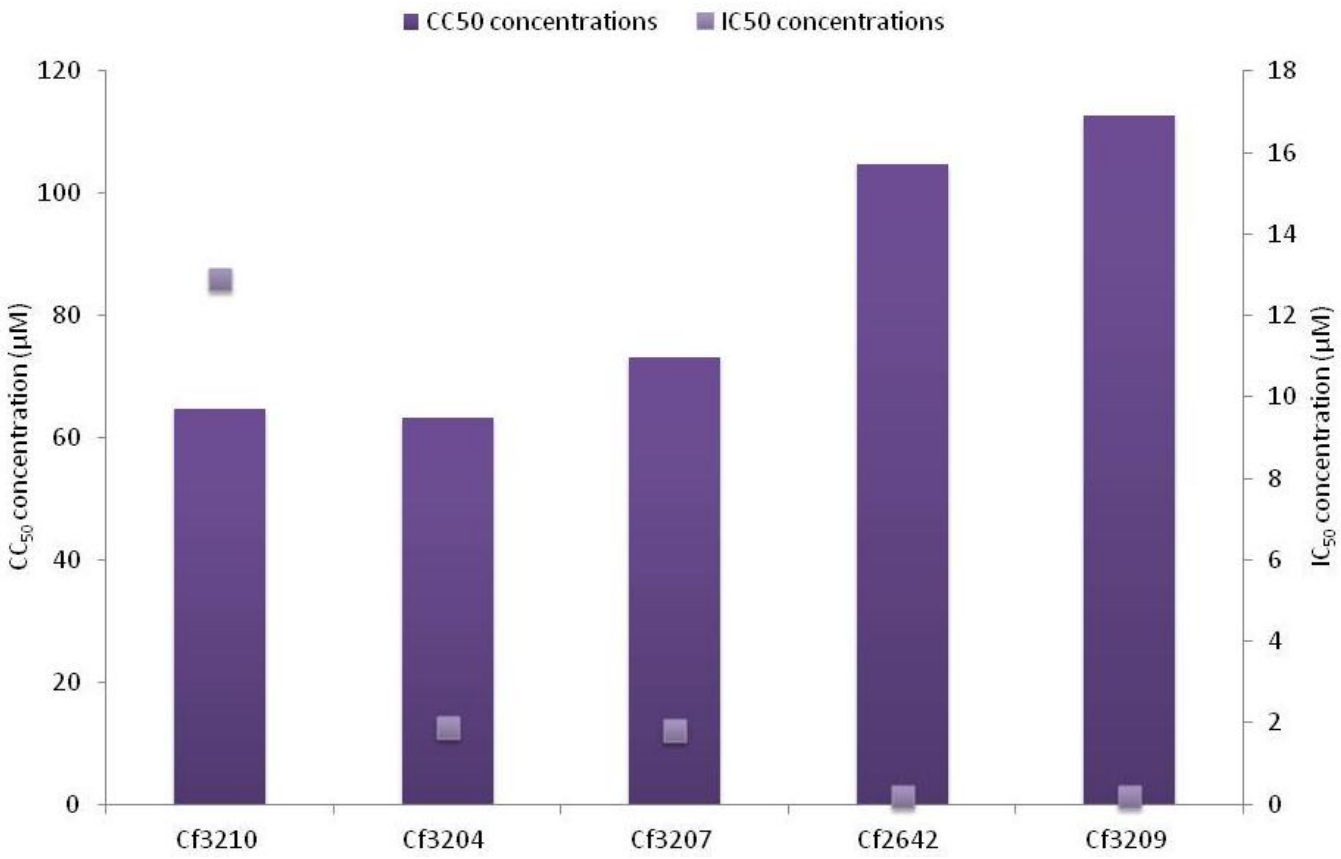

Figure 5.10 CC_{50} concentrations (bars against the left axis) compared with IC_{50} concentrations (points against the right axis). The two data sets do not follow the same trend across the ether series of L-ddBCNAs. As the activity increases with increasing side chain length, it appears that the toxicity decreases.

In addition to the cell titer-glo assays, further toxicity data was collected using an independent method, the caspase-glo 3/7 kit. This was to determine whether the loss in the viability described above was as a result of the cells entering apoptosis.

In the first of the caspase-glo 3/7 assays HeLa cells displayed a slight increase in the levels of caspases 3 and 7 in the presence of drug. At 10 µM the levels appear to increase by around 50%. It was noted though that in the absence of drug the background luminescence readings for this cell line were higher than for the others (data not shown). This suggests that these cells have higher background levels of the caspases.

The initial data also suggested that the B95a cells are sensitive to the drug after 24 hours exposure to Cf2642 at 10 µM, with an almost doubling in the levels of caspases 3 and 7. Beyond this, the drug did not appear to induce apoptosis in the other cells tested.

At this stage, the data points to a strong apoptotic response specifically in the B95a cells. Since these cells had been transformed with EBV, the next phase of caspase assays focused on distinguishing the difference in levels of apoptosis induced in EBV positive and EBV negative cells. It was thought that if it could be confirmed that the ddBCNAs induce apoptosis specifically in cells transformed with EBV then the ddBCNAs may have potential as anti-cancer agents in EBV induced cancers. Cidofovir has been described as having potential therapeutic use against EBV induced cancers; it has been shown to reduce the production of the EBV oncoproteins. Another effect of cidofovir on EBV positive cells was increasing their sensitivity to ionising radiation, causing them to enter apoptosis (Abdulkarim et al. 2003).

It was hoped that the second phase of testing would be particularly informative since a direct comparison could be made between a selection of B cell derived cell lines (i.e. essentially including EBV positive and EBV negative versions of the same cell line). However, the results of these investigations proved to be inconclusive. Contrary to the initial caspase assay, the apoptotic response of the B95a cells was

found to remain consistent whether the drug was present or not. The reason for this discrepancy remains unclear. Furthermore, the two other EBV positive cell lines did not display increased apoptosis in response to the drug. The results of the second assay implied that the ddBCNAs are unlikely to be inducing apoptosis in the cells tested. As such, this line of investigation was terminated owing to too little time and money, though ideally further repeats involving more conditions would have been attempted.

Interestingly, BSC-1 cells showed a decrease in the level of the caspases in the presence of the ddBCNAs. This work supports the conclusion that the ddBCNAs are having an inhibitory effect on the viruses without leading to increases in caspase 3 and 7 levels (and resultant apoptosis) in the host cells.

Over the course of several experiments carried out in the study of the ddBCNAs, it has been noted that the medium of the cells turns yellow at higher concentrations of the active ddBCNAs. This observation suggests a decrease in the pH of the cell medium at higher concentrations of Cf2642. It appears that the reduction in cellular viability closely corresponds to the change in pH/colour of the medium. The pH change had been noticed 24 hours after the addition of the drug to the cells while the loss in viability is seen after this point. This suggests that the drug itself is not leading to a loss in the viability of the cells, but is acting on the cells in a way that causes them to release acidic substances into the medium. It was thought that this decrease in pH of the medium could be the cause of the loss in cell viability.

B95a cells appear to be particularly prone to ‘medium acidification’ in the presence of the ddBCNAs, possibly explaining why the viability of these cells is more affected than the others. It could also be the reason that these cells enter apoptosis. It has been shown by Park et al. (1999) that an acidic environment can lead to apoptosis in the cell line HL-60 as a result of upregulation in caspases 1 and 3. This occurs at a pH of 6.2-6.6 within a couple of hours. As it takes up to 24 hours for the Cf2642 to cause a visible decrease in the pH of the medium, this could be the cause of the increase in the caspases 3 and 7 after this time in some cases. Another group to show that extracellular acidity may induce apoptosis (this time in MDCK cells) was

Schwerdt et al. (2004). Here it was demonstrated that extracellular acidification increased the levels of Ochratoxin A, which in turn induced apoptosis through caspase 3 activation.

To truly ascertain the effect of pH change on cell viability, an assay was devised that simply involved replacing the medium at regular intervals. Fresh medium (± Cf2642) was applied on a daily bases over the course of four days and cellular viability was compared between the cells with and without medium change. The data suggested that changing the medium did improve/extend the viability of the cells even in the presence of Cf2642 over the four days. This provided further evidence that the ddBCNAs are not directly having a toxic effect on the cells, and the loss in viability is due to the decrease in pH of the cell medium.

This effect of the pH on the viability requires further study to be confirmed and quantified. It would be interesting to see if using a medium with a higher buffering capacity (more concentrated medium) could extend the viability of the cells in the presence of the ddBCNAs when not replenished regularly. Beyond this, it would be very useful to see if a dynamic cell culture system could undo the effect of the decrease in the pH. For example the MinuCell system can be used to examine cells in a 3D tissue like cell culture model and has a constant supply of fresh medium. This would be a closer mimic of a living/dynamic system and would provide more pertinent information about the survival of the cells when supplied with a constant flow of fresh medium (± ddBCNA).

Following on from this model the next stage would ultimately be to study the toxicity effects of the ddBCNAs in animal models. This is the most accurate way of determining whether the compounds can be tolerated in a living system without causing toxicity issues.

It has already been shown in chapter 3 section 3.3.7 that the lead compound Cf2642 has been tested in a small pilot animal study in mice. In this experiment, mice that were administered with Cf2642 (up to 100 μg/kg) were unharmed and displayed no signs of discomfort in comparison to the control mice over the three

day experiment. The compound was injected into the peritoneal cavity of the mice and so the fact that it was well tolerated was a positive sign as this region of the mice is particularly sensitive. Dissection of the mice confirmed that there were no signs of internal inflammation at this site.

The discovery that the compound decreases the pH of the cell medium over time contributes yet further indications as to its MoA. This will be discussed further in chapter 6. Critically, this effect is observed in the absence of any virus and, therefore, it must be an effect that the compound is having on the cells that causes them to release acidic substances into the cell medium. It is also this effect that is thought to be the cause for the loss in the viability of the cells.

Chapter six - Mechanism of action

6.1 Introduction

Determining the MoA of a small molecule antiviral compound with a suspected cellular target is not a trivial task. For compounds that are synthesised with a target in mind, the MoA is potentially more obvious. The compound will either work against that target or not. If the target of the compound is unknown, searching for its precise target involves a complex process of elimination.

Each of the experiments previously described (in chapters 3, 4, and 5) have hinted at the MoA of the ddBCNAs tested. The work described in this chapter highlights assays that specifically focused on determining this MoA. It is believed that the compounds have a specific target as evidenced by the clear SAR shown in chapter 3, sections 3.3.1.2 and 3.3.5 and chapter 4, section 4.3.9. These indicate that the compounds can be rendered effective or ineffective simply through the addition or removal of carbon atoms to/from their side chain. It is also believed that the compounds have a cellular rather than viral target due to the fact that they display the same SAR profiles for cells infected with both VACV and measles virus. Cf2642 has been shown to work in several different cell lines but to different extents, pointing to a target that may be more prominent in some cells than others. This target is likely to be a host cell target which both VACV and measles take advantage of as part of their replication process.

In order to investigate what this target might be, specific assays were carried out focusing on one potential cellular target at a time. This could be either affected or unaffected by the drug. This elimination process, whilst laborious, proved effective in narrowing down the MoA.

The fact that it has been discovered that the ddBCNAs work against both VACV and measles viruses (shown in chapters three and four), suggests that the target of the ddBCNAs is cellular rather than viral since these are completely different viruses, VACV is from the poxvirus family while measles is from the paramyxovirus family. There is also some evidence that suggests that they may be active against HIV-1,

which is a lentivirus. It is highly unlikely that the ddBCNAs would be acting on a viral target within all three of these viruses. However, it is much more likely that they target a part of the host cell, one which all of these viruses take advantage of during their replication cycle.

Here, initial experiments studied the effect of Cf2642 on the entry and the spread of VACV. Confocal microscopy of VACV containing YFP attached to a structural protein (A3L), suggested that the entry of the viruses was possibly being inhibited by the compound as the virus particles appeared to accumulate on the surface of treated cells. This was later ruled out as the antiviral effect by using an acid wash to remove all external virus particles and counting all particles per cell in presence and absence of the drug. These results indicated that there was no difference in the number of particles inside the cells both treated with Cf2642 and untreated. Another theory was that the compound was affecting the spread of the virus from one cell to another by inhibiting the formation of actin tails. However confocal images taken in the presence of the compound clearly show actin tails at the surface of infected cells, indicating that this is also not the cause of the antiviral effect.

As mentioned in the toxicity chapter the active ddBCNAs lead to a change in colour of the cell medium at higher concentrations of the compounds (from red to yellow). The cell medium (DMEM) contains the pH indicator phenol red, which is red at a pH optimum for cell growth (7.4) but begins to turn orange at pH 7.2 and becomes bright yellow at pH 6.8 and below. This suggests that the compound is acting on the cell in a way that causes it to release acidic substances into the cell medium. A time course assay was carried out in order to determine at which point the medium initially visibly changes colour. This point was then used as the time scale for further studies based on the pH change effect.

After consideration as to why the ddBCNAs would be causing the medium to become acidic, one theory put forward was the possibility of the compound causing the migration of intracellular acidic vesicles such as lysosomes towards the cell membrane, where they may fuse and release their contents extra-cellularly. In

order to investigate this theory, an assay was devised that focussed on Cd63, a transmembrane receptor located on intracellular vesicles such as lysosomes. The purpose of this was to establish if there was a difference in its distribution in the presence and absence of Cf2642.

An ELISA for human IL-6 was carried out in order to determine if the ddBCNAs have an effect on the intracellular innate immune response. Most of the ddBCNAs tested had no effect on the levels of IL-6, with the exception of Cf3242. This compound was found to have increased toxicity against the cells as described in chapter 3, therefore this is likely to be the reason for the increase in the inflammatory response of the cell in the presence of this compound.

In order to verify if the early effect of the ddBCNAs against VACV could be due to inhibition of transcription at the enzymatic level, a cell-free transcription assay was carried out. This measured the amount of mRNA production based on the signal from incorporation of radioactively labelled [α^{32}P]UTP in permeabilised VACV and MCV virions (Bugert et al. 1998).

6.2 Materials and Methods

6.2.1 Flourescent vYFP-A3L confocal microscopy

HeLa cells were seeded into a 12-wp containing coverslips and left overnight to settle and reach confluency. The cells were pre-treated for 30 minutes with Cf2642/no drug control before being infected with a strain of VACV modified to contain YFP attached to the structural protein A3L (vYFP-A3L; gift from M Way, 2010), at an moi of 5. Cells were fixed 30 minutes pi. The cells were stained with phalloidin-594 to visualise the actin cytoskeleton of the cells (red) and mounted onto slides using Vectashield plus DAPI to visualise the nuclei of the cells (blue). The cells were imaged using confocal microscopy to verify if there was any difference in the distribution in the virus particles in relation to the cells with and without treatment.

6.2.2 Acid wash

In order to be able to visualise just virus particles that were inside the cell, an acid wash step was added to the protocol prior to fixation. This removed all external virus particles, including those attached to the surface of the cell, allowing a clear view of the inside of the cell.

The experiment was carried out as before, but an acid wash was employed immediately prior to the cells being fixed. The acid wash involved the following. Firstly the cells were placed on ice, then they were washed twice with ice cold PBS. After this, ice cold acid wash buffer was added to the cells on ice for one minute. This was then removed and they were washed three times with PBS at room temperature. Finally the cells were stained and mounted onto slides as usual.

The acid wash buffer consisted of 0.2M acetic acid and 0.2M NaCl at pH 2.0.

6.2.3 3D reconstruction confocal microscopy

A random area of cells was selected in the field of the microscope. The top and the bottom of the cells were determined visually and used to define the top and the bottom of the stack as the points for the program to measure between. Images were then taken at 20 regular intervals between the top and the bottom of this stack, the distance between these calculated by the software based on the selected boundaries (i.e. the size of the cells selected, divided by 20). These images were then combined using the accompanying software allowing the user to view any specific point from above as well as from both sides. Therefore, by focussing on a virus particle, the combination of images allow the user to confirm that it truly lies within the boundaries of the cell.

6.2.4 Virus particle and cell counting

A, Virus counting

Stacks of images of cell nuclei and virus particles were taken at 8 randomly selected areas for each of the coverslips. The images within each stack were combined using

Image J software, producing a single image from which a total number of virus particles could be counted. The fluorescence signal for the combined stack was then transformed into a two tone (black and white) binary image. In order to do this the threshold (to decide the level of fluorescence that should be converted to black signal against a white background) had to be adjusted in order to determine what was classed as 'signal' and what should be ignored as 'background'. When the settings had been selected for one of the stacks, the same settings were transposed to all remaining stacks for fair comparison. The number of particles was counted using Image J software.

B, Nuclei (and cell) counting

This process was repeated for each of the stacks but focussed on a blue DAPI signal in order to count the number of nuclei. Since each cell contains only one nucleus, the number of cells can be counted. It is important to ensure that this count is accurate and as such additional measures were adopted to ensure accuracy. This involved adjusting the signal to remove any holes in the signal areas and to separate nuclei that were in such close proximity that they would otherwise have been counted as one object (using the 'watershed tool'). For the nuclei is was also important to change the settings so that only particles equal to or greater than a certain size were measured in order to make sure that background signals were not measured.

The virus particle and cell counts from each stack were used to calculate an average number of virus particles per cell. This experiment was done in triplicate and the overall results were combined. Average counts were compared in the presence and absence of Cf2642. A T test was performed using SPSS to determine if there was any significant difference between the two sets of data.

6.2.5 Fluorescence microscopy of actin cytoskeleton plus other markers

The following was performed by Mr Preet Shah (from the Jones laboratory Cardiff school of pharmacy and pharmaceutical sciences). Hela cells were seeded into 12-wp containing coverslips and left overnight to settle and reach confluency. These were pretreated for 30 minutes with Cf2642 (10 μM) plus no drug controls. They

were infected with vWR (at moi of 1), and one of the no drug control wells were left uninfected as a 'mock' (no drug, no virus control). The cells were collected four hours pi and fixed in 3% PFA for 15 minutes. The cells were stained with Rhodamine-Phalloidin (to visualise the actin cytoskeleton in red) and with Hoescht (to stain the nuclei in blue) before mounting them onto slides for confocal microscopy.

This method was repeated as above substituting Rhodamine-Phalloidin with antibodies against a series of other cellular markers including α-Tubulin, TFR, TGN46, EEA1 and LAMP-2. This was also repeated using an anti-VACV antibody (Rabbit anti-VACV generated in the laboratory of Proffessor Bernhard Moss, Bethesda, USA) at 1:100 dilution, plus an Alexa Flour 488 chicken anti-rabbit IgG secondary antibody (Molecular Probes) at 1:400 dilution for detection.

6.2.6 Time course – pH change of cell medium

B95a and A549 cells were seeded into 96-wp and left overnight to settle and reach confluency. These were treated with Cf2642 (50, 20, 10, 5, 1 and 0 µM) and Chloroquine (100, 50, 20, 10, 5 and 0 µM), half the cells were infected with mWT Fb and the other half were left uninfected. The plates were scanned at four hour intervals over a 24 hour period and the subsequent images were used to visualise when the colour change of the medium occured.

6.2.7 Cd63 staining

In an effort to investigate the observation that the ddBCNAs cause the cell medium to become more acidic at active concentrations, A549 cells were treated with Cf2642 (10 µM) and fixed 16 hours after the addition of the drug. This fixation point was based on the time that the initial colour change (acidity exceeding the buffering capacity) of the medium was observed. Fixed cells were stained with a FITC labelled antibody for cd63 (ab18235; Abcam). Cd63 is a member of the transmembrane 4 family and is mainly associated with the intracellular vesicle membranes such as late endosomes and lysosomes (Pols and Lumperman, 2009).

The cells were also mounted with Vectashield containing DAPI so that the nuclei of the cells could be visualised via confocal microscopy. The microscope software was also used to produce graphs of intensity of the fluorescence through a selection of cells in an attempt to quantify the difference in the level/distribution of cd63 staining in the presence/absence of Cf2642.

6.2.8 IL-6 ELISA

Cells were seeded into a 96-wp and left overnight to reach confluency. They were treated with the selected ddBCNAs (Cf3242, Cf1821, Cf2095 and the ether series) at 10 µM for 24 hours at 37^{o}C, and then collected for the ELISA. The ELISA assay was carried out according to the kit protocol (Invitrogen Hu IL-6 chemiluminescence ELISA kit).

6.2.9 *In vitro* cell-free poxvirus transcription assay

The following was performed by Dr. Joachim Bugert using the previously described in vitro poxvirus transcription method (Bugert et al. 1998). Briefly, this involves measuring the level of transcription by tracking the amount of UTP containing radioactive phosphate (P^{32}) that is incorporated into the mRNA subsequently produced.

VACV and MCV were tested for transcription levels in the presence and absence of Cf2642 (2 µM). This was done by incubating 50 µL of virus suspension in a total volume of 200 µL *in vitro* transcription buffer (Shand et al. 1976) at 35^{o}C. Four 20 µL aliquots were taken at 0, 60, 120 and 180 minutes. The level of incorporated radioactivity was measured using Beckman scintillation counter.

6.3 Results

6.3.1 Cf2642 effect on vYFP-A3L entry into host cells

In chapter 3 luciferase assay data demonstrated that the ddBCNAs can have an inhibitory effect on VACV within two hours of infection. This suggests that the target of the ddBCNAs is something that the virus requires at an early stage of its

lifecycle. This time period covers the entry and early transcription stages of the VACV lifecycle. This led to the theory that the drugs MoA might be that they inhibit the virus' entry into the cell.

In order to investigate this, Cf2642 treated/untreated cells were infected with vYFP-A3L. The cells were fixed 30 minutes pi in order to establish the distribution of the virus fluorescence at the very early stages of infection. Initial confocal experiments with vYFP-A3L were performed, imaging cells in both the absence and the presence of Cf2642.

One coincident observation made during this experiment was the presence of many more virus particles than predicted from the virus titres. Many of them also appeared to be fixed onto the glass coverslip. In the absence of drug the virus particles appeared to be randomly distributed throughout the cells. However, in the presence of Cf2642 the virus particles appeared to be much more concentrated at the cell surface (figure 6.1). This observation seemed to correlate with the theory that the ddBCNAs are inhibiting the entry stage of the virus lifecycle. i.e. the images suggest that whilst viral attachment is not affected, viral entry into the cell might be being blocked – evidenced by their accumulation at the cell membrane.

To confirm this, the confocal assay was repeated with the inclusion of an acid wash step immediately prior to cell fixation. The aim of this acid wash was to remove any external virus particles from the cells and coverslips, including those attached to the surface of, but not yet internalised by, the cells. This resulted in much fewer virus particles being present in both the drug treated and untreated cells. Stacks of images were taken for random selections of the acid washed infected cells and, using a 3D reconstruction of the stack, it was demonstrated that fluorescent particles could be detected inside the cells in both the presence and absence of Cf2642 (figure 6.2).

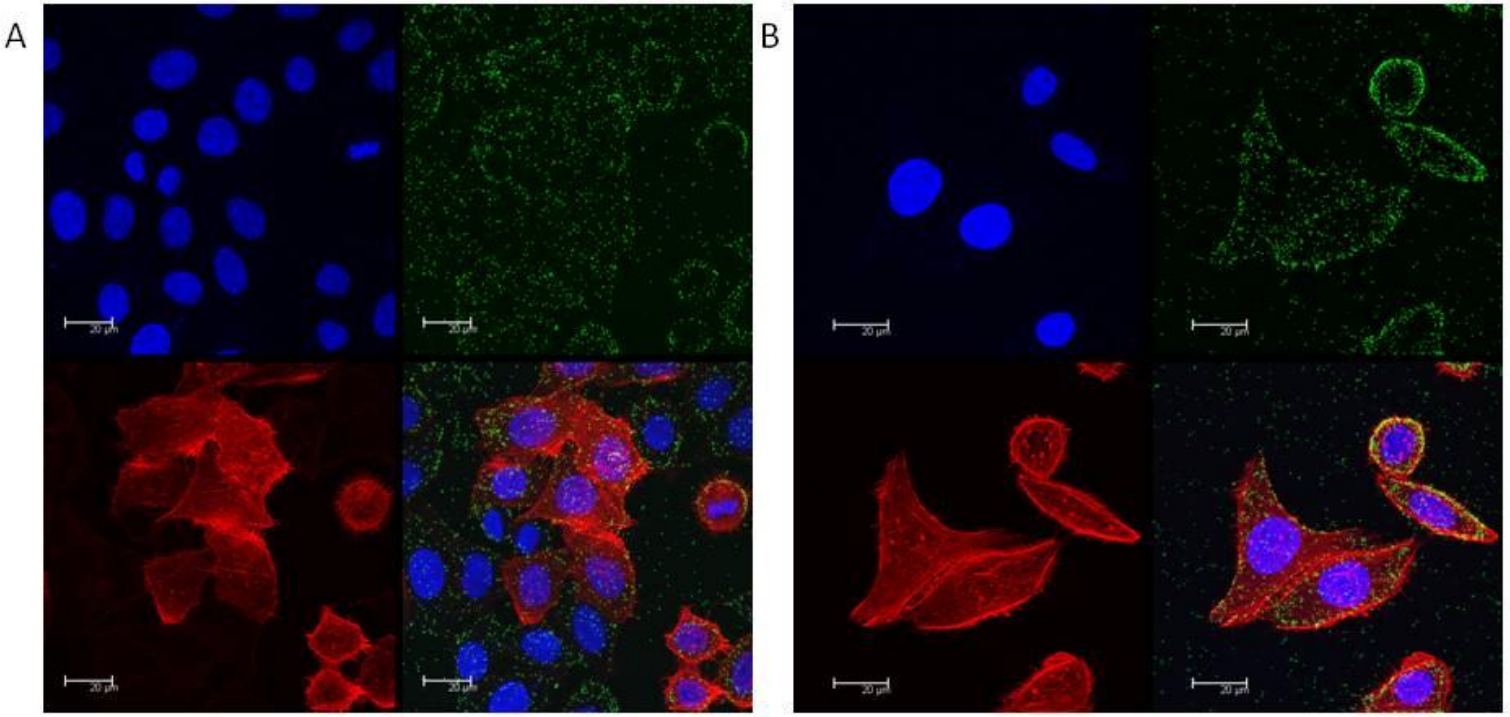

Figure 6.1 A: HeLa cells infected with vYFP-A3L fixed 30 minutes pi, no drug control B: HeLa cells infected with vYFP-A3L fixed 30 minutes pi, with 30 minute pre-treatment with 10 µM Cf2642. The images suggest that in the absence of the drug the fluorescent virus particles are randomly distributed throughout the image, both inside and outside of the cells. In the presence of drug the localisation of the virus particles appears to be more concentrated at the surface of the cell. Nuclei are stained blue, the virus particles are green and the actin cytoskeleton is stained red.

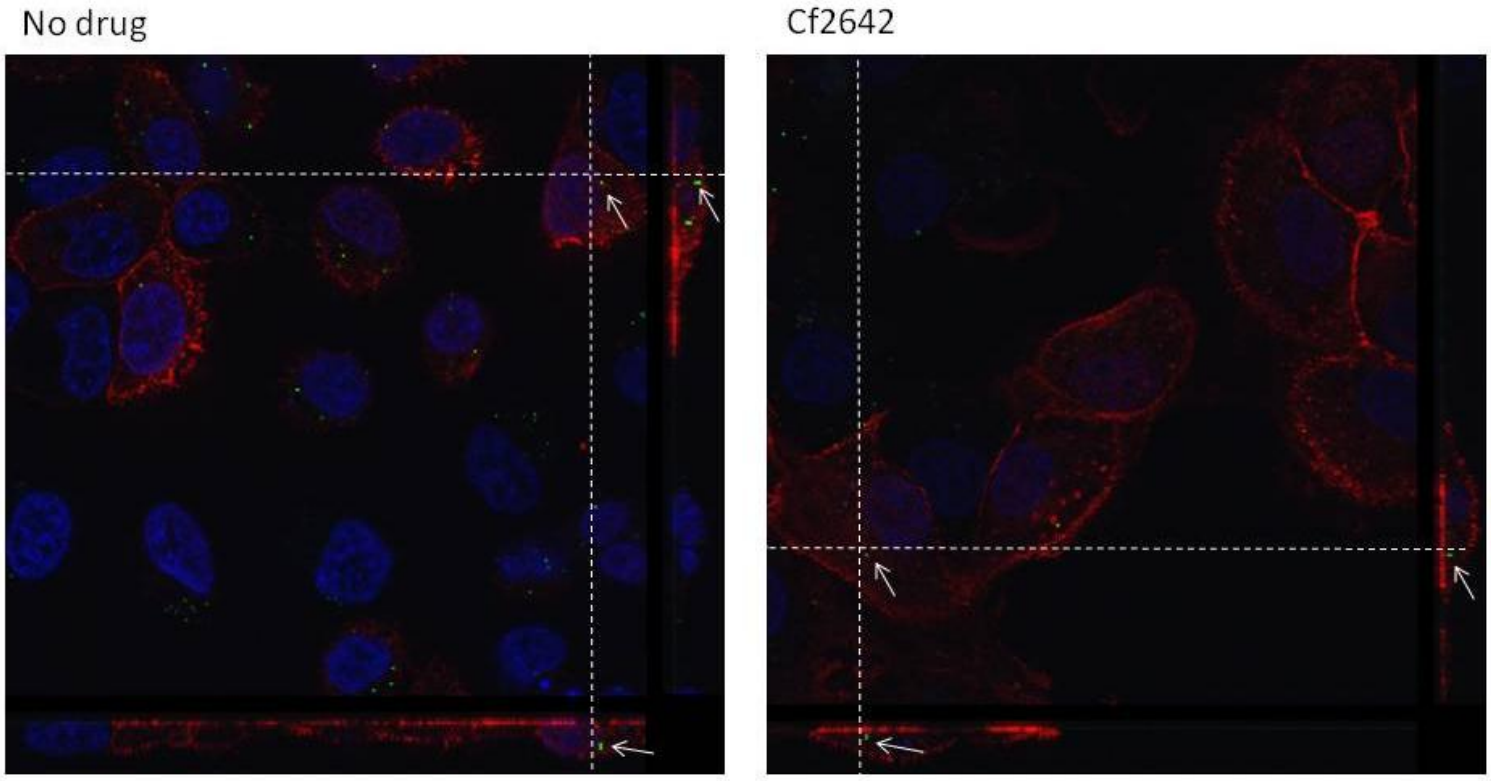

Figure 6.2 Using a 3D reconstruction of the images taken through a stack on the confocal microscope a view of the cells from the side and the bottom can be reconstructed. Using these images, it was possible to ascertain as to whether the flourescent particles were actually inside the cells. Images taken in the presence and absence of Cf2642 (10 µM) are shown. The cross bars (white dotted lines) indicate the slice of the cells that is being viewed from the side and the bottom. The particle immediately adjacent to cross bar intersection point is visible simultaneously from below and from the side (as indicated by white arrows).

Virus particles were visibly present inside the cells in both the presence and absence of Cf2642. However, from these images it was not evident as to whether there was a difference in the particle numbers between the two conditions. As such, this experiment was taken further in an attempt to quantify the number of virus particles per cell, the total number of virus particles and the total number of nuclei in combined stacks of images. Comparing the values generated, there was no apparent difference in the number of particles inside treated and untreated cells (figure 6.3) – with the counts from both conditions being about 5 virus particles per cell ($P = 0.484$). Contrary to the initial evidence, this data suggests that the ddBCNAs do not inhibit virus entry into the host cell.

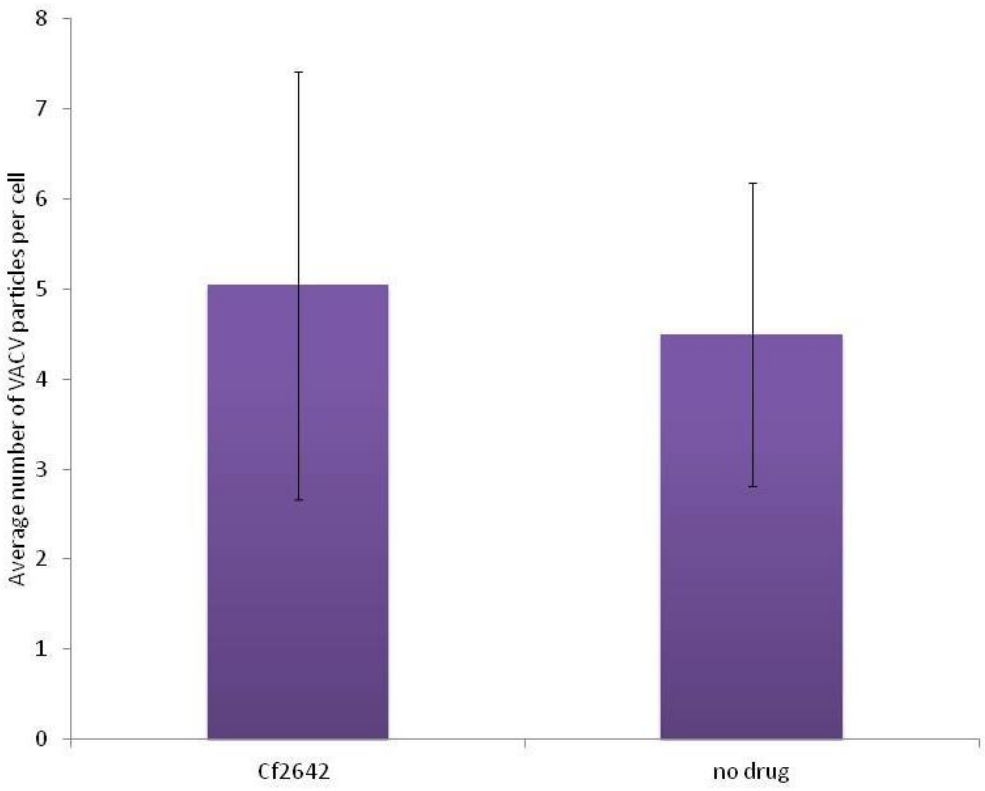

Figure 6.3 The average number of virus particles per cell calculated from the average of three experiments. There is no significant difference in the number of particle per cell in the presence and absence of Cf2642. P=0.484

6.3.2 Cf2642 effect on actin tail formation

As previously shown in plaque assays (chapter 3 section 3.3.5), cells treated with the ddBCNAs exhibit a reduced plaque size phenotype. This same phenotype has been described by others using the drug Terameprocol (Pollara et al. 2010). They found that their drug causes a reduction in the size of the plaques because actin tails (which would normally aid virus spread) are no longer induced at the surface of the cells. In order to determine whether actin tails at the surface of infected cells were inhibited in the presence of the ddBCNAs, confocal microscopy was employed, specifically using HeLa cells infected with vWR and fixed four hours pi. The cells were stained with Rhodamine-Phalloidin to visualise the structure of actin in the cells and Hoechst to stain the nuclei. In the images obtained, actin tails and membrane blebbing are clearly visible at the surface of both the treated and untreated cells infected with vWR (figure 6.4 A). This finding suggests that the ddBCNAs are not working in the same way as Terameprocol and that they do not prevent the formation of actin tails. The 'mock' cells show no signs of blebbing or actin tails at the surface, therefore confirming that these are induced by the presence of the virus.

Further evidence in support of this result is displayed in figure 6.4 B. This shows BSC-1 cells infected with vYFP-A3L in the presence of Cf2642 (50 μM). The cells were fixed 30 minutes pi. Actin tails can be seen at the surface of the cell.

A

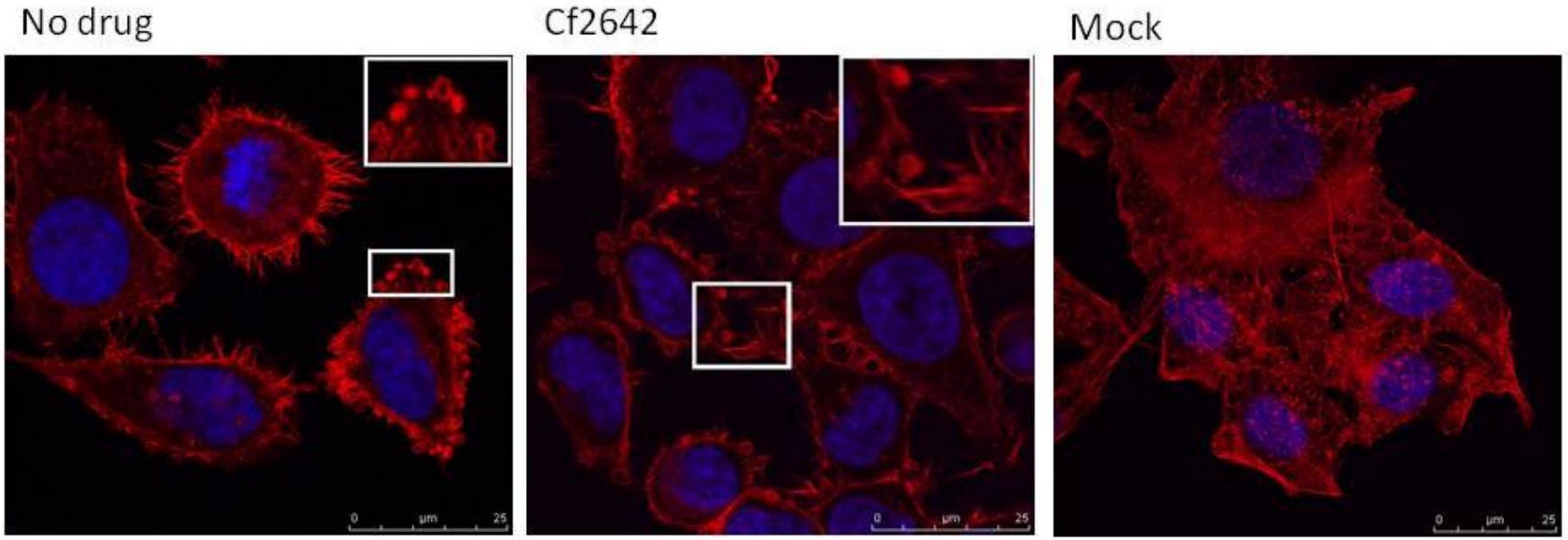

B

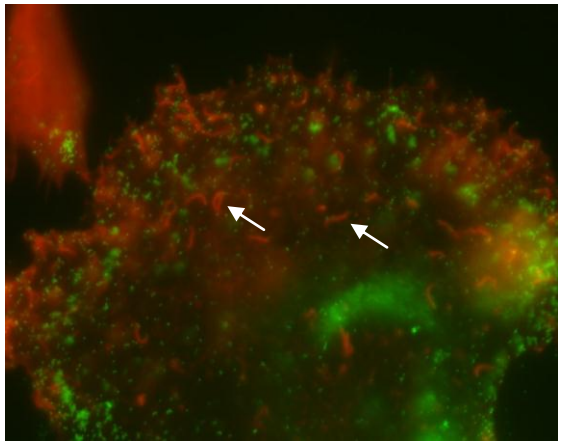

Figure 6.4 A: HeLa cells stained with Phalloidin-Rhodamine to visualise the actin cytoskeleton in red and Hoechst to visualise the nuclei in blue, untreated cells infected with vWR, Cf2642 (10 µM) treated and infected with vWR, 'Mock' untreated, uninfected control. Cf2642 appears to have no effect on the membrane blebbing and actin tail formation caused by the vWR. The blebbing and actin tails are not present in the mock cells indicating that these are induced by the virus. (Images from Preet Shah MSc dissertation).

B: Wide field fluorescene image of Cf2642 (50 µM) treated BSC-1 cell infected with vYFP-A3L (green). Cells fixed 30 minutes pi and stained with Phalloidin-594 to view the actin cytoskeleton (red). The image indicates that Cf2642 does not inhibit the formation of VACV induced actin tails at the surface of the host cells as there appear to be many at the surface of the cell (two of which are indicated by white arrows).

6.3.3 Change in pH of cell medium

In several of the assays involving the use of Cf2642 at higher concentrations (typically ≥ 5 µM), it has been noted that the cell medium changes in colour from pink to yellow, in-turn suggesting an increase in its acidity. Here, a time course experiment was carried out in order to determine exactly when the visible change in the pH of the medium occurs.

Initially this experiment was performed using $5x10^3$ cells per well in a 96-wp. Cf2642 and Choroquine were each added to the cells at a series of concentrations. The plates were scanned at 2 hour intervals over the course of 24 hours. Ultimately, this starting cell count proved too low to produce meaningful results during this time frame. However, a coincident observation of this plate was that, after one week in the incubator, A549 cells exposed to high concentrations of Cf2642 (≥ 5 µM) did indeed show a colour change of their medium (figure 6.5). Critically, this effect was inhibited by the Chloroquine (i.e. the colour change became less evident as the Cholorquine concentration increased. This could provide evidence that Cf2642 acts on the lysosomes of the cells.

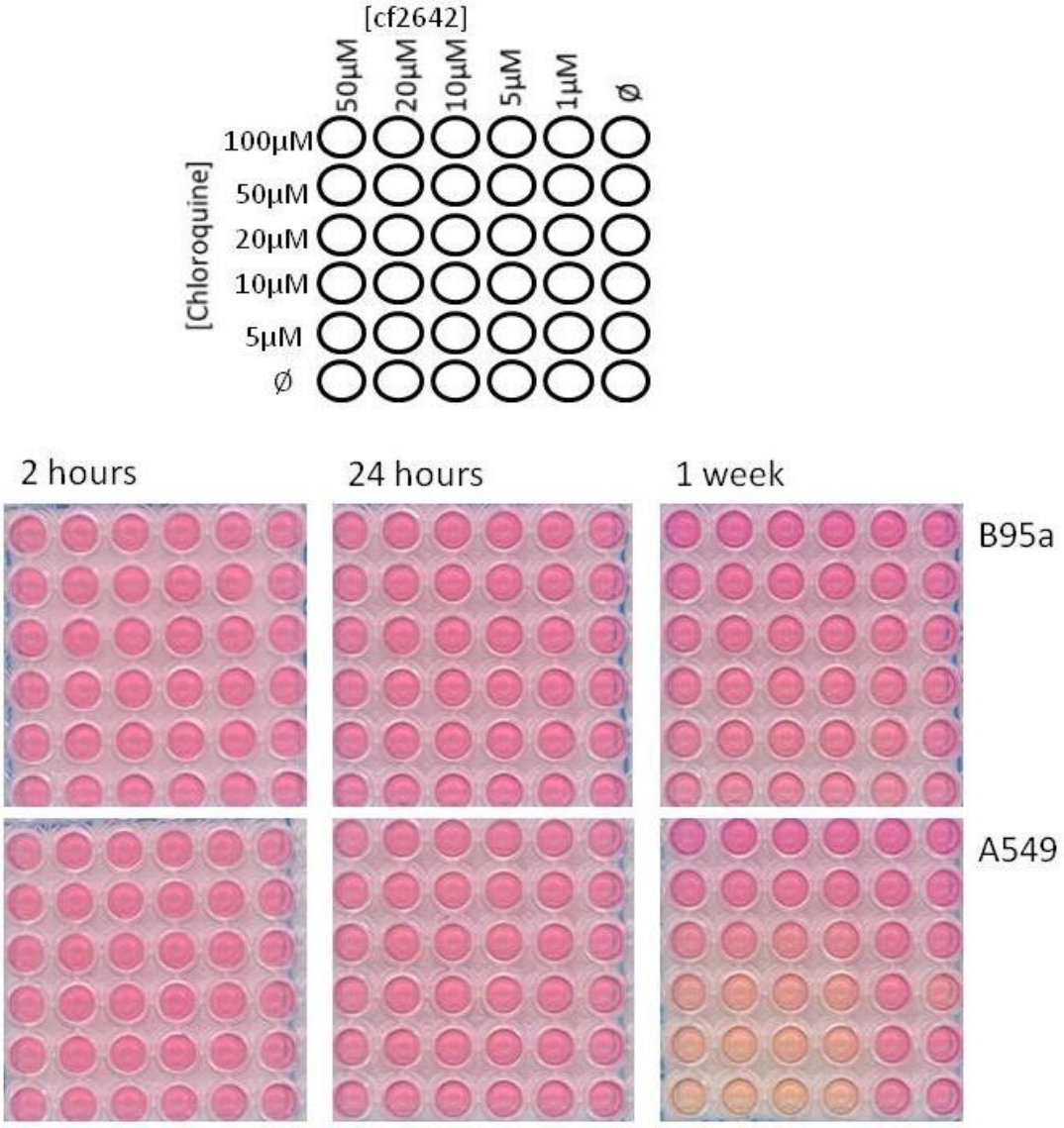

Figure 6.5 B95a and A549 cells at 5x103 cells/well, treated with Cf2642 and Chloroquine at a range of concentrations. Plate scans after 2 hours, 24 hours and 1 week are shown. A change in the colour of the medium can be seen in the A549 cells after one week at concentrations of Cf2642 ≥ 5 µM and Chloroquine ≤ 10 µM.

The experiment was repeated with 10 times the starting number of cells i.e. $5x10^4$ cells/well. This time the cells were treated with the drugs in duplicate. One half were left uninfected and the other half were infected with wild type measles virus. This was to establish whether the virus also contributed to the change in the colour of the medium, or if it was an effect of the drug alone. The plates were scanned at four hour intervals over a 24 hour period. A final scan was taken after 72 hours.

This experiment indicated that the initial noticeable change in colour occurs 16 hours after the addition of the drug to the cells (figure 6.6). In most of the wells it seemed that there was no obvious difference in the colour of the wells that were infected with the measles and those that were uninfected, suggesting that the virus is not contributing to the colour change and that it is an effect caused by the action of the compound on the cells. The only exception to this was in the B95a cells with 0 and 1 µM Cf2642; after three days the wells containing the virus appeared more yellow than those that were uninfected. This is likely to be due to the virus infection killing the cells after this length of time.

In this experiment, with the high number of cells it seemed that the Chloroquine did not have an effect on the colour change of the medium. Indeed, the yellow colour appears only in wells with higher (5 µM and above) concentrations of Cf2642 and is the same across all concentrations of Chloroquine. It is possible that with the high number of cells present, Choroquine is not able to counteract the effect of the ddBCNA within the 16 hours it takes for the Cf2642 to cause a change in the pH.

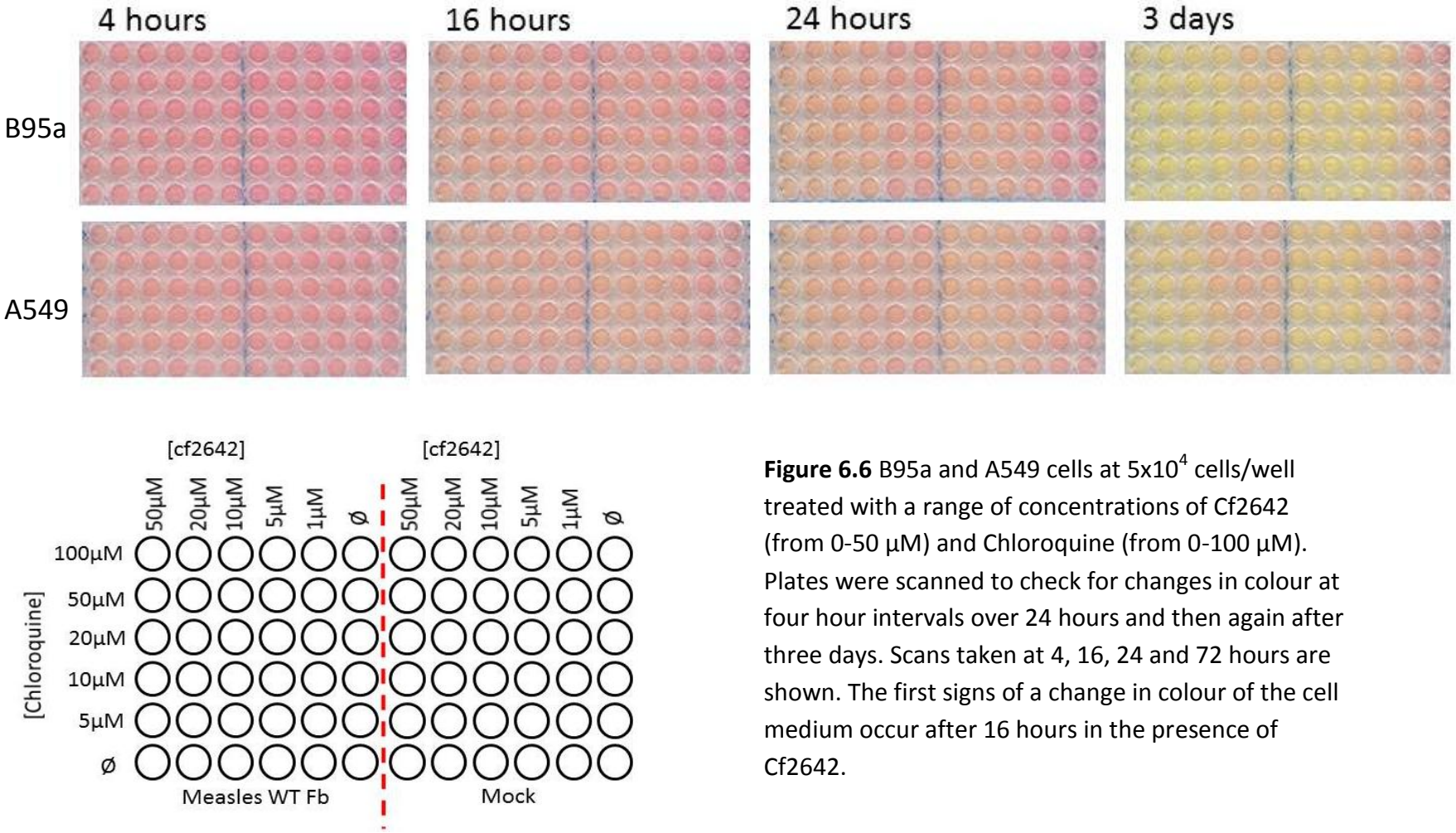

Figure 6.6 B95a and A549 cells at $5x10^4$ cells/well treated with a range of concentrations of Cf2642 (from 0-50 µM) and Chloroquine (from 0-100 µM). Plates were scanned to check for changes in colour at four hour intervals over 24 hours and then again after three days. Scans taken at 4, 16, 24 and 72 hours are shown. The first signs of a change in colour of the cell medium occur after 16 hours in the presence of Cf2642.

6.3.4 Cd63 confocal assay

In a further attempt to investigate the observation that the ddBCNAs cause the cell medium to become more acidic at active concentrations, A549 cells were treated with Cf2642 and fixed and stained with antibody for the detection of cd63. When comparing cells treated for 16 hours against untreated control cells, it appeared that the localisation of cd63 protein was more widespread throughout the cell in the former (figure 6.7). In the latter, the protein appeared to be concentrated around the nuclei of the cells and was typically brighter/more intense. This might suggest that Cf2642 is causing intracellular vesicles to migrate/fuse with the cell membrane and release their contents, in-turn offering a possible explanation for the pH change observed.

Leica microscopy software was used in an attempt to quantify this data. A selection of cells were measured for the level of fluorescence intensity across their length, and these values were used to generate graphs of the intensity signal profiles. A sample of three cells in the presence and absence of drug were selected to produce intensity graphs of the cd63 staining (figure 6.8). In the absence of drug, the staining intensity appeared to be higher and the maximum intensity point observed was 160. In Cf2642 treated cells the intensities of the signals appeared reduced; the maximum intensity observed was 100. The distribution of the intensities also appeared to be different. In untreated samples the areas of greatest intensity appeared to be in close proximity to the nucleus, while in Cf2642 treated samples the high intensity peaks appeared more evenly distributed across the length of the cell cytoplasm. The corresponding cells selected for the intensity graphs are shown figure 6.9.

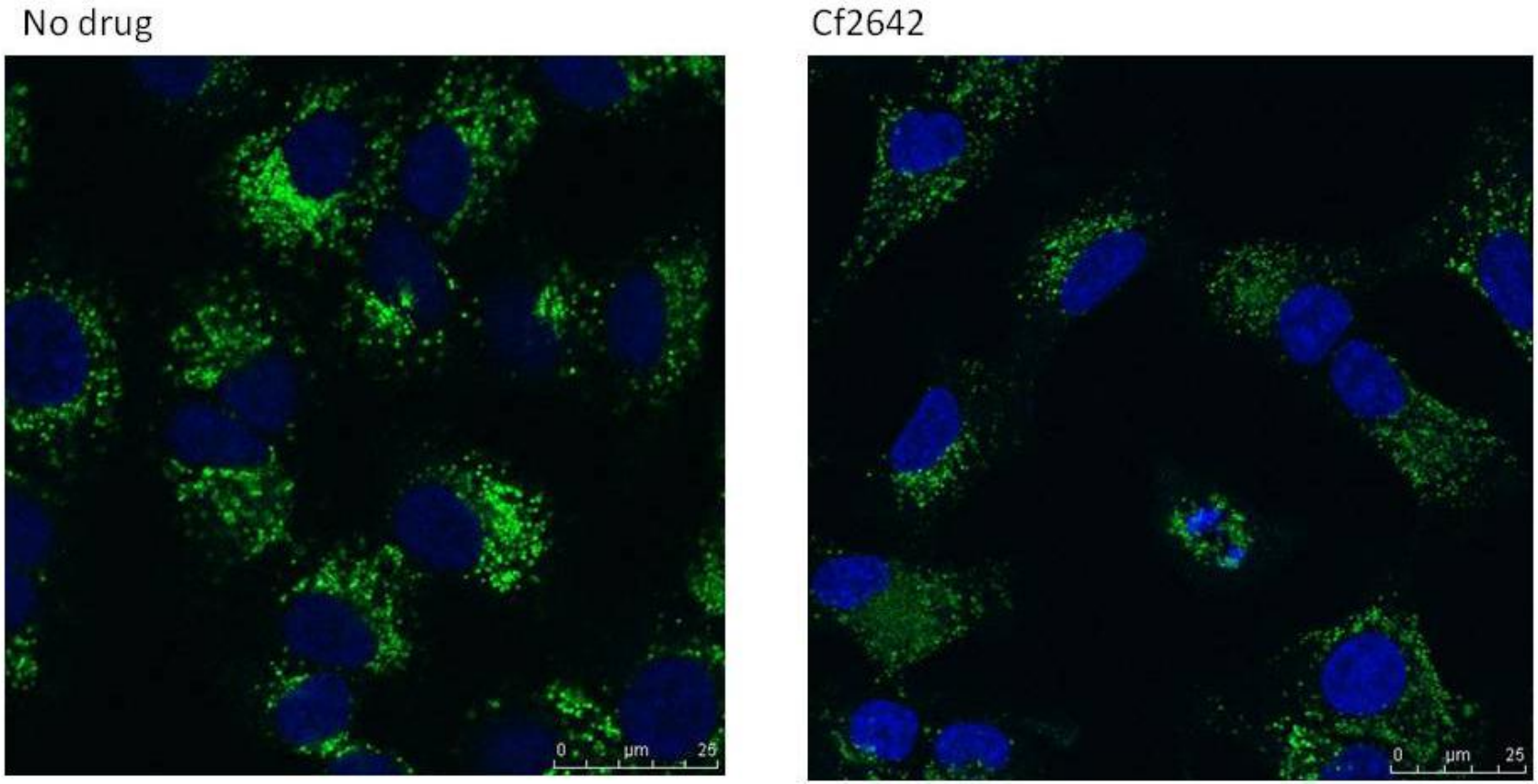

Figure 6.7 Hela cells stained for cd63 (green) in the absence (left panel) and presence (right panel) of Cf2642 (10 µM). Cells were fixed at 16 hours after drug addition. Confocal images show that cd63 appears more intensely clustered around the nucleus of the cells in the absence of the drug. However, in the presence of 10 µM Cf2642, cd63 staining is weaker and more evenly spread throughout the cell cytoplasm.

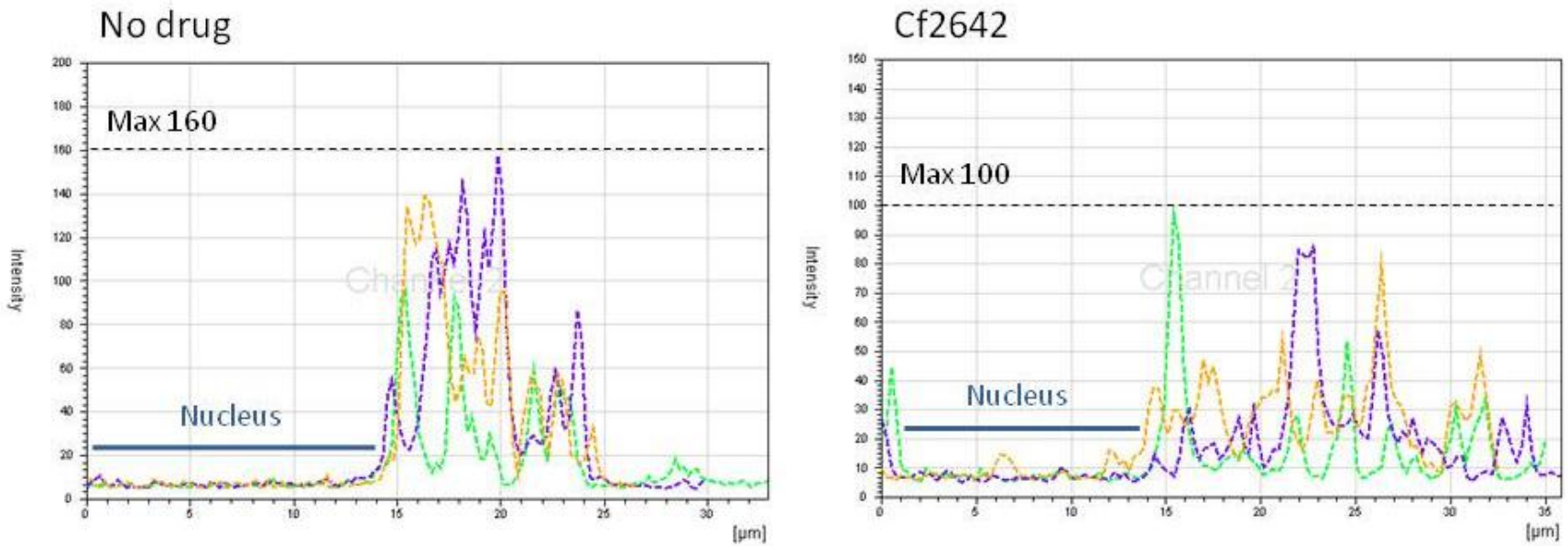

Figure 6.8 Signal profiles for three cells (displayed as dashed green, orange and purple lines) that were either untreated (left) or treated with Cf2642 (10 µM, right). The x axis represents distance along the length of the cell. The y axis represents the intensity of the green staining, indicating the presence of cd63. The maximum intensity signal observed is represented by the black dotted line, for the untreated cells the maximum signal was 160 and for the Cf2642 treated cells the maximum signal was 100. The location of the nucleus of the cells is represented on the graph by the dark blue solid line. The cells used to generate this data, and the axes studied, are shown in figure 6.9.

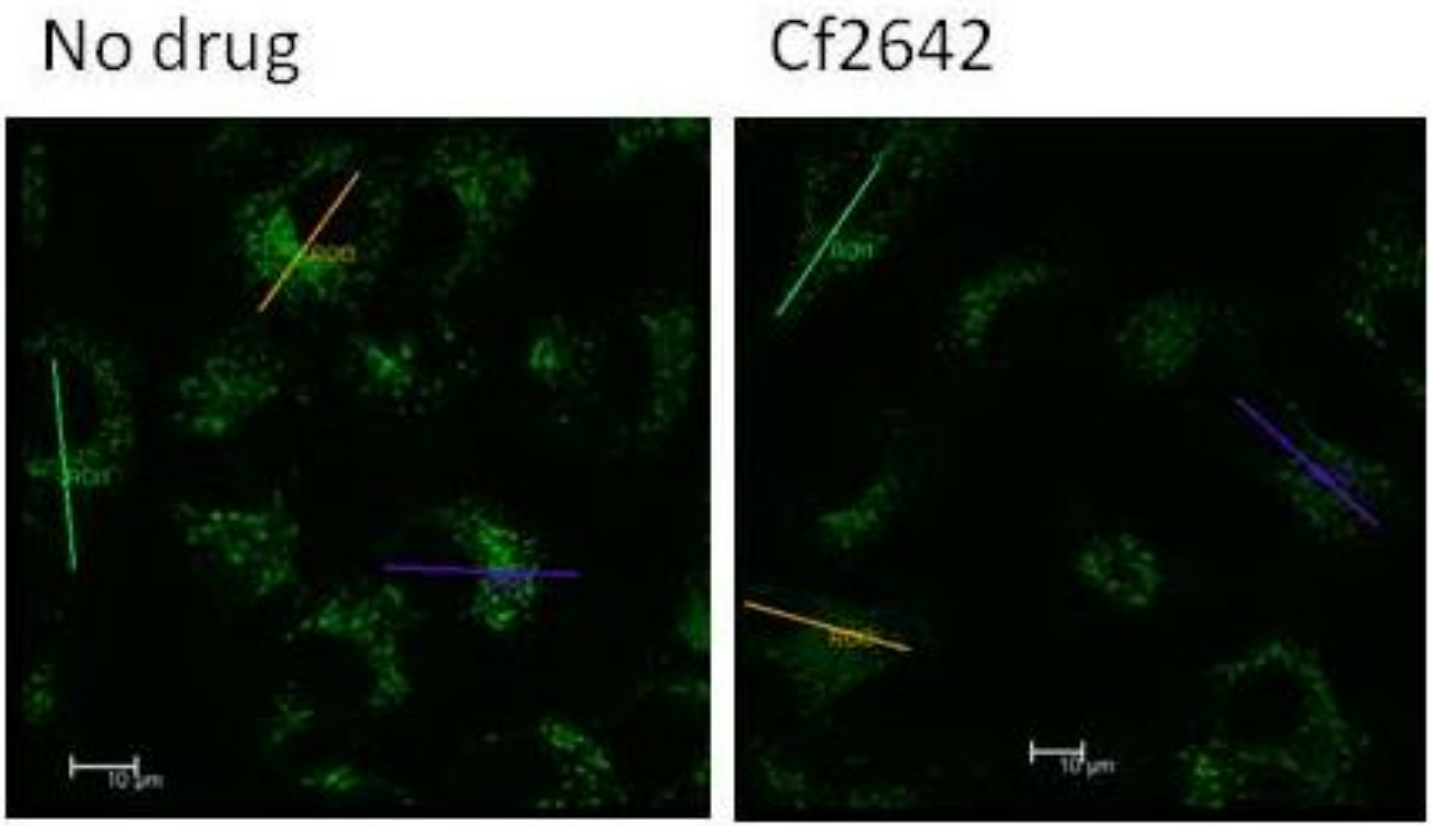

Figure 6.9 Images of cd63 staining in HeLa cells untreated (left) or treated (right) with Cf2642 (10 µM).The green, orange and purple lines correspond to the signal profiles displayed in figure 6.8. Leica microscope software measures the intensity of the staining across the length of these lines.

6.3.5 Other staining experiments

Cf2642 has also been tested in cells stained for a variety of different markers. The results from this project suggested no difference in the staining distribution of α-Tubulin (staining microtubules), transferrin receptor (TFR), trans golgi network (TGN46) and early endosomes (EEA1), suggesting that Cf2642 has no effect on any of these cellular locations (data not shown). LAMP-2 staining was also performed and the images suggest a slight difference in its distribution with it appearing less intense around the nucleus when in the absence of drug (data not shown). The infected HeLa cells were also stained for VACV in the presence and absence of Cf2642 and the images suggest that there are fewer VACV containing vesicles in the presence of Cf2642 and an increase in staining throughout the cytoplasm figure 6.10.

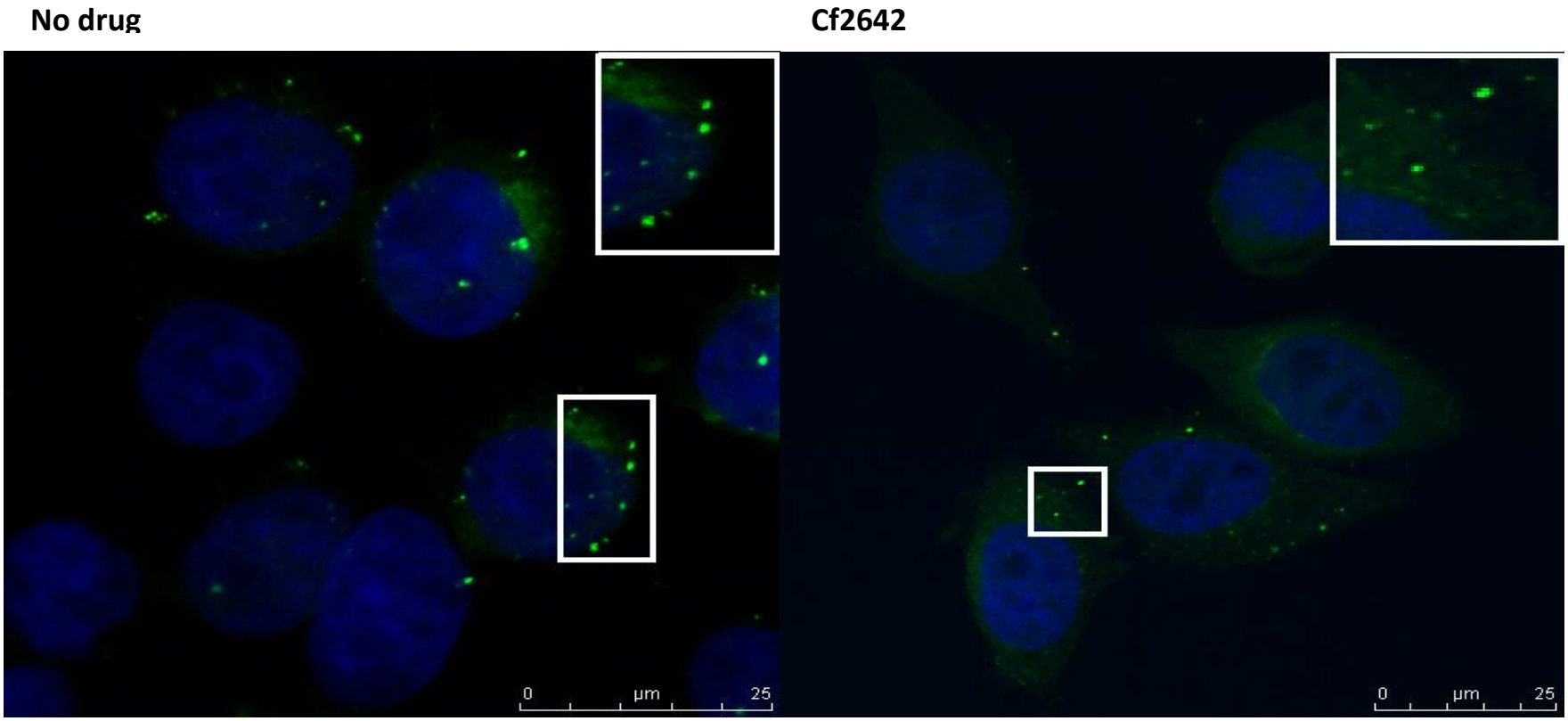

Figure 6.10 HeLa cells infected with vWR and fixed four hours pi. Cells were stained with Hoechst (to allow visualisation of their nuclei in blue) and rabbit anti-Vaccinia antibody plus Alexa-488 conjugated anti-rabbit secondary antibody (to allow visualisation of virus in green). There appear to be fewer VACV containing vesicles in the Cf2642 treated cells than in the untreated cells. (Images from Preet Shah MSc dissertation).

6.3.6 Human IL-6 ELISA

An ELISA was carried out to determine whether the ddBCNAs have an effect on the levels of human IL-6 in HeLa cells. This in turn indicated as to whether the compounds have an MoA that involves some effect on the intracellular innate immune response i.e. do they trigger an immune response in the host cell which acts against the virus. The results displayed in figure 6.11 indicate that the active ether series of L-ddBCNAs (Cf3210, Cf3204, Cf3207, Cf2642 and Cf3209) and the initial D-ddBCNAs (Cf2095 and Cf1821) do not alter the levels of Hu IL-6 as compared to the no drug control (all display levels of around 20 pg/mL). The only exception to this lies in the IL-6 concentration observed in the Cf3242 treated cells, where the levels are about double the control (i.e ~40 pg/mL). However, it has previously been noted (chapter 3, section 3.3.5) that this compound has a clear toxic effect on the cells. This observation requires further experiments, firstly repeats to confirm the results with statistical significance and secondly to investigate why cf3242 seems to trigger an IL-6 response, whereas all the others do not, the structure of this compound includes nitrogen methyl instead of oxygen (chapter 3 section 3.3.1.3).

Taken together, it appears that alteration of the levels of IL-6 and induction of the intracellular innate immune response is not the MoA of the compounds.

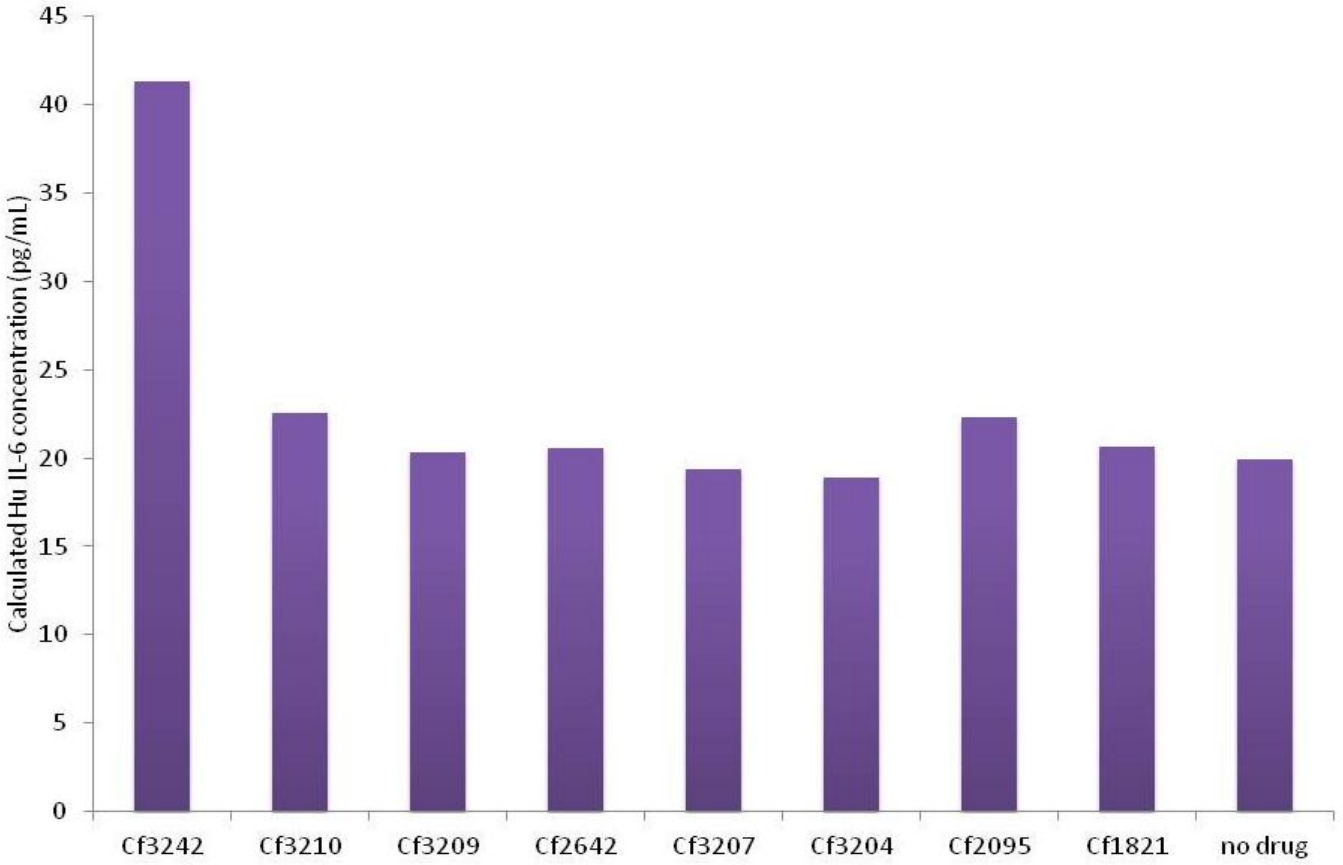

Figure 6.11 Human IL-6 ELISA in HeLa cells treated with 10 µM of the shown ddBCNAs. Cf3242 is the only compound to show increased IL-6 production (concentration calculated as ~40pg/mL). The rest of the ddBCNAs tested display similar levels of IL-6 concentrations to the no drug control (all were ~20 pg/mL).

6.3.7 Cf2642 effect on transcription

A cell free *in vitro* experiment was carried out in order to verify whether the ddBCNAs may be having an effect on the level of viral transcription. This experiment studied VACV and MCV in both the presence and absence of Cf2642 (2 µM). The results are displayed in figure 6.12. The data suggest that Cf2642 has no effect on the level of transcription. Indeed, transcription levels at one, two and three hours were almost identical in treated and untreated samples. The readings were higher with the MCV than with the VACV.

For either virus, the transcription signal increases over the first two hours before appearing to descend. This is likely to be because the reaction is ATP dependant and in the isolated system, ATP would eventually be used up and mRNA production would cease. At this point, mRNA would break down leading to the decrease in signal.

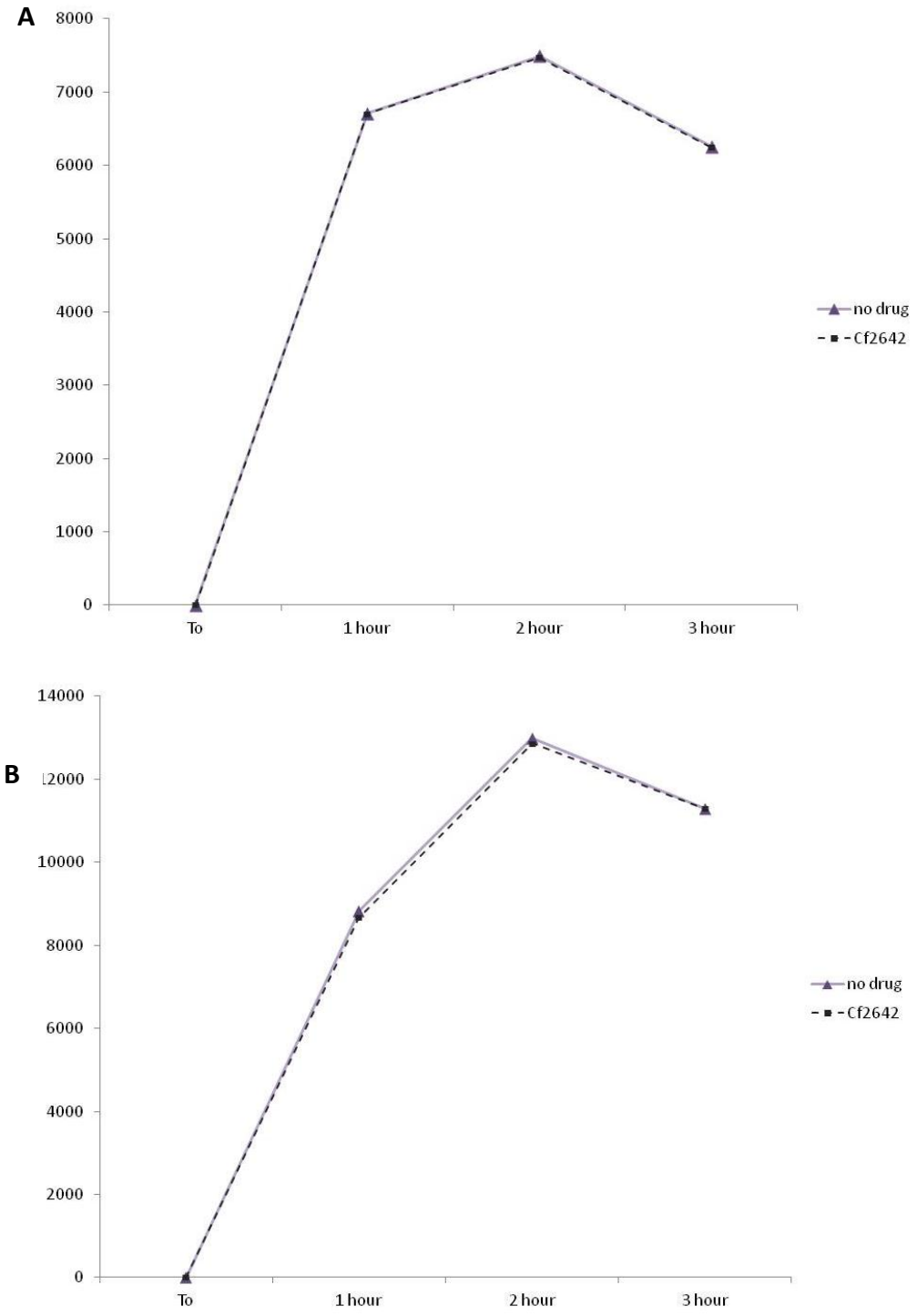

Figure 6.12 The effect of Cf2642 (2 µM) on the level of transcription (as radioactive counts per minute on the y-axis) compared with no drug. A: VACV B: MCV. Cf2642 appears to have no effect on the amount of mRNA production (Figure reproduced from Bugert data).

6.4 Discussion

Data from previous chapters have contributed hints as to the MoA of the ddBCNAs. In this chapter, the MoA has been narrowed down further. Initially confocal microscopy images of untreated/Cf2642 treated cells infected with vYFP-A3L appeared to indicate that the MoA might be inhibition of virus entry. This was evidenced by the localisation of virus particles on the cells; in Cf2642 treated cells, particles clustered at the membranes of the cells. In an extension of this study, an acid wash step was used to remove external virus particles. Subsequently, virus particles could be visualised inside cells in both the presence and absence of the drug. Quantification of this data confirmed that there was no significant difference between the two settings. The conclusion drawn from this set of data was that the ddBCNAs do not appear to be entry inhibitors.

Following on from observations made in previous chapters about the change in colour of the medium in the presence of the ddBCNAs, further studies into this effect were conducted. Initially this involved a time course assay to look at cells treated with various concentrations of Cf2642 to determine when the initial colour change occurred. The first of these experiments with a lower cell count displayed a colour change at concentrations of 5 µM and above of Cf2642. This effect was reversed by chloroquine. This finding could suggest that the acidification caused by the ddBCNAs might be due to them causing migration and fusion of the lysosomes with the cell membrane and subsequent release of their acidic contents into the cell medium. This could be reversed by chloroquine as this drug targets the lysosomes of cell and raises their pH.

The second experiment displayed an initial colour change after 16 hours in the presence of Cf2642 at 5 µM and above. This effect was not reversed by Chloroquine. This could be due to the number of cells overwhelming the capacity of Chloroquine to increase the pH. Ideally repeats of this experiment using a wider range of cell counts would need to be performed in order to confirm the effect of the cell numbers on acidification of the medium when ddBCNA treated.

Most of the cells cultured in this laboratory grow best at an optimum pH of around 7.4. The DMEM contains phenol red indicator which has a bright red colour at this pH. It also contains a buffering system that maintains this pH as the cells metabolise and produce acidic by-products. In the presence of the compound, the release of acid into the medium exceeds the buffering capacity of the medium much earlier than would be expected when resulting from normal cell respiration alone. After 16 hours there is already a visible colour change in the medium compared to untreated cells. After 24 hours the medium becomes orange, indicating a pH of around 7. The medium gradually turns yellow over the next 24-48 hours, indicating a pH of less than 6.5. This pH has an effect on the viability of the cells.

Based on these findings, a 16 hour time period was chosen to analyse cd63 distribution. The images produced suggest a decrease in the intensity of cd63 staining in the presence of Cf2642 compared with the untreated cells. However it must be noted that these images (and the plots generated from them) are the result of an individual experiment that would need to be repeated for confirmation of the effect. Ideally repeats would also include staining with a plasma membrane marker or with phalloidin-594 (to stain the actin cytoskeleton) in order to more accurately define the boundaries of the cells.

Experiments looking more specifically into this change in pH are necessary. This might include using pH trackers to detect any changes in the internal cellular pH in the presence of Cf2642. As viral processes can be pH dependant, changes in internal pH caused by the ddBCNAs could also be a potential MoA.

It has been demonstrated that during measles infection, the virus induces prolonged autophagy of the cell to aid its replication (Richetta et al. 2013). If the drug was affecting the cellular lysosomes this may have an effect on the virus lifecycle. Interestingly, VACV have also been shown to adopt intracellular vesicles to form its own virus factories (de Castro et al. 2013). As such, were ddBCNAs to affect lysosomes/endosomes, this could explain the antiviral effects previously observed.

The images of Cf2642 treated/ untreated infected HeLa cells stained for VACV suggest that Cf2642 treatment appears to reduce the number of the virus factories forming in the cell. The cytoplasm of the treated cells appears to have a greater level of general green staining and fewer virus containing vesicles. This observation potentially provides evidence towards the theory that the ddBCNAs have an effect on the formation of VACV virus factories.

In order to rule out induction of the intracellular immune response as the MoA, an ELISA for IL-6 was carried out. The results for this ELISA suggest that (with the exception of Cf3242) the ddBCNAs tested do not induce an increased inflammatory/immune response.

Finally the *in vitro* transcription assay indicates that the ddBCNAs do not have an effect on the viral components of transcription as they are able to produce the same amount of mRNA in the presence of Cf2642 in the cell free system. This finding provides further evidence toward the MoA of the ddBCNAs being a cellular rather than a viral target.

Chapter seven – General Discussion

7.1 Combining the findings of the project

In each of the chapters of this project, the experiments performed have provided clues towards the MoA of the ddBCNAs. Here these results are summarised with further interpretation of their relevance.

The luciferase assays have demonstrated that the ddBCNAs have an inhibitory effect on VACV within two hours pi. This finding implies that they have a viral or cellular target that is required in the early stages of infection. The first stages of the VACV lifecycle involve attachment and entry of the virus particles into the host cell. Therefore possible targets were considered within this time scale.

Our studies using a core labelled VACV (YFP-A3L) and confocal analysis of the location of viral particles 30 minutes pi (chapter 6 section 6.3.1) show an equal amount of viral particles inside cells in the presence and absence of Cf2642. This finding indicates that the processes involved with viral attachment and entry, including lipid raft mediated pathways (Chung et al. 2005), and macropinocytosis (Mercer and Helenius, 2008), are unlikely inhibited by ddBCNAs.

VACV early viral transcription is another process that occurs within the two hour time scale, and therefore was considered as a possible target of the ddBCNAs. The *in vitro* transcription data presented in chapter 6 section 6.3.7 suggest that viral early transcription is not inhibited by Cf2642. The *in vitro* transcription assay (Shand et al. 1976) uses VACV virions containing the complete early poxviral transcription complex: DNA dependent RNA polymerase with nine subunits, as well as capping enzyme, nucleoside hydrolases, the poly A polymerase and VACV early transcription factor (Broyles, 2003). The assay tests this system in its entirety, instead of testing component parts. It is well established as an assay suitable for testing inhibitory effects on VACV early transcription (Melquiot and Bugert, 2004).

However, it does not take into account the intracellular requirements for transcription in VACV infected cells, as the VACV virus particles are tested in a cell

free system. While it is therefore possible to say that mRNA transcription from viral genome templates by the early transcription complex in poxviral cores is not inhibited by Cf2642, components contributed to VACV transcription by the cell are not tested.

It has been demonstrated by Mallardo et al. (2002) that VACV cores need to be transported to specific locations within the cell cytoplasm for transcription to occur. So it is possible that the intracellular transport mechanism transporting VACV cores from the point of entry to the site of early transcription could be inhibited by the ddBCNAs. This possible MoA is the subject of ongoing work (confocal imaging of VACV transcription sites).

The fact that the effect is observed within two hours pi suggests that the target is not specific to a process that is only required at later stages of the virus life cycle, e.g. virus DNA replication. This occurs from about 3-4 hrs pi at specific sites in the cytoplasm that are different to those where early transcription occurs (Mallardo et al. 2002). To distinguish ddBCNA effects at the stage of VACV transcription, from later stages in the viral lifecyle, we used cidofovir (Snoeck et al. 1988) as a control. Cidofovir is a known inhibitor of viral DNA polymerases including vaccinia DNA polymerase (De Clercq, 1998). In the two hour luciferase assays the ddBCNAs cause significant reductions in the v3 luciferase transcription luminescence signals, where as cidofovir does not. It is reasonable to assume that the early inhibitory effect of ddBCNAs is not inhibition of the VACV DNA polymerase. This is further underlined by the fact that the D-ddBCNAs active against hCMV (on which the compounds in this project are based) were also found not to be DNA polymerase inhibitors (McGuigan et al. 2004).

As part of our systematic efforts to define the likely cell/viral processes affected by ddBCNAs, we conducted time of addition experiments. Our results (chapter 3 section 3.3.4) show that ddBCNAs have an effect on virus transcription even if given up to 8 hours pi. At this point in the VACV lifecycle viruses have passed DNA replication and start particle assembly/egress. The sites of early transcription have been shown to be in different locations to the sites of DNA replication and late

transcription. The latter appear to occur at the cytosolic side of the endoplasmic reticulum (ER), and the viral DNA replication process appears to attract further ER cisternae, leading to the enclosure of the site in ER membranes (Mallardo et al. 2002). It was also shown that the viral cores and mRNA associate with microtubules, indicating that the viral components are transported to their required location within the cell cytoplasm via microtubules.

The ToA method gives an indication as to the amount of time that the addition of a drug may be delayed without loss of its effect. This approach has been described by Daelemans et al. (2011) in regards to HIV-1 antivirals. Here we used it to provide an indication of the MoA. Our findings imply that it is not simply an early effect. If for example the inhibition was of viral entry alone, then adding the compound after completion of the entry stage of infection would have no effect against the virus. From the ToA experiment we conclude that the ddBCNA target is not likely to be an entry inhibitor, but rather targets a process that is required throughout the lifecycle of VACV.

It has been shown that antiviral compounds may exhibit differing levels of antiviral activity within different cell lines. An example of this effect was shown using poly(rI).poly(rC) (a homopolymer pair of polyriboinosinic and polyribocytidylic acid) which is a nucleotide inducer of interferon. This drug was tested for antiviral activity against bovine vesicular stomatitis virus in primary rabbit kidney (PRK) cells, human skin fibroblasts (HSF), mouse embryo fibroblasts (MEF), mouse L-929 cells, rabbit kidney (RK 13) cells, HeLa, BSC-1 and vero cells. The activity of the drug was found to have decreasing levels of activity through this list of cells (De Clercq and De Somer, 1971). Furthermore, an anti-orthopoxvirus compound, the carbocyclic thymidine analogue; N-methanocarbathymidine ((N)-MCT) was found to display differing levels of activity against VACV and cowpox in nine different cell lines (Smee et al. 2006). The activity of (N)-MCT was discovered to be dependent on cellular thymidine kinase.

We tested for such a difference using a cell range assay (chapter 3, section 3.3.2) which indicated that there was an antiviral effect of Cf2642 in a range of different cell lines of both human and animal origin. This finding confirms that the activity of the ddBCNAs is not specific to a single cell line. Of note, human lung cell line (A549) and skin keratinocytes (HaCaT) were both included in the assay and each represents an area of entry for natural infection with both pox and measles viruses (airborne route/direct contact). As such, our results contribute evidence that the drug may perform well as a measure against clinical infection. They also suggest that the target of the ddBCNAs could be cellular since the level of antiviral activity varies between different cells. The target of the ddBCNAs may also vary in abundance between cell lines.

In order to follow up with this line of thought, the ddBCNAs would need to be further tested in an animal model. The compounds and virus would be administered through different routes in order to determine the activity in a model that better simulates natural infection. Only more extensive animal testing would answer the question as to whether the ddBCNAs are suitable for development as drug candidates. This work has been proposed as the subject of a follow-up Phd /postdoctoral project.

The VACV assay giving the best indication of ddBCNA activity over the whole lifecycle of the virus are plaque assays. VACV plaques reach a size of ~3 mm in diameter in BSC-1 cell culture over a period of 3 days (Doceul et al. 2010). Plaque size is dependent on morphogenesis proteins (e.g. F13L, the VACV protein present of the outer envelope of the EEV form of the virus) being present (Blasco and Moss, 1991) and functionality of the cell cytoskeleton, especially the formation of actin tails to facilitate viral spread (Doceul et al. 2010).

In VACV plaque assays the effect of the ddBCNAs was observed as a reduced plaque size phenotype (chapter 3, section 3.3.4). This small plaque phenotype has been described for other VACV antiviral compounds such as ST-246. This compound targets the viral protein F13L leading to the reduced plaque size (Duraffour et al. 2008). As this compound targets a specific viral protein, the virus may mutate and

develop resistance to the drug. Indeed, strains of VACV that are resistant to ST-246 have already been described (Yang et al. 2005).

Another experimental antiviral active against VACV that causes a reduction in plaques size is Terameprocol (Pollara et al.2010). The reduction was found to be due to the inhibition of actin tail formation in-turn reducing the spread of the virus from one cell to the next. Actin tail formation propels incoming virus particles from already infected cells to cells further away, in the manner of a conveyor belt (Doceul et al. 2010). Actin tail formation is not inhibited at the surface of VACV infected cells in the presence of Cf2642 (chapter 6, section 6.3.2) ruling out an effect on actin polymerisation.

Blebbing has been described by Mercer and Helenius (2009) as a VACV triggered method for entry into host cells. Blebbing of the membrane was apparent in infected cells both in the presence and absence of Cf2642 (chapter 6, section 6.3.2).

The question at this point was to assess whether a cellular target is affected, rather than a VACV specific viral function. One way to answer this question was by investigating the effect of ddBCNAs/Cf2642 against a series of other viruses. A panel of viruses was chosen that represented a wide variety of different types. It included DNA viruses with and without envelopes i.e. HSV-1/HSV-2 and Adenovirus respectively, and the RNA viruses measles and Influenza. Assay systems for all of these viruses were established in the Bugert laboratory and high titer stocks were available. Yellow fever virus and HIV-1 were added to the panel at a later stage of the project.

The results, as presented in chapter 4, revealed significant antiviral activity against measles virus, while all other viruses in the panel were not affected. The measles virus lifecycle and gene products are sufficiently different from VACV, to rule out a virus specific target at this point. This is further evidenced by the fact that the ddBCNAs, in measles virus infected cells, inhibit the formation of syncytia, a CPE that is not observed in VACV infected cells. Syncytia formation is brought about by

the measles virus fusion (F), and hemagglutinin (H) proteins (Cattaneo and Rose, 1993), both of which have no correlates among known poxviral gene products.

This would support the notion of a ddBCNA cellular target relevant in the lifecycle of both VACV and measles viruses, but not the other viruses tested. Unfortunately, finding the MoA of a cell targeting drug is not trivial (Yan et al. 2013). With the vast number of cellular processes possibly affected, one way to show whether a compound has any specific activity versus a cryptic target is to determine SAR. SAR can establish whether specific chemical modifications have an effect on biological activity. Medicinal chemists use the method to improve the potency of a bioactive compound by chemical modification. The specificity of antiviral activity based on side chain length of other nucleoside analogues (against VZV) has previously been demonstrated through the establishment of an SAR (McGuigan et al. 1999).

In this project experiments were carried out in order to define SAR using the compound's activity versus VACV and measles viruses as biological readouts (chapter 3, sections 3.3.1 and 3.3.4 and chapter 4, section 4.3.9). This work was done in depth, using five of the L-ddBCNA compounds (including Cf2642) with specific modifications to the length of the ether side chain. Although not all ddBCNAs produced were tested in all antiviral assays they were all tested using luciferase assays in triplicate (a total of 38 compounds with various modifications), to establish the most active structures.

The two principal findings of the SAR study are: 1) that only L-ddBCNAs (and not D-ddBCNAs) nucleoside analogues have significant antiviral activity versus both VACV and measles virus and 2) that the most effective chemical modification was the lengthening of a hydrophobic side chain, with solubility aided by the presence of an ether bridge. Cf2642 emerged from this study as the lead ddBCNA, an L-enantiomer with the ether side chain C9-O-C5. Both the effects of chirality and the existence of an optimal side chain modification indicate a sterically specific molecular interaction as the cause of Cf2642 antiviral activity. This is demonstrated by the fact that altering the length of the side chain by just one or two carbon atoms can render the L-ddBCNAs less active.

Critically, the SAR established for the ether series of L-ddBCNAs follows the same trend in three very different biological assays: VACV luciferase assays at two hours pi, VACV plaque assays (IC_{50} of plaque size reduction) over four days, and measles virus IC_{50} assays two days pi (inhibition of syncytia inhibition). This indicates that the same target is affected in cells infected by either virus, over a period of two hours to four days pi, giving more credence to the hypothesis of one cellular target required for mRNA transcription, virus spread/ plaque formation, and syncytia formation of two very different viruses.

This work was used to make EU / US patent applications in 2012 (filed and upheld by Cardiff University) and published as an SAR study (McGuigan et al. 2013).

As all of the above processes involve intracellular transport and membrane trafficking, this work points at a cellular membrane compartment as the ddBCNA drug target. This is all the more plausible as the long hydrophilic side chain with specific length requirements suggest a membrane interaction/insertion of the L-ddBCNAs. An example of a drug that interacts with membrane bound compartments is chloroquine which in an unprotonated form may cross the lipid membrane. The compound accumulates in acidic lysosomes as once it has passed through the membrane into them it becomes protonated and with the positive charge it is unable to cross back through the membrane. Chloroquine has been shown to have potential as an antiviral compound as it inhibits pH dependant stages of viral lifecycles (Savarino et al. 2003). The MoA of chloroquine (increasing endosomal vesicle pH) turns out to be of special interest in light of our further findings regarding ddBCNA cellular toxicity and pH changes. We have addressed the question of cellular toxicity in depth as described in chapter five.

For evaluation of toxic effects on our cell lines the CELLTiter-glo assay was used, an extremely sensitive luminescence based test (Petty et al. 1995), which is now the accepted gold-standard for toxicity testing of biologically active compounds prior to testing in animal models. Four different cells lines were tested including B95a, Vero, RK13 and BSC-1 selected as the cells used in the majority of the antiviral assays. We have shown that loss in viability (ATP production) caused by the lead ether series of

L-ddBCNAs is not occurring at active concentrations within the timescale at which activity is observed (chapter 5, section 5.3.1). This implies that the activity is not simply a result of a loss in cell viability.

To our knowledge, this study exceeds other published work in terms of range of cells tested, and observation time for possible toxic effects *in vitro*. Indeed, cell viability was measured at four days post treatment, when most cell lines require medium changes sooner than that, especially at high cell densities. Usual timescales for published toxic effects do not exceed 72 hours.

Further to this, CC_{50} concentrations were calculated using BSC-1 cells (used for the four day VACV plaque assay). The most active ddBCNAs (Cf2642 and Cf3209), were found to have CC_{50} concentrations over 500 times greater than the IC_{50} concentrations (VACV) in the same cell line over the same time frame (i.e. they display a selectivity index of over 500). The *in vitro* selectivity index for Cidofovir against VACV has been shown to be 42 in experiments that used semi continuous foetal lamb muscle (FLM) cells (Nettleton et al. 2000).

It was also demonstrated that the CC_{50} concentrations calculated for the ether series of L-ddBCNAs do not follow the same trend as the IC_{50} concentrations for the same compounds. This is encouraging as it suggests that the loss in viability of the cells observed in some of the cell titer-glo assays (after 24 hours) is not the reason for the antiviral activity of the compounds. So loss of cell viability observed as a result of our lead series of ddBCNA compounds are independent of drug activity in SAR, indicating that the MoA is not an effect leading to cell toxicity between zero and four days post treatment.

This does however not correlate with the theory that the pH change of the medium is linked to the MoA. This theory requires that the pH would become more acidic when more active compounds are used. This is exactly what we observe: the colour change of the medium occurs at the same concentrations at which activity is observed (dose effect), and the more active compounds turn the medium yellow at lower concentrations than the less active ones (SAR pH effect). This effect is clearly

evident in images taken of the plates as part of the measles IC_{50} assays (supplementary material).

In order to find out if extracellular acidity as a cause for loss of viability, a medium replacement assay was devised (chapter 5, section 5.3.5). The results demonstrate that, by replacing the drug and medium with fresh aliquots on a daily basis, the viability of the cells over the four days is improved without a concomitant reduction in antiviral activity.

We interpret the above observations as follows: the cells tested (least and most sensitive BSC-1 and B95a, respectively) show reduced loss of viability after four days if the extracellular acidity is removed on a daily bases. This, along with the fact that antiviral activity can be observed within two hours, indicates that while extracellular acidity affects cell viability, it is not the cause of the antiviral effect, but is a side effect of the MoA of the ddBCNAs. The fact that there is a difference in the trend of the CC_{50} concentrations and the IC_{50} concentration suggests that extracellular acidity is not the sole reason for the loss in viability, and that the compounds with lower activity have other possible unwanted side effects.

At this point it is reasonable to conclude that increased extracellular acidity is a side effect that may lead to loss of cell viability, but is not the actual MoA. The mechanisms however, leading to increased extracellular acidity may still be linked to the MoA. Preliminary work into intracellular pH effects, looking at a lysosomal marker (cd63) at fixed time points (chapter 6, section 6.3.4), suggested that there was a reduction in cd63 staining in the presence of Cf2642. However this effect was difficult to accurately quantify and, therefore, further work using pH tracker dyes and live cell microscopy is currently ongoing.

In order to rule out apoptosis as a side effect of the ddBCNAs, Cf2642 was tested in a selection of cells using the caspase-glo 3/7 kit (chapter 5, sections 5.3.3 and 5.3.4) which measures the levels of effector caspases 3 and 7 (i.e. the level of apoptosis triggered through the caspase cascade (Thornberry and Lazebnik, 1998).

Initial results for caspase 3/7 levels in HeLa and B95a cell lines indicated a dose dependent induction of apoptosis by Cf2642. However, these results could not be repeated, and later experiments suggested both cell lines were completely unaffected. Some studies have shown that a decrease in the extracellular pH may in some cases lead to apoptosis (Park et al. 1999; Schwerdt et al. 2004). As discussed in chapter 6 section 6.3.3, the pH change time course assays indicate that the time of change in the pH brought about by the ddBCNAs is dependent on cell density. If there were slight differences in the number of cells in the wells between the two caspase-glo 3/7 assays (pipetting margin of error), this could be the reason for the differences in the level of caspases between the different assays i.e. a slight increase in the number of cells in the first assay could have been enough to tip the pH over the threshold before cells enter apoptosis.

This finding however also raised the possibility that at least in the case of measles virus syncytium inhibition (24 hrs pi) the antiviral effect may actually be preceded by cell apoptosis. To make sure that apoptosis is not actually the cause of the antiviral effect against measles, Cf2642 was tested in a human B cell line BJAB (derived from human Burkitt lymphoma), where it did not induce apoptosis in either of the caspase assays, but still inhibited syncytia formation by mWT Fb and mEdATCC (supplementary material).

Based on the combined data we feel confident to say that the antiviral effect of the ddBCNAs is not due to apoptosis or a loss in viability of the host cells, especially as initial antiviral activity against VACV can be observed after 2 hours pi (earlier than any loss in viability and/or apoptosis is observed).

The pH effects following ddBCNA treatment are the most interesting current lead for ddBCNA MoA. It is thought that the effect of the ddBCNAs may be linked to effects on cellular lysosomal vesicle turnover (chapter 6, section 6.3.4) and by extension another interesting and topical cellular effect: autophagy.

Measles have been described as inducing successive waves of autophagy (where lysosomes fuse with autophagosomes to form autolysosomes), leading to the

formation of syncytia, which aids dissemination of the infection (Richetta et al. 2013). Therefore if the action of the ddBCNAs on lysosomes were to inhibit autophagy, this could be the reason that the ddBCNAs inhibit syncytia formation in measles infection. A difference in autophagy induction between measles wild type and vaccine strains and the measles receptors involved is also described (Richetta et al. 2013). H protein adaptation to the cellular receptor Cd46 allows measles vaccine viruses to induce an initial wave of autophagy immediately upon infection of non-B cell types (e.g. Vero). Cd150 dependant wild-type measles strains are not able to induce early autophagy, but rather exploit the late and sustained phase of autophagy (Richetta et al. 2013). The difference in the way that these two receptors may induce autophagy may account for the differences observed between the effect of the ddBCNAs against the Edmonston strain of measles in B95a and Vero cells (chapter 4, sections 4.3.7 and 4.3.8).

We hypothesize, that early/pre-treatment with ddBCNAs leads to total suppression of syncytia and late autophagy in wild type strains, but is not always successful in the case of the vaccine strain, where autophagy starts sooner.

If the same MoA were assumed to apply to all viruses affected by ddBCNAs, this case is harder to make for VACV. VACV has been described as being able to replicate in cells deficient for autophagy, implying that they do not require autophagy for their replication (Zhang et al. 2006).

However this does not exclude lysosomes as a possible target for the MoA of the ddBCNAs against VACV. VACV require ER and other intracellular membrane compartments for their assembly and to set up virus factories (de Castro et al. 2013). It has also been found that VACV envelopes contain phospholipids typically found in lysosomal membranes (Hiller et al. 1981), suggesting that they may derive part of their envelope from lysosomal membranes.

While virus factories and the assembly of the VACV particles including the envelope are all occurring late in virus infection, effects on the setup of early transcription sites would also explain, how the ddBCNAs are able to inhibit VACV within two

hours of infection. Mallardo et al. (2002) describe specific intracellular sites of VACV early transcription which are distinct from DNA replication and virus assembly sites. Movement of viral cores to these sites is dependent on dynamic parts of the cytoskeleton, specifically microtubules.

It is well documented, that VACV use actin tails to spread between cells, however this appears not to be affected by the ddBCNAs (chapter 6, section 6.3.2). This leaves other (presumably membrane based) transport mechanisms within the cell that may affect the virus' ability to transport themselves to their required locations within the cell.

So we hypothesise that ddBCNAs are having an effect on the cellular trafficking of VACV components through interference with or disruption of lysosomes within the ddBCNA treated cells.

It has been shown that both measles (Berghäll et al. 2004) and VACV (Schepis et al. 2007) require the use of microtubule based transport during their replication cycles. Transport along microtubules is also required for the clustering of lysosomes in the region of the microtubule-organising centre (Matteoni and Kreis, 1987). From confocal images staining for the marker α-tubulin it appeared that the distribution of microtubules was not affected by Cf2642 (Prett Shah MSc data not shown).

Also, if microtubules themselves were the target of ddBCNAs, this would affect all viruses using this cellular transport system. However, the viruses that have been described as unaffected by the ddBCNAs also use microtubules for intracellular transport, including Adenovirus (Kelkar et al. 2004) Influenza (De Conto et al. 2012) and HSV (Mabit et al. 2002).

The ddBCNAs may affect viral/intracellular membranes (lysosomal/autophagosome compartments) in a way that makes them unable to bind with microtubule transport proteins.

From the cell range assay it was apparent that the antiviral effect against VACV was strongest in RK13 cells (chapter 3, section 3.3.2). Information provided on this cell

line from ATCC states that these cells are positive for keratin by immunoperoxidase staining. Keratin could be another possible target to consider. Keratin-like proteins have been found to associate with VACV factories (Murcia-Nicolas et al. 1999). It has also been shown that in cells infected with respiratory syncytial virus (related to measles), cytokeratin 17 is expressed and localises to sites of syncytia formation (Domachowske et al. 2000). We are following up the leads and hypotheses outlined above one by one.

Ongoing work on intracellular pH imaging and high resolution/EM imaging of poxviral factories, is testing the hypothesis that the cellular target is the lysosomal/autophagosome compartment, which is known to be involved in measles virus syncytia formation and presumably also affects poxviral assembly in factories.

7.2 Future work with the ddBCNAs

A number of leads for MoA of the ddBCNAs have been developed based on a cellular target which we would like to follow up with the following planned experiments:

1. Intracellular pH tracker live microscopy experiments ± Cf2642 using U2OS FYVE gfp cells (these cells are derived from human osteosarcoma and are stably express the FYVE finger fused to GFP, this is thought to localise FYVE-finger proteins with early endosomes; Thermo scientific) and lysotracker RED (selective marker for acidic organelles). The distribution of the green and red stained vesicles will be observed in the presence and absence of Cf2642. The effect of chloroquine on the results will also be established to see if this drug counteracts the effects of Cf2642. This work is currently in progress by Angela Williams and Elizabeth Roquemore at GE Healthcare Whitchurch.
2. An *in vitro* syncytia assay has recently been established using plasmids containing the genes for the Edmonston strain measles F and H proteins (from Caltech). Transfection of HeLa cells with these two plasmids has been shown to produce syncytia in the absence of the virus (supplementary

material). This effect is to be tested in the presence of Cf2642 to see if the effect can be reversed. This will establish if the ddBCNAs are able to inhibit syncytia formation in the absence of virus in different cell lines. Plasmids containing the wild type strains of measles F and H proteins are also in the process of being produced.

3. Depending on the results of the *in vitro* syncytia assay, it may be beneficial to test the effect of the ddBCNAs against the wild type measles virus in an alternative cell type e.g. cord blood cell (COBL) (Kobune et al, 2007).
4. The ddBCNAs will ultimately need to be tested to confirm antiviral activity in animal models for both VACV using black 6 mice (as used in chapter 3, section 3.3.6) and for measles using the cotton rat model (Niewiesk, 1999) which has been found suitable as a model for antiviral testing (Wyde et al, 2000). The compound would be administered through different routes in order to see if the level of infection may be reduced. The testing would need to be extended including administering repeated doses to ensure that no toxic effects occur at any stage during treatment with the compound.
5. The ddBCNAs should be tested against other viruses to find out if there are other viruses that may be inhibited by the drug. Further experiments against HIV-1 are necessary to to confirm if there is a clear effect against this virus.
6. Further medium replacement assays would need to be carried out to determine if maintaining the cell medium pH has an effect on the IC_{50} and CC_{50} concentrations.
7. Autophagosome assays to, firstly, determine the effects of Cf2642 on cells treated with either autophagy inhibitors (e.g. balfilomycin, wortmannin or chloroquine) or autophagy inducers (e.g. rapamycin) and secondly for use with fluorescence microscopy using markers for autophagosomes such as p62 and/or LC3B during measles infection in the presence/absence of Cf2642.

7.3 Addressing the aims of the project

In the introduction (section 1.5) a list of aims for the PhD project were presented. These aims have been addressed over the course of the project as follows:

1. All of the novel ddBCNAs were tested using luciferase assays and statistical significance was assessed in order to ascertain their levels of activity. SAR profiles were established for the alkyl and ether series of L-ddBCNAs (based on their side chain length) using the luciferase assay data. Similarly, SAR were also established for the same ether series using the IC_{50} concentrations developed from the plaque assays.
2. The ddBCNAs were found to be inactive against YFV, HSV-1, HSV-1, Adenovirus and Influenza. Possible activity was displayed against MCV and HIV-1. Activity of the L-ddBCNAs was established against measles. IC_{50} concentrations against measles virus of the ether series displayed similar SAR profiles to those previously established against VACV.
3. The ddBCNAs were found to not cause loss in viability at the active concentrations over the time scales at which activity is observed. The calculated CC_{50} concentrations for the ether series of L-ddBCNAs did not show the same trend as the SAR shown against measles and VACV. The selectivity index for Cf2642 was 500 as based upon the CC_{50} and IC_{50} concentrations for this compound. It was also demonstrated that it is unlikely that the ddBCNAs are inducing cellular apoptosis.
4. Experiments focussing solely on the MoA have ruled out certain targets for the MoA of the ddBCNAs. These include: viral entry, viral transcription, viral DNA polymerisation, cellular actin polymerisation and cellular innate immune responses. Combined, these suggest a specific cellular target which requires further investigation.

7.4 Merit of the project results

In summary this project has investigated the potential of novel compounds (the ddBCNAs) as antiviral drug candidates against pox and measles viruses. Structure

activity relationships have been established and revealed the most active of the compounds to be Cf2642. Initial toxicity testing has been successful and not ruled these out as drug candidates. The MoA has also been narrowed down by a series of experiments.

The MoA of the ddBCNAs is thought to involve a cellular target. Drugs that have cellular rather than viral targets are sometimes not preferred due to the increased likelihood of toxic side effects in the host. However in this project, it has been demonstrated that the ddBCNAs have an acceptable selectivity index *in vitro* and as long as these compounds can be proved safe in future *in vivo* assays, they may have potential for use as clinical antiviral drugs. A benefit of a cellular rather than viral target is that the capacity of the virus to become resistant to the drug is limited. It also has been demonstrated that the compounds display activity against more than one type of virus, presumably any virus that uses the target of the ddBCNAs as part of their replication cycle may also be inhibited by them.

The ddBCNAs are worth pursuing as antiviral compounds as there are currently no approved specific treatments for measles infection and the only recommended treatment against pox viruses in an emergency is cidofovir. Despite the existence of a successful vaccine, measles is still causing outbreaks worldwide and in many cases causes severe side effects. For example, in 2013 an outbreak in Swansea led to 1200 cases of infection, 88 of these individuals required hospital treatment for complications and 1 person died due to giant cell pneumonia caused by the infection (Griffith, 2013). An antiviral candidate for treatment in these situations would be of great benefit.

References

ABDULKARIM, B., SABRI, S., ZELENIKA, D., DEUTSCH, E., FRASCOGNA, V., KLIJANIENKO, J., VAINCHENKER, W., JOAB, I. & BOURHIS, J. 2003. Antiviral agent Cidofovir decreases Epstein-Barr virus (EBV) oncoproteins and enhances the radiosensitivity in EBV-related malignancies. *Oncogene,* 22**,** 2260-2271.

ALBRECHT, P., ENNIS, F. A., SALTZMAN, E. J. & KRUGMAN, S. 1977. PERSISTENCE OF MATERNAL ANTIBODY IN INFANTS BEYOND 12 MONTHS - MECHANISM OF MEASLES-VACCINE FAILURE. *Journal of Pediatrics,* 91**,** 715-718.

ANDREI, G. & SNOECK, R. 2010. Cidofovir Activity against Poxvirus Infections. *Viruses-Basel,* 2**,** 2803-2830.

ARAKAWA, Y., CORDEIRO, J. V., SCHLEICH, S., NEWSOME, T. P. & WAY, M. 2007. The release of vaccinia virus from infected cells requires RhoA-mDia modulation of cortical actin. *Cell Host & Microbe,* 1**,** 227-240.

ARITA, I. 1979. Farewell to smallpox vaccination. *Developments in biological standardization,* 43**,** 283-96.

ARTENSTEIN, A. W., JOHNSON, C., MARBURY, T. C., MORRISON, D., BLUM, P. S., KEMP, T., NICHOLS, R., BALSER, J. P., CURRIE, M. & MONATH, T. P. 2005. A novel, cell culture-derived smallpox vaccine in vaccinia-naive adults. *Vaccine,* 23**,** 3301-3309.

ATMAR, R. L., ENGLUND, J. A. & HAMMILL, H. 1992. COMPLICATIONS OF MEASLES DURING PREGNANCY. *Clinical Infectious Diseases,* 14**,** 217-226.

AVOTA, E., MULLER, N., KLETT, M. & SCHNEIDER-SCHAULIES, S. 2004. Measles virus interacts with and alters signal transduction in T-cell lipid rafts. *Journal of Virology,* 78**,** 9552-9559.

BANKAMP, B., WILSON, J., BELLINI, W. J. & ROTA, P. A. 2005. Identification of naturally occurring amino acid variations that affect the ability of the measles virus C protein to regulate genome replication and transcription. *Virology,* 336**,** 120-129.

BARNARD, D. L. 2004. Inhibitors of measles virus. *Antiviral Chemistry & Chemotherapy,* 15**,** 111-119.

BECKER, M. N., OBRAZTSOVA, M., KERN, E. R., QUENELLE, D. C., KEITH, K. A., PRICHARD, M. N., LUO, M. & MOYER, R. W. 2008. Isolation and characterization of cidofovir resistant vaccinia viruses. *Virology Journal,* 5.

BEHBEHANI, A. M. 1983. THE SMALLPOX STORY - LIFE AND DEATH OF AN OLD DISEASE. *Microbiological Reviews,* 47**,** 455-509.

BELLINI, W. J. & ROTA, P. A. 2011. Biological feasibility of measles eradication. *Virus Research,* 162**,** 72-79.

BELLINI, W. J., ROTA, J. S., LOWE, L. E., KATZ, R. S., DYKEN, P. R., ZAKI, S. R., SHIEH, W. J. & ROTA, P. A. 2005. Subacute sclerosing panencephalitis: More cases of this fatal disease are prevented by measles immunization than was previously recognized. *Journal of Infectious Diseases,* 192**,** 1686-1693.

BERG, J., TYMOCZKO, J. & STRYER, L. 2006. *Biochemistry 6th Edition*, New York : W. H. Freeman.

BERGHALL, H., WALLEN, C., HYYPIA, T. & VAINIONPAA, R. 2004. Role of cytoskeleton components in Measles virus replication. *Archives of Virology,* 149**,** 891-901.

BERTRAND, R., SOLARY, E., OCONNOR, P., KOHN, K. W. & POMMIER, Y. 1994. INDUCTION OF A COMMON PATHWAY OF APOPTOSIS BY STAUROSPORINE. *Experimental Cell Research,* 211**,** 314-321.

BLASCO, R. & MOSS, B. 1991. EXTRACELLULAR VACCINIA VIRUS FORMATION AND CELL-TO-CELL VIRUS TRANSMISSION ARE PREVENTED BY DELETION OF THE GENE ENCODING THE 37,000-DALTON OUTER ENVELOPE PROTEIN. *Journal of Virology,* 65**,** 5910-5920.

BLASCO, R. & MOSS, B. 1992. ROLE OF CELL-ASSOCIATED ENVELOPED VACCINIA VIRUS IN CELL-TO-CELL SPREAD. *Journal of Virology,* 66**,** 4170-4179.

BLASCO, R. & MOSS, B. 1995. SELECTION OF RECOMBINANT VACCINIA VIRUSES ON THE BASIS OF PLAQUE-FORMATION. *Gene,* 158**,** 157-162.

BODNAR, A. G., OUELLETTE, M., FROLKIS, M., HOLT, S. E., CHIU, C. P., MORIN, G. B., HARLEY, C. B., SHAY, J. W., LICHTSTEINER, S. & WRIGHT, W. E. 1998. Extension of life-span by introduction of telomerase into normal human cells. *Science,* 279**,** 349-352.

BRANCALE, A., MCGUIGAN, C., ANDREI, G., SNOECK, R., DE CLERCQ, E. & BALZARINI, J. 2000. Bicyclic nucleoside inhibitors of varicella-zoster virus (VZV): The effect of a terminal halogen substitution in the side-chain. *Bioorganic & Medicinal Chemistry Letters,* 10**,** 1215-1217.

BRAY, M. 2003. Pathogenesis and potential antiviral therapy of complications of smallpox vaccination. *Antiviral Research,* 58**,** 101-114.

BRAY, M. & ROY, C. J. 2004. Antiviral prophylaxis of smallpox. *Journal of Antimicrobial Chemotherapy,* 54**,** 1-5.

BRESLOW, R. & CHENG, Z. L. 2009. On the origin of terrestrial homochirality for nucleosides and amino acids. *Proceedings of the National Academy of Sciences of the United States of America,* 106**,** 9144-9146.

BROYLES, S. S. 2003. Vaccinia virus transcription. *Journal of General Virology,* 84**,** 2293-2303.

BUCKLEY, R. & SMITH, K. 1999. Topical imiquimod therapy for chronic giant molluscum contagiosum in a patient with advanced human immunodeficiency virus 1 disease. *Archives of Dermatology,* 135**,** 1167-1169.

BUGERT, J. J., LOHMULLER, C., DAMON, I., MOSS, B. & DARAI, G. 1998. Chemokine homolog of Molluscum contagiosum virus: Sequence conservation and expression. *Virology,* 242**,** 51-59.

BULLER, R. M., OWENS, G., SCHRIEWER, J., MELMAN, L., BEADLE, J. R. & HOSTETLER, K. Y. 2004. Efficacy of oral active ether lipid analogs of cidofovir in a lethal mousepox model. *Virology,* 318**,** 474-481.

CATTANEO, R. & ROSE, J. K. 1993. CELL-FUSION BY THE ENVELOPE GLYCOPROTEINS OF PERSISTENT MEASLES VIRUSES WHICH CAUSED LETHAL HUMAN BRAIN DISEASE. *Journal of Virology,* 67**,** 1493-1502.

CELLO, J., PAUL, A. V. & WIMMER, E. 2002. Chemical synthesis of poliovirus cDNA: Generation of infectious virus in the absence of natural template. *Science,* 297**,** 1016-1018.

CHAKRABARTI, S., SISLER, J. R. & MOSS, B. 1997. Compact, synthetic, vaccinia virus early/late promoter for protein expression. *Biotechniques,* 23**,** 1094-1097.

CHANG, S. J., CHANG, Y. X., IZMAILYAN, R., TANG, Y. L. & CHANG, W. 2010. Vaccinia Virus A25 and A26 Proteins Are Fusion Suppressors for Mature Virions and Determine Strain-Specific Virus Entry Pathways into HeLa, CHO-K1, and L Cells. *Journal of Virology,* 84**,** 8422-8432.

CHUNG, C. S., VASILEVSKAYA, I. A., WANG, S. C., BAIR, C. H. & CHANG, W. 1997. Apoptosis and host restriction of vaccinia virus in RK13 cells. *Virus Research,* 52**,** 121-132.

CHUNG, C. S., HUANG, C. Y. & CHANG, W. 2005. Vaccinia virus penetration requires cholesterol and results in specific viral envelope proteins associated with lipid rafts. *Journal of Virology,* 79**,** 1623-1634.

CONDIT, R. C. 2007. Vaccinia, Inc. - Probing the functional substructure of poxviral replication factories. *Cell Host & Microbe,* 2**,** 205-207.

CROUCH, S. P. M., KOZLOWSKI, R., SLATER, K. J. & FLETCHER, J. 1993. THE USE OF ATP BIOLUMINESCENCE AS A MEASURE OF CELL-PROLIFERATION AND CYTOTOXICITY. *Journal of Immunological Methods,* 160**,** 81-88.

DAELEMANS, D., PAUWELS, R., DE CLERCQ, E. & PANNECOUQUE, C. 2011. A time-of-drug addition approach to target identification of antiviral compounds. *Nature Protocols,* 6**,** 925-933.

DE CASTRO, I. F., VOLONTE, L. & RISCO, C. 2013. Virus factories: biogenesis and structural design. *Cellular Microbiology,* 15**,** 24-34.

DE CLERCQ, E. 1998. Towards an effective chemotherapy of virus infections: Therapeutic potential of cidofovir (S)-1- 3-hydroxy-2-(phosphonomethoxy)propyl cytosine, HPMPC for the treatment of DNA virus infections. *Collection of Czechoslovak Chemical Communications,* 63**,** 480-506.

DE CLERCQ, E. & NEYTS, J. 2009. Antiviral Agents Acting as DNA or RNA Chain Terminators. *In:* KRAUSSLICH, H. G. & BARTENSCHLAGER, R. (eds.) *Handbook of Experimental Pharmacology.* Springer-Verlag Berlin, Heidelberger Platz 3, D-14197 Berlin, Germany.

DE CONTO, F., DI LONARDO, E., ARCANGELETTI, M. C., CHEZZI, C., MEDICI, M. C. & CALDERARO, A. 2012. Highly Dynamic Microtubules Improve the Effectiveness of Early Stages of Human Influenza A/NWS/33 Virus Infection in LLC-MK2 Cells. *Plos One,* 7**,** 11.

DECLERCQ, E., COOLS, M., BALZARINI, J., SNOECK, R., ANDREI, G., HOSOYA, M., SHIGETA, S., UEDA, T., MINAKAWA, N. & MATSUDA, A. 1991. ANTIVIRAL ACTIVITIES OF 5-ETHYNYL-1-BETA-D-RIBOFURANOSYLIMIDAZOLE-4-CARBOXAMIDE AND RELATED-COMPOUNDS. *Antimicrobial Agents and Chemotherapy,* 35**,** 679-684.

DECLERCQ, E. & DESOMER, P. 1971. ANTIVIRAL ACTIVITY OF POLYRIBOCYTIDYLIC ACID IN CELLS PRIMED WITH POLYRIBOINOSINIC ACID. *Science,* 173**,** 260-&.

DEFILIPPIS, R. A., GOODWIN, E. C., WU, L. L. & DIMAIO, D. 2003. Endogenous human papillomavirus E6 and E7 proteins differentially regulate proliferation, senescence, and apoptosis in HeLa cervical carcinoma cells. *Journal of Virology,* 77**,** 1551-1563.

DELPEUT, S., RUDD, P. A., LABONTE, P. & VON MESSLING, V. 2012. Membrane Fusion-Mediated Autophagy Induction Enhances Morbillivirus Cell-to-Cell Spread. *Journal of Virology,* 86**,** 8527-8535.

DEVAUX, P. & CATTANEO, R. 2004. Measles virus phosphoprotein gene products: Conformational flexibility of the P/V protein amino-terminal domain and C protein infectivity factor function. *Journal of Virology,* 78**,** 11632-11640.

DIETZEL, E., KOLESNIKOVA, L. & MAISNER, A. 2013. Actin filaments disruption and stabilization affect measles virus maturation by different mechanisms. *Virology Journal,* 10**,** 11.

DOCEUL, V., HOLLINSHEAD, M., VAN DER LINDEN, L. & SMITH, G. L. 2010. Repulsion of Superinfecting Virions: A Mechanism for Rapid Virus Spread. *Science,* 327**,** 873-876.

DOMACHOWSKE, J. B., BONVILLE, C. A. & ROSENBERG, H. F. 2000. Cytokeratin 17 is expressed in cells infected with respiratory syncytial virus via NF-kappa B activation and is associated with the formation of cytopathic syncytia. *Journal of Infectious Diseases,* 182**,** 1022-1028.

DORIG, R. E., MARCIL, A., CHOPRA, A. & RICHARDSON, C. D. 1993. THE HUMAN CD46 MOLECULE IS A RECEPTOR FOR MEASLES-VIRUS (EDMONSTON STRAIN). *Cell,* 75**,** 295-305.

DULBECCO, R. 1952. PRODUCTION OF PLAQUES IN MONOLAYER TISSUE CULTURES BY SINGLE PARTICLES OF AN ANIMAL VIRUS. *Proceedings of the National Academy of Sciences of the United States of America,* 38**,** 747-752.

DUPREX, W. P., COLLINS, F. M. & RIMA, B. K. 2002. Modulating the function of the measles virus RNA-dependent RNA polymerase by insertion of green fluorescent protein into the open reading frame. *Journal of Virology,* 76**,** 7322-7328.

DURAFFOUR, S., SNOECK, R., DE VOS, R., VAN DEN OORD, J. J., CRANCE, J. M., GARIN, D., HRUBY, D. E., JORDAN, R., DE CLERCQ, E. & ANDREI, G. 2007. Activity of the anti-orthopoxvirus compound ST-246 against vaccinia, cowpox and camelpox viruses in cell monolayers and organotypic raft cultures. *Antiviral Therapy,* 12**,** 1205-1216.

DURAFFOUR, S., VIGNE, S., VERMEIRE, K., GARCEL, A., VANSTREELS, E., DAELEMANS, D., YANG, G., JORDAN, R., HRUBY, D. E., CRANCE, J.-M., GARIN, D., ANDREI, G. & SNOECK, R. 2008. Specific targeting of the F13L protein by ST-246 affects orthopoxvirus production differently. *Antiviral therapy,* 13**,** 977-90.

DURAFFOUR, S., DRILLIEN, R., HARAGUCHI, K., BALZARINI, J., TOPALIS, D., VAN DEN OORD, J. J., ANDREI, G. & SNOECK, R. 2014. KAY-2-41, a Novel Nucleoside Analogue Inhibitor of Orthopoxviruses In Vitro and In Vivo. *Antimicrobial Agents and Chemotherapy,* 58**,** 27-37.

ENDERS, J. F., PEEBLES, T. C., CHANG, Y. & HOLLOWAY, A. 1954. PROPAGATION IN TISSUE CULTURES OF CYTOPATHOGENIC AGENTS FROM PATIENTS WITH MEASLES. *Proceedings of the Society for Experimental Biology and Medicine,* 86**,** 277-286.

ENGLER, R. J. M., KENNER, J. & LEUNG, D. Y. M. 2002. Smallpox vaccination: Risk considerations for patients with atopic dermatitis. *Journal of Allergy and Clinical Immunology,* 110**,** 357-365.

ERLENHOFER, C., DUPREX, W. P., RIMA, B. K., TER MEULEN, V. & SCHNEIDER-SCHAULIES, J. 2002. Analysis of receptor (CD46, CD150) usage by measles virus. *Journal of General Virology,* 83**,** 1431-1436.

ESPOSITO, J. J. & NAKANO, J. H. 1991. *POXVIRUS INFECTIONS IN HUMANS*.

FORNI, A. L., SCHLUGER, N. W. & ROBERTS, R. B. 1994. SEVERE MEASLES PNEUMONITIS IN ADULTS - EVALUATION OF CLINICAL CHARACTERISTICS AND THERAPY WITH INTRAVENOUS RIBAVIRIN. *Clinical Infectious Diseases,* 19**,** 454-462.

FURUSE, Y., SUZUKI, A. & OSHITANI, H. 2010. Origin of measles virus: divergence from rinderpest virus between the 11(th) and 12(th) centuries. *Virology Journal,* 7**,** 4.

GEADA, M. M., GALINDO, I., LORENZO, M. M., PERDIGUERO, B. & BLASCO, R. 2001. Movements of vaccinia virus intracellular enveloped virions with GFP tagged to the F13L envelope protein. *Journal of General Virology,* 82**,** 2747-2760.

GEDDES, A. M. 2006. The history of smallpox. *Clinics in Dermatology,* 24**,** 152-157.

GRACI, J. D. & CAMERON, C. E. 2006. Mechanisms of action of ribavirin against distinct viruses. *Reviews in Medical Virology,* 16**,** 37-48.

GRANT, S. 1998. Ara-C: Cellular and molecular pharmacology. *Advances in Cancer Research, Vol 72,* 72**,** 197-233.

GRIFFIN, D. E. 2007. *Fields Virology- Measles virus*, Lippincott Williams and Wilkins.

GRIFFITH, R. 2013. Protecting health through public health law. *British journal of nursing (Mark Allen Publishing),* 22**,** 1324-5.

GRIFFITHS, G., WEPF, R., WENDT, T., LOCKER, J. K., CYRKLAFF, M. & ROOS, N. 2001. Structure and assembly of intracellular mature vaccinia virus: Isolated-particle analysis. *Journal of Virology,* 75**,** 11034-11055.

HALLER, S. L., PENG, C., MCFADDEN, G. & ROTHENBURG, S. 2014. Poxviruses and the evolution of host range and virulence. *Infection, genetics and evolution : journal of molecular epidemiology and evolutionary genetics in infectious diseases,* 21**,** 15-40.

HAMMARLUND, E., LEWIS, M. W., HANSEN, S. G., STRELOW, L. I., NELSON, J. A., SEXTON, G. J., HANIFIN, J. M. & SLIFKA, M. K. 2003. Duration of antiviral immunity after smallpox vaccination. *Nature Medicine,* 9**,** 1131-1137.

HASHIMOTO, K., ONO, N., TATSUO, H., MINAGAWA, H., TAKEDA, M., TAKEUCHI, K. & YANAGI, Y. 2002. SLAM (CD150)-independent measles virus entry as revealed by recombinant virus expressing green fluorescent protein. *Journal of Virology,* 76**,** 6743-6749.

HEINER, G. G., FATIMA, N., RUSSELL, P. K., HAASE, A. T., AHMAD, N., MOHAMMED, N., THOMAS, D. B., MACK, T. M., KHAN, M. M., KNATTERU.GL, ANTHONY, R. L. & MCCRUMB, F. R. 1971. FIELD TRIALS OF METHISAZONE AS A PROPHYLACTIC AGENT AGAINST SMALLPOX. *American Journal of Epidemiology,* 94**,** 435-&.

HENDERSON, D. A. 1999. Biological terrorism - The looming threat of bioterrorism. *Science,* 283**,** 1279-1282.

HILLER, G., EIBL, H. & WEBER, K. 1981. ACYL BIS(MONOACYLGLYCERO)PHOSPHATE, ASSUMED TO BE A MARKER FOR LYSOSOMES, IS A MAJOR PHOSPHOLIPID OF VACCINIA VIRIONS. *Virology,* 113**,** 761-764.

HOMEWOOD, C. A., WARHURST, D. C., BAGGALEY, V. C. & PETERS, W. 1972. LYSOSOMES, PH AND ANTI-MALARIAL ACTION OF CHLOROQUINE. *Nature,* 235**,** 50-&.

HUANG, C. Y., LU, T. Y., BAIR, C. H., CHANG, Y. S., JWO, J. K. & CHANG, W. 2008. A novel cellular protein, VPEF, facilitates vaccinia virus penetration into HeLa cells through fluid phase endocytosis. *Journal of Virology,* 82**,** 7988-7999.

HUGHES, A. L., IRAUSQUIN, S. & FRIEDMAN, R. 2010. The evolutionary biology of poxviruses. *Infection Genetics and Evolution,* 10**,** 50-59.

HUMPHRIES, A. C. & WAY, M. 2013. The non-canonical roles of clathrin and actin in pathogen internalization, egress and spread. *Nature Reviews Microbiology,* 11**,** 551-560.

HUMPHRIES, A. C., DODDING, M. P., BARRY, D. J., COLLINSON, L. M., DURKIN, C. H. & WAY, M. 2012. Clathrin Potentiates Vaccinia-Induced Actin Polymerization to Facilitate Viral Spread. *Cell Host & Microbe,* 12**,** 346-359.

HUSSEY, G. D. & CLEMENTS, C. J. 1996. Clinical problems in measles case management. *Annals of Tropical Paediatrics,* 16**,** 307-317.

IWASAKI, M., TAKEDA, M., SHIROGANE, Y., NAKATSU, Y., NAKAMURA, T. & YANAGI, Y. 2009. The Matrix Protein of Measles Virus Regulates Viral RNA Synthesis and Assembly by Interacting with the Nucleocapsid Protein. *Journal of Virology,* 83**,** 10374-10383.

IZMAILYAN, R., HSAO, J. C., CHUNG, C. S., CHEN, C. H., HSU, P. W. C., LIAO, C. L. & CHANG, W. 2012. Integrin beta 1 Mediates Vaccinia Virus Entry through Activation of PI3K/Akt Signaling. *Journal of Virology,* 86**,** 6677-6687.

JACOBS, B. L., LANGLAND, J. O., KIBLER, K. V., DENZIER, K. L., WHITE, S. D., HOLECHEK, S. A., WONG, S., HUYNH, T. & BASKIN, C. R. 2009. Vaccinia virus vaccines: Past, present and future. *Antiviral Research,* 84**,** 1-13.

JAROSZYN.B 1970. TREATMENT WITH METHISAZONE OF COMPLICATIOND FOLLOWING SMALLPOX VACCINATION. *Archives of Disease in Childhood,* 45**,** 573-&.

JEENINGA, R. E., KEULEN, W., BOUCHER, C., SANDERS, R. W. & BERKHOUT, B. 2001. Evolution of AZT resistance in HIV-1: The 41-70 intermediate that is not observed in vivo has a replication defect. *Virology,* 283**,** 294-305.

KAPLAN, C., BENSON, P. F. & BUTLER, N. R. 1965. IMMUNOGENICITY OF ULTRAVIOLET-IRRADIATED NON-INFECTIOUS VACCINIA-VIRUS VACCINE IN INFANTS AND YOUNG CHILDREN. *Lancet,* 1**,** 573-&.

KAPLAN, L. J., DAUM, R. S., SMARON, M. & MCCARTHY, C. A. 1992. SEVERE MEASLES IN IMMUNOCOMPROMISED PATIENTS. *Jama-Journal of the American Medical Association,* 267**,** 1237-1241.

KELKAR, S. A., PFISTER, K. K., CRYSTAL, R. G. & LEOPOLD, P. L. 2004. Cytoplasmic dynein mediates adenovirus binding to microtubules. *Journal of Virology,* 78**,** 10122-10132.

KEMPE, C. H., BERGE, T. O. & ENGLAND, B. 1956. HYPERIMMUNE VACCINAL GAMMA-GLOBULIN - SOURCE, EVALUATION, AND USE IN PROPHYLAXIS AND THERAPY. *Pediatrics,* 18**,** 177-188.

KHANNA, N., DALBY, R., CONNOR, A., CHURCH, A., STERN, J. & FRAZER, N. 2008. Phase I clinical trial of repeat dose terameprocol vaginal ointment in healthy female volunteers. *Sexually Transmitted Diseases,* 35**,** 577-582.

KINGSBURY, D. W. 1991. PARAMYXOVIRIDAE AND THEIR REPLICATION. *Fields, B. N. And D. M. Knipe.*

KOBUNE, F., AMI, Y., KATAYAMA, M., TAKAHASH, M., TUUL, R., KORUKLUOGLU, G., KIYOHARA, T., MIURA, R., SATO, H., YONEDA, M. & KAI, C. 2007. A novel monolayer cell line derived from human umbilical cord blood cells shows high sensitivity to measles virus. *Journal of General Virology,* 88**,** 1565-1567.

KRUMM, S. A., NDUNGU, J. M., YOON, J.-J., DOCHOW, M., SUN, A., NATCHUS, M., SNYDER, J. P. & PLEMPER, R. K. 2011. Potent Host-Directed Small-Molecule Inhibitors of Myxovirus RNA-Dependent RNA-Polymerases. *Plos One,* 6.

KRUMM, S. A., YAN, D., HOVINGH, E. S., EVERS, T. J., ENKIRCH, T., REDDY, G. P., SUN, A., SAINDANE, M. T., ARRENDALE, R. F., PAINTER, G., LIOTTA, D. C., NATCHUS, M. G., VON MESSLING, V. & PLEMPER, R. K. 2014. An orally available, small-molecule polymerase inhibitor shows efficacy against a lethal morbillivirus infection in a large animal model. *Science translational medicine,* 6**,** 232ra52.

KUDCHODKAR, S. B. & LEVINE, B. 2009. Viruses and autophagy. *Reviews in Medical Virology,* 19**,** 359-378.

LALIBERTE, J. P., WEISBERG, A. S. & MOSS, B. 2011. The Membrane Fusion Step of Vaccinia Virus Entry Is Cooperatively Mediated by Multiple Viral Proteins and Host Cell Components. *Plos Pathogens,* 7.

LANE, J. M. & MILLAR, J. D. 1971. RISKS OF SMALLPOX VACCINATION COMPLICATIONS IN UNITED-STATES. *American Journal of Epidemiology,* 93**,** 238-&.

LE MENACH, A., BOXALL, N., AMIRTHALINGAM, G., MADDOCK, L., BALASEGARAM, S. & MINDLIN, M. 2014. Increased measles-mumps-rubella (MMR) vaccine uptake in the context of a targeted immunisation campaign during a measles outbreak in a vaccine-reluctant community in England. *Vaccine,* 32**,** 1147-1152.

LEVY, O., ORON, C., PARAN, N., KEYSARY, A., ISRAELI, O., YITZHAKI, S. & OLSHEVSKY, U. 2010. Establishment of cell-based reporter system for diagnosis of poxvirus infection. *Journal of Virological Methods,* 167**,** 23-30.

LIN, C. C., PHILIPS, L., XU, C. & YEH, L. T. 2004. Pharmacokinetics and safety of viramidine, a prodrug of ribavirin, in healthy volunteers. *Journal of Clinical Pharmacology,* 44**,** 265-275.

MABIT, H., NAKANO, M. Y., PRANK, U., SAM, B., DOHNER, K., SODEIK, B. & GREBER, U. F. 2002. Intact microtubules support adenovirus and herpes simplex virus infections. *Journal of Virology,* 76**,** 9962-9971.

MAGEE, W. C., HOSTETLER, K. Y. & EVANS, D. H. 2005. Mechanism of inhibition of vaccinia virus DNA polymerase by cidofovir diphosphate. *Antimicrobial Agents and Chemotherapy,* 49**,** 3153-3162.

MALLARDO, M., SCHLEICH, S. & LOCKER, J. K. 2001. Microtubule-dependent organization of vaccinia virus core - derived early mRNAs into distinct cytoplasmic structures. *Molecular Biology of the Cell,* 12**,** 3875-3891.

MALLARDO, M., LEITHE, E., SCHLEICH, S., ROOS, N., DOGLIO, L. & LOCKER, J. K. 2002. Relationship between vaccinia virus intracellular cores, early mRNAs, and DNA replication sites. *Journal of Virology,* 76**,** 5167-5183.

MATTEONI, R. & KREIS, T. E. 1987. TRANSLOCATION AND CLUSTERING OF ENDOSOMES AND LYSOSOMES DEPENDS ON MICROTUBULES. *Journal of Cell Biology,* 105**,** 1253-1265.

MCFADDEN, G. 2010. Killing a Killer: What Next for Smallpox? *Plos Pathogens,* 6**,** 4.

MCGUIGAN, C., YARNOLD, C. J., JONES, G., VELAZQUEZ, S., BARUCKI, H., BRANCALE, A., ANDREI, G., SNOECK, R., DE CLERCQ, E. & BALZARINI, J. 1999. Potent and selective inhibition of varicella-zoster virus (VZV) by nucleoside analogues with an unusual bicyclic base. *Journal of Medicinal Chemistry,* 42**,** 4479-4484.

MCGUIGAN, C., BRANCALE, A., BARUCKI, H., SRINIVASAN, S., JONES, G., PATHIRANA, R., CARANGIO, A., BLEWETT, S., LUONI, G., BIDET, O., JUKES, A., JARVIS, C., ANDREI, G., SNOECK, R., DE CLERCQ, E. & BALZARINI, J. 2001. Furano pyrimidines as novel potent and selective anti-VZV agents. *Antiviral Chemistry & Chemotherapy,* 12**,** 77-89.

MCGUIGAN, C., PATHIRANA, R. N., SNOECK, R., ANDREI, G., DE CLERCQ, E. & BALZARINI, J. 2004. Discovery of a new family of inhibitors of human cytomegalovirus (HCMV) based upon lipophilic alkyl furano pyrimidine dideoxy nucleosides: Action via a novel non-nucleosidic mechanism. *Journal of Medicinal Chemistry,* 47**,** 1847-1851.

MCGUIGAN, C., BUGERT, J. J., JONES, A. T., PATHIRANA, R. & FARLEIGH, L. E. 2013. *Chemical compounds*.

MCGUIGAN, C., HINSINGER, K., FARLEIGH, L., PATHIRANA, R. N. & BUGERT, J. J. 2013. Novel Antiviral Activity of L-Dideoxy Bicyclic Nucleoside Analogues

versus Vaccinia and Measles Viruses in Vitro. *Journal of Medicinal Chemistry,* 56**,** 1311-1322.

MELQUIOT, N. V. & BUGERT, J. J. 2004. Preparation and use of molluscum contagiosum virus from human tissue biopsy specimens. *Methods in molecular biology (Clifton, N.J.),* 269**,** 371-84.

MERCER, J. & HELENIUS, A. 2008. Vaccinia virus uses macropinocytosis and apoptotic mimicry to enter host cells. *Science,* 320**,** 531-535.

MERCER, J. & HELENIUS, A. 2009. Virus entry by macropinocytosis. *Nature Cell Biology,* 11**,** 510-520.

MERCER, J., KNEBEL, S., SCHMIDT, F. I., CROUSE, J., BURKARD, C. & HELENIUS, A. 2010. Vaccinia virus strains use distinct forms of macropinocytosis for host-cell entry. *Proceedings of the National Academy of Sciences of the United States of America,* 107**,** 9346-9351.

MOLOUGHNEY, J. G., MONKEN, C. E., TAO, H. L., ZHANG, H. Y., THOMAS, J. D., LATTIME, E. C. & JIN, S. K. 2011. Vaccinia virus leads to ATG12-ATG3 conjugation and deficiency in autophagosome formation. *Autophagy,* 7**,** 1434-1447.

MOSS, B. 1991. POXVIRIDAE AND THEIR REPLICATION. *Fields, B. N. And D. M. Knipe.*

MOSS, B. 2006. Poxvirus entry and membrane fusion. *Virology,* 344**,** 48-54.

MOSS, B. 2012. Poxvirus Cell Entry: How Many Proteins Does it Take? *Viruses-Basel,* 4**,** 688-707.

MOSS, W. J., OTA, M. O. & GRIFFIN, D. E. 2004. Measles: immune suppression and immune responses. *International Journal of Biochemistry & Cell Biology,* 36**,** 1380-1385.

MURCIA-NICOLAS, A., BOLBACH, G., BLAIS, J. C. & BEAUD, G. 1999. Identification by mass spectroscopy of three major early proteins associated with virosomes in vaccinia virus-infected cells. *Virus Research,* 59**,** 1-12.

MYSKIW, C., PIPER, J., HUZAREWICH, R., BOOTH, T. F., CAO, J. & HE, R. 2010. Nigericin is a potent inhibitor of the early stage of vaccinia virus replication. *Antiviral Research,* 88**,** 304-310.

NETTLETON, P. F., GILRAY, J. A., REID, H. W. & MERCER, A. A. 2000. Parapoxviruses are strongly inhibited in vitro by cidofovir. *Antiviral Research,* 48**,** 205-208.

NIEWIESK, S. 1999. Cotton rats (Sigmodon hispidus): an animal model to study the pathogenesis of measles virus infection. *Immunology Letters,* 65**,** 47-50.

NITSCHE, A. & PAULI, G. 2007. Sporadic human cases of cowpox in Germany. *Euro surveillance : bulletin Europeen sur les maladies transmissibles = European communicable disease bulletin,* 12**,** E070419.3.

NOYCE, R. S., BONDRE, D. G., HA, M. N., LIN, L. T., SISSON, G., TSAO, M. S. & RICHARDSON, C. D. 2011. Tumor Cell Marker PVRL4 (Nectin 4) Is an Epithelial Cell Receptor for Measles Virus. *Plos Pathogens,* 7**,** 24.

OGBUANU, I. U., ZEKO, S., CHU, S. Y., MUROUA, C., GERBER, S., DE WEE, R., KRETSINGER, K., WANNEMUEHLER, K., GERNDT, K., ALLIES, M., SANDHU, H. S. & GOODSON, J. L. 2014. Maternal, fetal, and neonatal outcomes associated with measles during pregnancy: namibia, 2009-2010. *Clinical infectious diseases : an official publication of the Infectious Diseases Society of America,* 58**,** 1086-92.

OHNO, S., ONO, N., TAKEDA, M., TAKEUCHI, K. & YANAGI, Y. 2004. Dissection of measles virus V protein in relation to its ability to block alpha/beta interferon signal transduction. *Journal of General Virology,* 85**,** 2991-2999.

OSBORN, J. E. & WALKER, D. L. 1968. ENHANCEMENT OF INFECTIVITY OF MURINE CYTOMEGALOVIRUS IN VITRO BY CENTRIFUGAL INOCULATION. *Journal of Virology,* 2**,** 853-&.

PARK, H. J., LYONS, J. C., OHTSUBO, T. & SONG, C. W. 1999. Acidic environment causes apoptosis by increasing caspase activity. *British Journal of Cancer,* 80**,** 1892-1897.

PARKER, S., TOUCHETTE, E., OBERLE, C., ALMOND, M., ROBERTSON, A., TROST, L. C., LAMPERT, B., PAINTER, G. & BULLER, R. M. 2008. Efficacy of therapeutic intervention with an oral ether-lipid analogue of cidofovir (CMX001) in a lethal mousepox model. *Antiviral Research,* 77**,** 39-49.

PELKONEN, P. M., TARVAINEN, K., HYNNINEN, A., KALLIO, E. R. K., HENTTONEN, H., PALVA, A., VAHERI, A. & VAPALAHTI, O. 2003. Cowpox with severe generalized eruption, Finland. *Emerging Infectious Diseases,* 9**,** 1458-1461.

PERRY, R. T. & HALSEY, N. A. 2004. The clinical significance of measles: A review. *Journal of Infectious Diseases,* 189**,** S4-S16.

PETTY, R. D., SUTHERLAND, L. A., HUNTER, E. M. & CREE, I. A. 1995. COMPARISON OF MTT AND ATP-BASED ASSAYS FOR THE MEASUREMENT OF VIABLE CELL NUMBER. *Journal of Bioluminescence and Chemiluminescence,* 10**,** 29-34.

PLEMPER, R. K. & HAMMOND, A. L. 2014. Synergizing vaccinations with therapeutics for measles eradication. *Expert Opinion on Drug Discovery,* 9**,** 201-214.

PLEMPER, R. K. & SNYDER, J. P. 2009. Measles control - Can measles virus inhibitors make a difference? *Current Opinion in Investigational Drugs,* 10**,** 811-820.

PLOUBIDOU, A., MOREAU, V., ASHMAN, K., RECKMANN, I., GONZALEZ, C. & WAY, M. 2000. Vaccinia virus infection disrupts microtubule organization and centrosome function. *Embo Journal,* 19**,** 3932-3944.

POLLARA, J. J., LASTER, S. M. & PETTY, I. T. D. 2010. Inhibition of poxvirus growth by Terameprocol, a methylated derivative of nordihydroguaiaretic acid. *Antiviral Research,* 88**,** 287-295.

POLS, M. S. & LUMPERMAN, J. 2009. Trafficking and function of the tetraspanin CD63. *Experimental Cell Research,* 315**,** 1584-1592.

PRUSSIA, A. J., PLEMPER, R. K. & SNYDER, J. P. 2008. Measles Virus Entry Inhibitors: A Structural Proposal for Mechanism of Action and the Development of Resistance. *Biochemistry,* 47**,** 13573-13583.

QUENELLE, D. C., PRICHARD, M. N., KEITH, K. A., HRUBY, D. E., JORDAN, R., PAINTER, G. R., ROBERTSON, A. & KERN, E. R. 2007. Synergistic efficacy of the combination of ST-246 with CMX001 against orthopoxviruses. *Antimicrobial Agents and Chemotherapy,* 51**,** 4118-4124.

REED, L. J. & MUENCH, H. 1938. A simple method of estimating fifty per cent endpoints. *Amer Jour Hyg,* 27**,** 493-497.

RICHETTA, C., GREGOIRE, I. P., VERLHAC, P., AZOCAR, O., BAGUET, J., FLACHER, M., TANGY, F., RABOURDIN-COMBE, C. & FAURE, M. 2013. Sustained Autophagy Contributes to Measles Virus Infectivity. *Plos Pathogens,* 9**,** 15.

RIETDORF, J., PLOUBIDOU, A., RECKMANN, I., HOLMSTROM, A., FRISCHKNECHT, F., ZETTL, M., ZIMMERMANN, T. & WAY, M. 2001. Kinesin-dependent movement on microtubules precedes actin-based motility of vaccinia virus. *Nature Cell Biology,* 3**,** 992-1000.

RIMA, B. K. & DUPREX, W. P. 2006. Morbilliviruses and human disease. *Journal of Pathology,* 208**,** 199-214.

RIMA, B. K. & DUPREX, W. P. 2011. New concepts in measles virus replication: Getting in and out in vivo and modulating the host cell environment. *Virus Research,* 162**,** 47-62.

RIMOIN, A. W., MULEMBAKANI, P. M., JOHNSTON, S. C., LLOYD-SMITH, J. O., KISALU, N. K., KINKELA, T. L., BLUMBERG, S., THOMASSEN, H. A., PIKE, B. L., FAIR, J. N., WOLFE, N. D., SHONGO, R. L., GRAHAM, B. S., FORMENTY, P., OKITOLONDA, E., HENSLEY, L. E., MEYER, H., WRIGHT, L. L. & MUYEMBE, J. J. 2010. Major increase in human monkeypox incidence 30 years after smallpox vaccination campaigns cease in the Democratic Republic of Congo. *Proceedings of the National Academy of Sciences of the United States of America,* 107**,** 16262-16267.

ROBERTS, K. L. & SMITH, G. L. 2008. Vaccinia virus morphogenesis and dissemination. *Trends in Microbiology,* 16**,** 472-479.

ROBERTS, K. L., BREIMAN, A., CARTER, G. C., EWLES, H. A., HOLLINSHEAD, M., LAW, M. & SMITH, G. L. 2009. Acidic residues in the membrane-proximal stalk region of vaccinia virus protein B5 are required for glycosaminoglycan-mediated disruption of the extracellular enveloped virus outer membrane. *Journal of General Virology,* 90**,** 1582-1591.

ROSALES, R., SUTTER, G. & MOSS, B. 1994. A CELLULAR FACTOR IS REQUIRED FOR TRANSCRIPTION OF VACCINIA VIRAL INTERMEDIATE-STAGE GENES. *Proceedings of the National Academy of Sciences of the United States of America,* 91**,** 3794-3798.

ROSENTHAL, S. R., MERCHLINSKY, M., KLEPPINGER, C. & GOLDENTHAL, K. L. 2001. Developing new smallpox vaccines. *Emerging Infectious Diseases,* 7**,** 920-926.

SABELLA, C. 2010. Measles: Not just a childhood rash. *Cleveland Clinic Journal of Medicine,* 77**,** 207-213.

SAVARINO, A., BOELAERT, J. R., CASSONE, A., MAJORI, G. & CAUDA, R. 2003. Effects of chloroquine on viral infections: an old drug against today's diseases? *Lancet Infectious Diseases,* 3**,** 722-727.

SCHEPIS, A., STAUBER, T. & LOCKER, J. K. 2007. Kinesin-1 plays multiple roles during the vaccinia virus life cycle. *Cellular Microbiology,* 9**,** 1960-1973.

SCHMIDT, F. I. & MERCER, J. 2012. Vaccinia Virus Egress: Actin OUT with ClathrIN. *Cell Host & Microbe,* 12**,** 263-265.

SCHMIDT, F. I., BLECK, C. K. E., REH, L., NOVY, K., WOLLSCHEID, B., HELENIUS, A., STAHLBERG, H. & MERCER, J. 2013. Vaccinia Virus Entry Is Followed by Core Activation and Proteasome-Mediated Release of the Immunomodulatory Effector VH1 from Lateral Bodies. *Cell Reports,* 4**,** 464-476.

SCHRAMM, B. & LOCKER, J. K. 2005. Cytoplasmic organization of POXvirus DNA replication. *Traffic,* 6**,** 839-846.

SCHROEDER, N., CHUNG, C. S., CHEN, C. H., LIAO, C. L. & CHANG, W. 2012. The Lipid Raft-Associated Protein CD98 Is Required for Vaccinia Virus Endocytosis. *Journal of Virology,* 86**,** 4868-4882.

SCHWEGMANN, A. & BROMBACHER, F. 2008. INFECTIOUS DISEASE Host-Directed Drug Targeting of Factors Hijacked by Pathogens. *Science Signaling,* 1**,** 7.

SCHWERDT, G., FREUDINGER, R., SCHUSTER, C., SILBERNAGL, S. & GEKLE, M. 2004. Inhibition of mitochondria and extracellular acidification enhance ochratoxin A-induced apoptosis in renal collecting duct-derived MDCK-C7 cells. *Cellular Physiology and Biochemistry,* 14**,** 47-56.

SENKEVICH, T. G., KOONIN, E. V., BUGERT, J. J., DARAI, G. & MOSS, B. 1997. The genome of molluscum contagiosum virus: Analysis and comparison with other poxviruses. *Virology,* 233**,** 19-42.

SENKEVICH, T. G., OJEDA, S., TOWNSLEY, A., NELSON, G. E. & MOSS, B. 2005. Poxvirus multiprotein entry-fusion complex. *Proceedings of the National Academy of Sciences of the United States of America,* 102**,** 18572-18577.

SHAND, J. H., GIBSON, P., GREGORY, D. W., COOPER, R. J., KEIR, H. M. & POSTLETHWAITE, R. 1976. MOLLUSCUM CONTAGIOSUM - DEFECTIVE POXVIRUS. *Journal of General Virology,* 33**,** 281-295.

SHERWANI, S., BLYTHE, N., FARLEIGH, L. & BUGERT, J. J. 2012. New method for the assessment of molluscum contagiosum virus infectivity. *Methods in molecular biology (Clifton, N.J.),* 890**,** 135-46.

SIVAN, G., MARTIN, S. E., MYERS, T. G., BUEHLER, E., SZYMCZYK, K. H., ORMANOGLU, P. & MOSS, B. 2013. Human genome-wide RNAi screen reveals a role for nuclear pore proteins in poxvirus morphogenesis. *Proceedings of the National Academy of Sciences of the United States of America,* 110**,** 3519-3524.

SKIEST, D. J., DUONG, M., PARK, S., WEI, L. & KEISER, P. 1999. Complications of therapy with intravenous cidofovir: Severe nephrotoxicity and anterior uveitis. *Infectious Diseases in Clinical Practice,* 8**,** 151-157.

SMEE, D. F., WANDERSEE, M. K., BAILEY, K. W., WONG, M. H., CHU, C. K., GADTHULA, S. & SIDWELL, R. W. 2006. Cell line dependency for antiviral activity of N-methanocarbathymidine against orthopoxvirus infections. *Antiviral Research,* 70**,** A75-A75.

SMITH, G. L., VANDERPLASSCHEN, A. & LAW, M. 2002. The formation and function of extracellular enveloped vaccinia virus. *Journal of General Virology,* 83**,** 2915-2931.

SMOLEWSKI, P. 2008. Terameprocol, a novel site-specific transcription inhibitor with anticancer activity. *Idrugs,* 11**,** 204-214.

SNOECK, R., SAKUMA, T., DECLERCQ, E., ROSENBERG, I. & HOLY, A. 1988. (S)-1-(3-HYDROXY-2-PHOSPHONYLMETHOXYPROPYL)CYTOSINE, A POTENT AND SELECTIVE INHIBITOR OF HUMAN CYTOMEGALO-VIRUS REPLICATION. *Antimicrobial Agents and Chemotherapy,* 32**,** 1839-1844.

SUAREZ, C., WELSCH, S., CHLANDA, P., HAGEN, W., HOPPE, S., KOLOVOU, A., PAGNIER, I., RAOULT, D. & LOCKER, J. K. 2013. Open membranes are the precursors for assembly of large DNA viruses. *Cellular Microbiology,* 15**,** 1883-1895.

SUGAI, A., SATO, H., YONEDA, M. & KAI, C. 2013. Phosphorylation of Measles Virus Nucleoprotein Affects Viral Growth by Changing Gene Expression and Genomic RNA Stability. *Journal of Virology,* 87**,** 11684-11692.

TACK, D. M., KAREM, K. L., MONTGOMERY, J. R., COLLINS, L., BRYANT-GENEVIER, M. G., TIERNAN, R., CANO, M., LEWIS, P., ENGLER, R. J. M., DAMON, I. K. & REYNOLDS, M. G. 2013. Unintentional transfer of vaccinia virus associated with smallpox vaccines ACAM2000 (R) compared with Dryvax (R). *Human Vaccines & Immunotherapeutics,* 9**,** 1489-1496.

TAKEUCHI, K., MIYAJIMA, N., NAGATA, N., TAKEDA, M. & TASHIRO, M. 2003. Wild-type measles virus induces large syncytium formation in primary human small airway epithelial cells by a SLAM(CD150)-independent mechanism. *Virus Research,* 94**,** 11-16.

TATSUO, H., ONO, N., TANAKA, K. & YANAGI, Y. 2000. SLAM (CDw150) is a cellular receptor for measles virus. *Nature,* 406**,** 893-897.

TELENTI, A., MARSHALL, W. F. & SMITH, T. F. 1990. DETECTION OF EPSTEIN-BARR-VIRUS BY POLYMERASE CHAIN-REACTION. *Journal of Clinical Microbiology,* 28**,** 2187-2190.

THORNBERRY, N. A. & LAZEBNIK, Y. 1998. Caspases: Enemies within. *Science,* 281**,** 1312-1316.

TOOZE, J., HOLLINSHEAD, M., REIS, B., RADSAK, K. & KERN, H. 1993. PROGENY VACCINIA AND HUMAN CYTOMEGALOVIRUS PARTICLES UTILIZE EARLY ENDOSOMAL CISTERNAE FOR THEIR ENVELOPES. *European Journal of Cell Biology,* 60**,** 163-178.

TOWNSLEY, A. C., SENKEVICH, T. G. & MOSS, B. 2005. Vaccinia virus A21 virion membrane protein is required for cell entry and fusion. *Journal of Virology,* 79**,** 9458-9469.

TOWNSLEY, A. C., SENKEVICH, T. G. & MOSS, B. 2005. The product of the vaccinia virus L5R gene is a fourth membrane protein encoded by all poxviruses that is required for cell entry and cell-cell fusion. *Journal of Virology,* 79**,** 10988-10998.

TOWNSLEY, A. C., WEISBERG, A. S., WAGENAAR, T. R. & MOSS, B. 2006. Vaccinia virus entry into cells via a low-pH-dependent endosomal pathway. *Journal of Virology,* 80**,** 8899-8908.

VAN DER WOUDEN, J. C., VAN DER SANDE, R., VAN SUIJLEKOM-SMIT, L. W., BERGER, M., BUTLER, C. C. & KONING, S. 2009. Interventions for cutaneous molluscum contagiosum. *Cochrane database of systematic reviews (Online)***,** CD004767.

VANDERPLASSCHEN, A., HOLLINSHEAD, M. & SMITH, G. L. 1998. Intracellular and extracellular vaccinia virions enter cells by different mechanisms. *Journal of General Virology,* 79**,** 877-887.

VIGNE, S., DURAFFOUR, S., ANDREI, G., SNOECK, R., GARIN, D. & CRANCE, J.-M. 2009. Inhibition of Vaccinia Virus Replication by Two Small Interfering RNAs Targeting B1R and G7L Genes and Their Synergistic Combination with Cidofovir. *Antimicrobial Agents and Chemotherapy,* 53**,** 2579-2588.

VIJAYAN, M., SEO, Y. J., PRITZL, C. J., SQUIRES, S. A., ALEXANDER, S. & HAHM, B. 2014. Sphingosine kinase 1 regulates measles virus replication. *Virology,* 450**,** 55-63.

VOET, D. & VOET, J. G. 2004. *Biochemistry 3rd Edition*, New York ; Chichester : Wiley.

VOROU, R. M., PAPAVASSILIOU, V. G. & PIERROUTSAKOS, L. N. 2008. Cowpox virus infection: an emerging health threat. *Current Opinion in Infectious Diseases,* 21**,** 153-156.

WARD, B. M. 2005. Visualization and characterization of the intracellular movement of vaccinia virus intracellular mature virions. *Journal of Virology,* 79**,** 4755-4763.

WARD, B. M. & MOSS, B. 2004. Vaccinia virus A36R membrane protein provides a direct link between intracellular enveloped virions and the microtubule motor kinesin. *Journal of Virology,* 78**,** 2486-2493.

WEHRLE, P. F., POSCH, J., RICHTER, K. H. & HENDERSO.DA 1970. AIRBORNE OUTBREAK OF SMALLPOX IN A GERMAN HOSPITAL AND ITS SIGNIFICANCE WITH RESPECT TO OTHER RECENT OUTBREAKS IN EUROPE. *Bulletin of the World Health Organization,* 43**,** 669-&.

WELSCH, J. C., TALEKAR, A., MATHIEU, C., PESSI, A., MOSCONA, A., HORVAT, B. & POROTTO, M. 2013. Fatal Measles Virus Infection Prevented by Brain-Penetrant Fusion Inhibitors. *Journal of Virology,* 87**,** 13785-13794.

WILD, T. F., MALVOISIN, E. & BUCKLAND, R. 1991. MEASLES-VIRUS - BOTH THE HEMAGGLUTININ AND FUSION GLYCOPROTEINS ARE REQUIRED FOR FUSION. *Journal of General Virology,* 72**,** 439-442.

WILEMAN, T. 2006. Aggresomes and autophagy generate sites for virus replication. *Science,* 312**,** 875-878.

WYDE, P. R., MOORE-POVEDA, D. K., DE CLERCQ, E., NEYTS, J., MATSUDA, A., MINAKAWA, N., GUZMAN, E. & GILBERT, B. E. 2000. Use of cotton rats to evaluate the efficacy of antivirals in treatment of measles virus infections. *Antimicrobial Agents and Chemotherapy,* 44**,** 1146-1152.

WYMANN, M. P., BULGARELLILEVA, G., ZVELEBIL, M. J., PIROLA, L., VANHAESEBROECK, B., WATERFIELD, M. D. & PANAYOTOU, G. 1996. Wortmannin inactivates phosphoinositide 3-kinase by covalent modification of Lys-802, a residue involved in the phosphate transfer reaction. *Molecular and Cellular Biology,* 16**,** 1722-1733.

YAN, D., KRUMM, S. A., SUN, A., STEINHAUER, D. A., LUO, M., MOORE, M. L. & PLEMPER, R. K. 2013. Dual Myxovirus Screen Identifies a Small-Molecule Agonist of the Host Antiviral Response. *Journal of Virology,* 87**,** 11076-11087.

YANAGI, Y., ONO, N., TATSUO, H., HASHIMOTO, K. & MINAGAWA, H. 2002. Measles virus receptor SLAM (CD150). *Virology,* 299**,** 155-161.

YANAGI, Y., TAKEDA, M. & OHNO, S. 2006. Measles virus: cellular receptors, tropism and pathogenesis. *Journal of General Virology,* 87**,** 2767-2779.

YANG, G., PEVEAR, D. C., DAVIES, M. H., COLLETT, M. S., BAILEY, T., RIPPEN, S., BARONE, L., BURNS, C., RHODES, G., TOHAN, S., HUGGINS, J. W., BAKER, R. O., BULLER, R. L. M., TOUCHETTE, E., WALLER, K., SCHRIEWER, J., NEYTS, J., DECLERCQ, E., JONES, K., HRUBY, D. & JORDAN, R. 2005. An orally bioavailable antipoxvirus compound (ST-246) inhibits extracellular virus formation and protects mice from lethal orthopoxvirus challenge. *Journal of Virology,* 79**,** 13139-13149.

ZHANG, H. Y., MONKEN, C. E., ZHANG, Y., LENARD, J., MIZUSHIMA, N., LATTIME, E. C. & JIN, S. K. 2006. Cellular autophagy machinery is not required for vaccinia virus replication and maturation. *Autophagy,* 2**,** 91-95.

ZHANG, P., LI, L. Y., HU, C. L., XU, Q., LIU, X. & QI, Y. P. 2005. Interactions among measles virus hemagglutinin, fusion protein and cell receptor signaling lymphocyte activation molecule (SLAM) indicating a new fusion-trimer model. *Journal of Biochemistry and Molecular Biology,* 38**,** 373-380.

Supplementary material

1. IC_{50} calculation graphs (GraphPad)

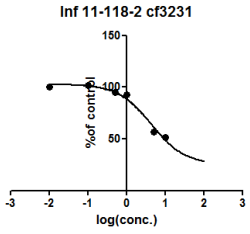

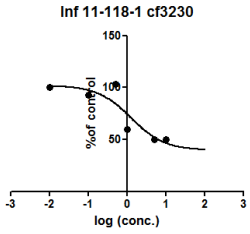

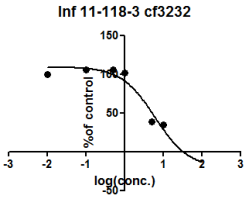

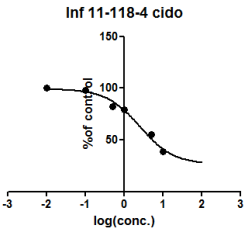

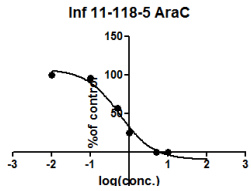

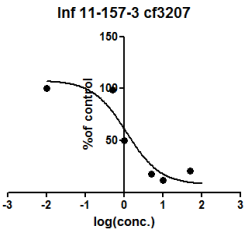

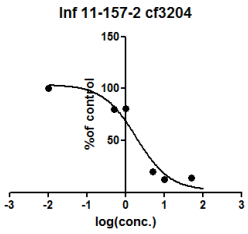

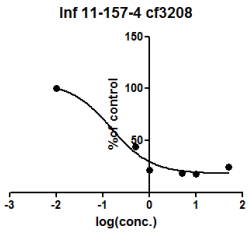

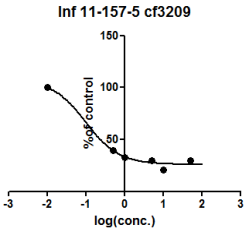

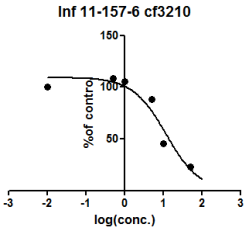

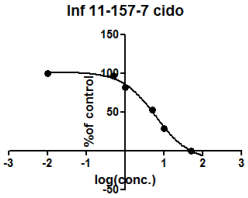

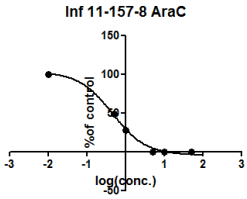

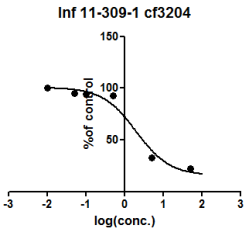

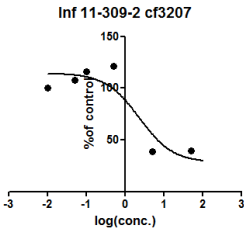

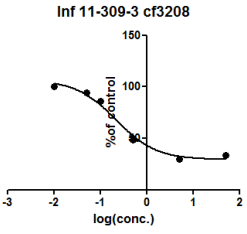

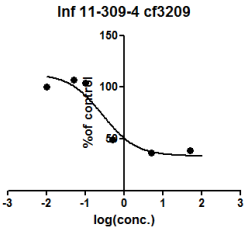

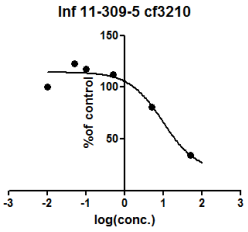

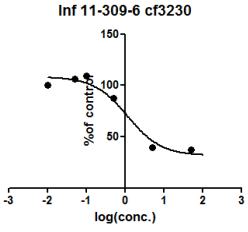

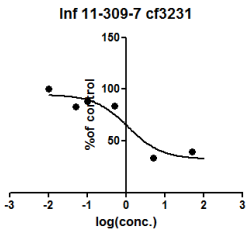

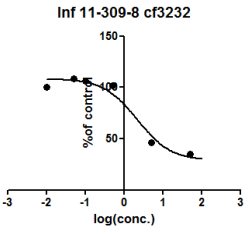

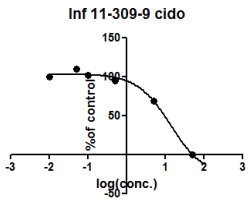

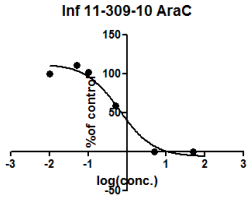

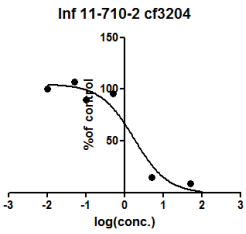
Inf 11-710-2 cf3204
%of control
log(conc.)

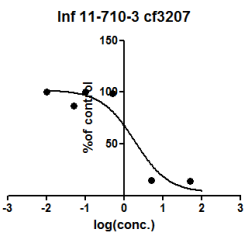
Inf 11-710-3 cf3207
%of control
log(conc.)

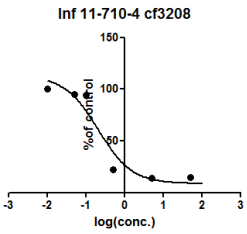
Inf 11-710-4 cf3208
%of control
log(conc.)

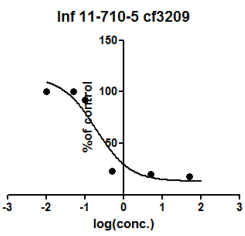
Inf 11-710-5 cf3209
%of control
log(conc.)

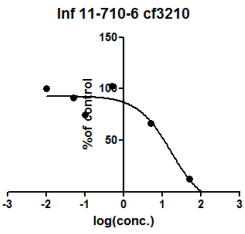
Inf 11-710-6 cf3210
%of control
log(conc.)

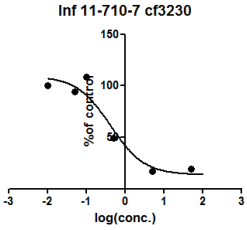
Inf 11-710-7 cf3230
%of control
log(conc.)

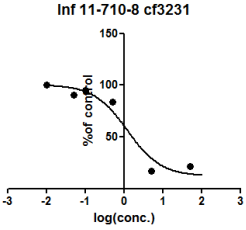
Inf 11-710-8 cf3231
%of control
log(conc.)

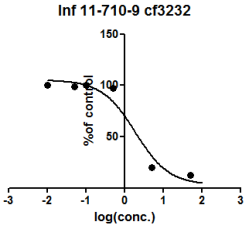
Inf 11-710-9 cf3232
%of control
log(conc.)

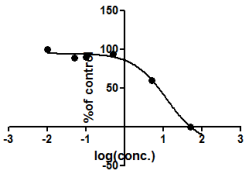
Inf 11-710-10 cido
%of control
log(conc.)

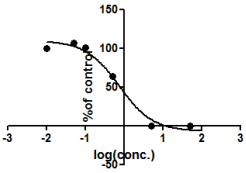
Inf 11-710-11 AraC
%of control
log(conc.)

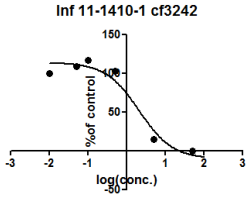
Inf 11-1410-1 cf3242
%of control
log(conc.)

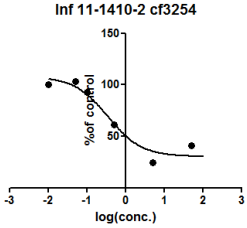
Inf 11-1410-2 cf3254
%of control
log(conc.)

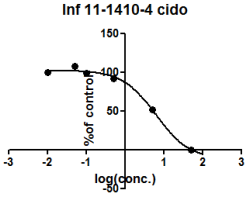
Inf 11-1410-4 cido
%of control
log(conc.)

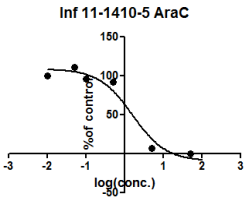
Inf 11-1410-5 AraC
%of control
log(conc.)

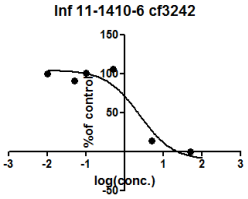
Inf 11-1410-6 cf3242
%of control
log(conc.)

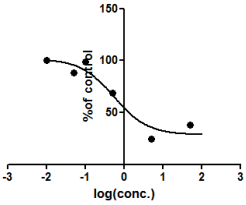
Inf 11-1410-7 cf3254
%of control
log(conc.)

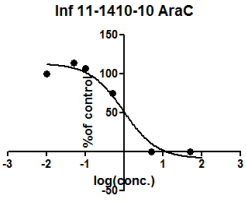
Inf 11-1410-10 AraC
%of control
log(conc.)

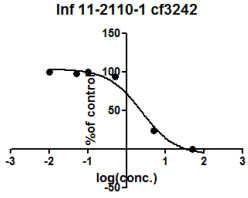
Inf 11-2110-1 cf3242
%of control
log(conc.)

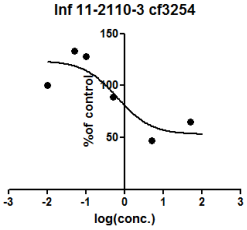
Inf 11-2110-3 cf3254
%of control
log(conc.)

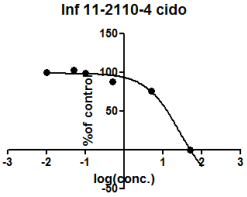
Inf 11-2110-4 cido
%of control
log(conc.)

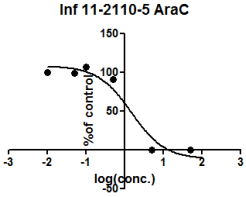
Inf 11-2110-5 AraC
%of control
log(conc.)

2. Transfection with measles F and H proteins – syncytia formation in the absence of virus

HeLa cells transfected with plasmids containing measles F and H proteins, in the absence of virus. Syncytia could be observed 24 hours post transfection.

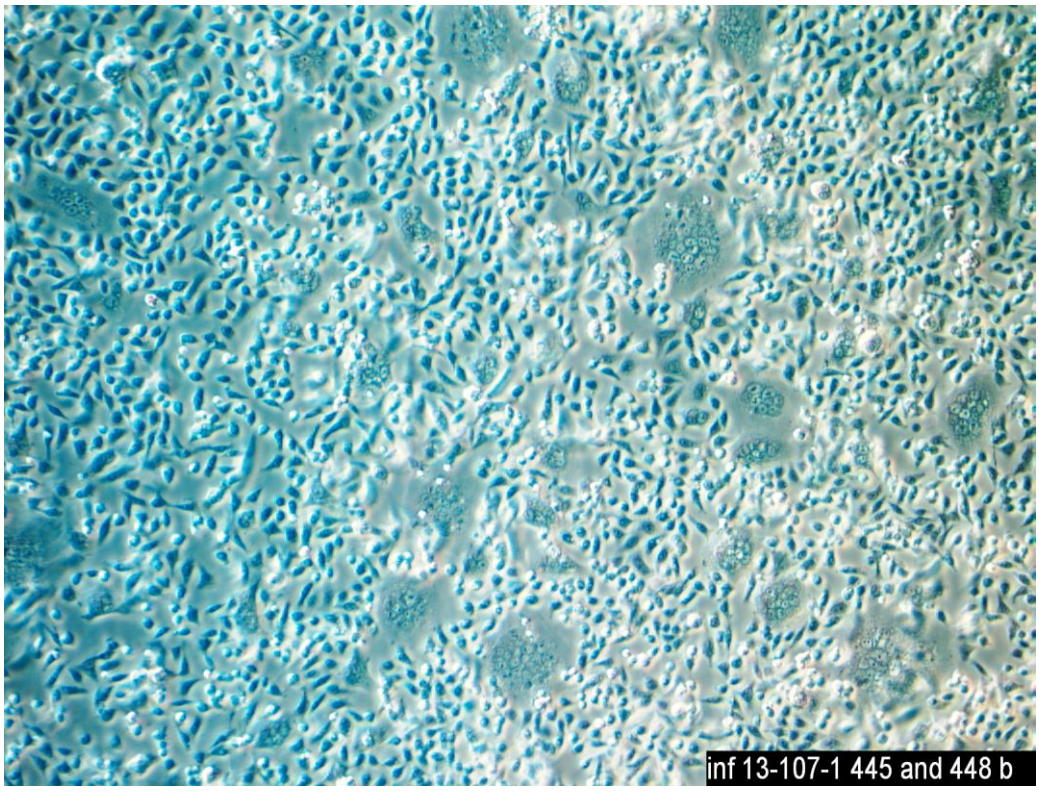

3. Measles IC_{50} experiment – Image of plates with medium colour change

Measles IC_{50} experiments showing that the medium in the wells containing active concentrations of the ddBCNAs become acidic (yellow), those where antiviral activity is not observed remain neutral (pink). The control compounds to not change the pH/colour of the cell medium.

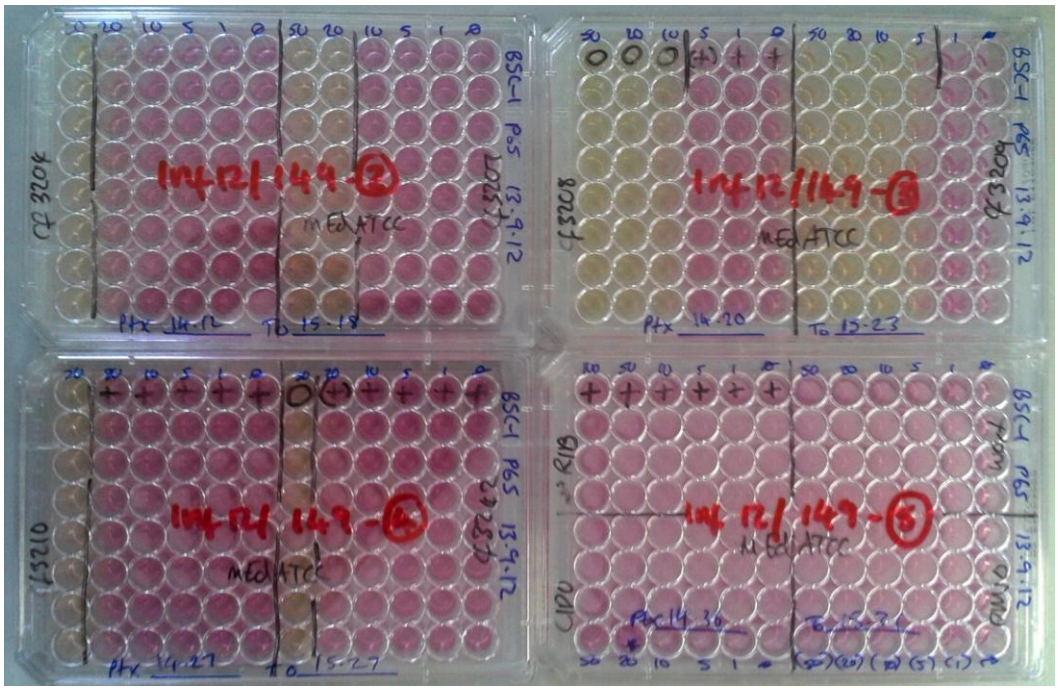

4. Cf2642 activity against measles in BJAB cells

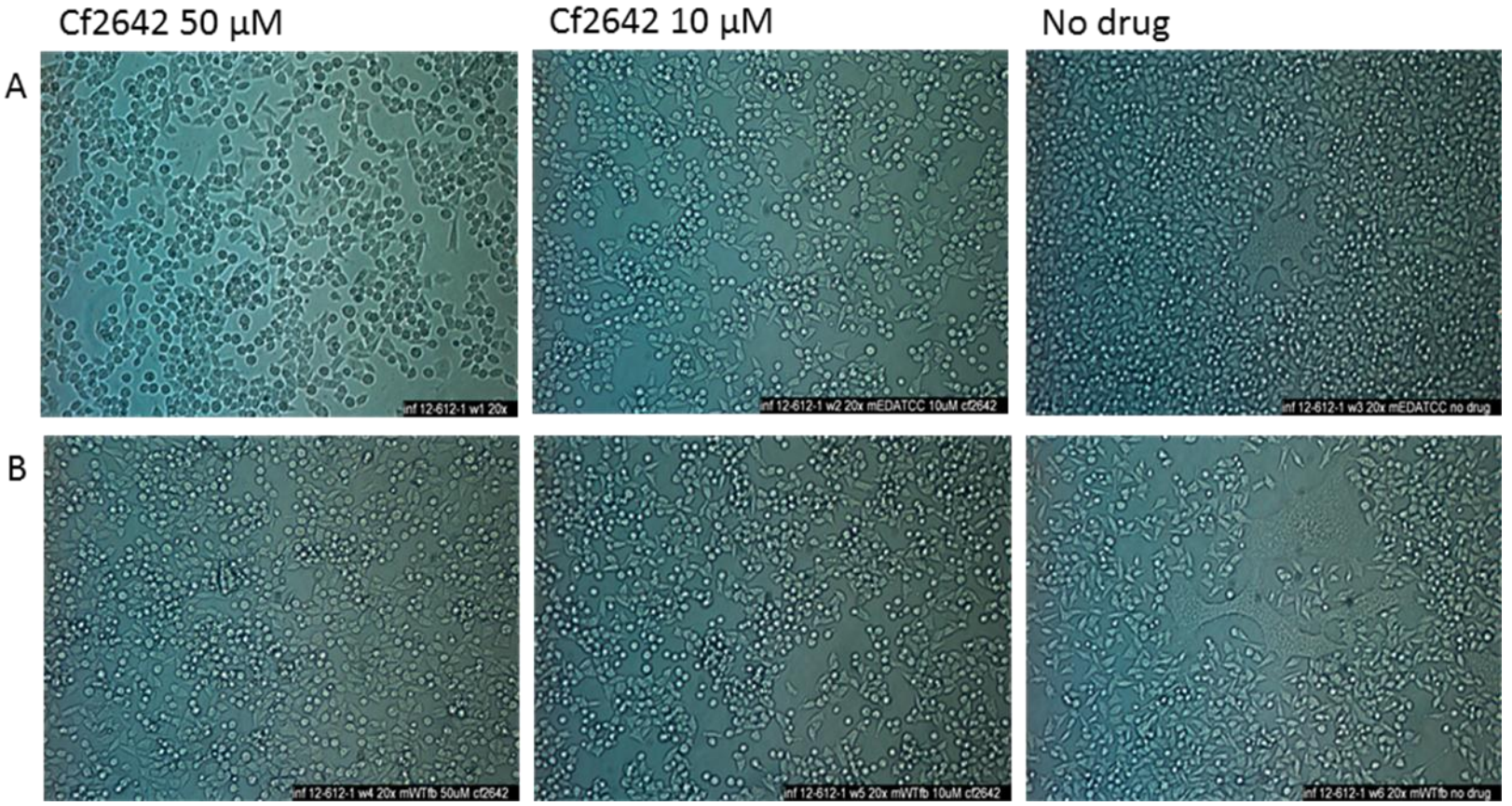

A: mEdATCC, B: mWT Fb

List of publications and presentations

Publications

MCGUIGAN, C., HINSINGER, K., **FARLEIGH, L**., PATHIRANA, R. N. & BUGERT, J. J. 2013. Novel Antiviral Activity of L-Dideoxy Bicyclic Nucleoside Analogues versus Vaccinia and Measles Viruses in Vitro. *Journal of Medicinal Chemistry,* 56**,** 1311-1322.

SHERWANI, S., BLYTHE, N., **FARLEIGH, L**. & BUGERT, J. J. 2012. New method for the assessment of molluscum contagiosum virus infectivity. *Methods in molecular biology (Clifton, N.J.),* 890**,** 135-46.

SHERWANI, S., **FARLEIGH, L**., AGARWAL, N., LOVELESS, S., ROBERTSON, N., HADASCHIK, E., SCHNITZLER, P. & BUGERT, J. J. 2014. Seroprevalence of Molluscum contagiosum Virus in German and UK Populations. *Plos One,* 9**,** 11.

Patent application

MCGUIGAN, C., BUGERT, J. J., JONES, A. T., PATHIRANA, R. & **FARLEIGH, L. E**. 2013. *Chemical compounds*.

Oral presentations

14.10.13 - Infection and Immunity Seminar, Institute of Infection and Immunity, Cardiff University School of Medicine, Cardiff, UK.

11.12.13 – Annual Symposium for translational infection research in Wales, The Liberty Stadium, Swansea

Poster Presentations

Laura Farleigh, Karen Hinsinger, Ranjith Pathirana, Arwyn T. Jones, Christopher McGuigan , and Joachim J. Bugert (12.09.12). Novel antiviral activity of L-ddBCNA versus vaccinia and measles viruses. Cardiff Institute of Infection and Immunity Annual Meeting 2012, Cardiff University, UK.

Laura Farleigh, Karen Hinsinger, Ranjith Pathirana, Arwyn T. Jones, Christopher McGuigan , and Joachim J. Bugert (21.09.12). Novel antiviral activity of L-ddBCNA versus vaccinia and measles viruses. MITReG: Interdisciplinary Postgraduate Research Day, Viriamu Jones Gallery, Cardiff University, UK.

Journal of Medicinal Chemistry

Article

pubs.acs.org/jmc

Novel Antiviral Activity of L-Dideoxy Bicyclic Nucleoside Analogues versus Vaccinia and Measles Viruses in Vitro

Christopher McGuigan,[†] Karen Hinsinger,[†] Laura Farleigh,[‡] Ranjith N. Pathirana,[†,§] and Joachim J. Bugert*[,‡]

[†]Cardiff School of Pharmacy & Pharmaceutical Sciences, Cardiff University, Redwood Building, King Edward VII Avenue, Cardiff, CF10 3NB, U.K.

[‡]Cardiff Institute of Infection and Immunity/Medical Microbiology and Infectious Diseases, School of Medicine, Cardiff University, Heath Park, Cardiff, CF14 4XN, U.K.

[§]Department of Chemistry, University of Ruhuna, Matara, Sri Lanka

ABSTRACT: Dideoxy bicyclic pyrimidine nucleoside analogues (ddBCNAs) with D-chirality have previously been described by us to inhibit replication of human cytomegalovirus. We herein report for the first time that activity against vaccinia virus (VACV) was achieved using novel L-analogues. A structure−activity relationship was established: Antiviral activity versus VACV was highest with an ether side chain with an optimum of n-C_9H_{18}−O−n-C_5H_{11}. This gave an IC_{50} of 190 nM, a 60-fold enhancement over the FDA-approved antiviral cidofovir. Interestingly, L-ddBCNAs also inhibit wild type measles virus syncytia formation with a $TCID_{50}$ of 7.5 μM for the lead compound. We propose that L-ddBCNAs represent significant innovative antiviral candidates versus measles and poxviruses, and we suggest a mechanism of action versus one or more cellular targets that are essential for viral replication.

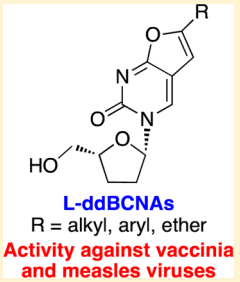

INTRODUCTION

Small pox variola was declared eradicated in 1979. However, threats of bioterrorism have reignited interest in finding suitable treatments that could be used in case of a small pox outbreak.[1] At present, the only drug that has been approved for treatment of poxviruses is cidofovir.[2] This drug is not ideal, as it has severe side effects. Vaccinia virus (VACV) is a convenient surrogate poxvirus for the development of new antipoxviral agents in vitro; VACV strains that are resistant to cidofovir have also been described.[3] Alternative treatments would also be useful for related infections with molluscum contagiosum virus[4] and human monkey pox virus.[5]

A number of new potential antipoxviral agents have recently been reported. These include ST-246, a molecule that targets the F13L protein of the virus,[6] although resistance to this drug has already been described,[7] and terameprocol, which reduces the spread of the virus by inhibiting the formation of actin tails at the surface of infected cells (cellular target).[8]

Human measles is usually a mild childhood infection but is a known cause of severe pneumonia in developing countries with over 1 million fatalities worldwide in 2005. The live measles vaccine is not given to infants under 12 months of age and maternal measles virus antibodies are lost at 4−9 months, so individuals are susceptible to the virus before the vaccination is given.[9] The ideal antiviral therapy for measles would be a small molecule inhibitor that is safe, effective, inexpensive to produce, and stable. Having a host target may offer the additional benefit of reducing the emergence of rapid resistance. Ribavirin inhibits measles virus in vitro only at supraphysiological levels (IC_{50} = 1160 μM), but it is not effective for the treatment of measles virus infections.[10] At present there are no measles antiviral drugs on the market.

Previously, we have reported novel potent and selective inhibitors of human cytomegalovirus based on D-dideoxy bicyclic furanopyrimidine nucleoside analogues (D-ddBCNAs) bearing alkyl side chains at the C5-position, with action suggested early in the virus lifecycle.[11] Further potency of D-ddBCNAs versus VACV[12] suggested a non-virus-specific mechanism of action and possibly a cellular target.

In order to further increase potency and explore the structure−activity relationships (SARs), we were interested in other unusual sugars and particularly in unnatural L-configuration nucleosides. Indeed, several L-nucleosides have emerged as potent antiviral agents,[13,14] which include β-L-[2-(hydroxymethyl)-1,3-oxathiolan-4-yl]cytosine (lamivudine, 3TC),[15] 5-fluoro-β-L-2′,3′-dideoxy-3′-thiacytidine (emtricitabine, FTC),[16] 5-fluoro-β-L-2′,3′-dideoxycytidine (L-FddC),[17] β-L-2′-fluoro-5-methylarabinofuranosyluracil (clevudine, L-FMAU),[18] 2′,3′-dideoxy-2′,3′-didehydro-β-L-5-fluorocytidine (elvucitabine, β-L-Fd4C),[19] and carbocyclic nucleoside L-Cd4U.[20] Moreover, it has been reported that some of them have more potent antiviral activity than their D-enantiomers with reduced toxicity.[21,22]

Therefore, it was of particular interest to synthesize and study the antiviral activity of L-dideoxy bicyclic furanopyrimidine nucleoside analogues (L-ddBCNAs) with different side chains.

Received: December 3, 2012
Published: January 15, 2013

dx.doi.org/10.1021/jm301778x | J. Med. Chem. 2013, 56, 1311−1322

RESULTS AND DISCUSSION

Chemistry. We previously presented the successful synthesis of different D-BCNAs.[11,23−26] For the D-dideoxy family, the bicyclic nucleosides were obtained from the key synthon D-5-iodo-2′,3′-dideoxyuridine (D-IddU) via Sonogashira reaction with different acetylenes followed by an intramolecular cyclization.[11] The described formation of the D-IddU started from the D-2′-deoxyuridine. We wanted to apply our methodology for the synthesis of the L-ddBCNAs. However, the L-2′-deoxyuridine is not commercially available. Thus, we sought a new route, illustrated in Scheme 1, starting from L-arabinose **1**.

Scheme 1. Synthetic Route to Target L-ddBCNAs[a]

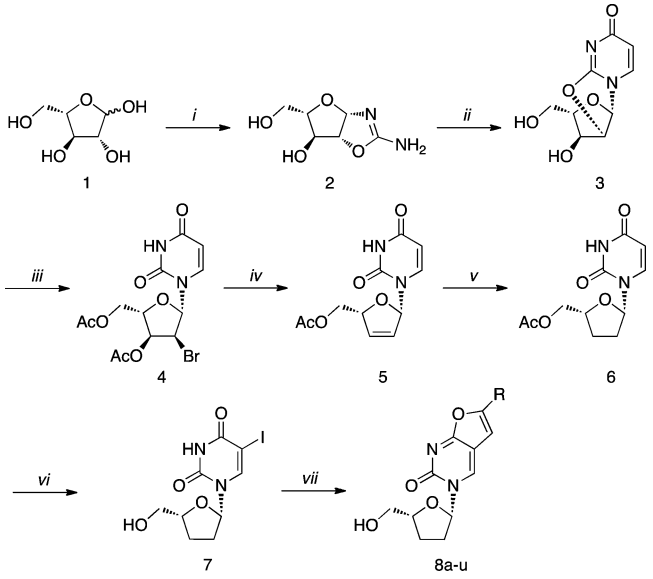

[a](i) NC−NH_2, NH_4OH, MeOH, rt, 3 days (70%); (ii) methyl propiolate, EtOH, reflux, 3 h (69%); (iii) AcBr, CH_3CN, reflux, 2 h (75%); (iv) Zn, glacial AcOH, EtOH, reflux, 2 h (53%); (v) H_2, Pd/C, MeOH, rt, 18 h (97%); (vi) (1) I_2, CAN, CH_3CN, reflux, 6 h, (2) MeONa, MeOH, rt, 18 h (60% over two steps); (vii) acetylenes, $Pd(PPh_3)_4$, CuI, DIPEA, DMF, rt, 18 h and then addition of Et_3N, CuI, 80 °C, 8 h (7−53%).

First, reaction of the carbohydrate **1** with cyanamide, according to the methodology reported by Ladurée et al.,[27] afforded the corresponding bicyclic oxazoline **2**. Treatment with methyl propiolate in methanol yielded the 2,2′-anhydronucleoside **3** which via a bromoacetylation reaction[28] with acetyl bromide in acetonitrile gave the nucleoside **4** in good yield. Reductive β-elimination with activated zinc powder in the presence of glacial acetic acid[29] afforded the 5′-*O*-acetyl-2′,3′-didehydro-2′,3′-dideoxyuridine **5**, which gave almost quantitatively the dideoxy nucleoside **6** upon catalytic hydrogenation. The L-5-iodo-2′,3′-dideoxyuridine **7** was obtained after first iodination at the C5-position of the base with iodine in the presence of ammonium cerium(IV) nitrate (CAN)[30] and then deacetylation using sodium methoxide, in 60% yield over two steps. Palladium-catalyzed Sonogashira coupling of the key synthon **7** with a series of acetylenes gave the corresponding 5-alkynyl nucleosides. Addition of copper(I) iodide in situ with heating of the reaction resulted in their intramolecular cyclization to afford the desired furanopyrimidine compounds **8a−u** with alkyl, aryl, or ether side chains. Indeed, we have reported in the case of D-deoxy BCNAs that aryl and ether groups decrease the lipophilicity of nucleosides and improve their activity.[24,26]

The alkyl- and arylacetylenes needed for the Sonogashira reaction were commercially available. However, the ether alkynes were synthesized following two different pathways depending on the target ethers (Scheme 2). The first method

Scheme 2. Synthetic Routes to Alkynyl Ethers 10a−j and 12a,b[a]

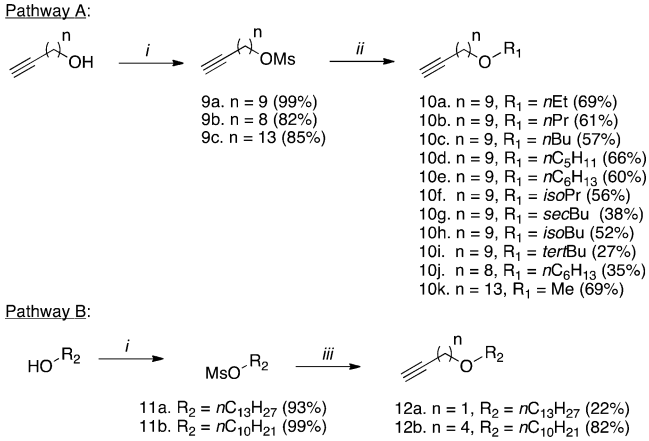

[a](i) MsCl, Et_3N, THF, rt, 18 h; (ii) alcohol, NaH, THF, 70 °C, 24 h; (iii) alkynol, NaH, THF, 60 °C, 36 h.

(pathway A) started with the mesylation of alkyn-1-ols to obtain the intermediates **9a−c**, which were then coupled with different alcohols to give the ethers **10a−j**. In the second method (pathway B), the starting materials were alcohols, which were first transformed into the mesylated compounds **11a** and **11b** and then reacted with selected alkynols to obtain the ethers **12a** and **12b**.

The structure and the purity of all L-ddBCNAs were confirmed by spectroscopic, chromotographic, and analytical data before they were tested for inhibition of viral infections.

Antiviral Activity. The L-ddBCNAs **8a−u** were evaluated by luciferase assay for their ability to inhibit the early stages of VACV replication from entry to early gene transcription in RK 13 cells (Table 1), following the initial notion of an effect early in the viral lifecycle.[11]

Luciferase inhibition was observed in compounds **8a−h** bearing alkyl and aryl chains, with an optimum at the analogue **8d** (n-C_9H_{19} chain). The apparent reduction in activity for longer alkyl chain derivatives **8e** (n-$C_{10}H_{21}$ chain) and **8f** (n-$C_{12}H_{25}$ chain) may be caused by their low water solubility (clogP data of 4.72 and 5.77). This led to the synthesis of ether compounds with a nonyl chain prior to oxygen (**8i−q**). The best reduction of luciferase values was then identified among the L-ddBCNAs **8j−m** with linear ether side chains, and a SAR regarding the length of the chain emerged; the best activity was found for compounds **8k** and **8l** with butyl and pentyl termini. Using the length of the side chain in **8l**, alteration of the oxygen atom position toward the base (analogues **8r−u**) did not improve the activity. However, the good luciferase values of derivatives **8r** (n-C_8H_{16}−O−n-C_6H_{13} chain) and **8s** (n-C_4H_8−O−n-$C_{10}H_{21}$ chain) in spite of high calculated log P data (of 4.89) shows that the lipophilicity of compounds is only one parameter in their mechanism of action.

These results were followed up for the most potent ether compounds by plaque assay and determination of IC_{50} in BSC-

dx.doi.org/10.1021/jm301778x | J. Med. Chem. 2013, 56, 1311−1322

Table 1. L-ddBCNA Structures, clogP, and Luciferase Reporter Assay Versus VAVC

compd	R	clogP[a]	luciferase reporter[b] (%)
8a	n-C_6H_{13}	2.60	70.7
8b	n-C_7H_{15}	3.13	43.2
8c	n-C_8H_{17}	3.68	41.9
8d	n-C_9H_{19}	4.19	38.1
8e	n-$C_{10}H_{21}$	4.72	45.7
8f	n-$C_{12}H_{25}$	5.77	96.4
8g	Ph-n-Bu	3.64	43.7
8h	Ph-n-C_5H_{11}	4.17	73.6
8i	n-C_9H_{18}–O–n-Et	3.30	79.9
8j	n-C_9H_{18}–O–n-Pr	3.83	46.8
8k	n-C_9H_{18}–O–n-Bu	4.36	27.5
8l	n-C_9H_{18}–O–n-C_5H_{11}	4.89	27.7
8m	n-C_9H_{18}–O–n-C_6H_{13}	5.42	35.7
8n	n-C_9H_{18}–O–i-Pr	3.61	79.9
8o	n-C_9H_{18}–O–s-Bu	4.14	69.9
8p	n-C_9H_{18}–O–i-Bu	4.23	64.3
8q	n-C_9H_{18}–O–t-Bu	4.01	70.7
8r	n-C_8H_{16}–O–n-C_6H_{13}	4.89	37.2
8s	n-C_4H_8–O–n-$C_{10}H_{21}$	4.89	26.1
8t	CH_2–O–n-$C_{13}H_{27}$	5.46	43.9
8u	n-$C_{13}H_{26}$–O–Me	5.03	60.5
cidofovir		−2.39	94.6

[a]clogP values calculated with Chemdraw ultra 12.0. [b]Luciferase reporter activity as percent of no drug control (100%) in RK13 cells.

1 cells with data shown in Table 2. The effect of L-ddBCNAs on cell viability (CC_{50}) was tested by measuring ATP levels in live BSC-1 cells (CellTiter-Glo Luminescent Cell Viability Assay).

Table 2. IC_{50} and CC_{50} Data Versus VACV of Selected Ether L-BCNAs

compd	R	IC_{50}[a] (μM)	CC_{50}[a] (μM)	CC_{50}[b] (μM)
8i	n-C_9H_{18}–O–n-Et	12.9	79.4	>100
8j	n-C_9H_{18}–O–n-Pr	1.9	89.1	>100
8k	n-C_9H_{18}–O–n-Bu	1.8	>100	>100
8l	n-C_9H_{18}–O–n-C_5H_{11}	0.19	>100	>100
8m	n-C_9H_{18}–O–n-C_6H_{13}	0.19	74.1	>100
8r	n-C_8H_{16}–O–n-C_6H_{13}	1.7	–	–
8s	n-C_4H_8–O–n-$C_{10}H_{21}$	2.2	–	–
8t	CH_2–O–n-$C_{13}H_{27}$	3.4	–	–
cidofovir		11.5	>100	>100

[a]In BSC-1 cells. [b]In HFFF cells.

The IC_{50} values from 4 day plaque assays of ethers with increasing chains (compounds **8i–m**) followed a similar SAR to that identified for the 2 h luciferase activity data. Both assays showed the same trend, perhaps implying the same mechanism of action. The 2 h luciferase assay was used as a predictor of compound efficacy. Moreover, all L-ddBCNAs with the exception of **8i** performed better than the cidofovir control. The IC_{50} of nucleosides **8l** and **8m** of 0.19 μM is a 60-fold improvement of activity.

The ether series L-ddBCNAs have a mild effect on BSC-1 cell viability with a selectivity index of >500 for the lead compound **8l** (IC_{50} = 0.19 μM and CC_{50} > 100 μM). BSC-1 cells did not show visible cytotoxicity in phase contrast microscopy after 2 h in the luciferase reporter assays or after 4 days at CC_{50} in the plaque reduction assays. The mild toxicity observed in BSC-1 cells for some compounds does not follow the SAR of the ether series L-ddBCNAs and is not predictive of antiviral activity. No cytotoxic effects of L-ddBCNAs **8i–m** were observed in HFFF cells up to 100 μM.

The lead bicyclic nucleoside **8l** was then evaluated by $TCID_{50}$ assay for its ability to inhibit formation of cytopathogenic effect of adenovirus, herpesvirus (types 1 and 2), and vaccine and wild type measles viruses (Table 3).

Table 3. $TCID_{50}$ (μM) of Compound 8l versus Other Viruses

	HFFF	BSC-1	B95a
adenovirus 5	>50	>50	nd
HSV 1 NCPV 17+	>50	>50	nd
HSV 2 NCPV 132349	>50	>50	nd
measles virus Edmonston (vaccine)	nd[a]	>50	>50
measles virus wild type *mWTFb*	nd[a]	nd[a]	7.5

[a]Cells not susceptible. nd: not determined.

Nucleoside **8l** was unable to suppress the cytopathogenic effects of adeno, herpes simplex, and measles vaccine viruses in BSC-1 and HFFF cells. However, it inhibits wild type measles virus syncytia formation by 50% at 7.5 μM. This is a 150-fold improvement over ribavirin in vitro (IC_{50} of 1160 μM;[10] Figure 1). When L-ddBCNAs **8i–m** of the ether series were tested

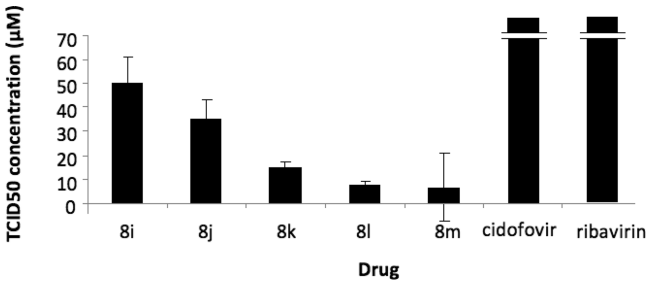

Figure 1. SAR of ether series of L-ddBCNAs versus wild type measles virus.

versus wild type measles virus in B95a cells (Figure 1), the SAR was found to follow closely the one found previously for VACV in RK13 (luciferase assay) and BSC-1 (plaque assay) cells. Cidofovir, a DNA polymerase inhibitor active against VACV, shows no effect in this assay, as expected. The ribavirin IC_{50} (1.2 mM, data not shown) is out of the range of this figure. Wortmannin, a furanosteroid inhibitor of PI3 like kinases,[31] inhibited measles wild type virus in this assay with an IC_{50} of 75 μM. (data not shown).

The SAR observed versus both vaccinia and wild type measles viruses is highly suggestive of a drug interaction with a specific target. While measles wild type viruses are only able to utilize the CD150 receptor found on human and simian B cells, the vaccine strain of measles virus uses the ubiquitous CD46 receptor. CD150 and CD46 receptors are located in different membrane microdomains, so a differential effect of L-ddBCNAs is possible. Membrane microdomains are involved in both measles and vaccinia virus replication.[32,33]

Is it possible that the reduction of VACV plaque size herein observed could be due to an effect on the dissemination of VACV in cell culture via the "conveyor belt".[34]

The phenolic antioxidant terameprocol[8] shows a similar activity profile to L-ddBCNAs, where the target of the antiviral

dx.doi.org/10.1021/jm301778x | J. Med. Chem. 2013, 56, 1311–1322

activity is the actin-cytoskeleton, clearly a cellular target. The main effect is a quantifiable reduction in plaque size, just as observed with the L-ddBCNAs. With a cellular target of this nature, viral infection in the host would not be completely shut down, but rather, the dissemination of the virus would be affected. Inhibiting specific aspects of a virus lifecycle induces the virus to develop resistance to the drug by altering the target of the drug. Targeting cellular processes means that there may be a possibility of increased toxicity but reduction in the opportunity for resistance. Antivirals versus cellular targets are not subject to viral resistance, which may develop quickly with all virus-targeting drugs.

CONCLUSION

In summary, we have described the successful synthesis of substituted L-dideoxy bicyclic furanopyrimidine nucleoside analogues in eight steps starting from L-arabinose.

A series of ether-substituted compounds has been shown to induce suppression of orthopox and measles virus replication in vitro. Actually, early (2 h p.i.) luciferase reporter assays against VACV and plaque/syncytium reduction assays against VACV and measles virus highlighted a SAR regarding the length of the chain. Notably, the lead L-ddBCNA **8l** with n-C_9H_{18}−O−n-C_5H_{11} side chain possessed an IC_{50} value of 0.19 μM against VACV, with good selectivity index, and a $TCID_{50}$ value of 7.5 μM against measles virus.

We propose that interactions between L-ddBCNAs and membrane microdomains are involved in the inhibition of virus replication. This kind of host targeting action would prevent drug resistance issues. Further studies about the mechanism of action of L-ddBCNAs are currently under investigation in our laboratory.

EXPERIMENTAL SECTION

Chemistry. The numbering of the bicyclic ring follows the recommended IUPAC nomenclature guidelines. The naming of the compounds follows IUPAC nomenclature and/or standard accepted nomenclature for nucleoside chemistry.

All solvents used were anhydrous and used as supplied by Aldrich. All nucleosides and solid reagents were dried for several hours under high vacuum over potassium hydroxide. All glassware was oven-dried at 130 °C for several hours or overnight and allowed to cool in a desiccator or under a stream of dry nitrogen. TLC was performed on precoated aluminum-backed plates (60 F-54, 0.2 mm thickness; supplied by E. Merck AG, Darmstadt, Germany) and spots visualized by UV (at 254 or 336 nm depending on the compound). Column chromatography was performed with silica gel supplied by Fisher (60A, 35−70 μm). ^{1}H and ^{13}C NMR spectra were recorded in a Bruker spectrometer (500 and 125 MHz, respectively) and autocalibrated to the deuterated solvent reference peak. All ^{13}C NMR spectra were proton-decoupled. Coupling constants (J) are measured in Hertz. The following abbreviations are used in the assignment of NMR signals: br (broad), s (singlet), d (doublet), t (triplet), q (quartet), m (multiplet), dd (doublet of doublet), ddd (doublet of doublet of doublet), dt (doublet of triplet). Low-resolution and accurate mass analysis were performed by the service at the Department of Chemistry, University of Wales, Cardiff, U.K., with electrospray (ES). The ≥95% purity of all the final compounds was confirmed using analytical HPLC analysis. HPLC experiments were done on a Thermo Fisher Scientific Spectra System SCM1000 provided with a System Controller SN4000, a pump Spectra System P4000, and a Spectra UV2000 detector set (detection at 254 nm) and using a 5 μM Hypersil GOLD (150 × 4.6 mm) reverse phase column eluting with the indicated mobile phase with a flow rate of 1 mL/min.

*2-Amino-[1,2-d]arabinosyloxazole (**2**).* A suspension of L-arabinose **1** (17 g, 113 mmol), cyanamide (10 g, 238 mmol, 2.1 equiv) in anhydrous MeOH (30 mL), and 6 M NH_4OH (5 mL) was stirred at room temperature for 65 h. The solvents were then evaporated from the resulting suspension under reduced pressure. The crude was triturated with MeOH to give a white solid (13.16 g, 66%). ^{1}H NMR (500 MHz, DMSO-d_6): δ 6.27 (2H, br s, NH_2), 5.67 (1H, d, J = 5.5 Hz, H-1′), 5.39 (1H, br s, OH-3′), 4.68 (1H, bs, OH-5′), 4.53 (1H, d, J = 5.5 Hz, H-2′), 4.02−3.99 (1H, m, H-3′), 3.67−3.62 (1H, m, H-4′), 3.31−3.23 (2H, m, H-5′). ^{13}C NMR (125 MHz, DMSO-d_6): δ 162.18 (C-2), 99.95 (C-1′), 88.04 (C-2′), 84.58 (C-4′), 75.62 (C-3′), 6.55 (C-5′).

*2,2′-Anhydrouridine (**3**).* A solution of 2-amino-[1,2-d]-arabinosyloxazole (**2**) (24.0 g, 137.81 mmol) and methyl propiolate (23 mL, 275.62 mmol, 2 equiv) in 50% aqueous ethanol solution (350 mL) was refluxed for 2 h. The solvent was removed under reduced pressure to obtain a residue that was dissolved in acetone (400 mL) and left at 0 °C overnight. The resulting precipitate was filtered and washed with acetone to obtain a white solid (23.06 g, 74%). ^{1}H NMR (500 MHz, DMSO-d_6): δ 7.83 (1H, d, J = 7.4 Hz, H-5), 6.31 (1H, d, J = 5.8 Hz, H-1′), 5.87 (1H, d, J = 4.3 Hz, OH-3′), 5.84 (1H, d, J = 7.4 Hz, H-6), 5.20 (1H, d, J = 5.5 Hz, H-2′), 4.97 (1H, t, J = 5.0 Hz, OH-5′), 4.41−4.37 (1H, m, H-3′), 4.08 (1H, t, J = 4.1 Hz, H-4′), 3.31−3.25 (1H, m, H-5′), 3.23−3.16 (1H, m, H-5′). ^{13}C NMR (125 MHz, DMSO-d_6): δ 171.10 (C-4), 159.77 (C-2), 136.77 (C-5), 108.59 (C-6), 89.97 (C-1′), 89.16 (C-4′), 88.71 (C-2′), 74.71 (C-3′), 60.81 (C-5′).

*5′,3′-Diacetyl-2′-bromo-2′-deoxyuridine (**4**).* 2,2′-Anhydrouridine (**3**) (22.0 g, 97.26 mmol) was suspended in CH_3CN (400 mL) and heated under reflux. Acetyl bromide (64.7 mL, 875.37 mmol, 9 equiv) was added dropwise. The mixture was stirred at reflux for 2 h. The solvent was removed under reduced pressure, and the residue obtained was dissolved in dichloromethane (400 mL), washed with a solution, dried over $MgSO_4$, and evaporated to obtain the title compound as a brown oil (33.0 g, 87%). ^{1}H NMR (500 MHz, $CDCl_3$): δ 8.99 (1H, s, NH), 7.45 (1H, d, J = 8.4 Hz, H-6), 6.22 (1H, d, J = 5.21 Hz, H-1′), 5.82 (1H, dd, J = 7.4 Hz, 1.57 Hz, H-5), 5.16 (1H, t, J = 5.04 Hz, H-3′), 4.61 (1H, t, J = 5.6 Hz, H-2′), 4.46−4.41 (1H, m, H-4′), 4.42−4.36 (1H, m, H-5′), 3.31−3.25 (1H, m, H-5′), 2.22 (3H, s, CH_3), 2.16 (3H, s, CH_3). ^{13}C NMR (125 MHz, $CDCl_3$): δ 171.04 (CO), 169.69 (CO), 162.50 (C-4), 149.93 (C-2), 138.92 (C-5), 103.29 (C-6), 91.01 (C-1′), 80.11 (C-4′), 70.76 (C-3′), 62.55 (C-5′), 48.41 (C-2′), 20.78 (CH_3), 20.61 (CH_3). MS (ES^+) m/z 413−415 (M + Na^+).

*5′-Acetyl-2′,3′-dideoxy-2′,3′-dehydrouridine (**5**).* Glacial acetic acid (1.5 mL, 26.20 mmol, 1.6 equiv) was added dropwise at 0 °C to a stirred suspension of zinc (4.20 g, 64.23 mmol, 4 equiv) and 5′,3′-diacetyl-2′-bromo-2′-deoxyuridine **4** (6.2 g, 15.85 mmol) in ethanol (195 mL). The resulting mixture was stirred at room temperature until the TLC (3% methanol in ethyl acetate) showed that the starting material had completely reacted. The mixture was filtered through a sintered funnel packed with Celite to remove zinc, and triethylamine (1.4 mL) was added to the filtrate. The solvent was removed under reduced pressure and the residue obtained was extracted with ethyl acetate (250 mL). Removal of solvent under reduced pressure gave a brown oil which was purified by column chromatography (1% methanol in ethyl acetate) to afford the title compound as a yellow oil (2.24 g, 53%). ^{1}H NMR (500 MHz, DMSO-d_6): δ 11.37 (1H, br s, NH), 7.44 (1H, d, J = 8.1 Hz, H-6), 6.79 (1H, m, H-1′), 6.42 (1H, dt, J = 6.1 Hz, 1.7 Hz, H-3′), 6.00 (1H, ddd, J = 6.1 Hz, 2.3 Hz, 1.3 Hz, H-2′), 5.66 (1H, d, J = 8.1 Hz, H-5), 4.97 (1H, m, H-4′), 4.17 (2H, d, J = 3.4 Hz, H-5′), 2.00 (3H, s, CH_3). ^{13}C NMR (125 MHz, DMSO-d_6): δ 170.07 (CO), 163.09 (C-4), 150.72 (C-2), 140.52 (C-6), 133.85 (C-3′), 126.37 (C-2′), 101.90 (C-5), 89.34 (C-1′), 83.80 (C-4′), 64.48 (C-5′), 20.56 (CH_3). MS (ES^+) m/z 275 (M + Na^+).

*5′-Acetyl-2′,3′-dideoxyuridine (**6**).* To a solution of 5′-acetyl-2′,3-dideoxy-2′,3′-dehydrouridine (**5**) (4.88 g, 19.34 mmol) in anhydrous methanol (80 mL) was added 10% Pd on carbon (0.23 g, 5% wt). The mixture was stirred under a hydrogen atmosphere for 6 h. The reaction was monitored by NMR analysis. The mixture was then filtered through a Celite pad. The solvent was removed under reduced pressure to afford the title compound as a pale brown oil (5.0 g, 99%). ^{1}H NMR (500 MHz, DMSO-d_6): δ 11.27 (1H, br s, NH), 7.66 (1H, d,

J = 8.0 Hz, H-6), 5.98 (1H, dd, J = 7.2 Hz, 3.8 Hz, H-1′), 5.64 (1H, d, J = 8.0 Hz, H-5), 4.21−4.18 (3H, m, H-5′, H-4′), 2.34−2.22 (1H, m, H-2′), 2.06−1.95 (5H, m, H-2′, H-3′, CH_3), 1.81−1.72 (1H, m, H-3′). ^{13}C NMR (125 MHz, DMSO-d_6): δ 170.21 (CO), 163.08 (C-4), 150.48 (C-2), 140.43 (C-6), 101.51 (C-5), 85.24 (C-1′), 77.95 (C-4′), 64.88 (C-5′), 30.8 (C-2′), 25.56 (C-3′), 20.60 (CH_3). MS (ES^+) m/z 277 (M + Na^+).

*L-5-Iodo-2′,3′-dideoxyuridine (**7**).* To a solution of 5′-acetyl-2′,3′-dideoxyuridine (**6**) (2.00 g, 7.86 mmol) in anhydrous acetonitrile (8 mL) were added I_2 (1.20 g, 4.72 mmol, 0.6 equiv) and CAN (2.16 g, 3.94 mmol, 0.5 equiv). The mixture was stirred at reflux for 3 h (progress of the reaction was monitored by TLC using 1% methanol in ethyl acetate as the eluent). The solvent was removed under reduced pressure and the residue was dissolved in dichloromethane (300 mL) and washed with a saturated solution of sodium bicarbonate. The two phases were separated, and the organic layer was dried over sodium sulfate and evaporated under reduced pressure to obtain the 5′-acetyl-2′,3′-dideoxy-5-iodouridine intermediate as a brown solid. This residue was dissolved in MeOH (60 mL), and MeONa (0.63 g, 11.66 mmol, 1.5 equiv) was added. The solution was stirred for 21 h. As the reaction was not complete, an additional amount of MeONa (0.21 g, 3.88 mmol, 0.5 equiv) was added, and the resulting mixture was stirred for further 1 h. Amberlite IR 120 was then added until the pH of the solution became 6.0 and the mixture was filtered. The solution was evaporated and the solid was washed with diethyl ether to yield the title compound (off-white solid, 1.57 g, 60%). ^{1}H NMR (500 MHz, DMSO-d_6): δ 11.27 (1H, br s, NH), 8.57 (1H, s, H-6), 5.87 (1H, dd, J = 6.6 Hz, 2.8 Hz, H-1′), 5.22 (1H, t, J = 5.0 Hz, OH), 4.05 (1H, m, H-4′), 4.72−4.53 (2H, m, H-5′), 2.26−1.83 (4H, m, H-2′, H3′). ^{13}C NMR (125 MHz, DMSO-d_6): δ 160.59 (C-4), 150.05 (C-2), 145.19 (C-6), 85.83 (C-1′), 82.10 (C-4′), 68.11 (C-5), 61.20 (C-5′), 32.45 (C-2′), 23.93 (C-3′). Reverse HPLC eluting with H_2O/MeOH (gradient from 90:10 to 0:100 in 30 min): t_R = 08.96 min.

General Procedure A: Formation of Mesylates (9a−c and 11a,b). To a stirred solution of alcohol in THF (0.7 mL/mmol) was added triethylamine (1.3 equiv) and methanesulfonyl chloride (1.3 equiv) dropwise at 0 °C under a nitrogen atmosphere. The reaction was left stirring for 18 h at room temperature. The solvent was evaporated; water was added to the reaction mixture and then extracted with dichloromethane. The organic layer was dried over sodium sulfate, filtered, and evaporated under reduced pressure to obtain the desired product.

*10-Undecynyl Mesylate (**9a**).* Procedure A was carried out using 10-undecyn-1-ol (10 g, 59.42 mmol) to give the desired compound as a yellow oil (15.5 g, 100%). ^{1}H NMR (500 MHz, $CDCl_3$): δ 4.26 (2H, t, J = 7.1 Hz, OCH_2), 3.05 (3H, s, CH_3), 2.20 (2H, dt, J = 7.1 Hz, 2.6 Hz, α-CH_2), 1.97 (H, t, J = 2.5 Hz, HC≡C), 1.60−1.28 (14H, m, 7 × CH_2).

*9-Decynyl Mesylate (**9b**).* Procedure A was carried out using 9-decyn-1-ol (2.50 g, 16.21 mmol) to give the desired compound as a yellow oil (3.10 g, 82%). ^{1}H NMR (500 MHz, $CDCl_3$): δ 4.24 (2H, t, J = 6.6 Hz, OCH_2), 3.02 (3H, s, CH_3), 2.01 (2H, dt, J = 7.1 Hz, J = 2.6 Hz, α-CH_2), 1.96 (1H, t, J = 2.6 Hz, HC≡C), 1.58−1.31 (12H, m, 6 × CH_2). ^{13}C NMR (125 MHz, $CDCl_3$): δ 84.64 (HC≡C), 70.13 (OCH_2), 68.19 (HC≡C), 37.39 (CH_3), 29.13, 2 × 28.89 (double intensity), 28.57, 28.39, 25.38 (6 × CH_2), 18.38 (α-CH_2).

*14-Pentadecynyl Mesylate (**9c**).* Procedure A was carried out using 14-pentadecyn-1-ol[30] (1.80 g, 8.022 mmol) to give the desired compound as a pale brown oil (2.07 g, 85%). ^{1}H NMR (500 MHz, $CDCl_3$): δ 4.24 (2H, t, J = 6.1 Hz, OCH_2), 3.01 (3H, s, CH_3), 2.20 (2H, dt, J = 7.1 Hz, 2.7 Hz, HC≡CCH_2), 1.95 (1H, t, J = 2.7 Hz, HC≡C), 1.76 (2H, m, CH_2), 1.56 (2H, m, CH_2), 1.43 (2H, m, CH_2), 1.40−1.23 (16H, m, 8 × CH_2). ^{13}C NMR (125 MHz, $CDCl_3$): δ 84.79 (HC≡C), 70.18 (OCH_2), 68.03 (HC≡C), 37.65 (CH_3), 29.59, 29.55, 29.47, 29.40, 29.13, 29.09, 28.89, 28.85, 28.74, 28.49, 25.73 (11 × CH_2), 18.63 (C≡CCH_2).

*Tridecyl Mesylate (**11a**).* Procedure A was carried out using 1-tridecanol (5.00 g, 24.95 mmol) to give the desired compound as a pale brown oil (6.39 g, 93%). ^{1}H NMR (500 MHz, $CDCl_3$): δ 4.25 (2H, t, J = 6.6 Hz, OCH_2), 3.03 (3H, s, CH_3), 1.76 (2H, m, OCH_2CH_2), 1.47−1.23 (20H, m, 10 × CH_2), 0.91 (3H, t, J = 7.0 Hz, CH_3). ^{13}C NMR (125 MHz, $CDCl_3$): δ 70.19 (OCH_2), 37.38 (CH_3), 31.91, 29.64, 29.62, 29.60, 29.51, 29.41, 29.34, 29.13, 29.03, 25.42 (10 × CH_2), 22.68 (CH_2CH_3), 14.10 (CH_3).

*Decyl Mesylate (**11b**).* Procedure A was carried out using 1-decanol (8.6 mL, 45 mmol) to give the desired compound as a pale brown oil (11.00 g, 100%). ^{1}H NMR (500 MHz, $CDCl_3$): δ 4.24 (2H, t, J = 6.6 Hz, OCH_2), 3.03 (3H, s, CH_3), 1.78 (2H, m, OCH_2CH_2), 1.46−1.23 (14H, m, 7 × CH_2), 0.91 (3H, t, J = 7.0 Hz, CH_3). ^{13}C NMR (125 MHz, $CDCl_3$): δ 70.19 (OCH_2), 37.38 (CH_3), 31.85, 29.46, 29.41, 29.25, 29.13, 29.02, 25.42 (7 × CH_2), 22.66 (CH_2CH_3), 14.08 (CH_3).

General Procedure B: Synthesis of Alkyloxyalkyne (10a−j and 12a,b). To a stirred solution of alcohol (1.2 equiv) in THF (2.5 mL/mmol) at 0 °C under a nitrogen atmosphere was added slowly NaH (dispersion, 60%, 1.25 equiv). After 5 min, the mesylate was added and the reaction was heated at 70 °C for 19 h. Then the solvent was removed under reduced pressure and the residue was dissolved in dichloromethane (100 mL) and washed with water (2 × 100 mL). The organic layer was dried over sodium sulfate, evaporated to dryness, and purified by column chromatography to obtain the desired compound.

*11-Ethyloxy-1-undecyne (**10a**).* Procedure B was carried out using ethanol (0.448 g, 9.735 mmol) and 10-undecynyl mesylate (**9a**) (2.04 g, 8.28 mmol). The crude product was purified by column chromatography (5% ethyl acetate in hexane) to give the product **10a** as a colorless oil (0.87 g, 69%). ^{1}H NMR (500 MHz, $CDCl_3$): δ 3.54−3.36 (4H, m, OCH_2), 2.20 (2H, m, α-CH_2), 1.95 (1H, ddd, J = 3.1 Hz, 2.2 Hz, 1.0 Hz, HC≡C), 1.64−1.27 (8H, m, 4 × CH_2), 1.21 (3H, dt, J = 7.4 Hz, 1.1 Hz, CH_3). ^{13}C NMR (125 MHz, $CDCl_3$): δ 84.76 (CH-*C*), 70.76 (OCH_2), 68.03 (*C*H−C), 66.04 (OCH_2CH_3), 29.81, 29.77, 29.43, 29.03, 28.72, 28.48, 28.25 (7 × CH_2), 18.39 (α-CH_2), 15.24 (CH_3).

*11-Propyloxy-1-undecyne (**10b**).* Procedure B was carried out using propanol (0.75 mL, 9.936 mmol) and 10-undecynyl mesylate (**9a**) (2.04 g, 8.28 mmol). The crude product was purified by column chromatography (5% ethyl acetate in hexane) to give the product **10b** as a colorless oil (1.06 g, 61%). ^{1}H NMR (500 MHz, $CDCl_3$): δ 3.50−3.36 (4H, m, 2 × OCH_2), 2.21 (2H, m, α-CH_2), 1.95 (1H, ddd, J = 3.1 Hz, 2.2 Hz, 1.0 Hz, HC≡C), 1.65−1.48 (8H, m, 4 × CH_2), 1.46−1.20 (8H, m, 4 × CH_2), 0.94 (3H, dt, J = 7.4 Hz, 1.1 Hz, CH_3). ^{13}C NMR (125 MHz, $CDCl_3$): δ 84.75 (CH-*C*), 72.55 (OCH_2), 70.94 (OCH_2), 68.01 (*C*H−C), 29.78, 29.69, 29.42, 29.03, 28.72, 28.48, 26.17, 22.94 (8 × CH_2), 18.38 (α-CH_2), 10.57 (CH_3).

*11-Butyloxy-1-undecyne (**10c**).* Procedure B was carried out using butanol (0.77 mL, 8.44 mmol) and 10-undecynyl mesylate (**9a**) (1.60 g, 6.49 mmol). The crude product was purified by column chromatography (5% ethyl acetate in hexane) to give the product **10c** as a colorless oil (0.83 g, 57%). ^{1}H NMR (500 MHz, $CDCl_3$): δ 3.47−3.38 (4H, m, 2 × OCH_2), 2.20 (2H, m, α-CH_2), 1.95 (1H, t, J = 2.6 Hz, HC≡C), 1.65−1.26 (18H, m, 9 × CH_2), 0.94 (3H, t, J = 6.5 Hz, CH_3). ^{13}C NMR (125 MHz, $CDCl_3$): δ 84.75 (HC≡C), 70.93 (OCH_2), 70.63 (OCH_2), 68.01 (HC≡C), 31.88, 29.77, 2 × 29.42 (double intensity), 29.03, 28.72, 28.48, 26.17, 19.37 (9 × CH_2), 18.38 (α-CH_2), 13.91 (CH_3).

*11-Pentyloxy-1-undecyne (**10d**).* Procedure B was carried out using pentanol (0.84 mL, 7.79 mmol) and 10-undecynyl mesylate (**9a**) (1.60 g, 6.49 mmol). The crude product was purified by column chromatography (5% ethyl acetate in hexane) to give the product **10d** as a colorless oil (1.00 g, 66%). ^{1}H NMR (500 MHz, $CDCl_3$): δ 3.48 (4H, m, 2 × OCH_2), 2.20 (2H, dt, J = 7.1 Hz, 2.7 Hz, α-CH_2), 1.95 (1H, t, J = 2.7 Hz, HC≡C), 1.67−1.22 (20H, m, 10 × CH_2), 0.92 (3H, t, J = 7.3 Hz, CH_3). ^{13}C NMR (125 MHz, $CDCl_3$): δ 84.75 (HC≡C), 70.96 (OCH_2), 70.94 (OCH_2), 68.01 (HC≡C), 31.59, 29.78, 29.49, 29.36, 29.04, 28.73, 28.49, 28.39, 26.17, 22.65 (10 × CH_2) 18.39 (α-CH_2), 14.03 (CH_3).

*11-Hexyloxy-1-undecyne (**10e**).* Procedure B was carried out using hexanol (0.98 mL, 7.79 mmol) and 10-undecynyl mesylate (**9a**) (1.60 g, 6.49 mmol). The crude product was purified by column chromatography (5% ethyl acetate in hexane) to give the product **10e** as a colorless oil (0.98 g, 60%). ^{1}H NMR (500 MHz, $CDCl_3$): δ 3.41 (4H, t, J = 6.7 Hz, 2 × OCH_2), 2.19 (2H, dt, J = 7.1 Hz, 2.6 Hz,

dx.doi.org/10.1021/jm301778x | J. Med. Chem. 2013, 56, 1311−1322

α-CH_2), 1.95 (1H, t, J = 2.7 Hz, HC≡C), 1.65−1.24 (22H, m, 11 × CH_2), 0.92 (3H, t, J = 7.2 Hz, CH_3). ^{13}C NMR (125 MHz, $CDCl_3$): δ 84.75 (HC≡*C*), 70.97 (OCH_2), 70.93 (OCH_2), 68.02 (HC≡C), 31.73, 29.78, 2 × 29.76 (double intensity), 29.43, 29.03, 28.73, 28.48, 26.18, 25.88, 22.63 (11 × CH_2), 18.39 (α-CH_2), 14.03 (CH_3).

*11-(Isopropyloxy)-1-undecyne (**10f**).* Procedure B was carried out using 2-propanol (0.372 mL, 4.86 mmol) and 10-undecynyl mesylate (**9a**) (1.00 g, 4.06 mmol). The mixture was heated for a total of 24 h at 70 °C, with a further 0.75 equiv of NaH added after the first 7 h. After treatment, the crude product was purified by column chromatography (5% ethyl acetate in hexane) to give the product **10f** as a colorless oil (0.484 g, 56%). ^{1}H NMR (500 MHz, $CDCl_3$): δ 3.56 (1H, m, J = 6.1 Hz, CH), 3.41 (2H, t, J = 6.8 Hz, OCH_2), 2.20 (2H, dt, J = 7.1 Hz, 2.7 Hz, α-CH_2), 1.96 (1H, t, J = 2.7 Hz, HC≡C), 1.58−1.52 (4H, m, 2 × CH_2), 1.44−1.29 (10H, m, 5 × CH_2), 1.18 (3H, s, CH_3), 1.17 (3H, s, CH_3). ^{13}C NMR (125 MHz, $CDCl_3$): δ 84.81 (HC≡*C*), 71.23 (OCH), 68.23 (OCH_2), 68.02 (HC≡C), 30.18, 2 × 29.44 (double intensity), 29.04, 28.73, 28.48, 26.18 (7 × CH_2), 22.16 (double intensity, 2 × CH_3), 18.39 (α-CH_2).

*11-(sec-Butyloxy)-1-undecyne (**10g**).* Procedure B was carried out using *sec*-butanol (0.447 mL, 4.87 mmol) and 10-undecynyl mesylate (**9a**) (1.00 g, 4.06 mmol). The crude product was purified by column chromatography (5% ethyl acetate in hexane) to give the product **10g** as a colorless oil (0.372 g, 38%). ^{1}H NMR (500 MHz, $CDCl_3$): δ 3.50−3.29 (3H, m, CH_2OCH), 2.20 (2H, dt, J = 7.1 Hz, 2.6 Hz, α-CH_2), 1.96 (1H, t, J = 2.7 Hz, HC≡C), 1.62−1.27 (16H, m, 8 × CH_2), 1.14 (3H, d, J = 6.1 Hz, CHC*H*$_3$), 0.92 (3H, t, J = 7.4 Hz, CH_2C*H*$_3$). ^{13}C NMR (125 MHz, $CDCl_3$): δ 84.79 (HC≡*C*), 76.59 (OCH), 68.47 (OCH_2), 68.01 (HC≡C), 30.21, 29.44 (double intensity), 29.26, 29.04, 28.74, 28.49, 26.18 (8 × CH_2), 19.30 (CH*C*H$_3$), 18.39 (α-CH_2), 9.86 (CH_2C*H*$_3$).

*11-(Isobutyloxy)-1-undecyne (**10h**).* Procedure B was carried out using isobutanol (0.450 mL, 4.87 mmol) and 10-undecynyl mesylate (**9a**) (1.00 g, 4.06 mmol). The mixture was heated for a total of 28 h at 70 °C, with a further 0.75 equiv of NaH and 0.6 equiv of isobutanol added after the first 18 h. After the treatment, the crude product was purified by column chromatography (5% ethyl acetate in hexane) to give the product **10h** as a light yellow oil (0.480 g, 52%). ^{1}H NMR (500 MHz; $CDCl_3$): δ 3.41 (2H, t, J = 6.7 Hz, CH_2C*H*$_2$O), 3.19 (2H, d, J = 6.7 Hz, OC*H*$_2$CH), 2.20 (2H, dt, J = 7.1 Hz, 2.6 Hz, α-CH_2), 1.96 (1H, t, J = 2.7 Hz, HC≡C), 1.92−1.85 (1H, m, CH), 1.59−1.53 (4H, m, 2 × CH_2), 1.36−1.28 (13H, m, 2 × CH_2), 0.93 (3H, s, CH_3), 0.91 (3H, s, CH_3). ^{13}C NMR (125 MHz, $CDCl_3$): δ 84.80 (HC≡*C*), 77.86 (OCH_2CH), 71.07 (OCH_2CH_2), 68.03 (HC≡C), 29.76, 2 × 29.44 (double intensity), 29.05, 28.75, 28.50, 28.45, 26.15, 25.89, 22.63 (10 × CH_2), 18.39 (α-CH_2), 14.04 (CH_3).

*11-(tert-Butyloxy)-1-undecyne (**10i**).* Procedure B was carried out using *tert*-butanol (0.925 mL, 9.74 mmol) and 10-undecynyl mesylate (**9a**) (2.00 g, 8.12 mmol). The mixture was heated for a total of 28 h at 70 °C, with a further 0.75 equiv of NaH added after the first 18 h. After treatment, the crude product was purified by column chromatography (5% ethyl acetate in hexane) to give the product **10i** as a colorless oil (0.478 g, 26%). ^{1}H NMR (500 MHz; $CDCl_3$): δ 3.41 (2H, t, J = 6.7 Hz, OCH_2), 2.21 (2H, dt, J = 7.1 Hz, 2.7 Hz, α-CH_2), 1.96 (1H, t, J = 2.7 Hz, HC≡C), 1.58−1.52 (4H, m, 2 × CH_2), 1.41−1.28 (10H, m, 5 × CH_2), 1.21 (9H, s, 3 × CH_3). ^{13}C NMR (125 MHz, $CDCl_3$): δ 84.81 (HC≡*C*), 72.97 (O*C*(CH$_3$)$_3$), 70.97 (OCH_2), 68.05 (HC≡C), 29.79, 2 × 29.45 (double intensity), 29.06, 28.76, 28.50, (6 × CH_2), 27.61 (3 × CH_3), 26.20, 18.42 (2 × CH_2).

*10-Hexyloxy-1-decyne (**10j**).* Procedure B was carried out using hexanol (1.2 mL, 9.29 mmol) and 9-decynyl mesylate (**9b**) (1.8 g, 7.74 mmol). The mixture was heated for a total of 55 h at 70 °C, with a further 1.2 equiv of NaH added after the first 19 h and again 0.5 equiv of NaH and 0.5 equiv of 9-decynyl mesylate (**9b**) added after 40 h. After treatment, the crude product was purified by column chromatography (5% ethyl acetate in hexane) to obtain the product **10j** as a pale brown oil (0.572 g, 35%). ^{1}H NMR (500 MHz, $CDCl_3$): δ 3.41 (4H, t, J = 6.6 Hz, 2 × OCH_2), 2.20 (2H, dt, J = 7.1 Hz, 2.6 Hz, α-CH_2), 1.96 (1H, t, J = 2.7 Hz, HC≡C), 1.70−1.26 (20H, m, 10 × CH_2), 0.92 (3H, t, J = 7.2 Hz, CH_3). ^{13}C NMR (125 MHz, $CDCl_3$): δ 84.75 (HC≡*C*), 70.98 (OCH_2), 70.91 (OCH_2), 68.04 (HC≡C), 31.73, 2 × 29.76 (double intensity), 29.34, 29.05, 28.70, 28.47, 26.15, 25.89, 22.63 (10 × CH_2), 18.39 (α-CH_2), 14.04 (CH_3).

*15-Methoxy-1-pentadecyne (**10k**).* Procedure B was carried out using methanol (0.36 mL, 8.76 mmol) and 14-pentadecynyl mesylate (**9c**) (2.04 g, 6.74 mmol) at 60 °C for 4 h. Some methanol (1.3 equiv) and NaH (1.35 equiv) were then added, and the mixture was heated further 3 h at 60 °C. After treatment, the crude product was purified by column chromatography (5% ethyl acetate in hexane) to obtain the product **10k** as a colorless oil (1.11 g, 69%). ^{1}H NMR (500 MHz, $CDCl_3$): δ 3.40 (2H, J = 6.7 Hz, OCH_2), 3.35 (3H, s, CH_3), 2.20 (2H, dt, J = 7.1 Hz, 2.7 Hz, CH_2C≡C), 1.95 (1H, t, J = 2.7 Hz, HC≡C), 1.64−1.50 (6H, m, 3 × CH_2), 1.46−1.23 (16H, m, 8 × CH_2). ^{13}C NMR (125 MHz, $CDCl_3$): δ 84.79 (HC≡*C*), 72.98 (OCH_2), 68.01 (HC≡C), 58.51 (CH_3), 31.58, 2 × 29.66 (double intensity), 29.61, 29.58, 29.50, 29.11, 28.76, 28.50, 26.14, 22.65 (11 × CH_2), 18.40 (*C*H$_2$C≡C).

*3-Tridecyloxy-1-propyne (**12a**).* Procedure B was carried out using 2-propyn-1-ol (0.56 g, 10.00 mmol) and tridecyl mesylate (**11a**) (4.2 g, 15.0 mmol). The mixture was heated for a total of 36 h at 60 °C with a further 1.0 equiv of NaH added after the first 24 h. After treatment, the crude product was purified by column chromatography (5% ethyl acetate in hexane) to give the desired compound as a pale brown oil (0.90 g, 22%). ^{1}H NMR (500 MHz, $CDCl_3$): δ 4.17 (2H, d, J = 2.6 Hz, OCH_2C≡C), 3.54 (2H, t, J = 7.1 Hz, OC*H*$_2$CH$_2$), 2.43 (1H, t, J = 2.6 Hz, HC≡C), 1.62 (2H, m, OCH_2C*H*$_2$), 1.62−1.22 (20H, m, 10 × CH_2), 0.91 (3H, t, J = 7.1 Hz, CH_3). ^{13}C NMR (125 MHz, $CDCl_3$): δ 80.09 (HC≡*C*), 73.97 (HC≡C), 70.32 (OCH_2CH_2), 57.99 (OCH_2C≡C), 31.92, 29.67, 29.65, 29.60, 29.57, 29.52, 29.44, 29.35, 26.21, 26 09 (10 × CH_2), 22.68 (α-CH_2), 14.10 (CH_3).

*6-Decyloxy-1-hexyne (**12b**).* Procedure B was carried out using hexyn-1-ol (0.66 mL, 6.11 mmol) and decyl mesylate (**11b**) (2.17 g, 9.17 mmol, 1.5 equiv). The mixture was heated for a total of 90 h at 60 °C, with a further 1 equiv of NaH added after the first 24 h and another 1 equiv of NaH and 1 equiv of decyl mesylate added after 48 h. After treatment, the crude product was purified by column chromatography (5% ethyl acetate in hexane) to obtain the desired compound as a brown oil (1.2 g, 82%). ^{1}H NMR (500 MHz, $CDCl_3$): δ 3.47−3.36 (4H, m, 2 × OCH_2), 2.24 (2H, dt, J = 7.0 Hz, J = 2.6 Hz, CH_2), 1.96 (1H, t, J = 2.6 Hz, HC≡C), 1.76−1.53 (6H, m, 3 × CH_2), 1.38−1.21 (14H, m, 7 × CH_2), 0.89 (3H, t, J = 7.0 Hz, CH_3). ^{13}C NMR (125 MHz, $CDCl_3$): δ 84.36 (HC≡*C*), 71.01 (OCH_2), 70.17 (OCH_2), 68.29 (HC≡C), 31.90, 29.80, 29.32, 29.11, 28.81, 26.20, 25.28, 24.85, 22.67, 22.64 (10 × CH_2), 18.23 (α-CH_2), 14.08 (CH_3).

General Procedure C: Synthesis of 3-(2′,3′-Dideoxy-ribo-β-L-furanosyl)-6-substituted-furo[2,3-d]pyrimidin-2(3*H*)-one analogues (8a−u). To a solution of L-5-iodo-2′,3′-dideoxyuridine **7** in DMF (5.5 mL/mmol) was added the alkyne (3 equiv), tetrakis-(triphenylphosphine) palladium(0) (0.1 equiv), CuI (0.2 equiv), and DIPEA (2 equiv). The mixture was stirred at room temperature for 16 h, and further CuI (0.2 equiv) and triethylamine (5.5 mL/mmol) were added. The mixture was stirred at 80 °C for 8 h. The solvent was removed under high vacuum and the residue was purified by flash column chromatography.

*3-(2′,3′-Dideoxy-ribo-β-L-furanosyl)-6-hexylfuro[2,3-d]pyrimidin-2(3H)-one (**8a**).* Procedure C was carried out using 1-octyne (0.29 g, 2.66 mmol), which gave the desired alkyne intermediate (0.130 g, 0.374 mmol, 34%). This compound was dissolved in DMF (5 mL), and to this solution Et_3N (5 mL) and CuI (0.014 g, 0.075 mmol, 0.2 equiv) were added. The resulting solution was heated at 80 °C for 8 h. Solvent was removed under high vacuum. The product **8a** was then obtained as an off-white solid (0.026 g, 22%) after purification by preparative thin layer chromatography using 20% chloroform in ethyl acetate as the eluent. ^{1}H NMR (500 MHz, $CDCl_3$): δ 876 (1H, s, H-4), 6.20 (1H, m, H-1′), 6.15 (1H, s, H-5), 4.31 (1H, m, H-4′), 4.16 (1H, ddd, J = 11.9 Hz, 4.2 Hz, 2.9 Hz, H-5′), 3.89 (1H, ddd, J = 11.9 Hz, 3.0 Hz, H-5′), 2.69−2.54 (3H, m, CH_2, H-2′), 2.25−2.16 (1H, m, H-2′), 1.99−1.90 (2H, m, H-3′), 1.72 (2H, m, J = 7.1 Hz, CH_2), 1.41−1.22 (6H, m, 3 × CH_2), 0.90 (3H, t, J = 6.3 Hz, CH_3). ^{13}C NMR (125

MHz, $CDCl_3$): δ 171.74 (C-7a), 159.47 (C-6), 155.05 (C-2), 135.98 (C-4), 107.25 (C-4a), 99.10 (C-5), 89.00 (C-1′), 82.93 (C-4′), 62.81 (C-5′), 33.79 (C-2′), 31.43, 28.69, 28.25 (3 × CH_2), 26.78 (C-3′), 23.89, 22.50 (2 × CH_2), 14.01 (CH_3). MS (ES^+) *m/z* 321 ($M + H^+$). Accurate mass: $C_{17}H_{25}N_2O_4$ requires 321.1814, found 321.1824. Reverse HPLC eluting with H_2O/MeOH (gradient from 100:0 to 0:100 in 25 min): t_R = 21.81 min.

*3-(2′,3′-Dideoxy-ribo-β-L-furanosyl)-6-septylfuro[2,3-d]pyrimidin-2(3H)-one (**8b**).* Procedure C was carried out using 1-nonyne (0.275 g, 2.22 mmol), which gave, after purification by flash column chromatography (5% methanol in ethyl acetate), the product **8b** as an off-white solid (0.128 g, 53%). ^1H NMR (500 MHz, $CDCl_3$): δ 8.84 (1H, s, H-4), 6.20 (1H, dd, *J* = 6.7 Hz, 2.5 Hz, H-1′), 6.16 (1H, s, H-5), 4.30 (1H, m, H-4′), 4.18 (1H, m, H-5′), 3.91 (1H, m, H-5′), 3.16 (1H, t, *J* = 5.4 Hz, OH), 2.70−2.54 (3H, m, α-CH_2, H-2′), 2.21 (1H, m, H-2′), 1.97 (2H, m, H-3′), 1.69 (2H, m, *J* = 7.1 Hz, CH_2), 1.44−1.22 (8H, m, 4 × CH_2), 0.90 (3H, t, *J* = 6.5 Hz, CH_3). ^{13}C NMR (125 MHz, $CDCl_3$): δ 171.72 (C-7a), 159.43 (C-6), 155.06 (C-2), 136.12 (C-4), 107.25 (C-4a), 99.15 (C-5), 89.00 (C-1′), 83.01(C-4′), 62.74 (C-5′), 33.81 (C-2′), 31.68, 28.98, 28.91, 28.25 (4 × CH_2), 26.83 (C-3′), 23.87, 22.59 (2 × CH_2), 14.04 (CH_3). MS (ES^+) *m/z* 335 (100%, $M + H^+$), 373 (9%, $M + K^+$), 398 (81%, $M + CH_3CN + Na^+$). Accurate mass: $C_{18}H_{27}N_2O_4$ requires 335.1971, found 335.1958. Reverse HPLC eluting with H_2O/MeOH (gradient from 100:0 to 10:90 in 15 min and with 10:90 for 10 min): t_R = 17.91 min.

*3-(2′,3′-Dideoxy-ribo-β-L-furanosyl)-6-octylfuro[2,3-d]pyrimidin-2(3H)-one (**8c**).* Procedure C was carried out using 1-decyne (0.31 g, 2.22 mmol). After purification by flash column chromatography (2% methanol in ethyl acetate) to obtain a pale brown oil and trituration with ethyl acetate, the product **8c** was obtained as an off-white solid (0.060 g; 23%). ^1H NMR (500 MHz, DMSO-d_6): δ 8.83 (1H, s, H-4), 6.42 (1H, s, H-5), 5.97 (1H, m, H-1′), 5.15 (1H, t, *J* = 5.1 Hz, OH), 4.14 (1H, m, H-4′), 3.80 (1H, m, H-5′), 3.60 (1H, m, H-5′), 2.61 (2H, t, *J* = 7.2 Hz, α-CH_2), 2.42 (1H, m, H-2′), 1.97 (1H, m, H-2′), 1.88−1.56 (2H, m, H-3′), 1.6 (2H, m, *J* = 7.5 Hz, CH_2), 0.84 (3H, t, *J* = 6.7 Hz, CH_3). ^{13}C NMR (125 MHz, DMSO-d_6): δ 170.99 (C-7a), 158.01 (C-6), 153.76 (C-2), 137.00 (C-4), 107.33 (C-4a), 99.72 (C-5), 88.02 (C-1′), 83.00 (C-4′), 61.33 (C-5′), 33.03 (C-2′), 31.16, 28.55, 28.50, 28.29, 27.29 (5 × CH_2), 26.35 (C-3′), 23.61, 22.00 (2 × CH_2), 13.88 (CH_3). MS (ES^+) *m/z* 349 ($M + H^+$). Accurate mass: $C_{19}H_{29}N_2O_4$ requires 349.2127, found 349.2141. Reverse HPLC eluting with H_2O/MeOH (gradient from 100:0 to 0:100 in 25 min and then at 0:100 for 5 min): t_R = 26.04 min.

*3-(2′,3′-Dideoxy-ribo-β-L-furanosyl)-6-nonylfuro[2,3-d]pyrimidin-2(3H)-one (**8d**).* Procedure C was carried out using 1-undecyne (0.405 g, 2.66 mmol), which gave, after purification by flash column chromatography (40% dichloromethane in ethyl acetate), the product **8d** as an off-white solid (0.150 g, 47%). ^1H NMR (500 MHz, $CDCl_3$): δ 8.76 (1H, s, H-4), 6.20 (1H, dd, *J* = 6.8 Hz, *J* = 2.6 Hz, H-1′), 6.15 (1H, s, H-5), 4.31 (1H, m, H-4′), 4.17 (1H, m, H-5′), 3.91 (1H, m, H-5′), 2.83 (1H, t, *J* = 5.5 Hz, OH), 2.70−2.55 (3H, m, α-CH_2, H-2′), 2.24 (1H, m, H-2′), 1.95 (2H, m, H-3′), 1.70 (2H, m, *J* = 7.2 Hz, CH_2), 1.45−1.21 (12H, m, 6 × CH_2), 0.90 (3H, t, *J* = 6.7 Hz, CH_3). ^{13}C NMR (125 MHz, $CDCl_3$): δ 171.75 (C-7a), 159.49 (C-6), 155.02 (C-2), 135.89 (C-4), 107.22 (C-4a), 99.07(C-5), 88.99 (C-1′), 82.88 (C-4′), 62.87 (C-5′), 33.78 (C-2′), 31.84, 29.45, 29.26, 29.04, 28.26 (5 × CH_2), 26.83 (C-3′), 23.91, 22.64 (2 × CH_2), 14.08 (CH_3). MS (ES^+) *m/z* 363 (53%, $M + H^+$), 426 (80%, $M + CH_3CN + Na^+$). Accurate mass: $C_{20}H_{31}N_2O_4$ requires 363.2284, found 363.2289. Reverse HPLC eluting with H_2O/MeOH (gradient from 100:0 to 10:90 in 15 min and then at 10:90 for 10 min): t_R = 21.57 min.

*3-(2′,3′-Dideoxy-ribo-β-L-furanosyl)-6-decylfuro[2,3-d]pyrimidin-2(3H)-one (**8e**).* Procedure C was carried out using 1-dodecyne (0.516 g, 3.11 mmol), which gave, after purification by flash column chromatography (40% dichloromethane in ethyl acetate), the product **8e** as an off-white solid (0.100 g, 33%). ^1H NMR (500 MHz, $CDCl_3$): δ 8.75 (1H, s, H-4), 6.21 (1H, m, H-1′), 6.15 (1H, s, H-5), 4.32 (1H, m, H-4′), 4.17 (1H, m, H-5′), 3.90 (1H, m, H-5′), 2.86 (1H, t, *J* = 5.4 Hz, OH), 2.68−2.57 (3H, m, α-CH_2, H-2′), 2.21 (1H, m, H-2′), 1.96 (2H, m, H-3′), 1.72 (2H, m, *J* = 7.0 Hz, CH_2), 1.44−1.21 (14H, m, 7 × CH_2), 9.00 (3H, t, *J* = 6.4 Hz, CH_3). ^{13}C NMR (125 MHz, $CDCl_3$): δ 171.75 (C-7a), 159.49 (C-6), 155.03 (C-2), 135.90 (C-4), 107.23 (C-4a), 99.07 (C-5), 88.99 (C-1′), 82.88 (C-4′), 62.86 (C-5′), 33.78 (C-2′), 31.87, 29.56, 29.50, 29.29, 29.27, 29.05, 28.26 (7 × CH_2), 26.83 (C-3′), 23.91, 22.66 (2 × CH_2), 14.09 (CH_3). MS (ES^+) *m/z* 377 (16%, $M + H^+$), 399 (6%, $M + Na^+$), 415 (8%, $M + K^+$), 440 (100%, $M + CH_3CN + Na^+$). Accurate mass: $C_{21}H_{33}N_2O_4$ requires 377.2440, found 377.2426. Reverse HPLC eluting with H_2O/MeOH (gradient from 100:0 to 0:100 in 30 min and then at 0:100 for 5 min): t_R = 33.00 min.

*3-(2′,3′-Dideoxy-ribo-β-L-furanosyl)-6-dodecylfuro[2,3-d]-pyrimidin-2(3H)-one (**8f**).* Procedure C was carried out using 1-tetradecyne (0.345 g, 1.77 mmol), which gave, after purification by flash column chromatography (40% dichloromethane in ethyl acetate), the product **8f** as an off-white solid (0.100 g, 42%). ^1H NMR (500 MHz, $CDCl_3$): δ 8.77 (1H, s, H-4), 6.23 (1H, dd, *J* = 6.6 Hz, 2.5 Hz, H-1′), 6.16 (1H, s, H-5), 4.32 (1H, m, H-4′), 4.18 (1H, m, H-5′), 3.90 (1H, m, H-5′), 2.90 (1H, br s, OH), 2.67−2.56 (3H, m, α-CH_2, H-2′), 2.21 (1H, m, H-2′), 1.94 (2H, m, H-3′), 1.69 (2H, m, *J* = 7.5 Hz, CH_2), 1.43−1.20 (18H, m, 9 × CH_2), 9.00 (3H, t, *J* = 6.5 Hz, CH_3). ^{13}C NMR (125 MHz, $CDCl_3$): δ 171.74 (C-7a), 159.48 (C-6), 155.03 (C-2), 135.95 (C-4), 107.24 (C-4a), 99.08 (C-5), 88.99 (C-1′), 82.91 (C-4′), 62.83 (C-5′), 33.79 (C-2′), 31.90, 29.64, 29.61, 29.51, 29.33, 29.28, 29.06, 28.26 (9 × CH_2), 26.84 (C-3′), 23.90, 22.67 (2 × CH_2), 14.10 (CH_3). MS (ES^+) *m/z* 405 ($M + H^+$). Accurate mass: $C_{23}H_{37}N_2O_4$ requires 405.2753, found 405.2739. Reverse HPLC eluting with H_2O/MeOH (gradient from 100:0 to 10:90 in 15 min, then at 10:90 for 10 min and another gradient from 10:90 to 0:100 in 5 min): t_R = 28.99 min.

*3-(2′,3′-Dideoxy-ribo-β-L-furanosyl)-6-(4-n-butylphenyl)furo[2,3-d]pyrimidin-2(3H)-one (**8g**).* Procedure C was carried out using 4-*n*-butylphenylacetylene (0.351 g, 0.39 mL, 2.22 mmol). The obtained residue was purified by column chromatography (5% methanol in dichloromethane) to give the product **8g** as an off-white solid (0.110 g, 40%). ^1H NMR (500 MHz, $CDCl_3$): δ 8.90 (1H, s, H-4), 7.63 (2H, d, *J* = 8.2 Hz, *Ph*), 7.22 (2H, d, *J* = 8.3 Hz, *Ph*), 6.71 (1H, s, H-5), 6.25 (1H, dd, *J* = 6.7 Hz, 2.3 Hz, H-1′), 4.32 (1H, m, H-4′), 4.2 (1H, m, H-5′), 3.92 (1H, m, H-5′), 2.92 (1H, t, *J* = 5.0 Hz, OH), 2.70−2.59 (3H, m, α-CH_2, H-2′), 2.25 (1H, m, H-2′), 2.00 (2H, m, H-3′), 1.65 (2H, m, CH_2), 1.39 (2H, m, CH_2), 0.98 (3H, t, *J* = 6.6 Hz, CH_3). ^{13}C NMR (125 MHz, $CDCl_3$): δ 171.58 (C-7a), 155.58 (C-6), 155.00 (C-2), 144.80 (C-*para Ph*), 136.79 (C-4), 128.96 (*Ph*), 125.98 (C-*ipso Ph*), 124.82 (*Ph*), 107.81 (C-4a), 97.22 (C-5), 89.11 (C-1′), 83.03 (C-4′), 62.79 (C-5′), 35.53 (CH_2), 33.85 (C-2′), 33.36 (CH_2), 23.83 (C-3′), 22.32 (CH_2), 13.91 (CH_3). MS (ES^+) *m/z* 369 (44%, $M + H^+$), 407 (70%, $M + K^+$), 432 (50%, $M + CH_3CN + Na^+$). Accurate mass: $C_{21}H_{25}N_2O_4$ requires 369.1814, found 369.1830. Reverse HPLC eluting with H_2O/MeOH (gradient from 100:0 to 0:100 in 35 min): t_R = 33.29 min.

*3-(2′,3′-Dideoxy-ribo-β-L-furanosyl)-6-(4-n-pentylphenyl)furo-[2,3-d]pyrimidin-2(3H)-one (**8h**).* Procedure C was carried out using 4-*n*-pentylphenylacetylene (0.382 g, 0.43 mL, 2.18 mmol). The obtained residue was purified by column chromatography (5% methanol in dichloromethane) to give the product **8h** as an off-white solid (0.102 g, 36%). ^1H NMR (500 MHz, $CDCl_3$): δ 8.80 (1H, s, H-4), 7.68 (2H, d, *J* = 8.2 Hz, *Ph*), 7.26 (2H, d, *J* = 8.3 Hz, *Ph*), 6.70 (1H, s, H-5), 6.26 (1H, dd, *J* = 6.67 Hz, 2.26 Hz, H-1′), 4.35 (1H, m, H-4′), 4.20 (1H, m, H-5′), 3.90 (1H, m, H-5′), 2.65 (3H, m, α-CH_2, H-2′), 2.30−2.18 (2H, m, H-2′, OH), 1.95 (2H, m, H-3′), 1.61 (2H, m, CH_2), 1.42−1.29 (4H, m, 2 × CH_2), 0.91 (3H, t, *J* = 6.5 Hz, CH_3). ^{13}C NMR (125 MHz, $CDCl_3$): δ 170.10 (C-7a), 156.00 (C-6), 155.50 (C-2), 144.91 (C-*para Ph*), 136.36 (C-4), 128.99 (*Ph*), 126.00 (C-*ipso Ph*), 124.87 (*Ph*), 125.98, 106.60 (C-4a), 97.04 (C-5), 89.10 (C-1′), 82.76 (C-4′), 63.04 (C-5′), 35.83 (C-2′), 33.78, 31.45, 30.92 (3 × CH_2), 23.91 (C-3′), 22.51 (CH_2), 13.99 (CH_3). MS (ES^+) *m/z* 383 (14%, $M + H^+$), 405 (3%, $M + Na^+$), 421 (7%, $M + K^+$), 446 (62%, $M + CH_3CN + Na^+$). Accurate mass: $C_{22}H_{27}N_2O_4$ requires 383.1971, found 383.1988. Reverse HPLC eluting with H_2O/MeOH (gradient from 100:0 to 10:90 in 15 min and then at 10:90 for 10 min): t_R = 21.00 min.

*3-(2′,3′-Dideoxy-ribo-β-L-furanosyl)-6-ethyloxynonylfuro[2,3-d]-pyrimidin-2(3H)-one (**8i**).* Procedure C was carried out using 11-ethyloxy-1-undecyne (**10a**) (0.348 g, 1.775 mmol). The obtained residue was purified by column chromatography (4% methanol in ethyl acetate) to give the product **8i** as an off-white solid (0.102 g, 42%). ^{1}H NMR (500 MHz, $CDCl_3$): δ 8.71 (s, 1H, H-4), 6.21 (1H, dd, *J* = 6.7 Hz, 2.2 Hz, H-1′), 6.13 (1H, s, H-5), 4.33−4.28 (1H, m, H-4′), 4.18−4.43 (1H, m, H-5′), 3.86 (1H, dt, *J* = 11.9 Hz, 3.8 Hz, H-5′), 3.49 (2H, q, *J* = 7.0 Hz, CH_3CH_2O), 3.42 (2H, t, *J* = 6.8 Hz, CH_2CH_2O), 2.65 (2H, t, *J* = 7.4 Hz, α-CH_2), 2.63−2.58 (1H, m, H-2′), 2.53 (1H, t, *J* = 4.7 Hz, OH), 2.26−2.19 (1H, m, H-2′), 1.99−1.90 (2H, m, H-3′), 1.72−1.65 (2H, m, β-CH_2), 1.62−1.54 (2H, m, CH_2CH_2O), 1.40−1.25 (10H, m, 5 × CH_2), 1.22 (3H, t, *J* = 7.0 Hz, CH_3). ^{13}C NMR (125 MHz, $CDCl_3$): δ 171.79 (C-7a), 159.47 (C-6), 154.98 (C-2), 135.70 (C-4), 107.15 (C-4a), 99.02 (C-5), 88.98 (C-1′), 82.76 (C-4′), 70.77 (CH_2CH_2O), 66.06 (CH_3CH_2O), 62.93 (C-5′) 33.76 (C-2′), 29.69, 29.39, 29.35, 29.09, 28.88, 28.21, 26.73, 26.15 (8 × CH_2), 23.91(C-3′), 15.24 (CH_3). MS (ES^+) *m*/*z* 429 (M + Na^+). Accurate mass: $C_{22}H_{34}N_2O_5Na$ requires 429.2365, found 429.2365. Reverse HPLC eluting with H_2O/MeOH (gradient from 100:0 to 0:100 in 35 min and then at 0:100 for 10 min): t_R = 33.25 min.

*3-(2′,3′-Dideoxy-ribo-β-L-furanosyl)-6-propyloxynonylfuro[2,3-d]pyrimidin-2(3H)-one (**8j**).* Procedure C was carried out using 11-propyloxy-1-undecyne (**10b**) (0.466 g, 2.218 mmol). The obtained residue was purified by column chromatography (4% methanol in ethyl acetate) to give the product **8j** as an off-white solid (0.105 g, 34%). ^{1}H NMR (500 MHz, $CDCl_3$): δ 8.84 (1H, s, H-4), 6.18 (1H, dd, *J* = 6.5 Hz, 2.0 Hz, H-1′), 6.15 (1H, s, H-5), 4.31−4.26 (1H, m, H-4′), 4.18−4.10 (1H, m, H-5′), 3.87 (1H, dt, *J* = 12.0 Hz, 3.0 Hz, H-5′), 3.50 (1H, m, OH), 3.40 (2H, t, *J* = 6.7 Hz, OCH_2), 3.40 (2H, t, *J* = 6.8 Hz, OCH_2), 2.63−2.54 (3H, m, α-CH_2, H-2′), 2.21−2.16 (1H, m, H-2′), 2.02−1.89 (2H, m, H-3′), 1.69−1.50 (6H, m, 3 × CH_2), 1.40−1.21 (10H, m, 5 × CH_2), 0.92 (3H, t, *J* = 7.4 Hz, CH_3). ^{13}C NMR (125 MHz, $CDCl_3$): δ 171.68 (C-7a), 159.33 (C-6), 155.10 (C-2), 136.32 (C-4), 107.24 (C-4a), 99.21 (C-5), 89.00 (C-1′), 83.10 (C-4′), 72.55 (OCH_2), 70.88 (OCH_2), 62.57 (C-5′), 33.82 (C-2′), 29.74, 29.39 (double intensity), 29.13, 28.93, 28.20, 26.76, 26.13 (8 × CH_2), 23.83 (C-3′), 22.91 (CH_2), 10.56 (CH_3). MS (ES^+) *m*/*z* 443 (M + Na^+). Accurate mass: $C_{23}H_{36}N_2O_5$ requires 443.2522, found 443.2539. Reverse HPLC eluting with H_2O/MeOH (gradient from 100:0 to 0:100 in 35 min and then at 0:100 for 10 min): t_R = 34.04 min.

*3-(2′,3′-Dideoxy-ribo-β-L-furanosyl)-6-butyloxynonylfuro[2,3-d]-pyrimidin-2(3H)-one (**8k**).* Procedure C was carried out using 11-butyloxy-1-undecyne **10c** (0.497 g, 2.217 mmol). The obtained residue was purified by column chromatography (4% methanol in ethyl acetate) to give the product **8k** as an off-white solid (0.090 g, 28%). ^{1}H NMR (500 MHz, $CDCl_3$): δ 8.76 (1H, s, H-4), 6.20 (1H, dd, *J* = 6.7 Hz, 2.4 Hz, H-1′), 6.14 (1H, s, H-5), 4.34−4.28 (1H, m, H-4′), 4.20−4.12 (1H, m, H-5′), 3.88 (1H, dt, *J* = 11.9 Hz, 3.5 Hz, H-5′), 3.41 (4H, q, *J* = 6.1 Hz, 2 × OCH_2), 2.88 (1H, t, *J* = 4.5 Hz, OH), 2.64 (2H, t, *J* = 7.3 Hz, α-CH_2), 2.60 (1H, m, H-2′), 2.24−2.18 (1H, m, H-2′), 1.99−1.90 (2H, m, H-3′),1.71−1.61 (2H, m, β-CH_2), 1.61−1.50 (4H, m, 2 × CH_2), 1.44−1.24 (12H, m, 6 × CH_2), 0.93 (3H, t, *J* = 7.4 Hz, CH_3). ^{13}C NMR ($CDCl_3$): δ 171.75 (C-7a), 159.42 (C-6), 155.02 (C-2), 135.94 (C-4), 107.18 (C-4a), 99.09 (C-5), 88.99 (C-1′), 82.90 (C-4′), 70.94 (OCH_2), 70.66 (OCH_2), 62.80 (C-5′), 33.79 (C-2′), 31.85, 29.76, 29.39, 29.37, 29.12, 28.92, 28.21, 26.75, 26.14 (9 × CH_2), 23.87 (C-3′), 19.36 (CH_2), 13.93 (CH_3). MS (ES^+) *m*/*z* 457 (M + Na^+). Accurate mass: $C_{24}H_{39}N_2O_5$ requires 435.2859, found 435.2839. Reverse HPLC eluting with H_2O/MeOH (gradient from 100:0 to 0:100 in 35 min and then at 0:100 for 10 min): t_R = 35.15 min.

*3-(2′,3′-Dideoxy-ribo-β-L-furanosyl)-6-pentyloxynonylfuro[2,3-d]-pyrimidin-2(3H)-one (**8l**).* Procedure C was carried out using 11-pentyloxy-1-undecyne (**10d**) (0.465 g, 1.952 mmol). The obtained residue was purified by column chromatography (4% methanol in ethyl acetate) to give the product **8l** as an off-white solid (0.102 g, 35%). ^{1}H NMR (500 MHz, $CDCl_3$): δ 8.76 (1H, s, H-4), 6.20 (1H, dd, *J* = 6.7 Hz, 2.5 Hz, H-1′), 6.14 (1H, s, H-5), 4.33−4.29 (1H, m, H-4′), 4.18−4.13 (1H, m, H-5′), 3.88 (1H, dt, *J* = 12.0 Hz, 3.9 Hz, H-5′), 3.41 (4H, dt, *J* = 6.7 Hz, 0.9 Hz, 2 × OCH_2), 2.90 (1H, br s, OH), 2.64 (2H, t, *J* = 7.5 Hz, α-CH_2), 2.63−2.56 (1H, m, H-2′), 2.25−2.18 (1H, m, H-2′), 2.00−1.91 (2H, m, H-3′), 1.72−1.63 (2H, m, β-CH_2), 1.61−1.55 (4H, m, 2 × CH_2), 1.35−1.28 (14H, m, 7 × CH_2), 0.91 (3H, t, *J* = 6.9 Hz, CH_3). ^{13}C NMR (125 MHz, $CDCl_3$): δ 171.75 (C-7a), 159.41 (C-6), 155.01 (C-2), 135.96 (C-4), 107.18 (C-4a), 99.09 (C-5), 88.99 (C-1′), 82.91 (C-4′), 70.98 (OCH_2), 70.94 (OCH_2), 62.79 (C-5′), 33.79 (C-2′), 29.76, 29.45, 29.39, 29.38, 29.12, 28.92, 28.36, 28.21, 26.75, 26.14 (10 × CH_2), 23.87 (C-3′), 22.54 (CH_2), 14.04 (CH_3). MS (ES^+) *m*/*z* 449 (11%, M + H^+), 471 (M + Na^+). Accurate mass: $C_{25}H_{41}N_2O_5$ requires 449.3015, found 449.3033. Reverse HPLC eluting with H_2O/MeOH (gradient from 100:0 to 0:100 in 35 min): t_R = 26.13 min.

*3-(2′,3′-Dideoxy-ribo-β-L-furanosyl)-6-hexyloxynonylfuro[2,3-d]-pyrimidin-2(3H)-one (**8m**).* Procedure C was carried out using 11-hexyloxy-1-undecyne (**10e**) (0.448 g, 1.775 mmol). The obtained residue was purified by column chromatography (4% methanol in ethyl acetate) to give the product **8m** as an off-white solid (0.120 g, 44%). ^{1}H NMR (500 MHz, $CDCl_3$): δ 8.76 (1H, s, H-4), 6.21 (1H, dd, *J* = 6.7 Hz, 2.3 Hz, H-1′), 6.14 (1H, s, H-5), 4.33−4.29 (1H, m, H-4′), 4.19−4.13 (1H, m, H-5′), 3.87 (1H, dt, *J* = 12.0 Hz, 3.9 Hz, H-5′), 3.41 (4H, dt, *J* = 6.7 Hz, 1.3 Hz, 2 × OCH_2), 2.87 (1H, t, *J* = 4.9 Hz, OH), 2.64 (2H, t, *J* = 7.3 Hz, α-CH_2), 2.63−2.57 (1H, m, H-2′), 2.24−2.19 (1H, m, H-2′), 1.98−1.92 (2H, m, H-3′), 1.71−1.65 (2H, m, β-CH_2), 1.69−1.53 (4H, m, 2 × CH_2), 1.38−1.26 (16H, m, 8 × CH_2), 0.90 (3H, t, *J* = 6.9 Hz, CH_3). ^{13}C NMR (125 MHz, $CDCl_3$): δ 171.75 (C-7a), 159.41 (C-6), 155.01 (C-2), 135.93 (C-4), 107.17 (C-4a), 99.08 (C-5), 88.98 (C-1′), 82.89 (C-4′), 71.00 (OCH_2), 70.94 (OCH_2), 62.80 (C-5′), 33.79 (C-2′), 31.71, 29.76, 29.73, 29.39, 29.38, 29.12, 28.92, 28.21, 26.75, 26.15, 25.86 (11 × CH_2), 23.87 (C3′), 22.62 (CH_2), 14.03 (CH_3). MS (ES^+) *m*/*z* 463 (5%, M + H^+), 485 (100%, M + Na^+), 501 (8%, M + K^+). Accurate mass: $C_{26}H_{43}N_2O_5$ requires 463.3172, found 463.3163. Reverse HPLC eluting with H_2O/MeOH (gradient from 100:0 to 10:90 in 15 min, then at 10:90 for 10 min and another gradient from 10:90 to 0:100 in 5 min): t_R = 26.91 min.

*3-(2′,3′-Dideoxy-ribo-β-L-furanosyl)-6-isopropyloxynonylfuro-[2,3-d]pyrimidin-2(3H)-one (**8n**).* Procedure C was carried out using 11-isopropyloxy-1-undecyne (**10f**) (0.280 g, 1.330 mmol). The obtained residue was purified by column chromatography (4% methanol in ethyl acetate) to give the product **8n** as an off-white solid (0.019 g, 10%). ^{1}H NMR (500 MHz, $CDCl_3$): δ 8.80 (1H, s, H-4), 6.20 (1H, dd, *J* = 6.6 Hz, 2.2 Hz, H-1′), 6.14 (1H, s, H-5), 4.30 (1H, ddt, *J* = 9.2 Hz, 6.0 Hz, 3.0 Hz, H-4′), 4.16 (1H, d, *J* = 11.8 Hz, H-5′), 3.88 (1H, dd, *J* = 12.0 Hz, 3.2 Hz, H-5′), 3.55 (1H, m, *J* = 6.1 Hz, OCH), 3.40 (2H, t, *J* = 6.7 Hz, OCH_2), 3.16 (1H, br s, OH), 2.63 (2H, t, *J* = 7.5 Hz, α-CH_2), 2.60−2.57 (1H, m, H-2′), 2.23−2.18 (1H, m, H-2′), 1.97−1.93 (2H, m, H-3′), 1.67 (2H, m, *J* = 7.2 Hz, β-CH_2), 1.55 (2H, m, *J* = 7.0 Hz, OCH_2CH_2), 1.38−1.26 (10H, m, 5 × CH_2), 1.17 (3H, s, CH_3), 1.15 (3H, s, CH_3). ^{13}C NMR (125 MHz, $CDCl_3$): δ 171.72 (C-7a), 159.38 (C-6), 155.05 (C-2), 136.10 (C-4), 107.21 (C-4a), 99.15 (C-5), 89.00 (C-1′), 83.00 (C-4′), 71.29 (OCH), 68.24 (OCH_2), 62.68 (C-5′), 33.83 (C-2′), 30.16, 29.41, 29.39, 29.13, 28.92, 28.21, 26.75, 26.19 (8 × CH_2), 23.85 (C-3′), 22.19 (double intensity, 2 × CH_3). MS (ES^+) *m*/*z* 443 (100%, M + Na^+), 863 (30%, MM + Na^+). Reverse HPLC eluting with H_2O/CH_3CN (elution with mixture 0:100 for 35 min, then gradient from 0:100 to 90:10 in 2 min and at 90:10 for 3 min): t_R = 36.18 min.

*3-(2′,3′-Dideoxy-ribo-β-L-furanosyl)-6-sec-butyloxynonylfuro[2,3-d]pyrimidin-2(3H)-one (**8o**).* Procedure C was carried out using 11-*sec*butyloxy-1-undecyne (**10g**) (0.197 g, 0.877 mmol). The obtained residue was purified by column chromatography (4% methanol in ethyl acetate) to give the product **8o** as an off-white solid (0.032 g, 36%). ^{1}H NMR (500 MHz, $CDCl_3$): δ 8.84 (1H, s, H-4), 6.19 (1H, dd, *J* = 6.6 Hz, 2.3 Hz, H-1′), 6.14 (1H, s, H-5), 4.33−4.29 (1H, m, H-4′), 4.16 (1H, d, *J* = 11.0 Hz, H-5′), 3.87 (1H, dt, *J* = 12.0 Hz, 3.9 Hz, H-5′), 3.49−3.28 (4H, m, OCH_2, OH, OCH), 2.63 (2H, t, *J* = 7.6 Hz, α-CH_2), 2.59−2.56 (1H, m, H-2′), 2.23−2.18 (1H, m, H-2′), 2.02−1.90 (2H, m, H-3′), 1.69−1.63 (2H, m, β-CH_2), 1.59−1.25 (14H, m, 7 × CH_2), 1.12 (3H, d, *J* = 6.1 Hz, CH_3), 0.09 (3H, t, *J* = 7.4 Hz, CH_3). ^{13}C NMR (125 MHz, $CDCl_3$): δ 171.70 (C-7a), 159.33 (C-6), 155.08

(C-2), 136.28 (C-4), 107.21 (C-4a), 99.19 (C-5), 89.00 (C-1′), 83.09 (C-4′), 76.64 (OCH), 68.48 (OCH_2), 62.58 (C-5′), 33.86 (C-2′), 30.19, 29.41 (double intensity), 29.25, 29.12, 28.94, 28.22, 26.77, 26.22 (9 × CH_2), 23.82 (C-3′), 19.31 (CH_3), 09.87 (CH_3). MS (ES^+) m/z 457 (100%, M + Na^+), 891 (51%, MM + Na^+). Reverse HPLC eluting with H_2O/CH_3CN (mixture 0:100 for 35 min, then gradient from 0:100 to 90:10 in 2 min and with 90:10 for 3 min): t_R = 36.71 min.

*3-(2′,3′-Dideoxy-ribo-β-L-furanosyl)-6-isobutyloxynonylfuro[2,3-d]pyrimidin-2(3H)-one (**8p**).* Procedure C was carried out using 11-isobutyloxy-1-undecyne (**10h**) (0.297 g, 1.319 mmol). The obtained residue was purified by column chromatography (4% methanol in ethyl acetate) to give the product **8p** as an off-white solid (0.047 g, 41%). ^1H NMR (500 MHz, $CDCl_3$): δ 8.69 (1H, s, H-4), 6.22 (1H, dd, J = 6.7 Hz, 2.5 Hz, H-1′), 6.13 (1H, s, H-5), 4.34−4.29 (1H, m, H-4′), 4.16 (1H, d, J = 11.5 Hz, H-5′), 3.88 (1H, d, J = 12.0 Hz, H-5′), 3.41 (2H, t, J = 6.7 Hz, OCH_2), 3.19 (2H, d, J = 6.7 Hz, OCH_2), 2.65 (2H, t, J = 7.6 Hz, α-CH_2), 2.63−2.59 (1H, m, H-2′), 2.42 (1H, s, OH), 2.25−2.20 (1H, m, H-2′), 1.97−1.92 (2H, m, H-3′), 1.87 (1H, m, CH), 1.69 (2H, m, β-CH_2), 1.58 (2H, m, OCH_2CH_2), 1.36−1.31 (10H, m, 5 × CH_2), 0.92 (3H, s, CH_3), 0.91 (3H, s, CH_3). ^{13}C NMR (125 MHz, $CDCl_3$): δ 171.79 (C-7a), 159.51 (C-6), 154.97 (C-2), 135.67 (C-4), 107.18 (C-4a), 99.01 (C-5), 88.99 (C-1′), 82.75 (C-4′), 77.87 (OCH_2), 71.07 (OCH_2), 62.98 (C-5′), 33.76 (C-2′), 29.74, 29.40 (double intensity), 29.14, 28.93 (5 × CH_2), 28.43 (CH), 28.24, 26.77, 26.16 (3 × CH_2), 23.93 (C-3′), 19.31 (double intensity, 2 × CH_3). Reverse HPLC eluting with H_2O/MeOH (gradient from 90:10 to 0:100 in 40 min and then at 0:100 for 5 min): t_R = 37.72 min.

*3-(2′,3′-Dideoxy-ribo-β-L-furanosyl)-6-tert-butyloxynonylfuro-[2,3-d]pyrimidin-2(3H)-one (**8q**).* Procedure C was carried out using 11-*tert*-butyloxy-1-undecyne (**10i**) (0.296 g, 1.319 mmol). The obtained residue was purified by column chromatography (4% methanol in ethyl acetate) to give the product **8q** as an off-white solid (0.011 g, 7%). ^1H NMR (500 MHz, $CDCl_3$): δ 8.67 (1H, s, H-4), 6.22 (1H, dd, J = 6.7 Hz, 2.5 Hz, H-1′), 6.13 (1H, t, J = 1.1 Hz, H-5), 4.34−4.29 (1H, m, H-4′), 4.16 (1H, d, J = 12 Hz, H-5′), 3.88 (1H, dt, J = 11.9 Hz, 3.5 Hz, H-5′), 3.35 (2H, t, J = 6.8 Hz, OCH_2), 2.66 (2H, t, J = 7.5 Hz, α-CH_2), 2.64−2.59 (1H, m, H-2′), 2.27−2.21 (1H, m, H-2′, OH), 1.99−1.89 (2H, m, H-3′), 1.72−1.66 (2H, m, β-CH_2), 1.55−1.50 (2H, m, OCH_2CH_2), 1.39−1.28 (10H, m, 5 × CH_2), 1.21 (9H, s, 3 × CH_3). ^{13}C NMR (125 MHz, $CDCl_3$): δ 171.81 (C-7a), 159.53 (C-6), 154.94 (C-2), 135.54 (C-4), 107.16 (C-4a), 98.98 (C-5), 88.99 (C-1′), 82.68 (C-4′), 72.48 ($OC(CH_3)_3$), 63.04 (C-5′), 61.69 (OCH_2), 33.75 (C-2′), 30.72, 29.44, 29.39, 29.11, 28.89, 28.22 (6 × CH_2), 27.61 (3 × CH_3), 26.73, 26.22 (2 × CH_2), 23.96 (C-3′). MS (ES^+) m/z 457 (100%, M + Na^+), 891 (13%, MM + Na^+). Reverse HPLC eluting with H_2O/MeOH (gradient from 90:10 to 0:100 in 40 min and with 0:100 for 5 min): t_R = 36.23 min.

*3-(2′,3′-Dideoxy-ribo-β-L-furanosyl)-6-hexyloxyoctylfuro[2,3-d]-pyrimidin-2(3H)-one (**8r**).* Procedure C was carried out using 10-hexyloxy-1-decyne **10j** (0.352 g, 1.48 mmol, 2.5 equiv). The obtained residue was purified by column chromatography (4% methanol in ethyl acetate) to give the product **8r** as an off-white solid (0.080 g, 30%). ^1H NMR (500 MHz, $CDCl_3$): δ 8.73 (1H, s, H-4), 6.21 (1H, dd, J = 6.1 Hz, 1.8 Hz, H-1′), 6.13 (1H, s, H-5), 4.34−4.27 (1H, m, H-4′), 4.19−4.12 (1H, m, H-5′), 3.88 (1H, dt, J = 7.6 Hz, 4.0 Hz, H-5′), 3.41 (4H, t, J = 6.1 Hz, 2 × OCH_2), 2.71 (1H, t, J = 4.7 Hz, OH), 2.67−2.56 (3H, m, α-CH_2, H-2′), 2.26−2.18 (1H, m, H-2′), 2.00−1.91 (2H, m, H-3′), 1.77−1.64 (2H, m, β-CH_2), 1.62−1.52 (4H, m, 2 × CH_2), 1.42−1.23 (14H, m, 7 × CH_2), 0.90 (3H, t, J = 6.8 Hz, CH_3). ^{13}C NMR (125 MHz, $CDCl_3$): δ 171.76 (C-7a), 159.44 (C-6), 154.99 (C-2), 135.83 (C-4), 107.17 (C-4a), 99.05 (C-5), 88.99 (C-1′), 82.83 (C-4′), 71.00 (OCH_2), 70.89 (OCH_2), 62.88 (C-5′), 33.77 (C-2′), 31.71, 29.73, 29.32, 29.19 (double intensity), 28.94, 28.23, 26.78, 26.14, 25.86 (10 × CH_2), 23.90 (C-3′), 22.62 (CH_2), 14.04 (CH_3). MS (ES^+) m/z 449 (11%, M + H^+), 471 (64%, M + Na^+), 487 (100%, M + K^+). Accurate mass: $C_{25}H_{41}N_2O_5$ requires 449.3015, found 449.3033. Reverse HPLC eluting with H_2O/MeOH (gradient from 100:0 to 0:100 in 35 min and then at 0:100 for 10 min): t_R = 38.17 min.

*3-(2′,3′-Dideoxy-ribo-β-L-furanosyl)-6-methyloxytridecylfuro[2,3-d]pyrimidin-2(3H)-one (**8s**).* Procedure C was carried out using 15-methoxy-1-pentadecyne (**10k**) (0.423 g, 1.774 mmol). The obtained residue was purified by column chromatography (3% methanol in ethyl acetate) to give the product **8s** as an off-white solid (0.050 g, 19%). ^1H NMR (500 MHz, $CDCl_3$): δ 8.75 (1H, s, H-4), 6.20 (1H, dd, J = 6.7 Hz, 2.4 Hz, H-1′), 6.15 (1H, s, H-5), 4.35−4.27 (1H, m, H-4′), 4.19−4.13 (1H, m, H-5′), 3.88 (1H, dt, J = 12.0 Hz, 4.0 Hz, H-5′), 3.38 (2H, t, J = 6.7 Hz, OCH_2), 2.35 (3H, s, OCH_3), 2.84 (1H, J = 4.8 Hz, OH), 2.64 (2H, t, J = 7.5, α-CH_2), 2.62−2.57 (1H, m, H-2′), 2.24−2.15 (1H, m, H-2′), 1.98−1.92 (1H, m, H-3′), 1.71−1.65 (2H, m, β-CH_2), 1.61−1.54 (2H, m, γCH_2), 1.40−1.23 (18H, m, 9 × CH_2). ^{13}C NMR (125 MHz, $CDCl_3$): δ 171.75 (C-7a), 159.47 (C-6), 155.02 (C-2), 135.90 (C-4), 107.22 (C-4a), 99.08 (C-5), 88.99 (C-1′), 82.88 (C-4′), 72.99 (OCH_2), 62.83 (C-5′), 58.52 (OCH_3), 33.77 (C-2′), 29.63, 29.56, 29.54, 29.48 (double intensity), 29.45 (double intensity), 29.23, 29.01, 28.25, 26.81, 26.12 (12 × CH_2), 23.91 (C-3′). MS (ES^+) m/z 449 (100%, M + H^+), 471 (68%, M + Na^+), 487 (84%, M + K^+). Accurate mass: $C_{25}H_{40}N_2O_5$ requires 449.3015, found 449.2997. Reverse HPLC eluting with H_2O/MeOH (gradient from 100:0 to 10:90 in 15 min, then at 10:90 for 5 min and another gradient from 10:90 to 0:100 in 5 min): t_R = 24.29 min.

*3-(2′,3′-Dideoxy-ribo-β-L-furanosyl)-6-tridecyloxymethylfuro[2,3-d]pyrimidin-2(3H)-one (**8t**).* Procedure C was carried out using 3-tridecyloxy-1-propyne **12a** (0.352 g, 1.776 mmol). The obtained residue was purified by column chromatography (4% methanol in ethyl acetate) to give the product **8t** as an off-white solid (0.024 g, 10%). ^1H NMR (500 MHz, $CDCl_3$): δ 8.87 (1H, s, H-4), 6.45 (1H, s, H-5), 6.21 (1H, dd, J = 6.8 Hz, 2.0 Hz, H-1′), 4.48 (2H, s, $CH_2OCH_2CH_2$), 4.34−4.29 (1H, m, H-4′), 4.20−4.15 (1H, m, H-5′), 3.90−3.87 (1H, m, H-5′), 3.56 (2H, t, J = 6.65 Hz, OCH_2CH_2), 2.68−2.57 (1H, m, H-2′), 2.28−2.18 (1H, m, H-2′), 1.98−1.89 (2H, m, H-3′), 1.67−1.58 (2H, m, J = 6.9 Hz, OCH_2CH_2), 1.40−1.22 (20H, m, 10 × CH_2), 0.90 (3H, t, J = 6.7 Hz, CH_3). ^{13}C NMR (125 MHz, $CDCl_3$): δ 171.78 (C-7a), 159.36 (C-6), 154.75 (C-2), 137.60 (C-4), 107.62 (C-4a), 102.36 (C-5), 88.13 (C-1′), 82.92 (C-4′), 71.49 (OCH_2CH_2), 64.95 ($CH_2OCH_2CH_2$), 62.79 (C-5′), 33.79 (C-2′), 31.91 (double intensity), 29.65, 29.61, 29.58 (double intensity), 29.47, 29.35, 26.06 (double intensity) (10 × CH_2), 23.74 (C-3′), 22.68 (CH_2), 14.10 (CH_3). MS (ES^+) m/z 449 (24%, M + H^+), 471 (36%, M + Na^+), 512 (100%, M + CH_3CN + Na^+). Accurate mass: $C_{25}H_{41}N_2O_5$ requires 449.3015, found 449.3024. Reverse HPLC eluting with H_2O/MeOH (gradient from 100:0 to 10:90 in 15 min, then at 10:90 for 5 min and another gradient from 10:90 to 0:100 in 5 min): t_R = 24.87 min.

*3-(2′,3′-Dideoxy-ribo-β-L-furanosyl)-6-decyloxybutylfuro[2,3-d]-pyrimidin-2(3H)-one (**8u**).* Procedure C was carried out using 6-decyloxy-1-hexyne (**12b**) (0.352 g, 1.776 mmol). The obtained residue was purified by column chromatography (4% methanol in ethyl acetate) to give the title compound as an off-white solid (0.070 g, 26%). ^1H NMR (500 MHz, $CDCl_3$): δ 8.72 (1H, s, H-4), 6.21 (1H, br d, J = 6.1 Hz, H-1′), 6.14 (1H, s, H-5), 4.34−4.28 (1H, m, H-4′), 4.19−4.12 (1H, m, H-5′), 3.91−3.86 (1H, m, H-5′), 3.45 (2H, t, J = 6.3 Hz, 2.1 Hz, OCH_2), 3.41 (2H, t, J = 6.7 Hz, 2.1 Hz, OCH_2), 2.69 (2H, t, J = 7.4 Hz, α-CH_2), 2.64−2.57 (2H, m, H-2′, OH), 2.23−2.19 (1H, m, H-2′), 1.98−1.92 (2H, m, H-3′), 1.81−1.73 (2H, m, β-CH_2), 1.69−1.62 (2H, m, CH_2), 1.60−1.54 (2H, m, CH_2), 1.35−1.24 (12H, m, 6 × CH_2), 0.90 (3H, t, J = 6.5 Hz, CH_3). ^{13}C NMR (125 MHz, $CDCl_3$): δ 171.75 (C-7a), 159.11 (C-6), 154.97 (C-2), 135.87 (C-4), 107.10 (C-4a), 99.23 (C-5), 89.00 (C-1′), 82.81 (C-4′), 71.15 (OCH_2), 70.23 (OCH_2), 62.92 (C-5′), 33.77 (C-2′), 29.74, 29.60, 29.57, 29.49, 29.31, 29.12 (6 × CH_2) 28.08 (α-CH_2), 26.18 (CH_2), 23.90 (C-3′), 23.68 (β-CH_2), 22.67 (CH_2), 14.10 (CH_3). MS (ES^+) m/z 449 (17%, M + H^+), 471 (6%, M + Na^+), 487 (4%, M + K^+), 512 (100%, M + CH_3CN + Na^+). Accurate mass: $C_{25}H_{41}N_2O_5$ requires 449.3015, found 449.3028. Reverse HPLC eluting with H_2O/MeOH (gradient from 100:0 to 10:90 in 15 min, then at 10:90 for 5 min, another gradient from 10:90 to 0:100 in 5 min and then at 0:100 for 10 min): t_R = 26.45 min.

dx.doi.org/10.1021/jm301778x | J. Med. Chem. 2013, 56, 1311−1322

Antiviral Assays. L-ddBCNAs were then prepared as 10 mM stock solutions in dimethyl sulfoxide (DMSO) to do the antiviral assays. Wortmannin (W3144; Sigma–Aldrich) was obtained as a 10 mM, 0.2-μm-filtered, ready-made solution in DMSO. Ribavirin (R9644; Sigma–Aldrich) and Cidofovir (C5874; Sigma–Aldrich) were prepared as 100 mM stock solution in water.

Cell Culture. Hela cells (ATCC CCL-2) were used for VACV stock production. BSC-1 cells (ATCC CCL-26), RK13 cells (ATCC CCL-37), HFFF (gift of G. Wilkinson), and B95a simian B cells [IZSBS–Istituto Zooprofilattico Sperimentale (Brescia, Italy)] were used for antiviral and proliferation assays. All cells were grown in Dulbecco's modified Eagle medium (DMEM; Invitrogen, Life Technologies, Paisley, U.K.) with 4.5g/L glucose and L-glutamine without sodium pyruvate 1× (Gibco, Life technologies, Paisley, U.K.), supplemented with 10% (v/v) heat-inactivated fetal bovine serum (FBS; Gibco; lot 41G6401K), used for the culture of all cells. Cells were cultured in the absence of antibiotics prior to assay, when penicillin/streptomycin was added (Gibco). Visibly contaminated cultures were discarded, mycoplasma contamination was ruled out by mycoplasma PCR (Geneflow).

Virus Culture. Vaccinia viruses were propagated in adherent HeLa cells, and mature intracellular virus (MV) was prepared using the method described by Townsley and co-workers[35] Vaccinia virus WR (VACV-WR) is a kind gift of Dr. Bernhard Moss, NIH, NIAID, LVD, to Joachim J. Bugert. VACV-WR luciferase reporter virus v3 was constructed to express firefly luciferase under the control of the synthetic–optimized early/late poxviral promoter using the pRB21-based donor plasmid p240.[36] The VACV-WR gfp reporter virus v300 was constructed to express enhanced green fluorescent protein (EGFP) under the control of the synthetic–optimized early/late poxviral promoter using the donor plasmid p300.[37]

Wild type measles viruses were propagated and titered in B95a cells and prepared as described by Hashimoto and co-workers[38] Wild type measles virus mWTFb is a kind gift of Jürgen Schneider Schaulies (Universität Würzburg, Germany). Wild type measles virus mIC323 expressing green fluorescent protein (GFP) is a kind gift of Yusuke Yanagi (NIID, Tokyo, Japan).

Measles virus vaccine strain Edmonston was purchased from ATCC (ATCC-VR24).

Measles virus Edmonston, adenovirus 5 (ATCC VR-5), and herpes simplex viruses type 1 (NCPV 17+) and type 2 (NCPV 132349) were propagated in Vero cells.[39]

VACV Luciferase Assays. RK13 cells in 96-well plates were pretreated for 30 min with each of the drugs at 10 μM and a DMSO control in triplicate. Luciferase producing vaccinia virus (v3) was then added to the wells at a multiplicity of infection (moi) of 0.2. The cells were collected 2 h p.i. A 100 μL portion of 1× passive lysis buffer (Promega, Madison, WI) per well was added to each well and the plate was agitated on a Bellydancer for 15 min. The plate was then frozen at −20 °C. After thawing, 20 μL of each of the samples was transferred to a black 96-well plate (NUNC, Roskilde, Denmark) and processed using the luciferase assay substrate and buffer II (Promega, Madison, WI). The luminescence was measured in a 96-well luminescence plate reader (FLUOstar OPTIMA FL, BMG Labtech). The percentages of the treated versus the no drug control readings were calculated.

VACV Plaque Reduction Assays (IC_{50}). BSC-1 cells grown to confluency in 24-well plates were pretreated with a series of dilutions of drug (50, 5, 0.5, 0.1, and 0.05 μM and no drug control) in quadruplicate. These were then infected with 30 plaque forming units (pfu) of vaccinia virus WR per well. The virus was left to adsorb onto the cells for 1 h, before the drug and the virus was removed and replaced with 1 mL of Avicel overlay (50% Avicel, 50% DMEM containing 1% P/S and drug to the required concentration). The plates were incubated for 4 days and were then rinsed with PBS and stained with crystal violet stain for 4–6 h. The plaque sizes were analyzed by scanning the plates at 600 dpi and measurement of the area of each of the plaques using Image J software. IC_{50} values were defined as the concentration of antiviral that reduced the size of plaques by 50% in comparison to cells infected in the absence of antiviral. The final IC_{50} values for all virus/antiviral combinations are each a mean from three experiments. The IC_{50} values were calculated for each drug using the GraphPad Prism software (GraphPad Software, Inc.).

$TCID_{50}$ Assays. Ten-fold dilutions of HSV-1/2, adenovirus 5, and measles viruses were used to infect HFFF, BSC-1 cells, and B95a cells in 96-well plates (10 dilutions, two mock, 8 times repeated) and evaluated 3 days postinfection for cytopathic effects in comparison to mock infected wells. Cells were grown in 96-well plates (NUNC) until 80% confluent. Cells were pretreated with medium containing the appropriate amount of antivirals for 30 min prior to infection. Each well was infected with 100 pfu of HSV-1/2 and adenovirus 5 or 100 syncytia forming units (sfu) of measles virus WTFb and incubated in DMEM without FBS or antibiotics containing no antivirals or antivirals at concentrations ranging from 1 to 100 μM for 3 days. Cytopathogenic effects were assessed by phase contrast microscopy. $TCID_{50}$ was defined as the concentration of antivirals that reduced the CPE by 50% in comparison to cells infected in the absence of antivirals as an average of three experiments. Controls consisting of virus and cell only (no drug) and cell only (no virus/no virus and no drug) were included in each experiment. $TCID_{50}$ values were calculated using the method of Reed and Muench.[40]

Cell Viability. L-ddBCNAs were tested for effects on cell viability over a period of 4 days in BSC-1 cells using a range of drug concentrations according to the manufacturer's instructions (G7571 CellTiter-Glo Luminescent Cell Viability Assay; Promega, Madison, WI). The assay measures the number of viable cells in culture based on quantitation of the ATP present, which signals the presence of metabolically active cells. CC_{50} values were calculated for each drug versus no drug using the GraphPad Prism software (GraphPad Software, Inc.).

AUTHOR INFORMATION

Corresponding Author

*Phone/Fax: +44 2920743583. E-mail: BugertJJ@cardiff.ac.uk.

Notes

The authors declare no competing financial interest.

ACKNOWLEDGMENTS

We thank the Severnside Alliance for Translational Research (SARTRE) for supporting this research with a DPFS grant to C.M. in 2010, and the Welsh Assembly Government for funding of this work as part of the NISCHR Ph.D. student award HS/10/33 to L.F. (2011-2014). We thank also Helen Murphy for excellent secretarial assistance, Bernhard Moss, Jürgen Schneider-Schaulies, Yusuke Yanagi, and Gavin Wilkinson for reagents, Danielle Donoghue for technical assistance, and Arwyn T. Jones and Teri Shors for critical comments.

ABBREVIATIONS USED

B95a, simian B lymphocyte strain 95 adherent; BCNA, bicyclic nucleoside analogue; BSC-1, grivet monkey kidney cell line; ddBCNA, dideoxy bicyclic nucleoside analogue; DIPEA, diisopropylethylamine; DMEM, Dulbecco's modified Eagle's medium; FBS, fetal bovine serum; HeLa, human cervical cancer cells taken from Henrietta Lacks; HFFF, human fetal foreskin fibroblast cell; IddU, 5-iodo-2′,3′-dideoxyuridine; MV, mature intracellular virus; nd, not done; pfu, plaque forming unit; p.i., postinfection; RK13, rabbit kidney epithelial cell line 13; sfu, syncytia forming unit; $TCID_{50}$, tissue culture inhibitory concentration 50%; VACV, vaccinia virus; Vero, kidney epithelial cells from an African green monkey; WR, Western Reserve strain of vaccinia virus.

REFERENCES

(1) Geddes, A. M. The history of smallpox. *Clin Dermatol.* **2006**, *24*, 152−157.

(2) Andrei, G.; Snoeck, R. Cidofovir activity against poxvirus infections. *Viruses-Basel.* **2010**, *2*, 2803−2830.

(3) Becker, M. N.; Obraztsova, M.; Kern, E. R.; Quenelle, D. C.; Keith, K. A.; Prichard, M. N.; Luo, M.; Moyer, R. W. Isolation and characterization of cidofovir resistant vaccinia viruses. *Virol. J.* **2008**, *5*, 58.

(4) van der Wouden, J. C.; van der Sande, R.; van Suijlekom-Smit, L. W.; Berger, M.; Butler, C. C.; Koning, S. Interventions for cutaneous molluscum contagiosum. *Cochrane Database of Systematic Reviews* (Online). **2009**, CD004767.

(5) Rimoin, A. W.; Mulembakani, P. M.; Johnston, S. C.; Lloyd-Smith, J. O.; Kisalu, N. K.; Kinkela, T. L.; Blumberg, S.; Thomassen, H. A.; Pike, B. L.; Fair, J. N.; Wolfe, N. D.; Shongo, R. L.; Graham, B. S.; Formenty, P.; Okitolonda, E.; Hensley, L. E.; Meyer, H.; Wright, L. L.; Muyembe, J. J. Major increase in human monkeypox incidence 30 years after smallpox vaccination campaigns cease in the Democratic Republic of Congo. *Proc. Natl. Acad. Sci. U. S. A.* **2010**, *107*, 16262−16267.

(6) Duraffour, S.; Vigne, S.; Vermeire, K.; Garcel, A.; Vanstreels, E.; Daelemans, D.; Yang, G.; Jordan, R.; Hruby, D. E.; Crance, J. M.; Garin, D.; Andrei, G.; Snoek, R. Specific targeting of the F13L protein by ST-246 affects orthopoxvirus production differently. *Antiviral Ther.* **2008**, *13*, 977−990.

(7) Yang, G.; Pevear, D. C.; Davies, M. H.; Collett, M. S.; Bailey, T.; Rippen, S.; Barone, L.; Burns, C.; Rhodes, G.; Tohan, S.; Huggins, J. W.; Baker, R. O.; Buller, R. L.; Touchette, E.; Waller, K.; Schriewer, J.; Neyts, J.; DeClercq, E.; Jones, K.; Hruby, D.; Jordan, R. An orally bioavailable antipoxvirus compound (ST-246) inhibits extracellular virus formation and protects mice from lethal orthopoxvirus challenge. *J. Virol.* **2005**, *79*, 13139−13149.

(8) Pollara, J. J.; Laster, S. M.; Petty, I. T. D. Inhibition of poxvirus growth by terameprocol, a methylated derivative of nordihydroguaiaretic acid. *Antiviral Res.* **2010**, *88*, 287−295.

(9) Yanagi, Y.; Takeda, M.; Ohno, S. Measles virus: Cellular receptors, tropism and pathogenesis. *J. Gen. Virol.* **2006**, *87*, 2767−2779.

(10) Zhang, N.; Chen, H. M.; Sood, R.; Kalicharran, K.; Fattom, A. I.; Naso, R. B.; Barnard, D. L.; Sidwell, R. W.; Hosmane, R. S. In vitro inhibition of the measles virus by novel ring-expanded ('fat') nucleoside analogues containing the imidazo[4,5-*e*]diazepine ring system. *Bioorg. Med. Chem. Lett.* **2002**, *2* (12), 3391−3394.

(11) McGuigan, C.; Pathirana, R. N.; Snoeck, R.; Andrei, G.; De Clercq, E.; Balzarini, J. Discovery of a new family of inhibitors of human cytomegalovirus (HCMV) based upon lipophilic alkyl furano pyrimidine dideoxy nucleosides: Action via a novel non-nucleosidic mechanism. *J. Med. Chem.* **2004**, *47*, 1847−1851.

(12) Bugert, J. J.; Jones, A. T.; McGuigan, C. Biological evaluation of cf1821 antiviral activity against vaccinia virus. Oral presentation W 3−4 at the 27th Annual Meeting of the American Society for Virology. Cornell University, Ithaca, NY. July 12−16, 2008.

(13) Mathé, C.; Gosselin, G. L-Nucleoside enantiomers as antivirals drugs: A mini-review. *Antiviral Res.* **2006**, *71*, 276−281.

(14) Buti, M.; Esteban, R. Entecavir, FTC, L-FMAU, LdT and others. *J. Hepatol.* **2003**, *39*, S139−S142.

(15) Coates, J. A. V.; Cammack, N.; Jenkinson, H. J.; Mutton, I. M.; Pearson, B. A.; Storer, R.; Cameron, J. M.; Penn, C. R. The separated enantiomers of 2′-deoxy-3′-thiacytidine (BCH 189) both inhibit human immunodeficiency virus replication in vitro. *Antimicrob. Agents Chemother.* **1992**, *36*, 202−205.

(16) Furman, P. A.; Davis, M.; Liotta, D. C.; Paff, M.; Frick, L. W.; Nelson, D. J.; Dornsife, R. E.; Wurster, J. A.; Wilson, L. J.; Fyfe, J. A.; Tuttle, J. V.; Miller, W. H.; Condreay, L.; Averett, D. R.; Schinazi, R. F.; Painter, G. R. The anti-hepatitis B virus activities, cytotoxicities, and anabolic profiles of the (−) and (+) enantiomers of *cis*-5-fluoro-1-[2-(hydroxymethyl)-1,3-oxathiolan-5-yl]cytosine. *Antimicrob. Agents Chemother.* **1992**, *36*, 2686−2692.

(17) Lin, T. S.; Luo, M. Z.; Liu, M. C.; Pai, S. B.; Dutschman, G. E.; Cheng, Y. C. Synthesis and biological evaluation of 2′,3′-dideoxy-L-pyrimidine nucleosides as potential antiviral agents against human immunodeficiency virus (HIV) and hepatitis B virus (HBV). *J. Med. Chem.* **1994**, *37*, 798−803.

(18) Chu, C. K.; Ma, T.; Shanmuganathan, K.; Wang, C.; Xiang, Y.; Pai, S. B.; Yao, G.-Q.; Sommadossi, J.-P.; Cheng, Y.-C. Use of 2′-fluoro-5-methyl-β-L-arabinofuranosyluracil as a novel anti-viral agent for hepatitis B virus and Epstein−Barr virus. *Antimicrob. Agents Chemother.* **1995**, *39*, 979−981.

(19) Lin, T. S.; Luo, M. Z.; Liu, M. C.; Zhu, Y.-L.; Gullen, E.; Dutschman, G. E.; Cheng, Y. C. Design and synthesis of 2′,3′-dideoxy-2′,3′-didehydro-β-L-cytidine (β-L-d4C) and 2′,3′-dideoxy-2′,3′-didehydro-β-L-5-fluorocytidine (β-L-Fd4C) cytidine, two exceptionally potent inhibitors of human hepatitis B virus (HBV) and potent inhibitors of human immunodeficiency virus (HIV) in vitro. *J. Med. Chem.* **1996**, *39*, 1757−1759.

(20) Wang, P.; Gullen, B.; Newton, M. G.; Cheng, Y. C.; Schinazi, R.; Chu, C. K. Asymmetric synthesis and antiviral activities of L-carbocyclic 2′,3′-didehydro-2′,3′-dideoxy and 2′,3′-dideoxy nucleosides. *J. Med. Chem.* **1999**, *42*, 3390−3399.

(21) Schinazi, R. F.; Chu, C. K.; Peck, A.; McMillan, A.; Mathis, R.; Cannon, D.; Jeong, L. S.; Beach, J. W.; Choi, W. B.; Yeola, S.; Liotta, D. C. Activities of the four optical isomers of 2′,3′-dideoxy-3′-thiacytidine (BCH-189) against human immunodeficiency virus type 1 in human lymphocytes. *Antimicrob. Agents Chemother.* **1992**, *36*, 672−676.

(22) Chang, C. N.; Doong, S. L.; Zhou, J. H.; Beach, J. W.; Jeong, L. S.; Chu, C. K.; Schinazi, R. F.; Liotta, D. C.; Cheng, Y. C. Deoxycytidine deamination-resistant stereoisomer is the active form of (−)-2′,3′-dideoxy-3′-thiacytidine in the inhibition of hepatitis B virus replication. *J. Biol. Chem.* **1992**, *267*, 13938−13942.

(23) McGuigan, C.; Yarnold, C.; Jones, G.; Velasquez, S.; Barucki, H.; Brancale, A.; Andrei, G.; Snoeck, R.; De Clercq, E.; Balzarini, J. Potent and selective inhibition of varicella-zoster virus (VZV) by nucleoside analogues with an unusual bicyclic base. *J. Med. Chem.* **1999**, *42*, 4479−4484.

(24) McGuigan, C.; Brancale, A.; Barucki, H.; Srinivasan, S.; Jones, G.; Pathirana, R.; Blewett, S.; Alvarez, R.; Yarnold, C.; Carangio, A.; Velasquez, S.; Andrei, G.; Snoeck, R.; De Clercq, E.; Balzarini, J. Fluorescent bicyclic furo pyrimidine deoxynucleoside analogs as potent and selective inhibitors of VZV and potential future drugs for the treatment of chickenpox and shingles. *Drugs Future* **2000**, *25*, 1151−1161.

(25) McGuigan, C.; Barucki, H.; Blewett, S.; Carangio, A.; Erichsen, J. T.; Andrei, G.; Snoeck, R.; De Clercq, E.; Balzarini, J. Highly potent and selective inhibition of varicella-zoster virus by bicyclic furo pyrimidine nucleosides bearing an aryl side chain. *J. Med. Chem.* **2000**, *43*, 4993−4997.

(26) McGuigan, C.; Brancale, A.; Barucki, H.; Srinivasan, S.; Jones, G.; Pathirana, R.; Carangio, A.; Blewett, S.; Luoni, G.; Bidet, O.; Jukes, A.; Jarvis, C.; Andrei, G.; Snoeck, R.; De Clercq, E.; Balzarini, J. Furano pyrimidines as novel potent and selective anti-VZV agents. *Antiviral Chem. Chemother.* **2001**, *12*, 77−89.

(27) Delbederi, Z.; Fossey, C.; Fontaine, G.; Benzaria, S.; Gavriliu, D.; Ciurea, A.; Lelong, B.; Ladurée, D.; Aubertin, A.; Kirn, A. Activity of C-5 substituted β-D- and β- L-D_4T analogues. *Nucleosides, Nucleotides Nucleic Acids* **2000**, *19*, 1441−1461.

(28) Sugeac, E.; Fossey, C.; Ladurée, D.; Schmidt, S.; Laumond, G.; Aubertin, A.-M. Synthesis and Anti-HIV activity of some heterodimers [NRTI]-glycyl-succinyl-[trovirdine analogue] of known HIV-1 reverse transcriptase inhibitors. *J. Enzyme Inhib. Med. Chem.* **2003**, *18*, 175−186.

(29) Classon, B.; Garegg, P. J.; Samuelsson, B. A facile preparation of 2′,3′-unsaturated nucleosides and hexopyranosides from acetylated halohydrins by reductive elimination. *Acta Chem. Scand.* **1982**, *B 36*, 251−253.

(30) Asakura, J.; Robins, M. Cerium(IV)-mediated halogenation at C-5 of uracil derivatives. *J. Org. Chem.* **1990**, *55*, 4928−4933.

(31) Vanhaesebroeck, B.; Leevers, S. J.; Ahmadi, K.; Timms, J.; Katso, R.; Driscoll, P. C.; Woscholski, R.; Parker, P. J.; Waterfield, M. D. Synthesis and function of 3-phosphorylated inositol lipids. *Annu. Rev. Biochem.* **2001**, *70*, 535−602.
(32) Chung, C. S.; Huang, C. Y.; Chang, W. Vaccinia virus penetration requires cholesterol and results in specific viral envelope proteins associated with lipid rafts. *J. Virol.* **2005**, *79*, 1623−1634.
(33) Avota, E.; Muller, N.; Klett, M.; Schneider-Schaulies, S. Measles virus interacts with and alters signal transduction in T-cell lipid rafts. *J. Virol.* **2004**, *78*, 9552−9559.
(34) Doceul, V.; Hollinshead, M.; van der Linden, L.; Smith, G. L. Repulsion of superinfecting virions: A mechanism for rapid virus spread. *Science* **2010**, *12* (327), 873−876.
(35) Townsley, A. C.; Weisberg, A. S.; Wagenaar, T. R.; Moss, B. Vaccinia virus entry into cells via a low-pH-dependent endosomal pathway. *J. Virol.* **2006**, *80*, 8899−8908.
(36) Bugert, J. J. Unpublished results. 2008.
(37) Farleigh, L. E ; Bugert, J. J. Unpublished results. 2011.
(38) Hashimoto, K.; Ono, N.; Tatsuo, H.; Minagawa, H.; Takeda, M.; Takeuchi, K.; Yanagi, Y. SLAM (CD150)-independent measles virus entry as revealed by recombinant virus expressing green fluorescent protein. *J. Virol.* **2002**, *76*, 6743−6749.
(39) Furesz, J.; Moreau, P. Plaque formation by polio and measles viruses in BS-C-1 (HOPPS) cells derived from the African green monkey. *Can. J. Microbiol.* **1965**, *11*, 435−439.
(40) Reed, L. J.; Muench, H. A simple method of estimating fifty percent endpoints. *Am. J. Hyg.* **1938**, *27*, 493−497.

Chapter 8

New Method for the Assessment of Molluscum Contagiosum Virus Infectivity

Subuhi Sherwani, Niamh Blythe, Laura Farleigh, and Joachim J. Bugert

Abstract

Molluscum contagiosum virus (MCV), a poxvirus pathogenic for humans, replicates well in human skin in vivo, but not in vitro in standard monolayer cell cultures. In order to determine the nature of the replication deficiency in vitro, the MCV infection process in standard culture has to be studied step by step. The method described in this chapter uses luciferase and GFP reporter constructs to measure poxviral mRNA transcription activity in cells in standard culture infected with known quantities of MCV or vaccinia virus. Briefly, MCV isolated from human tissue specimen is quantitated by PCR and used to infect human HEK293 cells, selected for ease of transfection. The cells are subsequently transfected with a reporter plasmid encoding firefly luciferase gene under the control of a synthetic early/late poxviral promoter and a control plasmid encoding a renilla luciferase reporter under the control of a eukaryotic promoter. After 16 h, cells are harvested and tested for expression of luciferase. MCV genome units are quantitated by PCR targeting a genome area conserved between MCV and vaccinia virus. Using a GFP reporter plasmid, this method can be further used to infect a series of epithelial and fibroblast-type cell lines of human and animal origin to microscopically visualize MCV-infected cells, to assess late promoter activation, and, using these parameters, to optimize MCV infectivity and gene expression in more complex eukaryotic cell culture models.

Key words: Molluscum contagiosum virus, Luciferase reporter construct, Eukaryotic cells, Infection, Transfection, Quantitative PCR

1. Introduction

Molluscum contagiosum virus (MCV) does not produce a quantifiable cytopathic effect and does not produce viral progeny in infected standard cell cultures. But small amounts of viral mRNA and protein expression can be detected indicating that MCV virions are transcriptionally active (1–3). Many investigators have observed

Stuart N. Isaacs (ed.), *Vaccinia Virus and Poxvirology: Methods and Protocols*, Methods in Molecular Biology, vol. 890,
DOI 10.1007/978-1-61779-876-4_8,

that poxvirus transcription complexes can drive luciferase reporters under the control of poxviral promoters in plasmids in poxvirus-infected cells. A recent paper uses this as a method to diagnose orthopoxvirus infections (4).

In the assay described in this chapter, the same principle is used. We introduce a luciferase reporter expression in trans as a new surrogate marker of infectivity and gene expression for MCV. To compare the infectivity of MCV with other poxviruses (11), the number of virions must be determined. Quantitation by EM or OD300 can be used (5), but requires relatively large amounts of gradient purified virons. However, currently, MCV can only be isolated from clinical specimens and thus is difficult to obtain amounts sufficient for gradient purification (5). PCR is an alternative method of quantitation of smaller amounts of poxviruses from clinical specimens, which is both reliable and highly specific for individual poxviruses. The method described in this chapter uses a novel PCR target in an area with significant DNA homology (~65%) between MCV and vaccinia virus strain WR (VACV-WR). The MCV gene is mc129R, which is homologous to the VAVWR144 (also called A24R gene encoding RPO132, the large subunit of the DNA-dependent RNA polymerase). The method provides a means to quantitate poxviral genome units in the same virus preparations used to compare transcriptional activity and infectivity of MCV and VACV-WR.

2. Materials

2.1. MCV Luciferase Reporter Assay

2.1.1. Infection–Transfection of Cell Cultures

1. OPTIMEM, stored at 4°C.
2. Plasmids described in Subheading 2.3 (see Note 1).
3. Lipofectamine 2000, stored at 4°C until used.
4. Human HEK 293 cells (ATCC CRL1573) (see Note 2).
5. Dulbecco's modified Eagle medium: DMEM, high glucose with glutamine, stored at 4°C until used.
6. Fetal calf serum: FCS, stored in aliquots at –70°C until used.
7. Cell growth medium: DMEM with 10% FCS.

2.1.2. Luciferase Assay (The Dual-Luciferase® Reporter Assay System from Promega)

1. Dual Luciferase Assay Substrate (lyophilized) stored at –20°C for up to 6 months reconstituted.
2. 10 ml Luciferase Assay Buffer II, stored in a 1-ml aliquots at –20°C for up to 6 months until used.
3. Stop and Glo Substrate (50×) stored at –20°C.

4. 10 ml of Stop & Glo Buffer, stored in a 1-ml aliquots at –20°C for up to 6 months until used.
5. 30 ml of Passive Lysis Buffer (5×) stored at –20°C, then diluted to 1× using sterile water, and kept at 4°C until used.
6. Clear film plate protectors (to prevent evaporation from wells).
7. FLUOStar Luminometer.

2.2. MCV and VACV Quantitative PCR Assay

1. Primers outlined in Table 1 suspended in injection-grade water to a final concentration of 100 pmol/μl and stored at –20°C.
2. MCV isolated from human skin biopsy material as described previously (5) and kept in 100-μl aliquots frozen at –70°C in PBS (see Note 3).
3. VACV-WR, vaccinia virus, strain WR (kind gift of B. Moss) was prepared and purified from infected HeLa cells, titrated in BSC-1 cells, and kept in 100-μl aliquots frozen at –70°C in PBS (see Note 3).
4. DNAse at 1 mg/ml.
5. DNAse/BamHI buffer: 78 μl water, 2 μl DNAse, 20 μl 10× BamHI buffer from New England Biolabs.
6. High Pure viral nucleic acid (HPVNA) kit (e.g., Roche).
7. Nanodrop-Spectrophotometer.

Table 1
MCV–VACV quantitative PCR assay primers

Primer ID	Primer sequence (nhb)	Primer length	Product size (nucleotide position), GenBank Acc. #
Mcv129 1-2F149275	5′-CCGCACTACTCCTGGATGCAGAA-3′	23	576 bp (149,275–149,850), U60315
Mcv129 1-3R149850	5′-CTGGATGTCGGAGAAGGTCATG-3′	22	
VACV-WR 1-2F132482	5′-CCTCACTATTCATGGATGCAGAA-3′ (3)	23	573 bp (132,482–122,054), AY243312
VACV-WR 1-3R133054	5′-CTGAATGTCAGAGAATGTCATG-3′ (3)	22	

nhb nonhomologous bases underlined (number of mismatches)
Primers were designed using BLAST2 (NCBI: http://blast.ncbi.nlm.nih.gov/) alignment of MCV (GenBank accession # U60315) and VACV-WR (GenBank accession # AY243312) genome sequences and Vector NTI vs. 4.0, 1994–1996 InforMax Inc.

8. ImageJ (Wayne Rasband (wayne@codon.nih.gov) Research Services Branch, National Institute of Mental Health, Bethesda, Maryland, USA).
9. Injection-grade water.
10. AmpliTaq 360 polymerase (5 U/μl).
11. dNTP (0.2 mM).
12. 10× PCR buffer.
13. 2% Agarose gel.
14. Ethidium bromide solution: 10 mg/ml stock solution in demineralized water and used at 20 μl per 200 ml.

2.3. Plasmids (See Fig. 1)

1. *PCR control plasmid*. The complete MCV-1 genome was cloned (6) and sequenced (7, 8) and the redundant MCV genome fragment library of MCV type 1 was submitted to

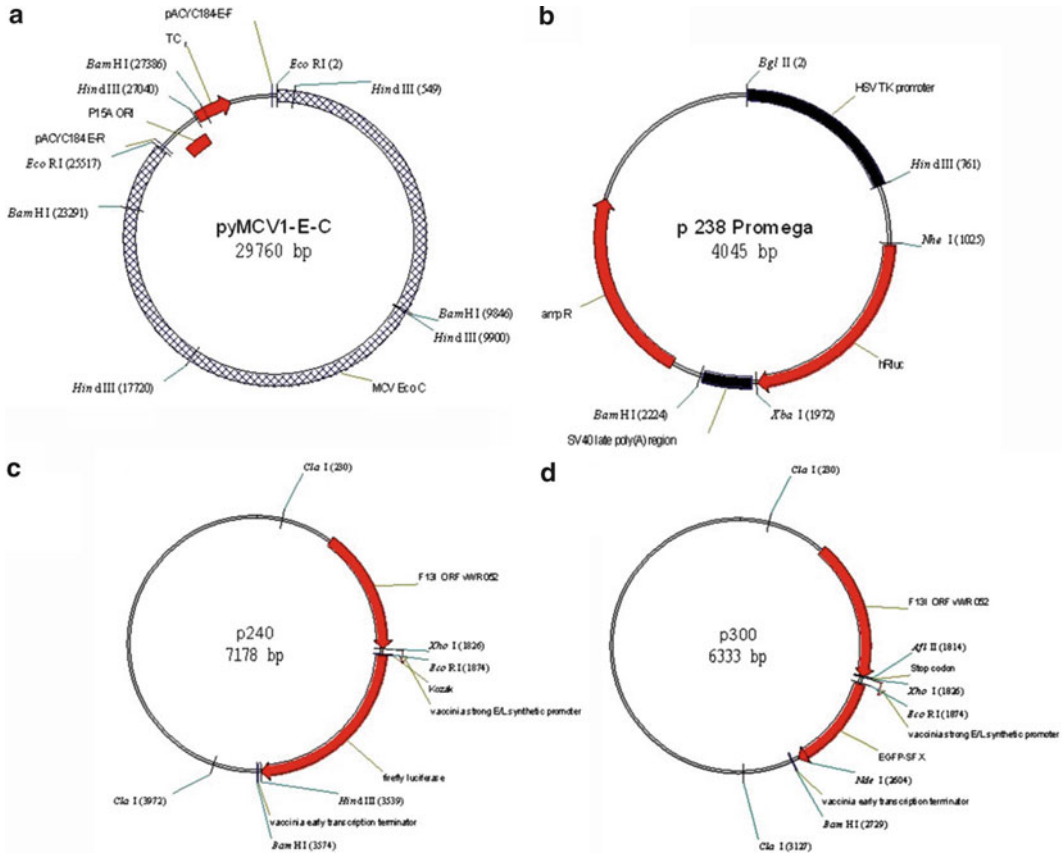

Fig. 1. Plasmid constructs. VectorNTI drawings for the recombinant plasmids (**a**) pyMCV1-EcoRI-fragment C (pyMCV1-E-C; available from ATCC molecular section), (**b**) phRG-TK (Promega; Internal lab reference number p238), (**c**) pRB21-pE/L-FF luciferase (p240), and (**d**) pRB21-pE/L-EGFP-SFX (p300).

ATCC for safekeeping in 2003 and 2008. For the quantitative PCR assay, the genomic MCV-1 *Eco*RI fragment C (25,516 bp) cloned into bacterial plasmid vectorp pACYC184 was used as a MCV target control (pyMCV1-E-C, see Fig. 1a).

2. *Transfection control plasmid*. Plasmid phRG-TK (Promega GenBank accession number AF362545: 4,045 bp), expressing renilla luciferase under the control of the herpes simplex virus TK gene promoter. In this protocol, this plasmid is called p238 and used as plasmid transfection control (p238 Promega; see Fig. 1b).
3. *Poxviral luciferase reporter plasmid*. The coding sequence of firefly luciferase (*Photinus pyralis* GenBank accession number M15077) was amplified with a modified Kozak sequence by PCR and ligated into the pRB21 donor plasmid (kind gift of B. Moss (9, 10)) using the EcoRI and HindIII restriction sites in the donor plasmid multiple cloning site, resulting in the pRB21-E-Koz-Fireflyluciferase-H(alsocalledpRB21-pE/L-FF luciferase) construct of 7,178 bp with the internal lab designation p240 (p240, see Fig. 1c).
4. *Poxviral EGFP reporter plasmid*. The coding sequence of EGFP was amplified from a commercially available plasmid with a modified Kozak sequence by PCR and ligated into the pRB21 donor plasmid using the EcoRI and NheI restriction sites in the donor plasmid multiple cloning site, resulting in the pRB21-E-Koz-EGFP-X-flag-strepII-N construct (also called pRB21-pE/L-EGFP-SFX) of 6,333 bp with the internal lab designation p300 (p300, see Fig. 1d).

3. Methods

3.1. Infection–Transfection: Luciferase Assay

3.1.1. Infection/Transfection

1. Prepare enough 12-well plates containing HEK 293 cells in growth media to allow for infection/transfection in triplicate for each experimental condition (including a mock that will be transfected but not infected, as well as wells that will be harvested at 16 h and wells that will be continued to be incubated for days) (see Note 4).
2. Thaw virus aliquots, sonicate, and keep on ice.
3. Thaw plasmid DNA and keep on ice.
4. Bring OptiMEM and Lipofectamine 2000 to room temperature (RT).
5. Prepare transfection mixes by adding a dilution of 2 µl of Lipofectamine 2000 in 50 µl of OptiMEM to a dilution of 0.3 µg of each plasmid DNA (p240 FF reporter and p238

transfection control plasmid, p300 EGFP reporter) in 50 µl of OptiMEM. Mix gently for 15 min at RT in the dark to allow formation of transfection complexes.

6. Remove growth media from HEK293 cells and put 100 µl of transfection mix in each well.
7. Combine 100 µl each of ice-cold virus in PBS and 100 µl of transfection mix at RT and transfer the mixture into appropriate wells of HEK293 cells (see Note 5).
8. Incubate for 16 h at 37°C in 5% CO_2 atmosphere (see Note 6).

3.1.2. Microscopy and Collection of Cells for Luciferase Assay

1. At 16 h post infection (p.i.), inspect cells transfected with the GFP reporter plasmid using live cell microscopy. Document GFP-positive cells noting that MCV does not show GFP-positive cells after 16 h, whereas WR shows multiple GFP-positive cells.
2. Upon further incubation for another 4 days (5 days p.i.), some individual cells in the MCV-infected wells will show medium to strong GFP signals (see Note 7). At the same time point, the WR-infected wells will show extensive plaques and cell degradation (see Fig. 2a–d).
3. For luciferase assay, at 16 h p.i., wash adherent cells in wells once with PBS and add 100 µl of 1× passive lysis buffer to each well (see Note 8).

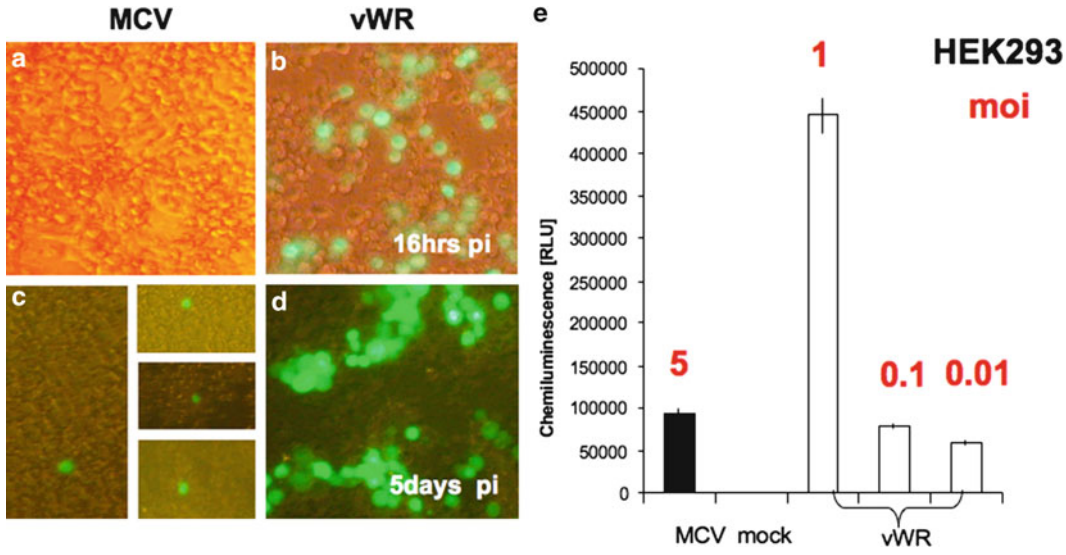

Fig. 2. Images of luciferase and GFP in infected/transfected cells and quantification of luciferase output. *Panels* (**a**–**d**) show HEK 293 cells infected with MCV (**a** and **c**), and vWR (**b** and **d**). Inserts in **c** show individual GFP-positive cells. *Panel* **e** shows a histogram of luciferase data giving chemiluminescence in RLU. HEK 293 cells were infected with MCV or vWR at the indicated moi, and collected at 16 h p.i.

4. Cover the 12-well plate with clear film plate protectors to stop evaporation and incubate with agitation on a belly-dancer at RT for 15 min. Plates are then frozen at −20°C for at least 15 min or stored overnight or for up to 2 weeks before assayed.
5. Cell lysates are tested for luciferase activity by adding 100 µl Dual Luciferase Assay Substrate to each well (see Note 9).
6. Luciferase activity is then measured in a FLUOStar Luminometer.
7. Data is compiled in a Microsoft EXCEL file and evaluated using standard statistical protocols (average, standard deviation, Student's *P* test). A typical result is shown in Fig. 2e (see Notes 6, 10, and 11).

3.2. Quantitative PCR Assay

1. Incubate equal volumes of freshly thawed virions (100-µl aliquot) in 100 µl DNAse/BamHI buffer for 30 min at 37°C.

3.2.1. Virus and DNA Preparation

2. Extract viral genomic DNA using a HPVNA kit following the manufacturer's instructions. The control plasmid pyMCV1-E-C (see Fig. 1a) is prepared using the same procedure.
3. Determine the DNA concentration of the control plasmid using a Nanodrop-Spectrophotometer or a similar device.
4. Calculate molecule numbers using the average molecular weight of DNA molecules and Avogadro's number (6.02×10^{23} per mole). The molecular weight of a plasmid (in Daltons) can be estimated as MW of a double-stranded DNA molecule (http://www.epibio.com/techapp.asp) = (# of base pairs) × (650 Da/base pair). The plasmid pyMCV1-E-C has 29,760 bp. Thus, the molecular weight is calculated as 19.344 MDa and thus 19.344 ng of plasmid would be 6.02×10^8 mol. The actual plasmid concentration was 21 ng/µl (±1.7) and, thus, represented 6.5×10^8 mol/µl. From this value, the molecule numbers for the pyMCV1-E-C twofold dilution series are calculated (see Fig. 3d). The molecule numbers are then correlated to the pixel numbers of bands on a gel quantitated by ImageJ (see Fig. 3d).

3.2.2. PCR Reaction (see Note 12)

1. Prepare twofold dilutions of viral genomic DNA and plasmid control in injection-grade water and store at −20°C.
2. Prepare PCR assays as outlined in Table 2. PCR reaction conditions are included in the table.
3. Visualize PCR bands by loading a 2% agarose gel with 10 µl from each PCR reaction and run for 1 h at 100 V (constant voltage). Stain with ethidium bromide, photograph with a digital unit, and export into a jpeg file (see Note 13).
4. To quantitate the PCR product, one can use the captured bands on the jpeg photograph with a series of identical gates

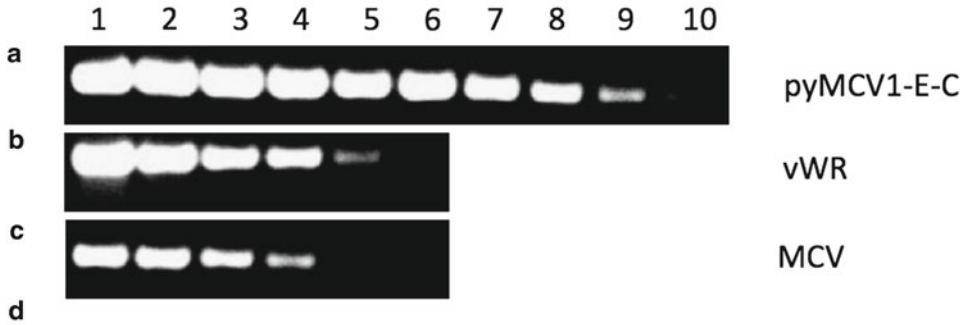

d

lane# (gel a)	1	2	3	4	5	6	7	8	9	data
DNA										
pyMCV	406,250	203,125	101,562	50,781	25,390	12,695	6,347	**3,173**	**1,586**	mol
pyMCV	138,794	159,136	140,851	129,871	107,126	112,165	89,590	67,495	27,779	pixel
lane# (gel b)					1	2	3	4	5	
vWR					156,659	126,644	87,696	71,008	15,102	pixel
lane# (gel c)						1	2	3	4	
MCV						77,875	73,384	55,270	28,726	pixel

Fig. 3. PCR quantification of purified DNA. *Panels* **a**–**c** show twofold dilutions of poxviral genomic DNA purified from DNAse-treated virions (**b** and **c**) and plasmid DNA repurified using the HPVNA kit (**a**). Lane numbers at the top of the figure refer to $\log_2$ dilutions from 1 to 10. *Panel* **d** tabulates the calculated molecular number for the reference plasmid pyMCV1-E-C (pyMC) (1,000× by nanodrop in 10 μl of original DNA prep) and the ImageJ pixels for each band in gels **a** to **c**. ImageJ (Wayne Rasband (wayne@codon.nih.gov) Research Services Branch, National Institute of Mental Health, Bethesda, Maryland, USA) was used to quantitate pixel densities in boxes of 212 × 42 pixels.

Table 2
PCR reaction

	Volume (μl)
Primer 1-2F[a] (100 pmol/μl)	0.5
Primer 1-3R[a] (100 pmol/μl)	0.5
Injection-grade water	36.8
10× PCR buffer	5.0
TaKaRa dNTP (0.2 mM)	2.0
Template (series of twofold dilutions)	5.0
AmpliTaq 360 polymerase (1 unit of 5 U/μl)	0.2
Total	50.0

PCR reaction: 2 min of denaturation at 96°C; and then 45 cycles of 1 min at 96°C, 2 min at 55°C, and 3 min at 72°C. Block and then cool to 10°C

[a]For MCV Primer 1-2F and Primer 1-3R, use Mcv129 1-2F149275 and Mcv129 1-3R149850, respectively. For WR Primer 1-2F and Primer 1-3R, use VACV-WR 1-2F132482 and VACV-WR 1-3R133054, respectively

using IMAGEJ software to produce a quantified pixel output that can be imported into a Microsoft EXCEL file.

5. Plot quantitative results of digital imaging (quantified pixel output) of a twofold dilution series of plasmid pyMCV1-E-C against molecule numbers using Microsoft EXCEL software.
6. Take molecule/genome equivalent numbers from the calibration plot and compare to the pixel readings obtained for VACV-WR. Tabulate results and evaluate using standard statistical protocols (average, standard deviation, Student's *P* test).
7. Results from a PCR reaction and the corresponding mole numbers and pixels are shown in Fig. 3d. In that figure, for gel a, lane 9, the signal (27,779 pixels) for the dilution of the MCV control plasmid (pyMCV1-E-C) correlates to 1.586×10^6 plasmid units. The band in gel c (MCV PCR) with comparable pixel density (i.e., within 10%) is in lane 4 with a pixel value of 28,726 pixels. If the 1.586×10^6 mol are multiplied by the dilution factor (16×), the MCV aliquot of 100 µl used for genomic DNA preparation contained 2.5×10^7 mol/genome units. If the pixel values obtained for vWR in gel b, lane 4 (71,008), are used in the same way and related to gel a, lane 8 (67,495 pixels), after multiplying by the dilution factor (16×), a molecule number of 5×10^7 is obtained. This can then be used to relate to the pfu. If WR was at 1.6×10^6 pfu in 100 µl, the pfu-to-genome unit ratio is 1:31 (see Notes 14–16).

4. Notes

1. All plasmid DNA should be purified using 100-µg capacity midiprep-columns (HPVNA) and then stored in elution buffer at –20°C until used.
2. The assay depends to a significant degree on the transfectability of the cell cultures involved. Human keratinocytes and fibroblast cell lines are most interesting as possible natural hosts for MCV, but they are also hard to transfect. We found HEK 293 cells to be the best transfected cell line. However, while this cell line shows robust reporter signals, it is clearly not the type of cell MCV naturally infects.
3. We prepare vaccinia virus and MCV preparations in 1 ml PBS and then immediately make ten 100-µl aliquots and freeze. The vaccinia virus stock was generated by infecting one T150 flask containing adherent HeLa cells. Harvest of the infected cells and resuspending them in 1 ml PBS yielded a titer of 2×10^7 pfu/ml. Thus, each of the ten 100-µl aliquots of vaccinia virus used here contained 2×10^6 pfu. The 100-µl aliquot MCV

contained an unknown number of MCV particles, but is quantified using the described PCR method.

4. Transfection efficiency can vary considerably from cell batch to cell batch. Passage number (best low), cell confluence (best below 60%), and time of culture prior to experiment (best no longer than 24 h) are determinant factors.
5. While in this protocol we transfect adherent cells, we have found that for some harder-to-transfect cells (e.g., human fibroblasts) we can get higher transfection efficiency when cells are in suspension.
6. The incubation time of 16 h allows for a robust signal from the transfection control plasmid p238, so firefly signal readings can be adjusted to renilla transfection efficiency readings between experiments.
7. Transfected plasmids with poxviral transcription signals can be transcribed by the poxviral transcription complex produced by transcriptionally active cores after entry. It is not clear whether the transcription complex is accessed inside partially uncoated virions, with plasmid DNA getting inside cores, or by transcription complex that is released into the cytoplasm. MCV-infected cells produce a robust luciferase signal after 16 h. However, GFP is only visibly expressed in a small number of individual cells, detectable after 5 days of incubation. Potentially, other cells may express GFP at a level undetectable by microscopy. The process where cores are accessible for the reporter plasmids may be delayed in MCV-infected cells.
8. The samples for the luciferase assay are collected at 16 h post infection. This allows the control plasmid ILR#238 to get to the nucleus and be expressed to yield a robust control signal. In 293 cells, the Renilla luciferase signal can be seen in vaccinia-infected cells after 2 h, and is seen in the MCV signal after 8 h.
9. If one does not have instrumentation that can add 100 μl of PROMEGA Dual luciferase firefly substrate one can hand, pipet series of four samples in a row, then load the plate, and read. The reading time, including the initial shake for four samples, is 20 s. Doing this results in a signal loss per reading of <1%, which is less than the sample-to-sample variation in triplicate samples, when compared to machine pipetting sample per sample.
10. The signal from early poxviral promoters can be used as a surrogate parameter of viral infectivity.
11. The signal can be further dissected and used to look at early and late transcription activity using transfected plasmids with a reporter gene behind the respective promoters in isolation.

12. The conventional PCR assay described has the problem of assay-to-assay variation due to agarose gel and staining artifacts. Future advances may be the development of a real-time PCR assay using molecular Taqman probes specific to either VAVC-WR or MCV and binding in the internal section of the rather large PCR product (550 bp).
13. The source template of the PCR products produced can also be determined by XhoI digest, which cleaves the MCV product into 227- and 349-bp subfragments but does not cleave the VAVC-WR PCR product.
14. It is unclear to which extent the different GC content of the two virus genomes would affect the PCR product. This was not further investigated.
15. It is clear that vaccinia plaque-forming units cannot be directly compared to MCV virion units because of the different nature of their biological activity. However, the PCR method described in Subheading 3.2 allows a relative quantification of MCV genome equivalents to VAVC-WR infectious units measured in pfu/ml based on amplifiable genomic DNA units/molecule numbers calculated for a relatively large plasmid containing 25,517 bp of MCV sequence. As described in Subheading 3.2.2, **step 7**, the pfu-to-molecule ratio for vaccinia virus (mature virions) comes out as 1:31, in keeping with previously published ratios (12). The PCR data can be used to calculate an MCV multiplicity of infection equivalents in relation to the control plasmid molecule numbers as well as in the form of pfu equivalents in relation to a titered vaccinia stock for comparison purposes. We have found this approach to be both more reproducible and more specific than electron microscopy or OD quantifications of virions.
16. The biological activity of virions can be assessed using an in vitro transcription reaction (1, 5, 13).

References

1. Bugert JJ, Lohmuller C, Darai G (1999) Characterization of early gene transcripts of molluscum contagiosum virus. Virology 257:119–129
2. Bugert JJ, Melquiot N, Kehm R (2001) Molluscum contagiosum virus expresses late genes in primary human fibroblasts but does not produce infectious progeny. Virus Genes 22:27–33
3. Stefan Mohr S, Grandemange S, Massimi P, Darai G, Banks L, Martinou J-C, Zeier M, Muranyi W (2008) Targeting the retinoblastoma protein by MC007L, gene product of the molluscum contagiosum virus: detection of a novel virus–cell interaction by a member of the poxviruses. J Virol 82:10625–10633
4. Levy O, Oron C, Paran N, Keysary A, Israeli O, Yitzhaki S, Olshevsky U (2010) Establishment of cell-based reporter system for diagnosis of poxvirus infection. J Virol Meth 167: 23–30
5. Melquiot NV, Bugert JJ (2004) Preparation and use of Molluscum Contagiosum Virus (MCV) from human tissue biopsy specimens. In: Isaacs SN (ed) Vaccinia virus and poxvirology: methods and protocols, 1st edn. Humana, Totowa, NJ, pp 371–383

6. Bugert JJ, Darai G (1991) Stability of molluscum contagiosum virus DNA among 184 patient isolates: evidence for variability of sequences in the terminal inverted repeats. J Med Virol 33: 211–217
7. Senkevich TG, Bugert JJ, Sisler JR, Koonin EV, Darai G, Moss B (1996) Genome sequence of a human tumorigenic poxvirus: prediction of specific host response-evasion genes. Science 273:813–816
8. Senkevich TG, Koonin EV, Bugert JJ, Darai G, Moss B (1997) The genome of molluscum contagiosum virus: analysis and comparison with other poxviruses. Virology 233:19–42
9. Blasco R, Moss B (1991) Extracellular vaccinia virus formation and cell-to-cell virus transmission are prevented by deletion of the gene encoding the 37,000-Dalton outer envelope protein. J Virol 65:5910–5920
10. Blasco R, Moss B (1995) Selection of recombinant vaccinia viruses on the basis of plaque formation. Gene 158:157–162
11. Bengali Z, Townsley AC, Moss B (2009) Vaccinia virus strain differences in cell attachment and entry. Virology 389:132–140
12. Payne LG, Kristensson K (1982) Effect of glycosylation inhibitors on the release of enveloped vaccinia virus. J Virol 41:367–375
13. Shand JH, Gibson P, Gregory DW, Cooper RJ, Keir HM, Postlethwaite R (1976) Molluscum contagiosum—a defective poxvirus? J Gen Virol 33:281–295

OPEN ACCESS Freely available online

PLOS ONE

Seroprevalence of Molluscum contagiosum Virus in German and UK Populations

Subuhi Sherwani[1], Laura Farleigh[1], Nidhi Agarwal[2], Samantha Loveless[3], Neil Robertson[3], Eva Hadaschik[4], Paul Schnitzler[5], Joachim Jakob Bugert[1]*

1 Cardiff University School of Medicine, Institute of Infection and Immunity/Medical Microbiology, Cardiff, United Kingdom, **2** Dr P N Behl Skin Institute and School of Dermatology, New Delhi, India, **3** Cardiff University Medical School, Institute of Psychological Medicine and Clinical Neuroscience, Cardiff, United Kingdom, **4** Universität Heidelberg, Hautklinik, Heidelberg, Germany, **5** Universität Heidelberg, Dept.of Infectious Diseases, Heidelberg, Germany

Abstract

Molluscum contagiosum virus (MCV) is a significant but underreported skin pathogen for children and adults. Seroprevalence studies can help establish burden of disease. Enzyme linked immunosorbent assay (ELISA) based studies have been published for Australian and Japanese populations and the results indicate seroprevalences between 6 and 22 percent in healthy individuals, respectively. To investigate seroprevalence in Europe, we have developed a recombinant ELISA using a truncated MCV virion surface protein MC084 (V123-R230) expressed in *E. coli*. The ELISA was found to be sensitive and specific, with low inter- and intra-assay variability. Sera from 289 German adults and children aged 0–40 years (median age 21 years) were analysed for antibodies against MC084 by direct binding ELISA. The overall seropositivity rate was found to be 14.8%. The seropositivity rate was low in children below the age of one (4.5%), peaked in children aged 2–10 years (25%), and fell again in older populations (11–40 years; 12.5%). Ten out of 33 healthy UK individuals (30.3%; median age 27 years) had detectable MC084 antibodies. MCV seroconversion was more common in dermatological and autoimmune disorders, than in immunocompromised patients or in patients with multiple sclerosis. Overall MCV seroprevalence is 2.1 fold higher in females than in males in a UK serum collection. German seroprevalences determined in the MC084 ELISA (14.8%) are at least three times higher than incidence of MC in a comparable Swiss population (4.9%). While results are not strictly comparable, this is lower than Australian seroprevalence in a virion based ELISA (n = 357; 23%; 1999), but higher than the seroprevalence reported in a Japanese study using an N-terminal truncation of MC133 (n = 108, 6%; 2000. We report the first large scale serological survey of MC in Europe (n = 393) and the first MCV ELISA based on viral antigen expressed in *E. coli*.

Citation: Sherwani S, Farleigh L, Agarwal N, Loveless S, Robertson N, et al. (2014) Seroprevalence of Molluscum contagiosum Virus in German and UK Populations. PLoS ONE 9(2): e88734. doi:10.1371/journal.pone.0088734

Editor: James P. Stewart, University of Liverpool, United Kingdom

Received October 28, 2013; **Accepted** January 10, 2014; **Published** February 18, 2014

Funding: Subuhi Sherwani is self funded. Consumables expenses were partially supported by a Wellcome Trust grant to Bernhard Moser (grant Number WT 092488). Wellcome Trust had no role in study design, data collection and analysis, decision to publish, or preparation of the manuscript.

Competing Interests: The authors have declared that no competing interests exist.

* E-mail: bugertjj@cf.ac.uk

Introduction

After the eradication of smallpox, MCV is the principal poxvirus causing human disease [1–4]. MCV is classified as a member of the family *Poxviridae*, in its own genus *Molluscipoxvirus* [5]. It has unique features that are distinct from other poxviruses pathogenic for humans, including smallpox and monkeypox [6]. MCV shares the highest level of amino acid (aa) similarity and unique proteins with parapoxviruses such as Orf viruses [7].

MCV infects the human skin and Molluscum contagiosum (MC) is a sexually transmitted disease, with infections occurring worldwide [1,8–10]. Clinical infection is characterized by a variable number of papules, each forming a central crater filled with a waxy plug of cell debris mixed with a large numbers of virus particles. Histopathologically, MC causes a benign epidermal hyperproliferation, known as an acanthoma [11]. MC is most common in young children and teenagers. MC in immunocompromised patients results in more numerous and extensive lesions [12]. In immune-competent patients, lesion may persist for up to 12 months [11]. Spontaneous regression of MC lesions is commonly preceded by clinical signs of inflammation [13], indicating a vigorous immune response [14].

The true prevalence of MC has probably been underestimated because of the benign clinical manifestation and rare complications. Development of assays which could assist in seroprevalence studies has been hampered by unsuccessful attempts to cultivate MCV efficiently *in vitro* [15–18]. The viral genome was sequenced in 1996 [2].

In the first known MCV antibody study in 1952, Mitchell found three out of 14 MC patients with complement-fixing antibody to an antigen prepared from human MC lesions [19]. Shirodaria *et al.* used MCV cryostat sections in an immunofluorescence study of MCV antibodies, reporting IgM class of antibodies only in MCV patients and IgG antibody responses in 16.7% of healthy control subjects (n = 30) [20]. Only two seroprevalence studies using ELISA, have been reported; one by Konya and Thompson [21] in 1999 and another by Watanabe *et al.* in 2000 [22].

Konya and coworkers described in 1992 a virion based enzyme linked immunosorbent assay [23]. MCV virions were isolated from human lesion material. The antigen was extracted from pooled

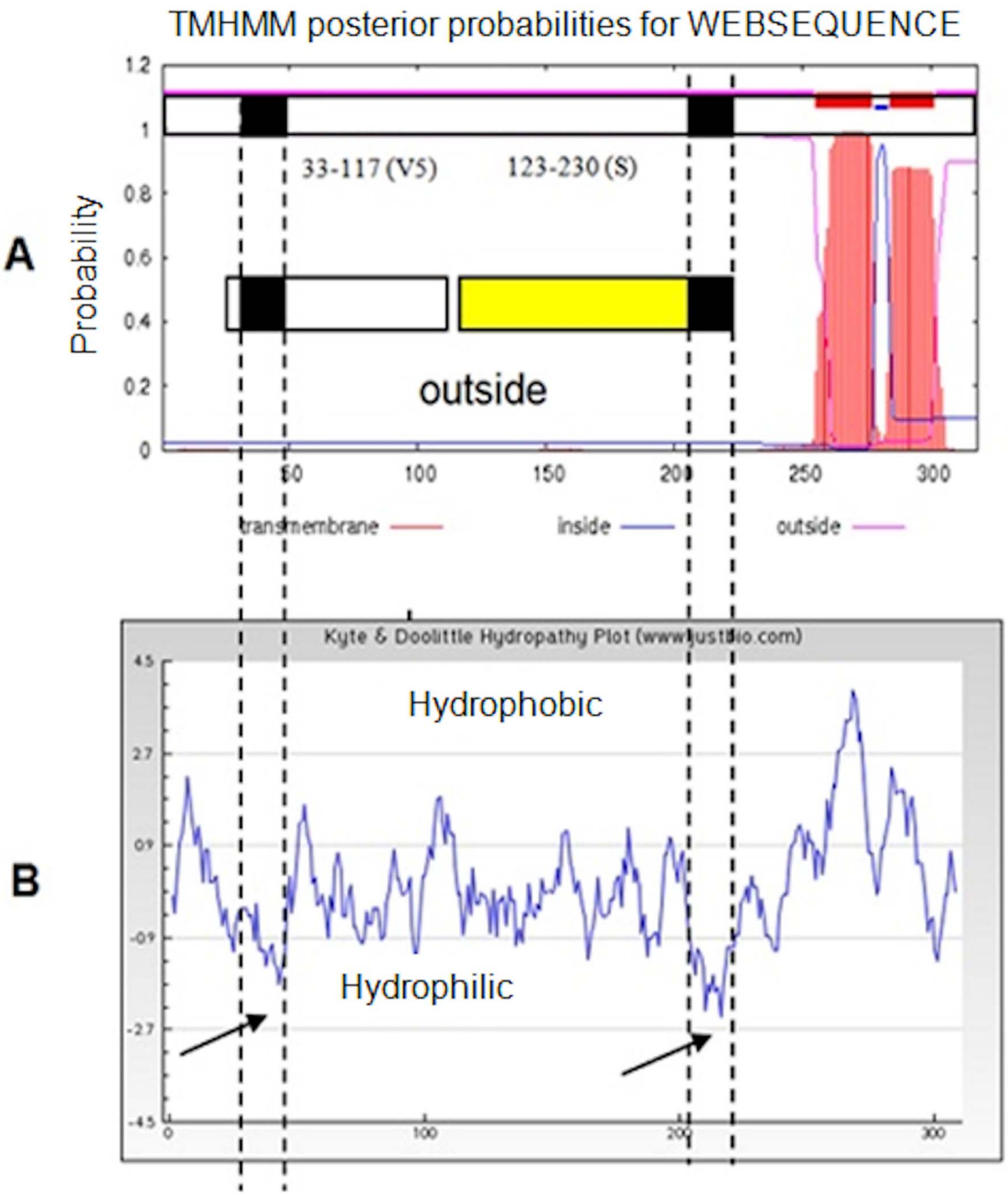

Figure 1. Bioinformatics. (A) Transmembrane plot (TMHMM Server v.2.0) [25] of mc084 amino acids 1–318; (B) hydropathy plot of MC084 protein with predicted high hydrophilic/antigenic regions indicated by black boxes. The full length ORF (MC084 1–318; predicted molecular weight 34.2 kD; shown on top) was cloned into vRB12 using specific primers tailed with restriction enzyme sites *BamHI-HindIII*) and C-terminal StrepII epitope tag. The resulting plasmid p319 was sequenced and the recombinant vaccinia virus v319 isolated on BSC-1 cells using the plaqueless mutant system [26]. N- and C-terminal (in yellow) truncations were subcloned from the original full length MCV gene into pGEX-2TK for overexpression in *E. coli* BL21 (RIL^{+}). TMHMM was used to determine transmembrane regions [26] whereas the Kyte-Doolittle plot was used to identify hydrophilic regions with predicted high antigenicity [27].
doi:10.1371/journal.pone.0088734.g001

lesions of different genotypes with epidermal protein extract used as a control. Their 1999 serological survey of a healthy Australian population (n = 357) revealed an overall seroprevalence of 23% and up to 77% in MCV infected HIV negative individuals [21].

Based on MCV sequence information then available, in 1998 Watanabe *et al.* identified two immunodominant proteins of 70 and 34 kDa and mapped them to the ORFs mc133L and mc084L, respectively [24]. The proteins are homologues of vaccinia virus proteins H3L and A27L, and major antigenic peptides of the virion particle [1,24].

Using this information they developed an ELISA, based on an N-terminal truncation of MCV virion protein MC133 produced in a Sendai virus expression system [22]. Their survey of a Japanese population of 508 subjects found mc133 specific antibodies only in

58% of patients with MC, and in only 6% of healthy controls (n = 108).

The objective of our current study was to develop a recombinant MCV ELISA using water soluble and highly antigenic truncations of MC084L expressed in *E. coli* and to establish seroprevalence in a German and a UK serum collection.

Materials and Methods

Ethics Statement

The study has ethical approval for the use of German tissues and sera (Ethikvotum S-091/2011 Hautklinik Heidelberg. Ethical approval was given by the Heidelberg University board in charge of ethical approvals, the 'Ethikkommission'. Ethical approval for UK samples was part of 'An Epidemiological study of Multiple sclerosis and other neuroinflammatory demyelinating disorders in South Wales', 05/WSE03/111. Ethical approval was given by the Cardiff University 'Biobank Ethics Board'. All patients provided prospective informed consent in writing upon admission. All children's' parents/guardians provided informed consent in writing. Class 2 GM work was notified to HSE with the project number GM 130/10.3.

pGEX-2TK Expression of Truncated MCV –GST Fusion Proteins

The plasmid pGEX-2TK was used for expression of truncated and epitope tagged MCV ORFs mc084 (V33-G117V5), MC084 (V123-R230 StrepII), and MC133 (M1-N370 StrepII) in *E. coli* with Glutathione S-Transferase (GST) fusion protein at the N terminus. Recombinant plasmids were constructed by PCR using specific primers tailed with restriction enzyme sites (*BamHI-EcoRI*) and C-terminal epitope tags.

Expression and Purification of MC084S (V123-R230) Protein

pGEX 2TK GSTmc084S (ILR#332; MC084 specific insert 107 amino acids; 14 kD) was transformed into *E. coli* BL21 (RIL^+).Cultures were induced with Isopropyl β-D-1-thiogalacto-pyranoside (IPTG) and fractions analysed for fusion protein expression by SDS-PAGE and StrepII tag expression by western blotting. Cultures were incubated at 37°C for 4 h after which the cells were harvested by centrifugation at 10,000×g for 20 min and lysed by sonification in buffer B (8 M urea, 0.1 M NaH_2PO_4, 0.01 M and Tris-HCl, pH 8.0). Lysate containing the protein of interest was added to glutathione sepharose beads and GST-MC084S was bound to beads using batch purification. The fusion protein was cleaved using Precision protease at RT overnight. AKTA-FPLC of the resulting 14 kD sized protein was done using size exclusion Superdex S200 column (GE Healthcare).

SDS-PAGE, Western Transfer and Immunodetection

Protein preparations were separated using denaturing sodium dodecyl sulphate polyacrylamide electrophoresis (SDS-PAGE) in NuPAGE Novex 4–12% Bis-tris Gels (Life technologies) and MOPS SDS running buffer (Invitrogen). Protein bands were visualised by staining with 0.01% Coomassie Brilliant Blue R-250. For immunodetection proteins prepared by SDS-PAGE were electrotransferred onto nitrocellulose and probed with Strep MAB Classic HRP conjugate (IBA). Detection by chemiluminescence was performed using Super Signal West Pico Chemiluminescent Substrate (Thermo Scientific) according to the manufacturer's recommendations.

Human Serum/Tissue Samples

314 serum samples and lesion material from patients with molluscum contagiosum were collected at University Hospital Heidelberg, Germany, between 2007–2011. 79 UK sera samples

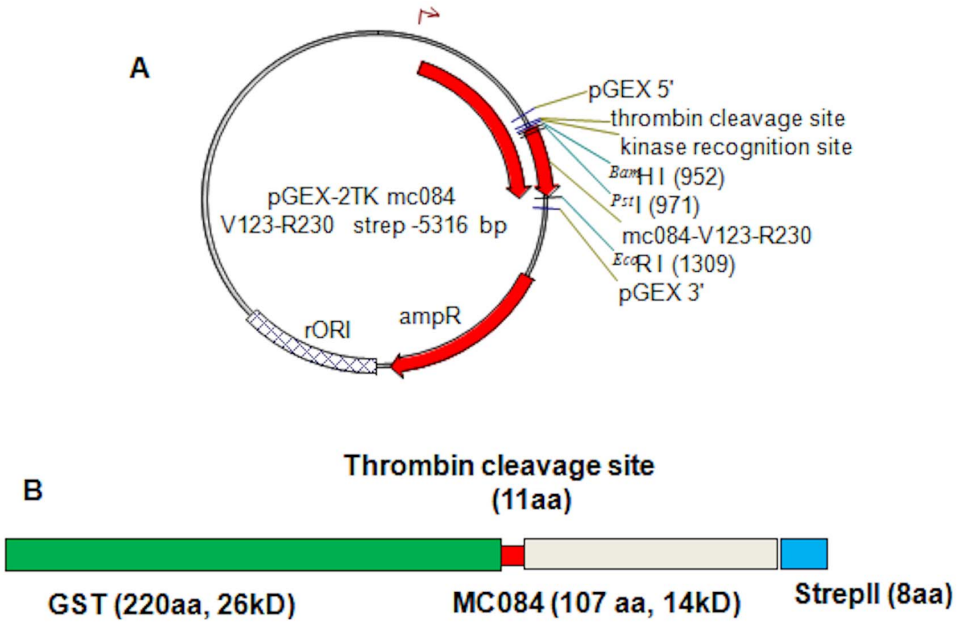

Figure 2. pGEX 2TK construct. (A) Schematic of recombinant plasmid p332 with a MC084 specific insert of 107 amino acids (V123-R230); predicted molecular weight 14 kD (B) Schematic of fusion protein of GST (green), followed by Thrombin kinase site (red), MC084 V123-R230 (grey), and strep II tag (blue); predicted antigenic site (black) (C) Western blot giving 40 kD GST fusion protein GST-MC084S (V123-R230) detected using Strep MAB-Classic HRP conjugate (IBA-lifesciences). Vector NTI (vNTI) was used to produce virtual molecules and schematic diagrams of constructs prior to molecular cloning (InforMax, Inc).
doi:10.1371/journal.pone.0088734.g002

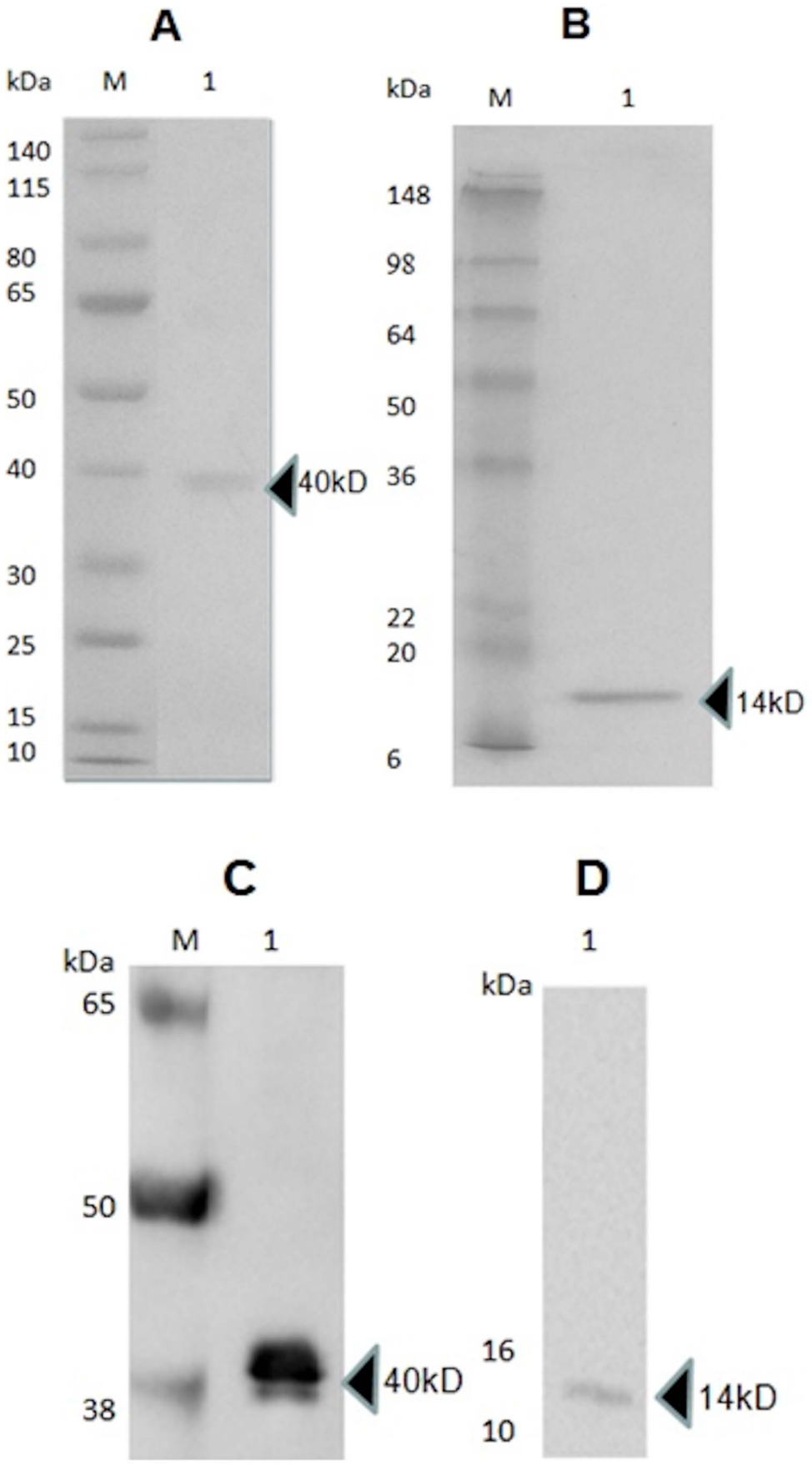
A
kDa
M
1
140
115
80
65
50
40
30
25
15
10
40kD
B
kDa
M
1
148
98
64
50
36
22
20
6
14kD
C
M
1
kDa
65
50
38
40kD
D
1
kDa
16
10
14kD

Figure 3. Protein purification. Characterisation of over expressed recombinant fusion protein GST-MC084S and FPLC purified recombinant MC084S protein by SDS-PAGE and Western Blot. M: Molecular weight markers expressed in kDa. (A) Over-expressed 40 kDa Recombinant GST-MC084S fusion protein separated in a 4–12% Bis-Tris gel. (B) FPLC purified 14 kDa protein separated in a 15% Bis-Arylamide gel. Both gels were stained with Coomassie Brilliant Blue R-250. (C) GST-MC084S fusion protein after transfer to nitrocellulose (D) FPLC purified MC084S. The membranes were probed with Strep MAB-Classic HRP conjugate (IBA-lifesciences). Arrow heads indicate the locations of proteins.
doi:10.1371/journal.pone.0088734.g003

were collected at Cardiff University. Twelve serum samples were collected from MCV patients (10 from Dr P N Behl Skin Institute and School of Dermatology, New Delhi, India; two from UK; aged 2–62 years) as diagnostic specimens.

MCV Direct Binding ELISA

Ninety six well Maxisorp ELISA plates (Nunc) were coated with 3 μg/ml of FPLC purified recombinant truncated MC084S (aa 123–230) protein per well in 100 μl of 0.05 M carbonate-bicarbonate buffer (pH9.6) and incubated at 37°C for 2 h and then overnight at 4°C. Plates were washed with PBS and blocked with 5% skim milk. Test sera, diluted 1:100 in dilution buffer, and were coated across the plate (100 μl/well). The plates were incubated at 37°C for 2 h and washed ten times with PBS-T. Secondary anti-human IgG conjugated to horseradish peroxidase (GE Healthcare), diluted 1:2000 in dilution buffer was subsequently added (100 μl/well). After incubation at 37°C for 2 h the plate was washed ten times with PBS-T and 100 μl of BD OptEIA™ substrate reagents (BD Biosciences) was added to each well. 50 μl of 1 M H_2SO_4 was used to stop the enzyme reaction after 20 min incubation at RT. The OD of the reaction product was read at 450 nm on an FLUROSTAR OPTIMA - ELISA plate reader (BMG Labtech).

Plate Description

42 serum samples were tested in duplicate on each plate along with a panel of four control sera consisting of two negative and two positive as well as four blanks, all in duplicate. The results were expressed as δODU (δODU = mean of duplicate wells minus mean of the blank wells).

ELISA Performance

Plate to plate variation was monitored by comparing the control panel results between the different wells of the same plate; same sera samples run on different plates on the same day as well as on different days.

Immunofluorescence and Immunohistochemistry

Paraffin embedded sections were deparaffinized and rehydrated. Dako Cytomation Envision®+Dual Link System-HRP (DAB^+) kit (Dako) was used as per manufacturer's instructions. For staining of tissue with human sera, ECL Anti-human IgG (1:2000) (GE Healthcare) was used. Staining was completed with Mayers haematoxylin and eosin counterstaining. All sections were analysed using an Olympus BX51 light microscope. Vaccinia virus infected HaCaT cells were grown on glass coverslips and fixed with 3% paraformaldehyde for 10 min, followed by staining with human serum antibodies (1:100) and an anti-human AlexaFluor 488 secondary antibody (Invitrogen).

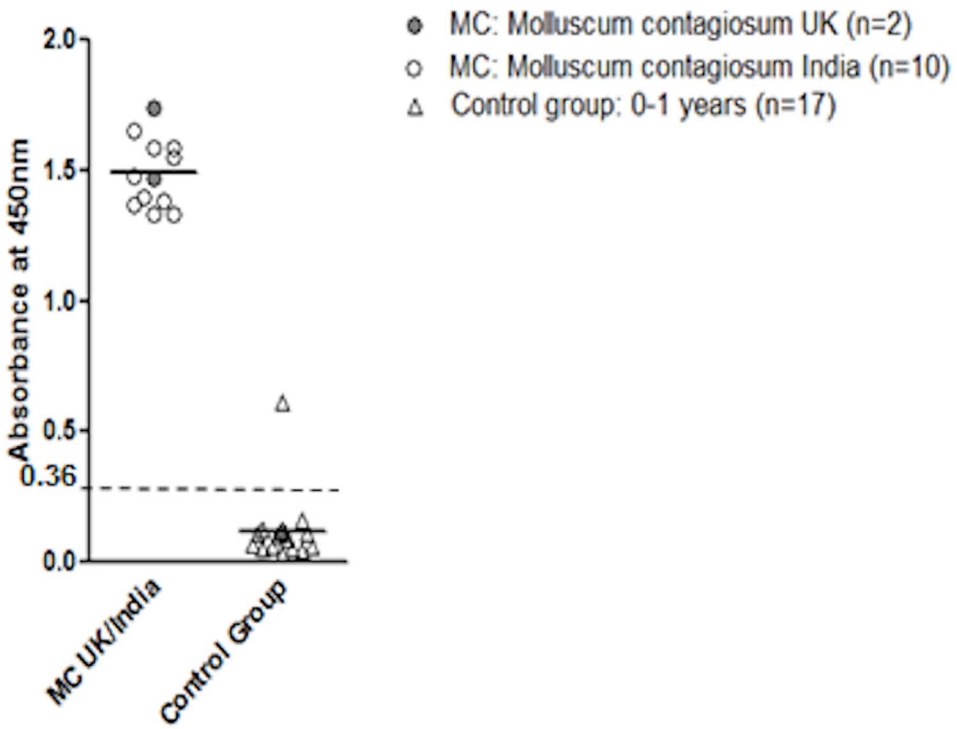

Figure 4. Sensitivity. Absorbance plot of twelve sera from patients clinically diagnosed with MCV (India n = 10; UK n = 2; control group of 0–1 year old individuals n = 17).
doi:10.1371/journal.pone.0088734.g004

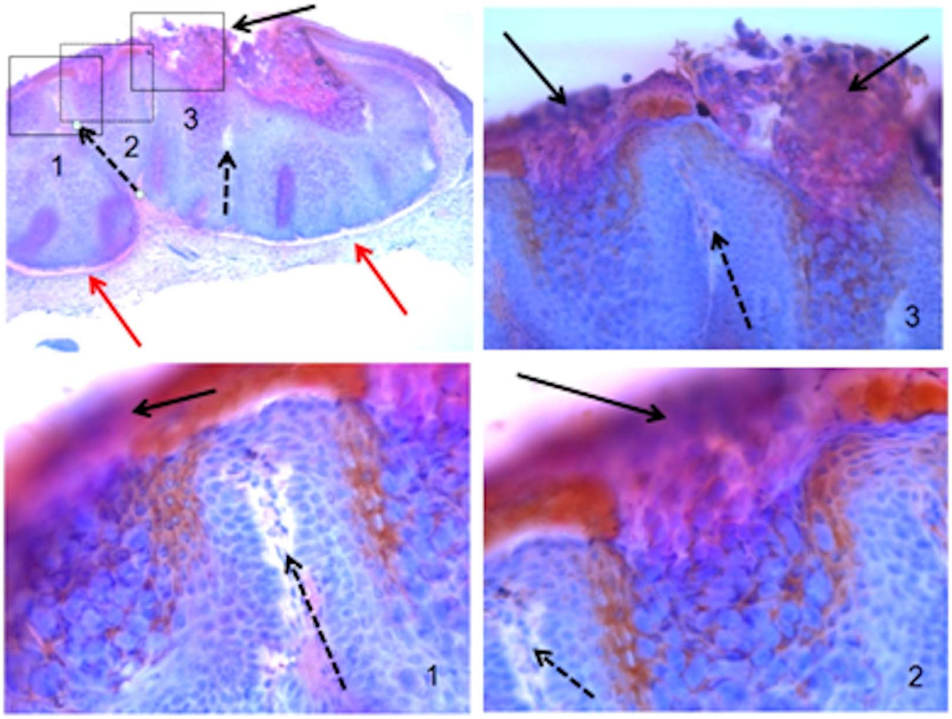

Figure 5. Tissue stain details. Microscopy (4×) of a Molluscum contagiosum lesion section (17315/11) stained with MC patient positive serum (CF2012-1) and haematoxylin-eosin counterstain (upper left hand corner). Three insets showing details at various magnifications [inset 1-(10×), inset 2-(20×) and inset 3-(20×)].
doi:10.1371/journal.pone.0088734.g005

Statistical Analysis

Serological data was stratified by age or diagnosis. Statistical significance of differences between the ELISA responses of different groups was assessed by one way ANOVA. Tukey post hoc anova was used to identify and compare statistically significant means and differences of different groups.

Additional information on material and methods is shown in supporting information.

Results

Selection of MC084 Antigen, Cloning and Purification

Amino acid sequences of MC084 (298 aa, 34 kD) were analysed to determine overall homology with related proteins in the GenBank and identify transmembrane regions and region of high hydrophilicity/high antigenicity. Two transmembrane regions predicted in the C-terminal end of the protein [26], were excluded to avoid solubility issues in the *E. coli* expression system (Figure 1A). Of the remaining amino acids, a N-terminal region (V33-G117) and a C-terminal region (aa V123-R230), both containing one region of high hydrophilicity in the Kyte–Doolittle plot (Figure 1B) [28] were further analysed for subcloning.

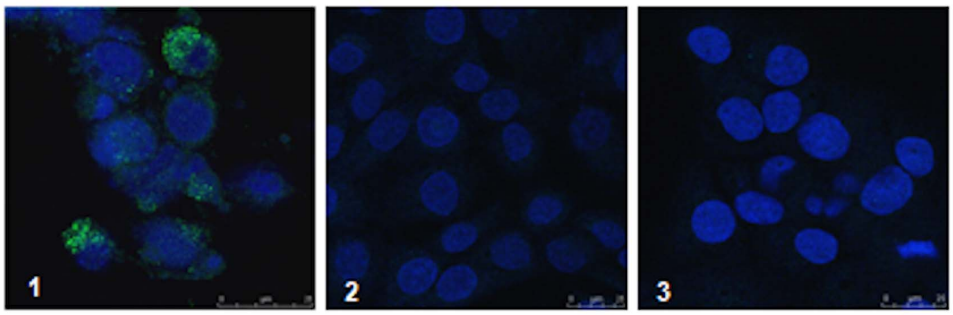

Figure 6. HaCaT Immunofluorescence. (A) HaCaT cell culture infected with recombinant vaccinia virus expressing MC084S (v319). Reactivity of high titre human serum HDV0901071 and secondary antibody AlexaFluor 488 (Green) goat anti-human IgG (H+L). (B) HaCaT cell culture infected with recombinant vaccinia virus expressing MC084S (v319). Reactivity of low titre human serum HDV0900040 and secondary antibody AlexaFluor 488 (Green) goat anti-human IgG (H+L). (C) Mock infected cells. Reactivity of high titre human serum HDV0901071 and secondary antibody AlexaFluor 488 (Green) goat anti-human IgG (H+L). Nuclei are stained with DAPI (Hoechst) and shown in blue. Samples were analysed for fluorescence emission properties by using confocal scanning laser microscopy Leica TCS SP2 AOBS.
doi:10.1371/journal.pone.0088734.g006

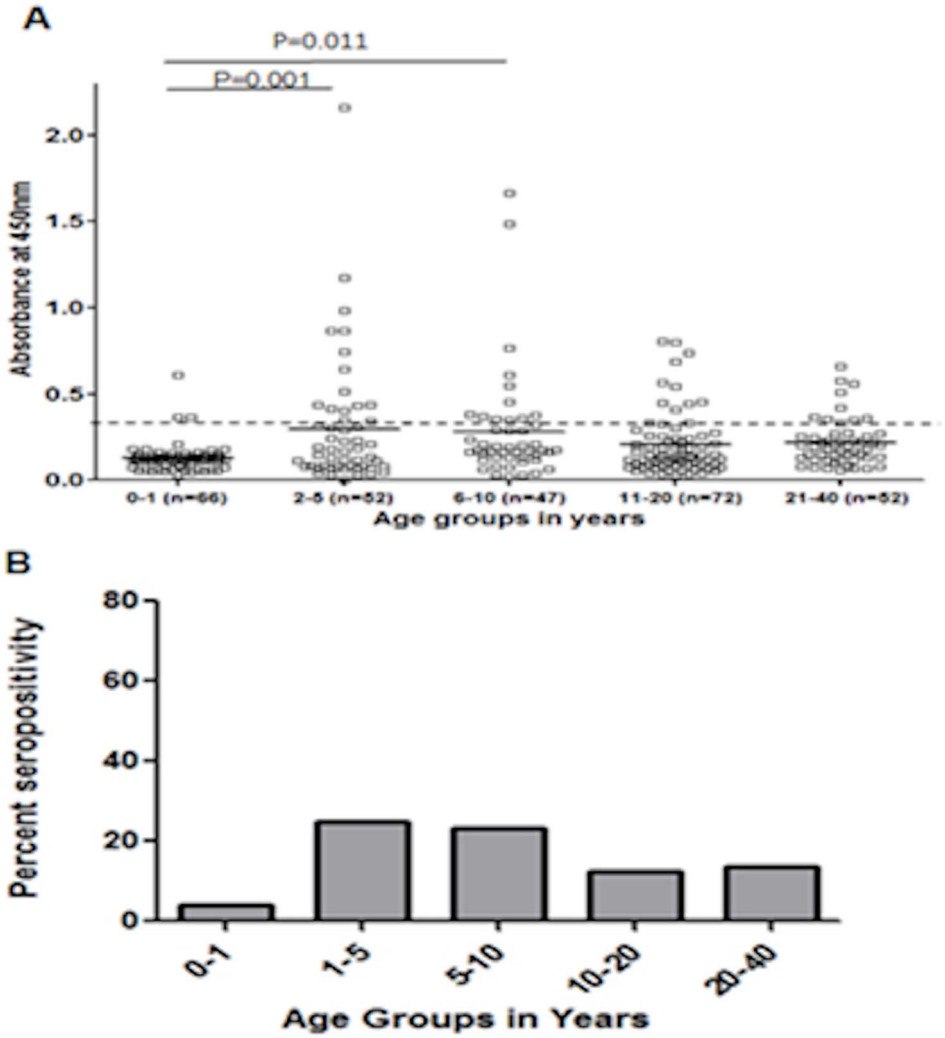

Figure 7. German seroprevalence. Distribution of anti-MC084S antibodies in a German population tested by direct binding ELISA (A) Serological responses to MCV antigen MC084 in a German population (n = 289; ages 0–40 years) expressed as the δODU value of an individual serum sample. The horizontal bar within each group represents the median absorbance measurement. (B) Percent seropositivities in different age groups after cut–off of 0.36 (i) 0–1 years (4.5%), (ii) 2–5 years (25%), (iii) 6–10 years (23.4%), 11–20 years (12.5%), and 21–40 years (13.5%).
doi:10.1371/journal.pone.0088734.g007

The C-terminal truncation of mc084 (V123-R230, predicted MW 14 kD), comprising 107 aa, has the lowest homology to orthopoxvirus proteins and contains a region of high antigenicity (218-NELRGREYGASLR-230) with no significant homology to vaccinia/cowpox virus. The C-terminal truncation MC084 (V123-R230) was then subcloned into the pGEX-2TK vector (Figure 2A) with a Strep II tag and in frame with glutathione S-transferase separated by a thrombin kinase site (Figure 2B) and overexpressed as a GST fusion protein in codon optimized *E. coli* (BL21 RIL$^+$).

The GST fusion protein was identified with an apparent molecular weight (MW) similar to the predicted MW of 40 kD in IPTG induced cultures (Figure 3A) and was absent in the uninduced cultures. The protein was protease cleaved and the C-terminal truncation of MC084 with an apparent MW of 14 kD was further purified via FPLC using a size exclusion Superdex S200 column (Figure 3B). The Strep II tag was identified in Western Blot in both the fusion protein and the cleaved MC084 (V123-R230)-Strep II truncation (Figures 3 C and D). Additional data on antigen selection and optimization can be found in Figures S1 and S2.

ELISA Sensitivity, Cut-off, and Specificity

MC084S (V123-R230) antigen coated ELISA plates were produced as described in material and methods. Serum samples were diluted 1:100.

To establish sensitivity a panel of 12 sera from patients with known and clinically active MCV was first screened in comparison to sera from 0–1 year old individuals from the neonatal screening program of the Heidelberg University Clinics. In the group of sera from patients with diagnosed Molluscum contagiosum (n = 12) the ELISA gave high readings for all (median δODU 1.5), with the most recent sample from Cardiff (CF2012-1) giving the highest (Figure 4). The control group of seventeen neonates from the Heidelberg University Clinics showed low readings with a mean of 0.1 δODU as shown in Figure 4, with one outlier (0.61 δODU). The confidence interval for the difference between positive and negative control groups was highly significant (Figure 4). Sensitivity was 100% for MC patients.

The cut-off for ELISA was calculated based on 66 sera from infants seen in the neonatal unit aged 0–1 years. The mean of δODU readings was 0.12043 and the SD was 0.08300. In

Table 1. Summary of seroprevalences in German and UK populations.

Groups	Total sera	Positive sera ≥ cut-off = Mean+3*SD (0–1 yr+outlier) 0·36
German sera		
0–1 years	66	3 (4·5%)
2–5 years	52	13 (25%)
6–10 years	47	11 (23·4%)
11–20 years	72	9 (12·5%)
21–40 years	52	7 (13·5%)
	289	**Seropositivity in healthy subjects** 14·87%
Psoriasis	10	2 (20%)
SLE*	3	1 (33·3%)
Autoimm†	12	2 (16·6%)
UK sera		
Healthy Humans	33	10 (30.3%)
PPMS#	9	1 (11·1%)
RRMS‡	37	6 (16·2%)
Total	393	65 (16.5%)

*SLE – Systemic Lupus Erythematosus.
†Autoimm. – General autoimmune conditions.
#PPMS – Primary progressive multiple sclerosis.
‡RRMS – Relapsing remitting multiple sclerosis.
doi:10.1371/journal.pone.0088734.t001

comparison the mean δODU for 12 MCV infected patients was 0.833 and the S.D. 0.571. The infant group was used to define negativity with the upper limit being the mean δODU plus 3 SD (i.e. 0.36). Assuming that these values are indicative of a negative response to the recombinant protein, we defined a positive antibody response as being a value greater than mean plus 3 SDs i.e. δODU 0.36. Two more outliers were identified in this group (δODU 0.36 and 0.35). The MCV status of these subjects (aged 2 months, 9 months and 11 months) could not be determined. Inter-well, intra-assay and inter-assay variability was found to be 3%, 5.2% and 6.7%, respectively.

In order to establish ELISA specificity, human MCV infected tissue section obtained from the Heidelberg University Dermatology Unit were tested with high and low titre sera form our serum collections (Figure S3). Reactivity of high titre sera are shown on the left (Figure S3 1A, B/transverse section-perpendicular to level skin and 2A, B/plane section-parallel to level skin). High titre sera show strong MC084 specific staining of cellular debris and MC bodies extruded from and in the centre of lesions, as well as infected cells in lobules extruding infectious virus into the centre of the lesion and upwards. Molluscum rich lipid debris areas are well preserved in these lesions. There is much weaker staining with low titre sera (same lesions in transverse and plane sections; Figure S3 1C, D and 2C, D).

Specific reactivity (MCV positive UK patient CF2012-1) is demonstrated in more detail in Figure 5. The section shows a dome-shaped contour with cup shaped lesions with central invagination, representing a typical MCV lesion consisting of two inverted lobules of hyperplastic squamous epithelium (red arrows) with several sub-lobules. The MC lesion shows acanthosis with the appearance of intraepidermal lobules with enlarged basophilic nuclei filled with cellular debris and molluscum bodies (black arrows). Intraepidermal lobules are separated by septa consisting of compressed dermis (dotted arrow). MCV inclusion bodies stain strongly golden-brown with the human polyclonal serum CF2012-1 taken from a patient with clinical MCV infection. The stain is confined to areas where MCV cores, mature and released virus particles would be expected. In a number of tissue sections stained, the pattern was repeatable and sensitive to tissue preparation. Interestingly, the debris areas filled with mature MCV particles and lipid debris are also sensitive to removal by xylene/ethanol treatment of paraffin sections. The area's most consistently stained are the suprabasal and spinous layers.

To further establish antigen specificity we also infected human HaCaT keratinocytes with a vaccinia virus expressing full length mc084 (v319; aa 1 to 318) as shown in Figure 6. Infected keratinocytes were tested with the high titre serum HD V0901071. Virus infected cells show a vesicular stain similar to an endosomal/lysosomal pattern. Uninfected cells show no background signal, indicating the human polyclonal does not recognize keratinocyte antigens in cultured HaCaT cells.

Antigen optimization and comparisons are described in supporting information (Figures S1 and S2).

ELISA Population Studies

Sera from 289 individuals aged 2 months to 40 years (median age 21 years) were randomly selected from frozen 'normal control sera' collected at the University of Heidelberg, Germany, and tested for the presence of anti-MC084S (aa 123–230) antibodies (Figure 7 A). Healthy subjects are divided into groups on the basis of age: 0–1 years (n = 66), 2–5 years (n = 52), 6–10 years (n = 47), 11–20 years (n = 72) and 21–40 years (n = 52). The reactivity in infants was significantly lower than in other groups. Based on the minimum cut-off value of δODU 0.36, 43 (14.8%) sera of the 289 sera from a representative healthy German population tested positive in the MC084S (123–230) ELISA. Positive antibody responses in the age groups were as follows: 4.5% (n = 3) 0–1 year olds, 25% (n = 13) in 2–5 year olds, 23.4% (n = 11) in 5–10 year olds, 12.5% (n = 9) in 10–20 year olds and 13.5% (n = 7) in 20–40

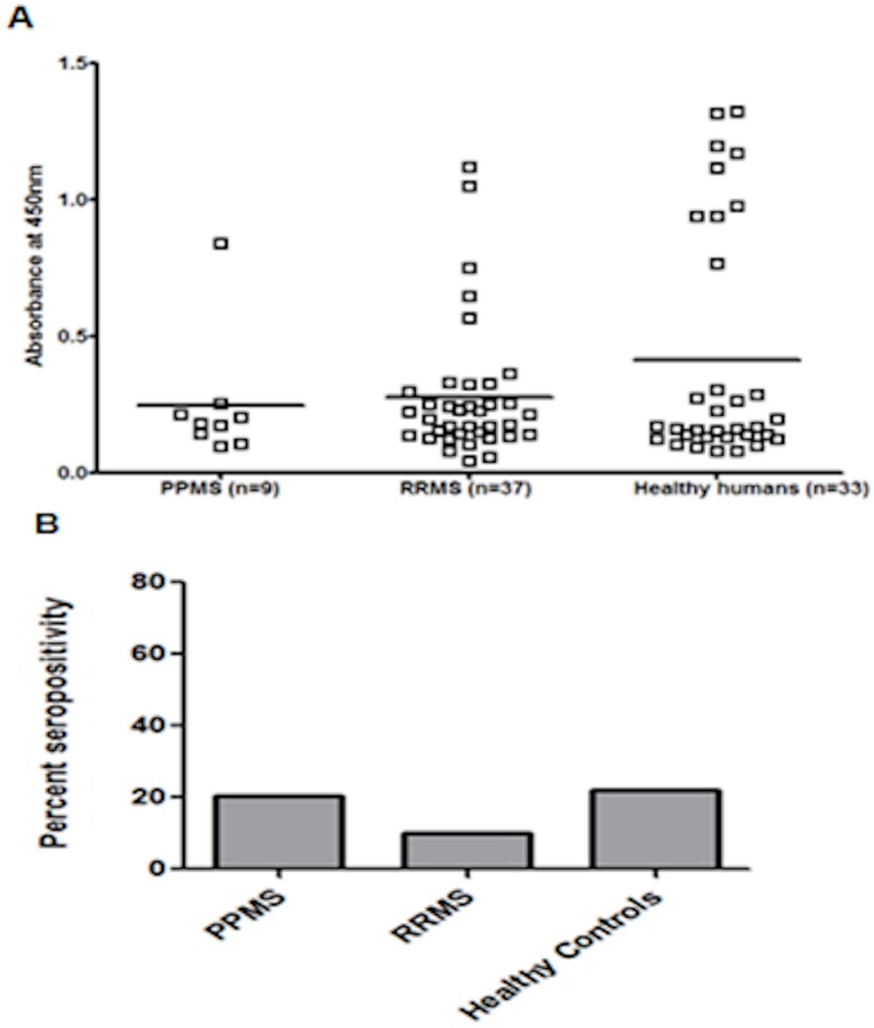

Figure 8. UK seroprevalence. Distribution of anti-MC084S antibodies in a UK population tested by direct binding ELISA. (A) Serological responses to MCV antigen MC084S (V123-R230) in UK population (n = 79) expressed as the δODU value of an individual serum sample in different groups (i) Primary progressive multiple sclerosis (PPMS; n = 9), (ii) Relapsing remitting multiple sclerosis (RRMS; n = 33) and (iii) Healthy humans (n = 37). The horizontal bar within each group represents the median absorbance measurement (B) Percent positivity in individual groups for MC084S after cut-off of 0.36 (i) PPMS (11.1%), (ii) RRMS (16.2%) and (iii) healthy humans (30.3%).
doi:10.1371/journal.pone.0088734.g008

year olds (Figure 7 B). A one way anova was used for preference differences between the different age groups. The test statistic (F value) is 4.587 and the p value is 0.001. Further post hoc analysis was done using Tukey test to identify and measure statistically significant difference between groups of data as pairs. From the multiple comparisons it can be concluded that there is a sharp increase in positive sera responses between 0–1 year olds and 2–5 year olds which are statistically significant at p value = 0.001. The differences in the sera responses between 0–1 year olds and 6–10 year olds are also statistically significant (p = 0.011). Differences in sera responses between all other groups are not statistically significant. The results of the serological survey in members of the German populations are shown in Table 1.

We analysed 25 patients (8–40 years of age) with dermatological conditions such as Systemic lupus erythematosus (n = 10), Psoriasis (n = 3) and general autoimmune conditions (n = 12), including patients with Autoimmune haemolytic anaemia, Autoimmune cerebilitis and Autoimmune hepatitis diagnosed at the University of Heidelberg. The findings are summarized in Table 1. MCV seroprevalence is above the average rate in skin specific autoimmune conditions, but similar in general autoimmune conditions.

79 serum samples from a UK population (aged 21–40 years; median age 27 years) were analysed which had been collected as part of a study on Multiple sclerosis (MS) at Cardiff University. These subjects were grouped as Primary progressive multiple sclerosis (n = 9), relapsing remitting multiple sclerosis (n = 37) and healthy humans (n = 33) (Figure 8A).

Using the same cut-off of 0.36, MCV antibodies were detected in 10 of 33 healthy UK serum samples (30.3%). In patients with primary progressive multiple sclerosis seroprevalence was 11.1% (n = 1/9), as compared to 16.2% (n = 6/37) in patients with relapsing remitting multiple sclerosis (Figure 8B). A one way anova was used for preference differences between the different groups. The test statistic (F value) is 1.756 and the p value is 0.180. Further post hoc analysis was done using Tukey test to identify and measure statistically significant difference between groups of data as pairs. From the multiple comparisons it can be concluded that

differences in sera responses between groups are not statistically significant. An overall gender ratio (M: F) of 1.4:1 (183:131) was found in the German serum collection, as compared to 1:2.1 (25:54) in the UK population. The results of the serological survey in members of all UK populations are shown in Table 1.

Discussion

We describe here for the first time a seroepidemiological study of MCV in Europe, the largest survey reported so far (n = 393) and the first MCV ELISA based on viral antigen expressed in *E. coli*.

Previously reported MCV ELISAs used antigen from human lesion material or Sendai virus expressed N-terminal amino acid sequences of MC133, raising issues with background skin antigens and posttranslational antigen processing. To improve water solubility and provide an expression platform more suitable for commercial production of a MCV ELISA, we decided to use hydrophilic antigenic regions of MC084 expressed in *E. coli*. On the basis of previous work by Watanabe *et al.* [22] and our own homology analyses we chose a C-terminal truncation of MC084 (V123-R230), upstream of A238-Q298 previously found non-reactive in ELISA by Watanabe [22], as our candidate ELISA antigen. Our choice of antigen minimizes the possibility of cross reactivity with vaccinia virus specific antibodies, exclude the membrane spanning domains of mc084, but include a possible major antigenic site, identified by hydrophilicity plotting (MC084 N218-R230).

The ELISA is sensitive (100%) and specific, with low inter- and intra-assay variability. This is in comparison to the lower sensitivities of 71% and 58%, in the ELISAs reported by Konya *et al.* [21] and Watanabe [22], respectively. We have determined specificity in MCV tissue sections, similar to Konya *et al.* [21]. To determine specificity quantitatively, a collection of sera would be needed.

We have calculated cut-off for our ELISA to include outlier results from our neonatal control group. The MC status of the outliers could not be determined, as the data was anonymised.

Any comparisons of our findings with previous ELISA results must be fundamentally flawed, because different antigen and expression systems were used. However, no other data are available, so with the above reservations, we compared the findings of our serological survey to results reported for Northern Ireland and two previous ELISA studies in Australia and Japan [20,21–22]. We find an overall seropositivity in a general German population of 14.8% and 30.3% in the UK. This correlates well with previous findings of 16.7% in Ireland (n = 30; IgG responses) [20], 23% in an Australian population [21] and less so with 6% reported in a Japanese survey [22].

The age profile determined using the MC084 ELISA correspond well with our understanding of the natural history of MCV infections, with low exposure of very young children and a high prevalence among toddlers and preschool children, where MCV smear infections is most likely to be transmitted among larger numbers of children. Our data confirm previously reported findings of stronger antibody responses in acute MC [21], mostly in the 2–10 age group [25,28], with waning antibody levels being detectable as the population ages. This would suggest very little re-exposure in older age groups.

In contrast to Konya *et al.* [21], who report a very high seropositivity rate in their 0–6 month old population of 31%, explaining this with maternal antibodies, our data do not indicate a high seropositivity rate in very young children. Seroprevalence with the mc084 (V123-R230) ELISA is below 5% in 0–1 year olds and only increases in the age group of 2–5 year olds, not exceeding 25%. Watanabe *et al.* explained their low overall seropositivity (n = 108, 6%) [22] in healthy subjects in comparison to the prior Australian study (n = 357; 23%) [21], with their mc133 ELISA failing to pick up sera with mc084 antibodies as shown in immunoblots, indicating that mc133 may not be the best choice of antigen, underestimating seroprevalence.

The findings in immunocompromised patients and patients with skin and other inflammatory disorders indicate an increased seroprevalence in skin disorders, and a decrease in generally or therapeutically immunocompromised populations, but lack statistical power because of low sample numbers. The gender ratios calculated, indicate a higher seroprevalence (2.1 fold) in females than males of in the UK serum collection, but a lower ratio in the German collection.

In summary, we propose MC084 (V123-R230) is a suitable antigen for MCV serological surveys when expressed in *E. coli*. It includes a probable highly antigenic site at amino acid position N219-R230. Importantly, the MC seroprevalence of 14.8% in our German population is a threefold increase over the reported incidence of MC in a comparable Swiss population of 4.9% [29], supporting the notion, that MC is an underreported infection. The assay will allow further investigations into the seroprevalence of MCV in other geographical areas, including the US, China, Japan and Australia.

Ongoing work includes possible use of a subpeptide of MC084 (N218-R230) comprising only the highly antigenic site for a capture ELISA and T cell studies, and the development of an IgM MC084 (V123-R230) ELISA. We are also in the process of investigating the MC084 (V123-R230) peptide for its potential to compete with MCV/VACV entry in a MCV/VACV reporter assay [30].

Supporting Information

Figure S1 MC084 antigen optimization. The figure shows the antigenicity of MC084S (aa123–230) as determined by direct binding ELISA using high titre human serum (HD V0901071). (A) Saturation was achieved at 3 μg/ml. (B) A maximum of 80% inhibition of anti-serum antibodies with MC084S as inhibitor was observed whereas negligible inhibition was observed with BSA and human IgG.
(TIF)

Figure S2 Comparison of antigen reactivity. The N-terminal truncation of MC084 i.e. MC084v5 (33–117), C-terminal truncation of MC084 i.e. MC084S (123–230), N-terminal truncation of MC133 i.e. MC133S (1–370) and GST tested as uncleaved fusion proteins on a GST affinity plate to compare antigen affinity and seroreactivities. The relative absorbance of individual sera was the same against all antigens tested with only minimal differences in absorbance.In direct antigen comparison there was no significant difference between truncations of mc084 and mc133, and no serum showed prevalent reactivity against one or another of the antigen used. A strep tag was used for detection of recombinant antigen in western blots. The tag did not interfere with ELISA results in a serum study of 149 serum samples.
(TIFF)

Figure S3 Tissue staining with high and low litre sera. Tissue sections stained with high (HD V0901071 (**1A, B**), HD V0903005 (**2A, B**) and low titre sera (HDV0900471 (**1C, D**), HDV0900040 (**2C, D**) in two magnifications (4x and 10x). High titre sera stained the spinous layers as well as cellular debris and MC bodies in and around the intraepidermal lobules golden-brown. The same section stained with low titre sera as determined

in MC084S ELISA showed much reduced or no reactivity in the same tissue areas.
(TIFF)

Acknowledgments

We thank Bernhard Moser for evaluating this manuscript and offering many helpful suggestions. We thank Arwyn T Jones and Edd Sayers for assistance with the confocal microscope, Bernard Moss of the NIH, NIAID LVD, Bethesda, Maryland, U.S.A. for the gift of the vRB12/pRB21 recombination system, Norbert Fusenig of the DKFZ, Heidelberg, Germany for HaCaT cells, Christopher Holland for assistance with protein purifications, Kamalpreet Banga for help with the statistics analyses and Frau S. Martinache for technical support with MCV section material provided by the Hadaschik group.

Author Contributions

Conceived and designed the experiments: SS JJB. Performed the experiments: SS LF JJB. Analyzed the data: SS JJB PS. Contributed reagents/materials/analysis tools: NA SL NR EH PS. Wrote the paper: SS JJB.

References

1. Chen X, Anstey A, Bugert JJ (2013) Molluscum contagiosum virus infection of the human skin: A comprehensive review of scientific studies and clinical practise. Lancet Infec Dis 13(10): 877–888.
2. Senkevich TG, Bugert JJ, Shisler JR, Koonin EV, Darai G, Moss B (1996) Genome sequence of a human tumorigenic poxvirus: prediction of specific host response-evasion genes. Science 273: 813–816.
3. Bugert JJ (2008) Molluscum Contagiosum Virus In: Mahy BWJ, Van Regenmortel MHV, editors. Encyclopedia of Virology. Oxford: Elsevier-Academic Press. pp. 319–24.
4. Breman JG, Arita I (1980) The confirmation and maintenance of smallpox eradication. New Engl J 303: 1263–73.
5. Esposito JJ (1991) Family: poxviridae in classification and nomenclature of viruses, 5th report. Arch Virol Suppl.2: 91–102.
6. Buller RM, Palumbo GJ (1991) Poxvirus pathogenesis. Microbiol Mol Biol Rev 55: 80–122.
7. Delhon G, Tulman ER, Afonso CL, Lu Z, de la Concha-Bermejillo A, et al. (2004) Genomes of the parapoxviruses Orf virus and Bovine popular stomatitis virus. J Virol 78(1): 168–177.
8. Postlethwaite R (1970) Molluscum contagiosum: A review. Arch Environ Health 21: 432–452.
9. Brown ST, Weinberger J (1974) Molluscum contagiosum: Sexually transmitted disease in 17 cases. J Am Vener Dis Assoc 1: 35–6.
10. Birthistle K, Carrington D (1997) Review: Molluscum contagiosum virus. J Infec Dis 34: 21–28.
11. Gottlieb SL, Myskowski PL (1994) Molluscum contagiosum. Int J Dermatol 33: 453–61.
12. Buckley R, Smith K (1999) Topical imiquimod therapy for chronic giant molluscum contagiosum in a patient with advanced human immunodeficiency virus 1 disease. Arch Dermatol 135: 1167–9.
13. Butala N, Siegfried E, Weissler A (2013) Molluscum BOTE sign: a predictor of imminent resolution. Pediatrics 131 (5): e1650–3. DOI: 10.1542/peds.2012–2933. Accessed Apr 1 2013.
14. Vermi W, Fisogni S, Salogni L, Schrer L, Kutzner H, Sozzani S, et al. (2011) Spontaneous regression of highly immunogenic molluscum contagiosum virus (MCV)-induced skin lesions is associated with plasmacytoid dendritic cells and IFN-DC infiltration. J Invest Dermatol 131: 426–34.
15. Burnett JW, Neva FA (1966) Studies on the mechanism of molluscum contagiosum cytotoxicity1. J Invest Dermatol 46: 76–83.
16. Burnett JW, Sutton JS (1968) Molluscum contagiosum cytotoxicity for primary human amnion cells in vitro as studied by electron microscopy. J Invest Dermatol. 50 (1): 67–84.
17. Buller RM, Burnett J, Chen W, Kreider J (1995) Replication of molluscum contagiosum virus. Virology 213: 655–9.
18. Fife KH, Whitfeld M, Faust H, Goheen MP, Bryan J, Brown DR (1996) Growth of molluscum contagiosum virus in a human foreskin xenograft model. Virology 226: 95–101.
19. Mitchell JC (1952) Observations on the virus of molluscum contagiosum. Br J Exp Pathol 34: 44–49.
20. Shirodaria PV, Matthews RS, Samuel M (1979) Virus specific and anti-cellular antibodies in molluscum contagiosum. B J Dermatol 101: 133–140.
21. Konya J, Thompson CH (1999) Molluscum contagiosum virus: antibody responses in persons with clinical lesions and seroepidemiology in a representative Australian population. J Infect Dis 179: 701–04.
22. Watanabe T, Nakamura K, Wakugawa M, et al. (2000) Antibodies to molluscum contagiosum virus in the general population and susceptible patients. Arch Dermatol 136: 1518–22.
23. Konya J, Thompson CH, De Zwart-Steffe RT (1992) Enzyme-linked immunosorbent assay for measurement of IgG antibody to Molluscum contagiosum virus and investigation of the serological relationship of the molecular types. J Virol Methods 40: 183–94.
24. Watanabe T, Morikawa S, Suzuki K, Miyamura T, Tamaki K, Ueda Y (1998) Two major antigenic polypeptides of molluscum contagiosum virus. J Infect Dis 177: 284–92.
25. Krogh B, Larssonn G, von Heijne, Sonnhammer ELL (2001) Predicting transmembrane protein topology with a hidden Markov model: Application to complete genomes. J Mol Biol 305(3): 567–580.
26. Blasco R, Moss B (1991) Extracellular vaccinia virus formation and cell-to-cell virus transmission are prevented by deletion of the gene encoding the 37,000-Dalton outer envelope protein. J Virol 65(11): 5910–20.
27. Kyte J, Doolittle R (1982) A simple method for displaying the hydropathic character of a protein. J. Mol. Biol 157: 105–132.
28. Reynolds MG, Holman RC, Yorita Christensen KL, Cheek JE, Damon IK (2009) The Incidence of Molluscum contagiosum among American Indians and Alaska Natives. PLOS ONE 4(4): e5255.
29. Wenk C, Itin PH (2003) Epidemiology of pediatric dermatology and allergology in the region of Aargau, Switzerland Pediatric Dermatol 20: 482–7.
30. Sherwani S, Blythe N, Farleigh L, Bugert JJ (2012) New method for the assessment of Molluscum contagiosum virus infectivity. In: Isaacs S, editors. Methods Mol Biol. Clifton, NJ. Vol. 890: pp135–46.